ERDC/EL TR-12-33

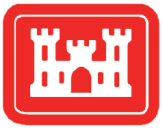

US Army Corps
of Engineers®
Engineer Research and
Development Center

Strategic Environmental Research and Development Program

Identification of Microbial Gene Biomarkers for *in situ* RDX Biodegradation

Project ER-1609

Fiona. H. Crocker, Karl J. Indest, Carina M. Jung,
Dawn E. Hancock, Megan E. Merritt, Christine Florizone,
Hao-Ping Chen, Gordon R. Stewart, Songhua Zhu,
Nicole Sukdeo, Marie-Claude Fortin, Steven J. Hallam,
William W. Mohn, Lindsay D. Eltis, Nancy N. Perreault,
Jian-Shen Zhao, Louise Paquet, Annamaria Halasz,
and Jalal Hawari

December 2012

Environmental Laboratory

Strategic Environmental Research and Development Program

ERDC/EL TR-12-33
December 2012

Identification of Microbial Gene Biomarkers for *in situ* RDX Biodegradation

Project ER-1609

Fiona. H. Crocker, Karl J. Indest, Carina M. Jung, Dawn E. Hancock, and Megan E. Merritt

Environmental Laboratory
U.S. Army Engineer Research and Development Center
3909 Halls Ferry Road
Vicksburg, MS 39180-6199

Christine Florizone, Hao-Ping Chen, Gordon R. Stewart, Songhua Zhu, Nicole Sukdeo, Marie-Claude Fortin, Steven J. Hallam, William W. Mohn, and Lindsay D. Eltis

Department of Microbiology and Immunology
University of British Columbia
2350 Health Sciences Mall
Vancouver, British Columbia
Canada V6T 1Z3

Nancy N. Perreault, Jian-Shen Zhao, Louise Paquet, Annamaria Halasz and Jalal Hawari

Biotechnology Research Institute, NRC
6100 Royalmount Avenue
Montreal, Quebec
Canada H4P 2R2

Final report

Prepared for U.S. Army Corps of Engineers
Washington, DC 20314-1000

Abstract

Objectives of this project were to: (a) elucidate RDX degradation pathways in model RDX-degrading bacteria, (b) design and develop molecular tools to identify genes responsible for RDX biodegradation, and (c) correlate the response of biomarker(s) to concentrations of RDX and/or rates of RDX degradation. *Gordonia* sp. KTR9 and *Shewanella oneidensis* MR-1 served as model bacterial systems for the aerobic and anaerobic degradation of RDX, respectively.

Genome annotation and functional characterization of the plasmid pGKT2 in KTR9 revealed that *xplA* gene is both necessary and sufficient for RDX degradation. *Shewanella oneidensis* MR-1 was shown to efficiently degrade RDX anaerobically via two initial routes: (a) sequential N-NO_2 reduction to the corresponding nitroso (N-NO) derivatives; and (b) mono-denitration followed by ring cleavage. The qPCR molecular tools described in this report have the potential to be used by remediation specialists for site characterization, treatment recommendations, and for evaluation and optimization of the treatment process.

The fundamental information gained in this study suggests that XplA-mediated aerobic denitration of RDX may be subjected to inhibitory effects in response to nitrogen availability. Additional research is required to determine reliable guidelines to inform site managers of specific field concentrations of ammonium and nitrate that will increase RDX treatment times. Also, techniques to effectively lower the inorganic nitrogen concentrations to non-inhibitory levels for the aerobic RDX biodegradation pathway will need to be determined.

Contents

Figures and Tables

Figures

Tables

Acronyms

2D	Two-dimensional
AICE	Actinomycetes integrative and conjugative elements
ANOVA	Analysis of variance
BLAST	Basic local alignment search tool
bp	Base pair
cDNA	Complimentary DNA
CFB	Canadian Forces Base
COG	Clusters of Orthologous Groups
*cyp151*s	PipA, Cytochrome P450, family 151 gene
Cyp151s	Cytochrome P450, family 151 protein
DNX	Hexahydro-1,3-dinitroso-5-nitro-1,3,5-triazine
DoD	Department of Defense
E-value	Expectation value
G+C	Guanosine plus cytosine
GI	Genomic island
glnA	Glutamine synthetase gene
GlnA	Glutamine synthetase protein
glnAxplB	Gene fusion between *glnA* and *xplB* genes

GlnAXplB	Fusion protein of glutamine synthetase and flavodoxin reductase
glnR	Global nitrogen transcriptional regulator gene
GlnR	Global nitrogen transcription regulator protein
HGT	Horizontal gene transfer
HMX	Octahydro-1,3,5,7-tetranitro-1,3,5,7-tetrazocine
HPLC	High performance liquid chromatography
IAAAP	Iowa Army Ammunition Plant
IMAC	Immobilized metal affinity chromatography
IPG	Immobilized pH gradient
IS	Insertion sequence
kb	Kilobase pairs
kDa	Kilodalton
KEGG	Kyoto Encyclopedia of Genes and Genomes
Km^r	Kanamcyin resistance marker
LB	Luria Bertani broth
MALDI-ToF	Matrix-assisted laser desorption ionization-time of flight
MB	Megabase pairs
MEDINA	Methylenedinitramine
MNX	Hexahydro-1-nitroso-3,5-dinitro-1,3,5-triazine
morA	Cytochrome P450 gene for morpholine degradation

MS	Mass spectrometry
MSM	Mineral salts medium
NCBI	National Center for Biotechnology Information
NDAB	4-nitro-2,4-diazabutanal
nfsI	Nitroreductase gene from *Enterobacter cloacae*
OD	Optical density
ORF	Open reading frame
PBS	Phosphate-buffered saline
PCR	Polymerase chain reaction
PFGE	Pulsed-field gel electrophoresis
pI	Isoelectric point
pipA	Piperidine-inducible Cytochrome P450 gene for degradation of piperidine and pyrrolidine
qPCR	Quantitative polymerase chain reaction
RDX	Hexahydro-1,3,5-trinitro-1,3,5-triazine
RTqPCR	Reverse transcription quantitative polymerase chain reaction
SERDP	Strategic Environmental Research and Development Program
TE	Tris ethylene dinitramine buffer
TMAO	Trimethylamine *N*-oxide
TNT	2,4,6-trinitrotoluene

TNX	Hexahydro-1,3,5-trinitroso-1,3,5-triazine
TSA	Trypticase soy agar
UMCD	Umatilla Chemical Depot
xplA	Flavodoxin-cytochrome P450 gene
XplA	Flavodoxin-cytochrome P450 protein
xplB	Flavodoxin reductase gene
XplB	Flavodoxin reductase protein

Preface

This report was prepared by the U.S. Army Engineer Research and Development Center (ERDC), Environmental Laboratory (EL), Vicksburg, Mississippi, in partnership with the Department of Microbiology and Immunology, University of British Columbia (UBC), Vancouver, British Columbia, Canada, and the Biotechnology Research Institute (BRI), National Research Council of Canada, Montreal, Quebec, Canada. The research was sponsored by the Strategic Environmental Research and Development Program (SERDP), Arlington, Virginia, Dr. Jeff Marqusee, Executive Director, under Environmental Restoration Project Number ER 1609. The principal investigator was Dr. Fiona H. Crocker, Research Microbiologist, Environmental Processes and Engineering Division (EPED), EL, ERDC. Co-principal investigators were Dr. Lindsay D. Eltis, UBC; Dr. Jalal Hawari, BRI; and Dr. Karl J. Indest, Research Microbiologist, EPED, EL, ERDC.

The authors acknowledge the assistance of the following organizations and people for their collaborative efforts made on behalf of this project:

U.S. Army Corps of Engineers, Environmental Quality and Installation Program funded the genome sequencing of *Gordonia* sp. KTR9. Genome British Columbia co-funded Drs. Eltis, Mohn, and Hallam. Defense Research and Development Canada, Department of National Defense is recognized for in-kind contribution.

Dr. Alan D. Hewitt, ERDC Cold Regions Research and Engineering Laboratory, Hanover, NH; Dr. Mandy M. Michalsen, Environmental Engineer, U.S. Army Corps of Engineers (USACE) Seattle District, Seattle, WA; Dr. Victor Medina, EL, ERDC; Mrs. Cynthia L. Price, Research Biologist, EPED, EL, ERDC; Dr. Rick Arnseth, Project Manager/ Geochemist, Tetra Tech Inc., Oak Ridge, TN; and Defense Research and Development Canada, Department of National Defense are recognized for soil and groundwater collection.

Drs. Jed O. Eberly and Tanwir Habib assisted with validation of the *xplA* TaqMan qPCR assay and the *Shewanella oneidensis* MR-1 network analysis, respectively.

This report was graciously reviewed by Denise L. Lindsay and Dr. Jed O. Eberly.

At the time of publication of this report, COL Kevin J. Wilson was Commander of ERDC. Dr. Jeffery P. Holland was Director.

1 Project Objectives

Project ER-1609 "*Identification of Microbial Gene Biomarkers for in situ RDX Biodegradation*" focused on understanding the genetics, physiology, and biochemistry of RDX biodegradation. This basic information was then used to develop molecular probes that would be applicable to predicting the potential for RDX biodegradation or monitoring the progress of RDX bioremediation in the field. The objectives of this project were:

1. To elucidate the RDX degradation pathways in aerobic and anaerobic RDX-degrading bacteria.
2. To identify and validate genetic biomarkers indicative of *in situ* RDX biodegradation.
3. To design and develop molecular tools, such as quantitative PCR primers or hybridization probes, to identify genes responsible for RDX biodegradation *in situ*.
4. To validate the selectivity and sensitivity of the molecular tools generated during this study.

To accomplish these goals, this project used a combination of analytical chemistry, physiological, proteomic and genomic approaches that were organized into five tasks (Figure 1).

The bacterial strains used for these tasks were *Gordonia* sp. KTR9 and *Shewanella oneidensis* MR-1 (ATCC 700550) as representative aerobic and anaerobic RDX-degrading bacteria. Each of these organisms uses distinct mechanisms to degrade RDX. Slightly different strategies were used for each strain, based on the available genomic resources at the time. Two-dimensional (2D) protein electrophoresis and mass spectrometry (MS), and genome annotation were initially used to characterize and identify RDX-related genes and proteins in strain KTR9. Later studies with KTR9 also included differential gene expression (transcriptomic) analysis using DNA microarrays developed from the annotated genome. Differential gene expression analysis was also conducted for strain MR-1 using commercially available microarrays and the publicly available annotated genome. These studies identified gene and protein targets that were considered as potential molecular biomarkers. A combination of genetic mutation/deletion studies,

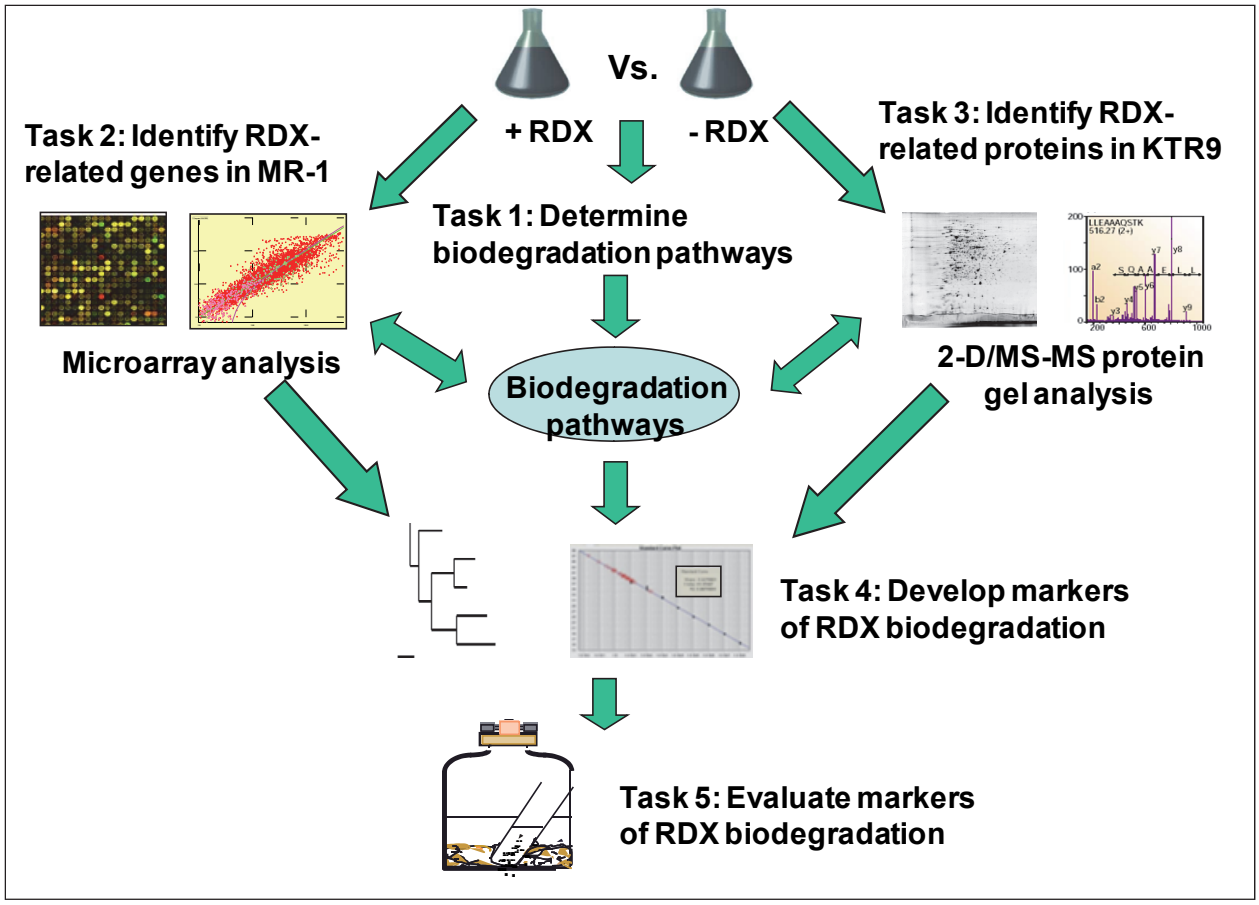

Figure 1. Technical approach for Project ER-1609.

and physiological and proteomics data was used to characterize putative functions of gene targets with respect to RDX degradation and regulation of RDX genes. An existing gene target for aerobic RDX biodegradation, *xplA,* which encodes for a cytochrome P450 enzyme, was used to develop and optimize a TaqMan quantitative polymerase chain reaction (qPCR) set of primers and hybridization probes. The ability of this TaqMan qPCR assay to detect the presence of RDX-degrading bacterial genes was validated with pure cultures and soil and groundwater samples.

This research is expected to yield at least four products:

1. Novel genes and enzymes responsible for the degradation of RDX.
2. Biomarker assays (i.e., qPCR assays) to assess the potential for RDX biodegradation and to monitor *in situ* restoration.
3. Sequencing of the *Gordonia* sp. KTR9 genome, representing the first XplA-mediated RDX degrading bacterium to be sequenced.

4. Annotation of the KTR9 genome and an associated microarray to assess the physiology of *Gordonia* sp. KTR9 following exposure to RDX and other explosives.

Genome annotation and functional characterization of the plasmid pGKT2 in KTR9 revealed that the *xplA* gene is both necessary and sufficient for RDX degradation. It was demonstrated that pGKT2 and its ability to degrade RDX could be disseminated via horizontal gene transfer (HGT) to other actinomycetes. Proteomic analysis of KTR9 grown on RDX as a nitrogen source identified multiple protein targets, including XplA, that were up-regulated. Physiological studies of KTR9 grown on RDX and competing inorganic nitrogen sources, in parallel with PCR analysis of *xplAB,* showed that ammonium sulfate (greater than 3 mM) and sodium nitrite (4 mM) have significant inhibitory effects on RDX degradation and *xplAB* expression. Transcriptome analysis of KTR9 grown on RDX suggested that the transcriptome response to RDX is likely a reaction to nitrogen limitation rather than a response to RDX. Of the gene targets identified as biomarker candidates, only *xplA* met criteria as a suitable biomarker. Validation of an *xplA* TaqMan quantitative polymerase chain reaction (qPCR) assay with field collected samples and microcosm incubations suggested that *xplA* may have value as a qualitative biomarker. The demonstration that *xplA* can be disseminated via HGT is significant, for bioaugmentation efforts utilizing *xplA*-containing bacteria may have the effect of seeding the indigenous microbial population with the ability to degrade RDX.

Shewanella oneidensis MR-1 was shown to efficiently degrade RDX anaerobically via two initial routes: (i) sequential N-NO_2 reduction to the corresponding nitroso (N-NO) derivatives; and (ii) mono-denitration followed by ring cleavage. Four RDX-defective mutants that had insertions in genes encoding for chorismate synthase, naphthoate synthase (MenB), and a cytochrome c, (CymA), were isolated. Characterization of RDX degradation in MenB and CymA mutants implied the participation of CymA in the nitrosation route, but could not definitively suggest a role for MenB. Network analysis of transcriptome data suggests that c-type cytochromes play a role in RDX transformation. However, CymA was not a suitable biomarker candidate due to its broad substrate specificity with other electron acceptors. While a functional gene was not identified in strain MR-1, a phylogenetic gene marker targeting *Shewanella* may have some benefit since a number of species from this genus transform RDX.

The qPCR molecular tools described in this report have the potential to be used by remediation specialists for site characterization, treatment recommendations, and for evaluation and optimization of the treatment process. Phylogenetic gene markers can provide information on the types and abundance of microorganisms associated with biodegradation of RDX. Catabolic gene markers can provide evidence of the potential for one of the specific pathways of RDX biodegradation at a site. These biomarkers could be used to complement traditional methods of determining the fate of RDX in the environment. Currently, the concentrations of RDX and the nitroso metabolites of RDX are routinely measured. This provides information only on the anaerobic pathways for degradation of RDX as a potential treatment scheme. Biomarker assays that target catabolic genes or microorganisms specific to each of the anaerobic RDX biodegradation pathways could potentially prescribe different schemes to promote either the reductive nitroso route or the ring-opening, mono-denitration route under anaerobic conditions. During treatment, the same biomarker assays could be used to evaluate and optimize the process based on quantitative changes in gene copy number. The environmental and genetic regulators that affect the anaerobic microbial processes were not discerned in this study and so catabolic gene biomarkers for these processes were unable to be developed. Three projects funded by SERDP (ER-1378 "Groundwater Chemistry and Microbial Ecology Effects on Explosives Biodegradation", ER-1606 "Development of Biomarkers for Assessing In situ RDX Biodegradation Potential", and ER-1607 "New Approaches to Evaluate the Biological Degradation of RDX in Groundwater") have expanded knowledge of the types of microorganisms that have the potential to degrade RDX, so that phylogenetic biomarkers for anaerobic RDX-degrading bacteria may be possible in the near future.

The *xplA* gene biomarker examined in this project is highly specific for the aerobic biodegradation pathway of RDX. The biomarker is found within a small group of bacteria belonging to the order *Actinomycetales*. These bacteria and their genetic marker have been found world-wide in aerobic surface soils and aerobic groundwater. This is significant to the application of the biomarker in prescribing an aerobic treatment scheme for shallow aerobic groundwater, surface waters, and soils. Compared to anaerobic treatment schemes, aerobic stimulation of RDX biodegradation is expected to require a smaller mass of electron donor, be less expensive, and not generate undesirable end-products, such as methane, sulfides, and nitroso-RDX metabolites.

The fundamental information gained in this study suggests that XplA-mediated aerobic denitration of RDX may be subjected to inhibitory effects in response to nitrogen availability. This has implications for the role of *xplA* as a biomarker of RDX degradation, as it will also be necessary for bioremediation site managers to measure soil and groundwater concentrations for ammonium and nitrate. Ammonium concentrations in excess of 125 mg/L and nitrate concentrations in excess of 250 mg/L inhibited the rate of RDX degradation for strain KTR9. At these inorganic nitrogen concentrations, the extent of RDX degradation after 68 h was inhibited by approximately 60% and 15%, respectively. Concentrations between 100 and 1000 mg/L of ammonium and nitrate have been reported to inhibit RDX degradation for other aerobic RDX-degrading *Rhodococcus* species (Bernstein et al. 2011, Coleman et al. 1998, Nejidat et al. 2008). It was not the goal of this project to determine the relationship between RDX degradation rates and inorganic nitrogen concentrations in soils and groundwater. As such, the above concentrations can only be used as estimates of ammonium or nitrate inhibition of aerobic RDX biodegradation in the field. Additional research is required to determine reliable guidelines to inform site managers of specific field concentrations of ammonium and nitrate that will increase RDX treatment times. Also, techniques to effectively lower the inorganic nitrogen concentrations to non-inhibitory levels for the aerobic RDX biodegradation pathway will need to be determined.

2 Project Background

The production of explosives and military training activities have resulted in explosives contamination of soils at military facilities around the world. The extent of this contamination is not well known outside of North America because only a limited number of site characterizations have been completed (Spain 2000, Wingfors et al. 2006). In the United States, approximately 15 million acres of military lands contain detectable levels of explosive compounds. The concentrations of 2,4,6-trinitrotoluene (TNT), TNT transformation products, hexahydro-1,3,5-trinitro-1,3,5-triazine (RDX), and octahydro-1,3,5,7-tetranitro-1,3,5,7-tetrazocine (HMX) in soils are generally low (<1 to around 50 µg/kg) except near low-order detonations, tank targets, and firing points where concentrations can be quite high (1,000 to >100,000 µg/kg) (Hewitt 2002; Jenkins et al. 1998, 2001; Pennington et al. 2001, 2005;Walsh et al. 2001). The ecotoxicology of TNT and RDX is well established (Sunahara et al. 2009); thus, contamination by explosives must be managed to reduce risks to human and ecological receptors.

Once present in soil, dissolution, transformation, and adsorption will primarily affect the fate and transport of the explosive compounds. Trinitrotoluene and its transformation products do not migrate quickly to or within groundwater due to their sorption capacity to soil and aquifer constituents. However, RDX and HMX are less reactive than TNT and they migrate easily through soil (Lynch et al. 2002, Martel et al. 2009, Sheremata et al. 2001). In groundwater, RDX and HMX have the potential to be transported with very little retardation due to their limited sorption to aquifer sediments (Clausen et al. 2004). However, knowledge of the extent of explosive contamination in groundwater is limited to a small number of training ranges. Groundwater beneath Demolition Area 1 at Camp Edwards, Massachusetts was found to contain RDX at concentrations as high as 370 µg/L, while most samples contained RDX at concentrations between 100-150 µg/L (Clausen et al. 2004). A consequence of the mobility of RDX is that the plume has migrated offsite where it has contaminated at least one private well. A similar characterization of Garrison Valcartier, Canada indicated that the groundwater beneath an anti-tank range was contaminated with low levels of TNT and RDX, as well as HMX at concentrations up to 180 µg/L (Martel et al. 2009).

In comparison, wastewater from manufacturing and load and pack facilities was often discharged to unlined lagoons and ditches. Thus, soils and groundwater at these facilities generally have higher concentrations of explosives. Recent investigations of groundwater at several of these facilities measured RDX concentrations between 25 µg/L and 17,000 µg/L (Table 1). At the Iowa Army Ammunition Plant near Burlington, Iowa, an RDX groundwater plume has migrated offsite where it has contaminated agricultural and drinking water wells (Tetra Tech 2010). In addition, groundwater at these sites was also found to contain TNT and its transformation products and sometimes HMX.

Table 1. Groundwater RDX concentrations at U.S. manufacturing and load and pack facilities.

Site	RDX Concentration (µg/L)	Reference
Nebraska Ordnance Plant, NE	400 – 500 Large plume	Wani et al. 2002
Cornhusker Army Ammunition Plant, NE	35 Hot spots = 2000	Wani et al. 2002
Louisiana Army Ammunition Plant, LA	20 – 17,000	Wani et al. 2002
Ft. Meade, MD	80 – 100	Wani et al. 2002
Pueblo Army Depot, CO	220; Hot spots = 10,000 0.3 – 21.8	Wani et al. 2002 Paquet et al. 2011
Iowa Army Ammunition Plant, IA		
Line 800	370 – 12,500	Beller and Tiemeier 2002
Offsite plume	2 – 120	Tetra Tech 2010
Umatilla Chemical Depot, OR Explosives washout lagoon	2 – 300	Michalsen 2011[1]
Picatinny Arsenal, NJ Former melt-pour facility	BD – 86	Fuller et al. 2010; Paquet et al. 2011
Virginia	18 – 99	Paquet et al. 2011
Texas	177 – 708	Paquet et al. 2011

BD: below detection limit of 0.2 µg/L

These examples illustrate the importance of managing contamination by mobile explosives, such as RDX and HMX, in order to sustain training ranges and ordnance production and storage facilities for future military obligations. Biotransformation of RDX occurs in a variety of environments from surface and subsurface soils (Coleman et al. 1998, Crocker et al.

[1] Personal Communication. 2011. M. Michalsen, Environmental Engineer, U.S. Army Engineer District, Seattle.

2005, Oh et al. 2001, Ringelberg et al. 2003, Seth-Smith et al. 2002), aquifers (Beller and Tiemeier 2002;Bernstein et al. 2011;Bradley and Dinicola 2005;Davis et al. 2004;Nejidat et al. 2008;Waisner et al. 2002), sewage sludges (Hawari et al. 2000), and cold marine sediments (Zhao et al. 2010). These environments indicate that RDX biotransformation is possible under a wide variety of electron donor and acceptor conditions and thus illustrate the difficulty in understanding the biogeochemistry of RDX-degrading bacteria. *In situ* bioremediation is an attractive remedial action for sites contaminated by explosives, but it is not widely accepted due to a lack of understanding about the biogeochemistry of nitramine-degrading bacteria (Fuller et al. 2010, Halasz and Hawari 2011).

The degradation of RDX is governed by both abiotic and biotic reactions (Bhushan et al. 2003, Fournier et al. 2002; Halasz et al. 2002; Halasz and Hawari 2011; Zhao et al. 2003). The pathways of RDX degradation include (1) sequential reduction ($2e^-/H^+$) of the $N\text{-}NO_2$ groups to the corresponding nitroso (-N-NO) derivatives: hexahydro-1-nitroso-3,5-dinitro-1,3,5-triazine (MNX), hexahydro-1,3-dinitroso-5-nitro-1,3,5-triazine (DNX), and hexahydro-1,3,5-trinitroso-1,3,5-triazine (TNX) (Figure 2B) and (2) cleavage of the $N\text{-}NO_2$ bond(s) (denitration) followed by spontaneous ring cleavage to give the key RDX intermediate(s) 4-nitro-2,4-diazabutanal (NDAB; Figure 2A) or methylenedinitramine (MEDINA; Figure 2B). Additional ring cleavage end products include nitrite, nitrous oxide, ammonium, formaldehyde, formic acid, and carbon dioxide. Whether MEDINA or NDAB is formed depends on how many nitro groups are lost prior to ring cleavage. When one nitro group is lost, MEDINA is formed (Figure 2B), while the loss of two nitro groups produces NDAB (Figure 2A).

Abiotic reducing conditions with zero-valent iron (Comfort et al. 2003, Shrout et al. 2005), iron and manganese oxides (Gregory et al. 2004, Szecsody et al. 2004), electron shuttles and humics (Bhushan et al. 2006, Kwon and Finneran 2006, 2008a, 2010) generally produce the nitroso derivatives as the major end products with denitration to MEDINA as a minor route. Aerobic and anaerobic metabolism by bacteria, fungi, and enzymes proceeds by either the nitroso or denitration pathways to varying extents (Crocker et al. 2006, Halasz and Hawari 2011). The nitroso pathway is a minor RDX degradation route in *Klebsiella pneumoniae* strain SCZ-1, *Clostridium bifermentans* strain HAW-1, *Shewanella halifaxensis* strain HAW-EB4 and *Shewanella* sp. HAW-EB5 (Zhao et al. 2002, 2003, 2004, 2006) while in *Methylobacterium* spp., enterobacteria, and *Shewanella* sp.

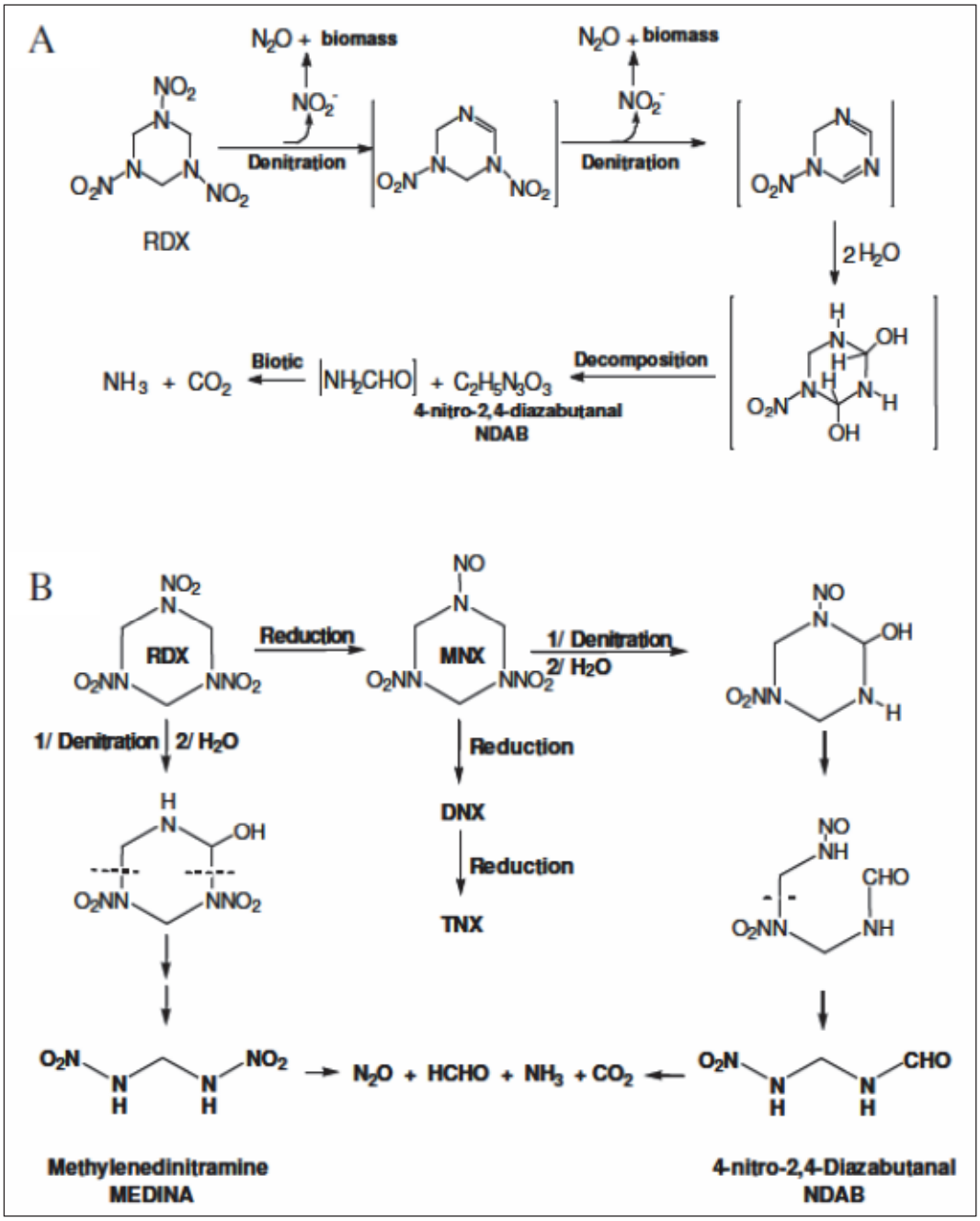

Figure 2. Degradation mechanisms for RDX under aerobic conditions (A), and anaerobic conditions (B). Mechanisms shown include aerobic denitration (A), anaerobic denitration (B), and reduction (B). Figure adapted from Bhushan et al. (2003), Fournier et al. (2002), Halasz et al. (2002), Zhao et al. (2003).

HAW-EB2 it is the major route of degradation (Fournier et al. 2005, Kitts et al. 1994, Van Aken et al. 2004; Zhao et al. 2004). Denitration of RDX via NDAB occurs by alkaline hydrolysis (Balakrishnan et al. 2003), photolysis (Hawari et al. 2002), and a select group of aerobic actinomycete bacteria (Andeer et al. 2009; Bernstein et al. 2011; Coleman et al. 1998; Nejidat et al.

2008; Ronen et al. 2008; Seth-Smith et al. 2002, 2008; Thompson et al. 2005). Among intermediates and end products detected in groundwater and soil, only the nitroso derivatives have been routinely sampled for and detected. Methylenedinitramine is not expected to be detected in field samples since it decomposes rapidly at ambient conditions in water. The extent of NDAB in groundwater and soils is currently unknown, since this compound has only recently been identified as an end-product of RDX degradation. Some preliminary research has detected NDAB in groundwater at the Iowa Army Ammunition Plant (Hawari, unpublished) and soil from an ammunition plant in Valleyfield, Quebec, Canada (Fournier et al. 2004).

In most bacteria, the ability to degrade RDX via the nitroso derivatives is co-metabolic, since the nitramine ring is preserved. This pathway is commonly observed under anaerobic conditions in groundwater following biostimulation with electron donors (Beller 2002; Davis et al. 2004; Ronen et al. 2008; TetraTech, Inc. 2010). The sequential reduction of RDX is hypothesized to occur by oxygen-insensitive nitroreductase enzymes that are present in both aerobic and anaerobic bacteria. However, only the NsfI enzyme from *Enterobacter cloacae* strain 96-3 (Bryant et al. 1991) has been shown to catalyze the two-electron reduction of RDX (Kitts et al. 2000).

Mono-denitration appears to be mainly an anaerobic process by anaerobic bacteria (Crocker et al. 2006) and by anaerobic incubation of several enzymes, including cytochrome P450 (XplA; (Rylott et al. 2006)), diaphorase (Bhushan et al. 2002a), and nitrate reductase (Bhushan et al. 2002b). Methylenedinitramine is unstable in water and decomposes to nitrous oxide and formaldehyde (Halasz et al. 2002). In comparison, NDAB is stable in water, is generally produced under aerobic conditions, and accumulates in culture supernatants of aerobic RDX-degrading bacteria (Fournier et al. 2002, 2004; Thompson et al. 2005). In the latter case, these bacteria do not degrade NDAB, but NDAB can be degraded by a *Methylobacterium* species and *Phanerochaete chyrsosoporium* (Fournier et al. 2004, 2005). The actual mechanism leading to the cleavage of the $N\text{-}NO_2$ bond(s) of RDX is not fully understood. It is possible that the reduction of RDX by a single electron produces a radical anion ($RDX^{\cdot-}$) followed by denitration and ring cleavage. Alternately, denitration could be caused by proton or hydrogen abstraction from the methylene (C-H) group in RDX (Halasz and Hawari 2011).

Aerobic actinomycete bacteria of the genera *Rhodococcus* (Bernstein et al. 2011; Coleman et al. 1998; Nejidat et al. 2008; Ronen et al. 2008; Seth-Smith et al. 2002, 2008), *Gordonia* (Thompson et al. 2005), *Williamsia* (Thompson et al. 2005), and *Microbacterium* (Andeer et al. 2009) degrade RDX by denitration to NDAB, nitrite, ammonia, formaldehyde, and carbon dioxide. All of these bacteria utilize the nitrite as a source of nitrogen for growth, while the *Gordonia* and *Williamsia* strains can use the RDX as both a carbon and nitrogen source for growth (Thompson et al. 2005). Interestingly, all of the aerobic RDX-degrading bacteria isolated to date from geographically distant soils and groundwater use a highly conserved enzyme system, XplAB, for the denitration of RDX (Andeer et al. 2009; Indest et al. 2010; Nejidat et al. 2008; Seth-Smith et al. 2008). The *xplA* and *xplB* genes encode a cytochrome P450 system composed of the fused flavodoxin-cytochrome P450 enzyme, XplA, and a flavodoxin reductase, XplB (Rylott et al. 2006; Seth-Smith et al. 2002). Characterization of this enzyme has shown it to be an oxygen-sensitive enzyme that catalyzes the di-denitration of RDX under aerobic conditions (Fournier et al. 2002; Rylott et al. 2006). Under anaerobic conditions this enzyme system primarily catalyzed the mono-denitration of RDX to MEDINA (Jackson et al. 2007). The global distribution and highly conserved nature of the *xplAB* genes suggested that these genes represented excellent candidates for the development of a real-time quantitative PCR (RTqPCR) assay for RDX biodegradation.

Shewanella strains have been isolated for their ability to degrade RDX in marine sediment (Zhao et al. 2005, 2006). *S. halifaxensis* was shown to degrade RDX anaerobically, under trimethylamine *N*-oxide (TMAO)-respiring condition, via a major route consisting of the sequential reduction of the $N\text{-}NO_2$ groups to produce the corresponding mono-, di-, and trinitroso derivatives MNX, DNX, and TNX, respectively, and a minor route involving denitration followed by ring cleavage to produce MEDINA and its decomposition products HCHO and N_2O (Halasz et al. 2002). A cytochrome C_{552} purified from *S. halifaxensis* was reported to degrade RDX anaerobically via initial denitration followed by ring cleavage to produce MEDINA (Zhao et al. 2008).

By analyzing the genomes of 15 *Shewanella* strains, Zhao et al. (2010) observed that the RDX-degrading strains had a higher number of genes for cytochromes and nitrate/nitrite reductases. Despite progress made towards understanding the anaerobic degradation routes of RDX, the genetic

determinants dictating the fate of RDX under anaerobic conditions are still unclear. *Shewanella oneidensis* MR-1, a freshwater sediment strain (Myers and Nealson 1988), can utilize numerous electron acceptors for anaerobic respiration including Fe(III), Mn(IV), fumarate, nitrate, TMAO, and a variety of metals (Nealson and Saffarini 1994). It was recently proposed that MR-1 can also use RDX as an electron acceptor (Kwon and Finneran 2008a).

Culture-independent techniques that assay biomarkers (proteins, nucleic acids, and lipids) can reveal the presence and/or abundance of microorganisms or metabolic activities directly from field-collected samples. These tools can therefore be used to assess whether natural attenuation or enhanced bioremediation are appropriate treatment options for contaminated soils and groundwater. In developing such tools, it is preferable to focus on functional genes associated with contaminant degradation (*e.g.*, genes encoding RDX-degrading enzymes) and to correlate the gene copy number with the levels of contaminant and the rate of degradation of the contaminant. Quantitative polymerase chain reaction (qPCR) is a method that can be used to quantify the number of gene copies in the original sample even if they are present in low abundance. Several studies have developed qPCR methods for functional genes and correlated the gene expression with field contaminant concentrations and degradative activity in microcosms (Beller et al. 2002, Hosada et al. 2005, Indest et al. 2007, Nyyssonen et al. 2006, Powell et al. 2006, Ritalahti et al. 2010). Commercially available qPCR assays that target the 16S rRNA gene of *Dehalococcoides* species and several reductive dehalogenase genes are currently in use to assess biostimulation or bioaugmentation of chlorinated solvent contaminated groundwater (Ritalahti et al. 2010). That only a few genes are currently known to be involved in RDX degradation pathways (Bryant et al. 1991, Fuller et al. 2009, Seth-Smith et al. 2002) presents a significant challenge to the development of biomarkers that can provide supporting evidence of *in situ* RDX bioremediation.

3 *Gordonia* sp. KTR9 Genome Annotation and Regulation of RDX Biodegradation

Introduction

Members of the genus *Gordonia* metabolize a variety of aliphatic, aromatic, and halogenated hydrocarbons, benzothiophenes, polyisoprenes, and heterocyclic compounds (Arenskotter et al. 2004, Bröker et al. 2004, Lee et al. 2001, Thompson et al. 2005). They are also able to produce novel bioactive compounds, such as gordonan, substituted imidazoles (cyclic N-C-N rings), biosurfactants, carotenoids, and L-lysine and its analogues (Arenskotter et al. 2004). It appears that many genes and enzymes within *Gordonia* species are potentially unique, since some species degrade xenobiotic compounds by rare or novel pathways (Lee et al. 2001, Linos et al. 2000, Mulbry 1994). Thus, while the environmental and biotechnological importance of biochemical processes mediated by this genus is becoming increasing clear, much of the biochemistry, enzymology, proteomics, and genetics of this genus remain ill-defined. Lack of this basic information for the genus *Gordonia* inhibits applied biotechnological development. *Gordonia* species belong to Actinomycetales, an order of Gram-positive bacteria that live in a broad range of environments including soil and water. This order includes some of the most important organisms known to mankind, including streptomycetes, which produce 55% of the antibiotics in use today (Strohl 1997), and *Mycobacterium tuberculosis*, responsible for the largest number of human deaths by bacterial infection (Karlson et al. 1993). Among the better characterized actinomycetes, *Gordonia* is most similar to *Rhodococcus* (Gurtler et al. 2004), an important industrial genus not used for antibiotic production (Larkin et al. 2005; van der Geize and Dijhuizen 2004). These genera share many fundamental physiological and ecological characteristics, such that many of the genetic tools developed for *Rhodococcus* are likely to function in *Gordonia*.

Gordonia sp. KTR9 genome assembly, annotation, and functional characterization of pGKT2

Gordonia sp. KTR9 is able to grow on RDX as a sole nitrogen source (Thompson et al. 2005), similar to *Rhodococcus rhodochrous* 11Y (Seth-Smith et al. 2002) and *Rhodococcus* sp. DN22 (Coleman et al. 1998; Fournier et al. 2002), and produces RDX degradation products consistent

with the involvement of a cytochrome P450 (Fournier et al. 2002). At the time this project was conceived, there was a lack of information regarding the genetic, regulatory, and enzymatic basis of RDX biotransformation. The genome of *Gordonia* sp. KTR9 was sequenced and annotated in order to characterize the ability of strain KTR9 to use RDX as a nitrogen source for growth. The objectives of annotating the genome of KTR9 were:

1. To identify genes surrounding the cytochrome P450 gene (*xplA*) in KTR9
2. To identify novel genes related to RDX degradation
3. To develop an *in silico* peptide database with which to compare the proteomes of RDX- and nitrite-grown KTR9 cultures
4. To develop a gene microarray for future physiological and genetic studies with KTR9

In addition, functional annotation of *xplA* and surrounding genes was established by heterologous gene expression, conjugal gene transfer, gene deletion, and physiological experiments.

Methods

KTR9 sequencing and genome assembly

Genomic DNA was isolated from stationary phase cultures of *Gordonia* sp. KTR9 grown in LBP (1% Bacto-peptone, 0.5% yeast extract, 1% NaCl). Approximately 5 µg of genomic DNA was extracted from washed cell pellets using the Qiagen DNeasy extraction kit. Sequencing of the genome was performed by 454 Life Science Corp., Branford, CT using the Genome Sequencer FLX™ System. This system, which uses the high throughput pyrosequencing procedure, generated a total of 816,115 sequence reads with an average length of 256 nucleotides.

These reads were assembled into contigs by the Genome Science Centre (Vancouver, B.C.) using Phrap (http://www.phrap.org/), a DNA sequence assembler and finishing tool (Phil Green Lab, Univ. of Washington Genome Center). In addition, a library of 1581 fosmid clones (EpiFOS™, Epicentre Biotechnologies) was constructed, fingerprint-mapped, and end-sequenced to assemble the contigs into scaffolds. Genomic DNA was purified from *Gordonia sp*. KTR9 by phenol/chloroform extraction methods as described by Saito and Miura (1963). Sequence analysis revealed that only 40% of the clones yielded high quality sequence from both ends. The fosmid end reads were aligned to the Newbler assembly contigs from 454 Life Science Corp

using BLAST. These alignment data were integrated with the physical map to assist with ordering and orienting the sequence contigs. The end reads and 454 Newbler assembly contigs were assembled using Phrap. Analysis and manual editing of the Phrap assembly and integration with the physical map yielded sequence scaffolds.

To improve the assembly, 38 fosmid clones were pooled and pyrosequenced using 454 technology (Genome Quebec, McGill University). Of these 38 fosmid clones, 16 spanned six large gaps within the scaffolds of the initial assembly (and that were located at the end of each scaffold), 16 were located at the end of unscaffolded contigs, and 6 crossed the gaps within scaffolds. Pyrosequencing of these 38 fosmids yielded 105 contigs of up to 43 kilobases (kb). These data reduced the number of scaffolds in the assembly to four and closed two of the gaps within scaffolds. The four scaffolds of the KTR9 assembly were then ordered using the genome of *Gordonia bronchialis* DSM 43247 as a reference and Mauve, a genome alignment software (Genome Evolution Laboratory, University of Wisconsin), designed for constructing alignments of multiple rearranged genomes. The last gaps within scaffolds were bridged by using a LongAmp™ PCR kit from New England Biolabs, Inc (Ipswitch, MA) using KTR9 chromosomal DNA as a template.

KTR9 genome annotation

The sequence of KTR9 scaffolds and unscaffold contigs was automatically annotated using a specialized software (FGENESB, Softberry Inc., Mount Kisco, NY, USA) and the RAST server (http://rast.nmpdr.org). FGENESB is a suite of operon and gene-finding programs for automatic annotation of bacterial genomes. The FGENESB gene prediction algorithm is based on Markov chain models of coding regions and translation and termination sites. (http://linux1.softberry.com/berry.phtml?topic=fgenesb&group=help&subgroup=gfindb). The genes that were identified were compared to databases of protein sequences using the NCBI nr database (http://blast.ncbi.nlm.nih.gov/Blast.cgi). Subsequently, the genes were subjected to a second round of automated annotation and the results were then manually verified.

Metabolic pathways of KTR9 were reconstructed using the annotated KTR9 genome and Pathway Tools (http://bioinformatics.ai.sri.com/ptools/). In this automated process, 901 “holes” in predicted metabolic pathways were identified. These holes represent reactions within a pathway that have no corresponding enzyme identified in the genome. Some of these holes were

filled using the Pathway Hole Filler/blastp program, which finds genes whose products are predicted to catalyze a missing reaction, by checking the major *de novo* biosynthetic pathways manually and, by using tblastn program to search the genome again. Any genes that were found using this approach were added to the annotation and overlapping genes were deleted. Once pathway holes were filled, the resulting annotated KTR9 genome was compared with the genomes of other *Actinobacteria*. The Clusters of Orthologous Groups (COG), Kyoto Encyclopedia of Genes and Genomes (KEGG), and RefSeq databases were searched for homologs using BLASTP and an e-value cutoff of 1x e^{-6}. The best result for each BLAST search was imported as the gene annotation. The automatic annotation results were then manually checked and adjusted as necessary. The COG analysis was used to cluster the annotated gene distribution into functional categories.

Use of transcriptomic data to validate sequence and annotation

The genome sequence and annotation was further refined using the deep-sequencing transcriptomic data (see below). The raw sequence data from the transcriptome were first aligned to the genome using the CLC Genomics Workbench software tool (http://www.clcbio.com/). Genome sequence files and annotation files were created using Artemis (Sanger Institute, Cambridge, U.K.), a genome browser and annotation tool that allows visualization of sequence features, next generation data and the results of analyses within the context of the sequence. These files were then sorted and indexed using Integrated Genomics Viewer (http://www.broadinstitute.org/igv/), which supports various data types including sequence alignments, microarrays, and genomic annotations in large datasets.

Functional expression of xplA in heterologous hosts

A 1668 bp fragment representing the KTR9 *xplA* putative coding region was synthesized (Celtek Biosciences, Nashville, TN) in expression vector pET-11a (New England Biolabs, Beverly, MA). The resulting plasmid, pEMTxplA, was cut with the restriction enzymes, *NdeI* and *HindIII,* liberating a 1953 bp DNA fragment containing the *xplA* gene. The resulting fragment was gel-purified and ligated with a NdeI/HindIII restricted pTip vector TypeII, an *E. coli-Rhodococcus* shuttle vector for heterologous protein production in *Rhodococcus* (Nakashima and Tamura 2004). The ligation mixture was used to transform *E. coli* DH5α. The plasmid that carries the *xplA* gene in the correct orientation was then used to transform *R. jostii* RHA1 by

electroporation. The empty pTip vector was also introduced by electroporation into RHA1 for use as a control. Precultures of both transformed strains were obtained by inoculating single colonies into 2 mL of PTYG broth (Balkwill and Ghiorse 1985) with 25 μg mL^{-1} chloramphenicol and incubated overnight at 30°C. Precultures of each strain were used to inoculate triplicate flasks of 40 mL PTYG with 25 μg mL^{-1} chloramphenicol at a 1% inoculum level. Cultures were induced at OD 0.5 by addition of thiostrepton dissolved in DMSO to a final concentration of 50 μg mL^{-1}. The cells were allowed to grow overnight, washed, resuspended, and concentrated two-fold in 0.1 M sodium phosphate, pH 7.0 with 60 μg mL^{-1} RDX. Flasks were incubated at 30°C with shaking. Samples were taken periodically over 5 h and analyzed by HPLC.

Similarly, an 1197 bp fragment containing *cyp151C* was synthesized (Celtek Biosciences, Nashville, TN) in expression vector pET-11a (New England Biolabs, Beverly, MA). The resulting plasmid construct, pEMTCyp151C, along with pEMTxplA were transformed into *E. coli* BL21 gold (DE3) competent cells (Stratagene, LaJolla, CA) and transformants were selected on LB plates with ampicillin (100 μg mL^{-1}). Overnight cultures of each recombinant *E. coli* strain were diluted 1/20 in LB supplemented with RDX (40 μg mL^{-1}), incubated at 37°C for 2 h, and induced with the addition of 1 mM IPTG. Final concentrations of RDX were determined after 18 h of incubation at 37°C. *E. coli* culture samples derived from each recombinant plasmid were mixed with an equal volume of Laemmli sample buffer (Maniatis et al. 1982) containing 5% β-mercaptoethanol and heated to 95°C for 5 min. Denatured samples along with a low range unstained protein standard (BioRad, Hercules, CA) were loaded on a 12.5% Tris-Cl polyacrylamide gel and proteins were separated by electrophoresis in 1×TGS buffer (25 mM Tris, 192 mM glycine, 0.1% w/v SDS, pH 8.3). Proteins were visualized with Biosafe Coomassie G250 stain (BioRad, Hercules, CA) according to the manufacturer's instructions.

Curing of pGKT2 in strain KTR9

Gene deletion constructs of *xplA* and *xplR* were synthesized (Celtek Biosciences) with 1.5 kb flanking sequences to create a 3 kb insert in the pCR2.1 vector (Invitrogen, Carlsbad, CA). Gene deletion inserts were liberated from the pCR2.1 vector via BamHI restriction enzyme digestion, gel purified with a Wizard SV Gel and PCR Clean-up System Kit (Promega, Madison, WI), and subcloned into the BamHI site of the mobilizable plasmid pK18*mobsacB* (Schafer et al. 1994). The resulting mutagenic

plasmids, pKTR9xplA and pKTR9xplR, were used for gene deletion analysis in *Gordonia* sp. KTR9 based on a conjugation strategy (van der Geize et al. 2001) using a *sacB* counter-selectable marker, with the exceptions of using kanamycin and nalidixic acid at 50 μg mL^{-1}. Transconjugants were replica plated onto the same media with and without 10% sucrose. Sucrose sensitive colonies were propagated overnight at 30°C in 25 mL of LBP medium and then spread plated onto LBP plates supplemented with 10% sucrose. Sucrose resistant colonies were checked for kanamycin sensitivity, and screened for the presence of the deleted gene by PCR amplification using the primers targeting the pGKT2 plasmid as described in Indest et al. (2010).

The ability of the KTR9 wild type and the two mutant strains to degrade RDX was evaluated as follows. KTR9 strains were pre-grown in MSM with 5 mM sodium succinate, 10 mM glycerol, 5 mM glucose, and 4 mM $(NH_4)_2SO_4$ until the stationary phase. The cultures were washed twice with MSM and then inoculated into LBP or MSM plus the three carbon sources media at an initial OD_{600} of 0.02. Both media were supplemented with 180 μM RDX. All cultures were grown at 30°C with shaking at 150 rpm and the growth (OD_{600}) and RDX concentrations determined throughout the incubation period.

The curing of plasmid pGKT2 was also confirmed by pulsed-field gel electrophoresis (PFGE) and Southern hybridization. The BioRad Chef DRII system (Bio-Rad, Hercules, CA) was employed for PFGE. Cultures of *Gordonia* sp. KTR9 and mutant strains, *Gordonia* sp. KTR9/pGKT2-1Δ and *Gordonia* sp. KTR9/pGKT2-2Δ, were grown in LBP and harvested from the late exponential phase. Cell plugs were prepared from approximately 1×10^8 cells per plug in accordance with the manufacturer's instructions, with the addition of 180 U mutanolysin (Sigma Aldrich, Saint Louis, MO) to increase cell lysis. Electrophoresis parameters consisted of 0.5×TBE at 5.5 V cm^{-1} with a switch time of 40-90 s at a 120° angle for 21 hr at a constant temperature of 14°C. The Lambda ladder marker (BioRad) was used as a size standard.

A 683 bp probe specific to pGKT2 was generated by PCR amplification with primers KTR9plas120505aF: 5'-cgaagggcttctcacttcac-3'; and KTR9plas121248aR: 5'- gacgagacctccttgcagac-3'. Amplification conditions consisted of a single step at 95°C for 5 min followed by 30 cycles at 94°C for 30 s, 63°C for 40 s, and 72°C for 40 s. The resulting PCR amplicon was gel purified and subsequently labeled by random primer extension

reaction with the NEBlot Phototope Kit (New England Biolabs, Ipswitch, MA) following the manufacturer's instructions. The DNA from the PFGE was transferred to a Nytran SuPerCharge nylon membrane using the alkaline transfer method and apparatus from the TurboBlotter Kit (Whatman). Hybridization was performed using the Phototope Star Detection Kit (New England Biolabs). The resultant blot was exposed to Lumi-Film Chemiluminescent Detection Film (Roche).

Results and Discussion

KTR9 genome assembly

The automatic annotation of scaffolds and unscaffolded contigs, manual editing of the Phrap assembly, and integration with the physical map yielded 10 sequence scaffolds: nine covering the chromosome (scaffolds 1-9) and one covering a circular plasmid (scaffold 10). The ten scaffolds included 43 gaps, of which six exceeded 10 kb. The 37 smaller gaps were bridged using PCR or direct sequencing of fosmid templates. Pyrosequencing of 38 strategically chosen fosmids clones yielded sequence data that reduced the number of scaffolds to 4 (Scaffolds A to D in Figure 3) and closed two of the six gaps within scaffolds. Using the genome of *Gordonia bronchialis* DSM 43247 as a reference allowed the ordering of the four remaining scaffolds (Figure 3). The alignment of the colored segments between the KTR9 scaffolds and the *G. bronchialis* genome illustrates that the two genomes have multiple regions of DNA sequence homology as well as a similar structural arrangement of genes.

KTR9 genome annotation

Automated annotation identified 5,070 genes that were annotated using a very strict statistical significance threshold of $1 \times e^{-6}$, to minimize the possibility of error (Table 2). After the final manual assembly of the genome, a total of 5,072 genes were identified. The genome comprises a 5.4 Mb chromosome and three plasmids (pGKT1: 89 kb; pGKT2: 182 kb; and pGKT3: 172 kb). The overall guanosine plus cytosine nucleotide (G+C) content of KTR9 genome was 67.5%, which is consistent with the G+C content of the genus *Gordonia*. Finally, validation of the KTR9 genome sequence and annotation using the deep sequencing transcriptomic data yielded the following result: the chromosome comprises 4,741 genes, plasmid pGKT1 contains 93 genes, plasmid pGKT2 contains 178 genes, and plasmid pGKT3 contains 163 genes.

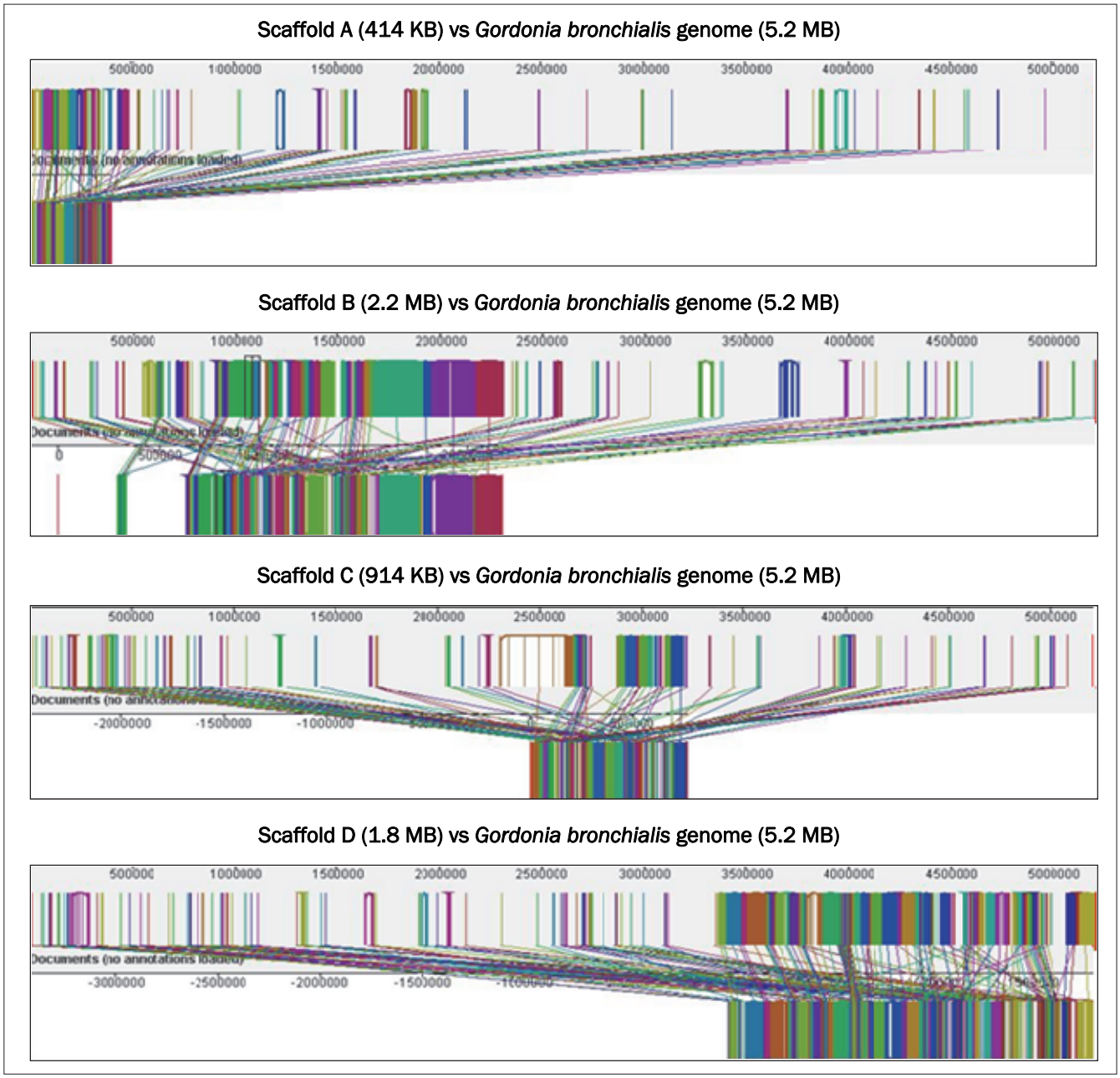

Figure 3. Alignment of assembled *Gordonia* sp. KTR9 (lower) scaffolds with the complete *Gordonia bronchialis* DSM 43247 (upper) genome. The homologous segments are shown as colored blocks that are connected between the KTR9 scaffolds and the *G. bronchialis* genome.

A total of 272 metabolic pathways were predicted using Pathway Tools. These pathways were classified into four main categories: 177 biosynthetic pathways, 118 degradation and assimilation pathways, 4 detoxification pathways, and 26 pathways involved in precursor metabolite production and/or energy generation. Some pathways belong to more than one category. These data suggest that strain KTR9, like other actinomycetes, has a diverse metabolic potential that could be exploited for additional environmental or biotechnological applications.

Table 2. Assembly of *Gordonia* sp. KTR9 genome using three consecutive methods.

Genome Element	Size (bp)	Number of Predicted Genes		
		Automatic Annotation	Manual Assembly	Validation Using Transcriptomic Data
Chromosome	5,441,391	4634	4695	4741
Plasmid GKT1	89,480	98	77	93
Plasmid GKT2	182,454	173	157	178
Plasmid GKT3	172,385	165	143	163
Total	5,885,710	5070	5072	5193

Protein encoding sequences in the *Gordonia* sp. KTR9 genome were compared to those of several related mycolic-acid containing actinomycetes: *G. bronchialis* DSM43247, *Rhodococcus jostii* RHA1, *Mycobacterium bovis* BCG, and *Corynebacterium glutamicum* ATCC 13032 (Figure 4). The dot-plots visualize the genomic positions of the orthologous segments identified between two different bacterial chromosomes. The gene arrangement order of G*ordonia* sp. KTR9 was most similar to that of *G. bronchialis* (Figure 4). The COG analysis of the annotated KTR9 genome showed that genes are distributed in 24 different functional categories. The category for lipid transport and metabolism includes 9.6% of the total number of genes (Figure 5). The COGs of proteins were ranked based on the number of genes in each cluster. The top cluster of COGs involved in lipid metabolism includes 45 Coenzyme F420-dependent N5,N10-methylene tetrahydromethanopterin reductase and related flavin-dependent oxidoreductases (Table 3).

A search of the assembled reads of the KTR9 genome for *xplA*-specific nucleotide sequences revealed the presence of an *xplA* homolog on pGKT2 that shares 97% to 99% amino acid sequence identity with characterized XplA cytochrome P450s (Andeer et al. 2009; Seth-Smith et al. 2002, 2008). The gene is the last in a cluster comprising *cyp151C*, a *glnAxplB* gene fusion, and *xplA* (Table 4). Approximately 1.5 kb upstream of this cluster is *xplR*, encoding a GntR-type transcriptional regulator. Cyp151C shares up to 71% amino acid sequence identity with the mycobacterial *pipA/morA*-encoded cytochrome P450s that are involved in the utilization of the secondary amines piperidine, pyrrolidine, and morpholine (Kim et al. 2006, Poupin et al. 1999, Sielaff and Andreesen 2005). The *glnAxplB* fusion is predicted to encode the first 85% of the residues of a glutamine synthetase fused to the entire XplB reductase. Polymerase chain reaction analysis of KTR9 DNA

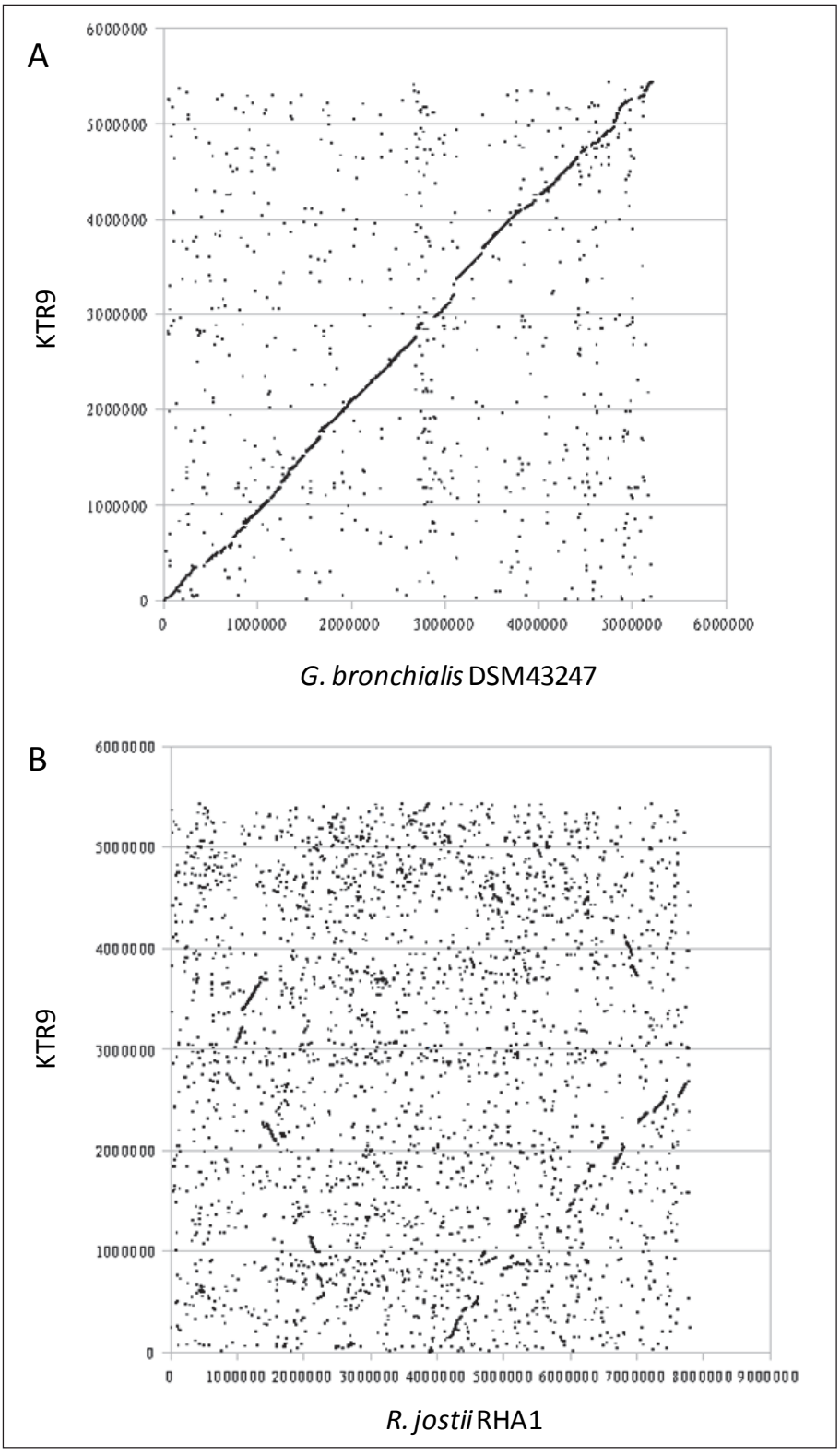

Figure 4. Comparative synteny analysis between the chromosome of *Gordonia* sp. KTR9 and those of *G. bronchialis* DSM 43247 (A), *R. jostii* RHA1 (B), *M. bovis* BCG (C) and *C. glutamicum* ATCC 13032 (D). Plasmids were not included in the comparison.

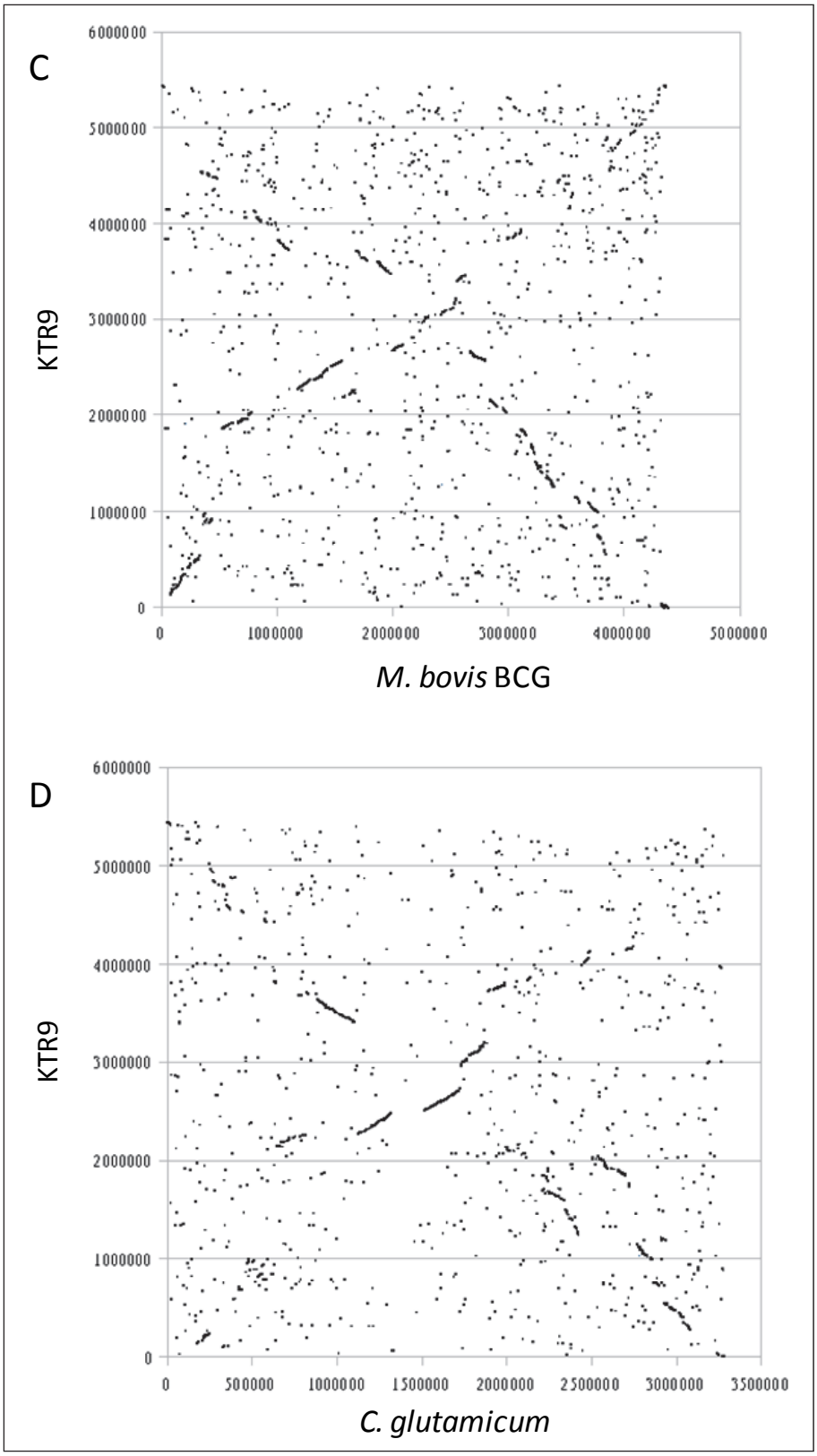

Figure 4. (continued).

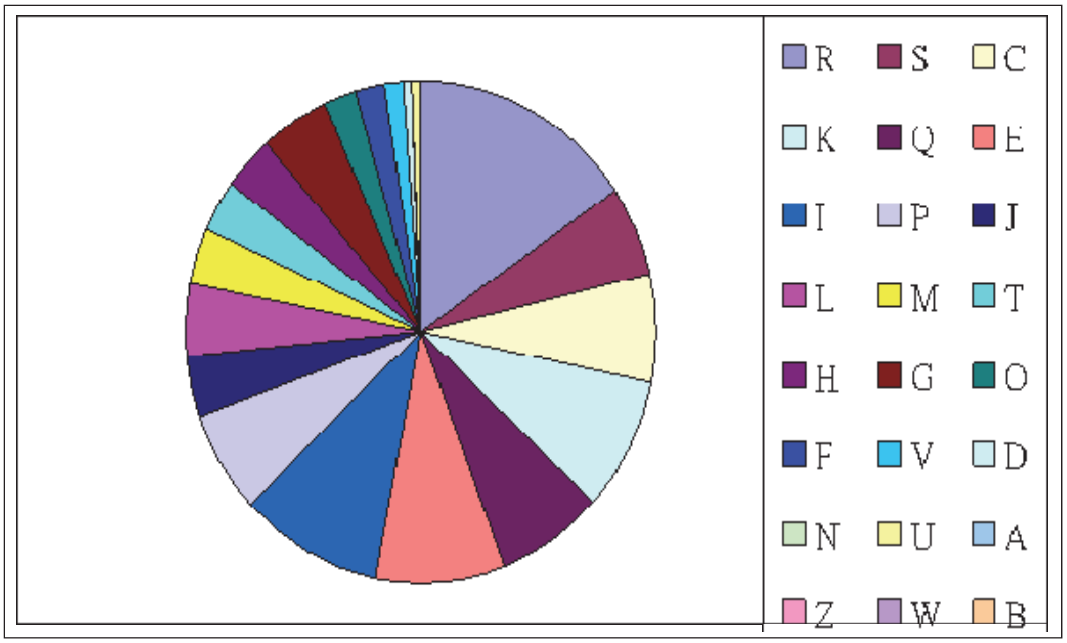

Figure 5. Annotated genes of *Gordonia* sp. KTR9 distributed into 24 functional categories. Legend: R: General function prediction only (15.5%); I: Lipid transport and metabolism (9.6%); E: Amino acid transport and metabolism (9.1%); K: Transcription (8.7%); C: Energy production and conversion (7.1)%; Q: Secondary metabolites biosynthesis: transport and catabolism (7.0)%; P: Inorganic ion transport and metabolism (6.6%); S: Function unknown (5.8%); L: Replication: recombination and repair (4.9%); G: Carbohydrate transport and metabolism (4.7%); J: Translation: ribosomal structure and biogenesis (4.0%); M: Cell wall/membrane/envelope biogenesis (3.6%); H: Coenzyme transport and metabolism (3.6%); T: Signal_transduction mechanisms (3.2%); O: Posttranslational modification: protein turnover: chaperones (2.2%); F: Nucleotide transport and metabolism (2.0%); V: Defense mechanisms (1.3%); D: Cell cycle control: cell division: chromosome partitioning (0.6%); U: Intracellular trafficking: secretion: and vesicular transport (0.5%); N: Cell motility (0%); B: Chromatin structure and dynamics (0%); A: RNA processing and modification (0%); Z: Cytoskeleton (0%); W: Extracellular structures (0%).

genomic template with primers that flank the gene fusion point confirmed that there is no gap between these genes (data not shown). Interestingly, the glutamine synthetase portion of the *glnAxplB* fusion and XplR share up to 70% and 49% sequence identity with the glutamine synthetases and GntR-type regulators, respectively, encoded by genes associated with the mycobacterial *cyp151*s (Kim et al. 2006, Poupin et al. 1999, Sielaff and Andreesen 2005).

Table 3. Ranking of clusters of orthologous groups in *Gordonia* sp. KTR9 (based on the number of genes in each cluster).

Rank	Gene Number	Clusters of Orthologous Groups of Proteins (COGs)
1	94	COG1028 short-chain alcohol dehydrogenases and related enzymes
2	88	COG1309 Transcriptional regulators
3	69	COG1960 Acyl-CoA dehydrogenases
4	57	COG0477 Permeases of the major facilitator superfamily
5	45	COG2141 Coenzyme F420-dependent N5,N10-methylene tetrahydromethanopterin reductase and related flavin-dependent oxidoreductases
6	44	COG0596 alpha/beta hydrolase superfamily, including related acyltransferases
7	40	COG0318 Acyl-CoA synthetases (AMP-forming)/AMP-acid ligases II
8	36	COG1024 Enoyl-CoA hydratase/carnithine racemase
9	32	COG1463 ABC-type transporters involved in resistance to organic solvents, periplasmic component
10	28	COG0183 Acetyl-CoA acetyltransferase
11	27	COG1012 NAD-dependent aldehyde dehydrogenases
12	20	COG0438 Glycosyltransferases
13	20	COG1020 Non-ribosomal peptide synthetase modules and related proteins
14	19	COG2072 Predicted flavoprotein involved in K+ transport
15	18	COG0515 Serine/threonine protein kinase

Overall, plasmid pGKT2 appears to be typical of those of *Gordonia* based on its G+C content (63 mol%), which is characteristic of DNA from several genera of *Corynebacterineae* (Arenskotter et al. 2004). Annotation of its nucleotide sequence initially identified 157 predicted ORFs (accession number CP002112). This number has since been updated to 178 based on the deep transcriptomic sequencing data (Table 2). A partial list of these ORFs is provided in Table 4 and discussed below. The functional classes of predicted genes on this plasmid are summarized in Table 5. The largest functional class comprises putative genes involved in replication (recombination and repair) including multiple transposase sequences, an integrase, two topoisomerases, and multiple helicases. Predicted genes involved in general functions encompass the second largest class (13.7%), with the majority categorized as ATPases, including a member of the AAA+ superfamily. Genes involved in biosynthesis of secondary metabolites (10.3%) and transcription (10.3%) constitute perhaps the most significant classes of plasmid genes with a subset of these involved in RDX degradation.

Table 4. Open reading frames (ORFs) with assigned functions from *Gordonia* sp. KTR9 plasmid pGKT2.

ORF[1]	Gene Name	Product Size[2]	Closest Characterized Homolog[3]	Sequence Identity[4]
KTR9_5080	*parA*		ParA, *Corynebacterium glutamicum* ATCC 13032 (BAB98814)	34%
KTR9_5085		635	Plasmid maintenance protein Orf8 of pKB-1 from *G. westfalica* Kb1 (NP_954749)	39%
KTR9_5225		679	Single-stranded DNA-specific exonuclease *C. glutamicum* ATCC 13032 (BAB99130)	43%
KTR9_5228	*xplR*	246	PipR,GntR-type transcriptional regulator *Mycobacterium smegmatis* MC2 155 (YP_890908)	49%
KTR9_5229	*cyp151c*	399	PipA, Cytochrome P450, family 151 *Mycobacterium smegmatis* MC2 155 (YP_890903)	71%
KTR9_5230	*glnA-xplB*	813	GlnA-XplB fusion protein, glutamine synthetase, flavodoxin reductase *Rhodococcus rhodochrous* (AAN27918)	99%
KTR9_5231	*xplA*	552	XplA, flavodoxin-cytochrome P450 *R. rhodochrous* (AAN27917)	99%
KTR9_5241		145	Prophage maintenance system killer protein *Nostoc* sp. PCC 7120 (NP_478676)	42%

[1]Numbered according to KTR9 genome.

[2]In number of amino acid residues.

[3]Gene product, organism (Accession number).

[4]Over length of KTR9 gene product.

Finally, IslandPick was used (Langille and Brinkman 2009) to search for regions within pGKT2 of probable horizontal origin. Such regions, known as genomic islands (GIs), are frequently associated with particular physiologic adaptations such as virulence, catabolism, or resistance to a toxic compound and can sometimes be identified based on abnormal sequence composition, such as G+C content and codon bias. The analysis revealed that pGKT2 contained no predicted GIs. Moreover, no insertion sequence (IS) elements were found using IS Finder (http://www-is.biotoul.fr/). However, the plasmid contains five genes predicted to encode transposases or integrases. Of these, the most proximal to *xplAB* is KTR9_4947, 15 kb away.

Table 5. COG functional classification of *Gordonia* sp. KTR9 plasmid pGKT2 ORFs.

Functional Classification	No. of Genes	%[1] of total genes on pGKT2
R. General function prediction only	4	13.7
Q. Secondary metabolites biosynthesis: transport and catabolism	3	10.3
K. Transcription	3	10.3
E. Amino acid transport and metabolism	1	3.4
J. Translation: ribosomal structure and biogenesis	1	3.4
L. Replication: recombination and repair	13	44.8
O. Posttranslational modification: protein turnover: chaperones	2	6.9
D. Cell cycle control: cell division: chromosome partitioning	1	3.4
U. Intracellular trafficking: secretion: and vesicular transport	1	3.4

[1]Percentages based on the manual annotation identification of a total of 157 genes on pGKT2.

Expression of xplA in heterologous hosts

The *xplA* gene was heterologously expressed in *Rhodococcus jostii* RHA1 using a pTip vector. Production of the *xplA*-encoded cytochrome P450 was verified using denaturing acrylamide gel analysis and visible absorption spectroscopy. More particularly, cells carrying pTipXplA but not pTip revealed the characteristic CO-dependent peak at 450 nm, indicating that XplA is both soluble and functional (data not shown). Moreover, RHA1::pXplA rapidly depleted RDX from culture medium within 2.5 h (Figure 6). In contrast, RHA1::pTip did not detectably deplete RDX in the culture media. This indicates that RHA1 efficiently takes up RDX and that the *xpl*A gene alone is sufficient to degrade RDX.

The *xplA* gene was also heterologously expressed in *E. coli* BL21 using the pET11a vector. Overnight cultures of the recombinant *E. coli* strain grown in LB + RDX (180 μM) that had been previously induced with the addition of 1 mM IPTG 18 h earlier showed significant reduction in RDX compared to control samples (Table 6). In contrast, *cyp151C* did not elicit degradation of RDX when expressed in *E. coli* (Table 6) despite the presence of a soluble, correctly folded cytochrome P450 as verified by denaturing gel analysis and visible absorption spectroscopy (data not shown).

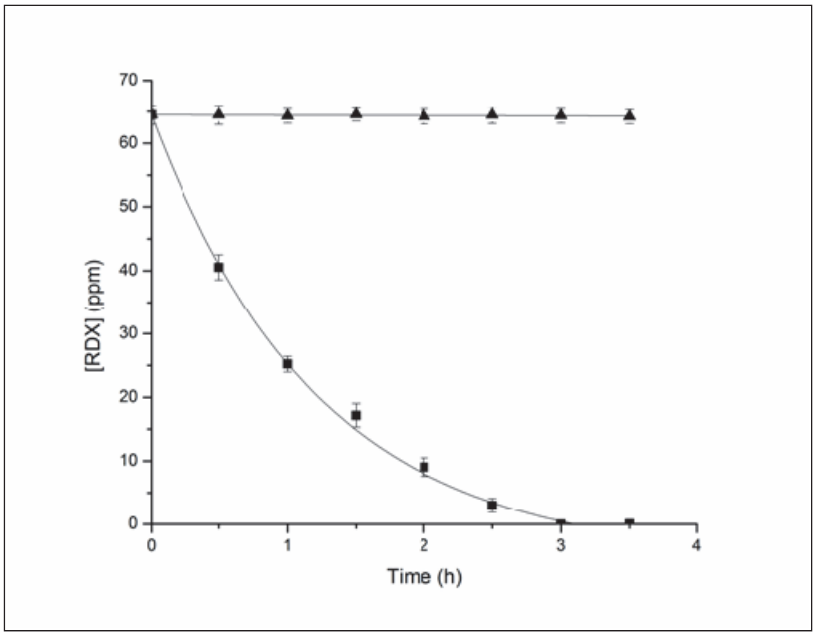

Figure 6. Degradation of RDX by *Rhodococcus jostii* RHA1 containing XplA. Exponentially growing cells containing pTipXplA (■) or an empty pTip vector (▲) were resuspended to an OD_{600} of 1.2 in 0.1 M sodium phosphate, pH 7.5 containing 60 ppm RDX. The fitted curve represents a first order decay with $t_{½}$ = 0.61± 0.05 h.

Table 6. Degradation of RDX by *E. coli* strains producing XplA and Cyp151C.

Strain	RDX Concentration (µg mL^{-1})[1]	
	Uninduced	Induced[2]
Control	42 ± 2	42 ± 2
XplA	37 ± 1	12 ± 1
Cyp151C	42 ± 1	42 ± 1

[1] RDX concentration after 18 h incubation. Values are averages ± standard deviation of three replicates.

[2] Genes were induced using IPTG.

Horizontal gene transfer of pGKT2

The ability of *Gordonia* sp. KTR9 to transfer pGKT2 via conjugation to *R. jostii* RHA1 was successfully demonstrated (Jung et al. 2011). The functional activity of *xplA* was assessed by comparing RDX degradation and growth with RDX as a sole nitrogen source between RHA1 transconjugant and wild type strains. The plasmid was stable up through 100 generations and conferred the ability to grow on and degrade RDX similar to KTR9, while the wild type was unable to grow on or degrade RDX (Figure 7).

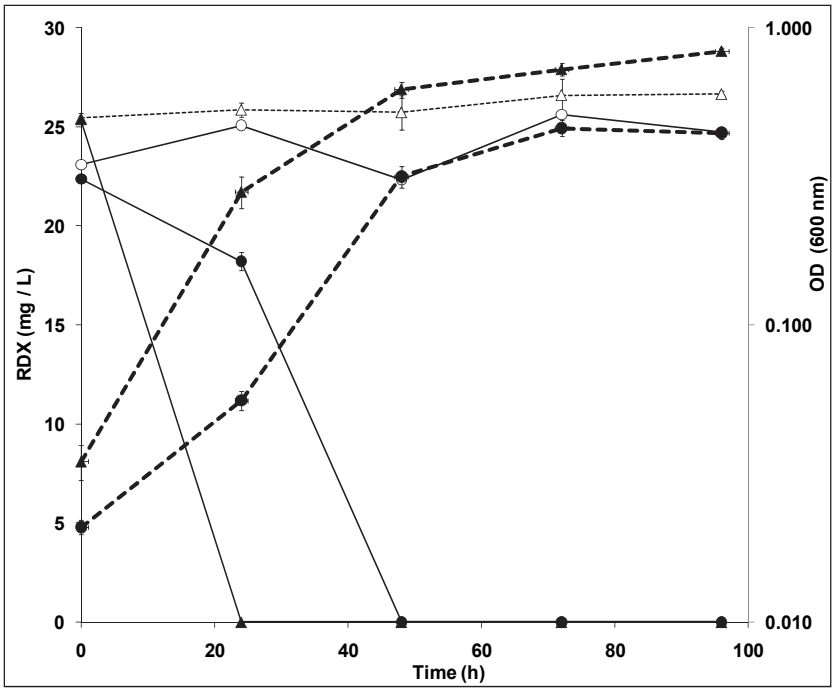

Figure 7. Growth of (dashed bold lines) and RDX degradation by *Gordonia* sp. KTR9 (•), *Rhodococcus jostii* RHA1 wild type (△), and *Rhodococcus jostii* RHA1 transconjugant (▲). Sterile control (○) was used to account for abiotic transformation.

Interestingly, as discussed in Jung et al. (2011), the genomic annotation of pGKT2 by Indest et al. (2010) did not immediately suggest a likely mechanism of conjugation by pGKT2. However, further inspection of the plasmid sequence found evidence for a partial cryptic Type IV secretion system with homologs of VirD4 (acc. no. ADK68942; E value $2e^{-18}$) and VirB4 (ADK68924; $3e^{-10}$) ATPase present on pGKT2. These components are responsible for substrate presentation and are involved with the energetics of DNA translocation across the membrane (Doroghazi and Buckley 2010, Indest et al. 2010, te Poele et al. 2008). Correspondingly, the proximity of putative recombinases (ADK68954, ADK68949), integrases (ADK68955), and tRNA synthase (ADK68956) to one another on pGKT2 (CP002112) is consistent with Actinomycetes integrative and conjugative elements (AICEs), which are commonly integrated in a specific tRNA gene within the host chromosome (te Poele et al. 2008). AICEs are often associated with secondary metabolite gene clusters and foreign DNA from previous hosts (te Poele et al. 2008). These similarly grouped putative elements may be a remnant of an AICE or an orthologous system specific to this plasmid.

Physiological characterization of KTR9 cured of pGKT2

Attempts to independently create unmarked gene deletions in the *xplA* or *xplR* loci using a *sacB* counter-selectable marker resulted in curing of plasmid pGKT2 from strain KTR9. Screening of sucrose resistant, kanamycin sensitive derivatives of KTR9 by PCR using multiple primer sets targeting different regions of pGKT2 including *xplA*, *xplR*, and *cyp151C* were not amplifiable when tested (data not shown). Loss of the plasmid was further confirmed by PFGE and Southern analysis of uncut and XbaI digested (one cut site resulting in linearization of the plasmid) DNA samples from both KTR9 and plasmid-cured strains (Figure 8A). Those lanes containing wild-type KTR9 DNA reacted with a labeled 683 bp probe known to be on the plasmid revealing the presence of a band in the expected size range for the plasmid. In contrast, neither KTR9 plasmid-cured strains produced a signal when probed (Figure 8B).

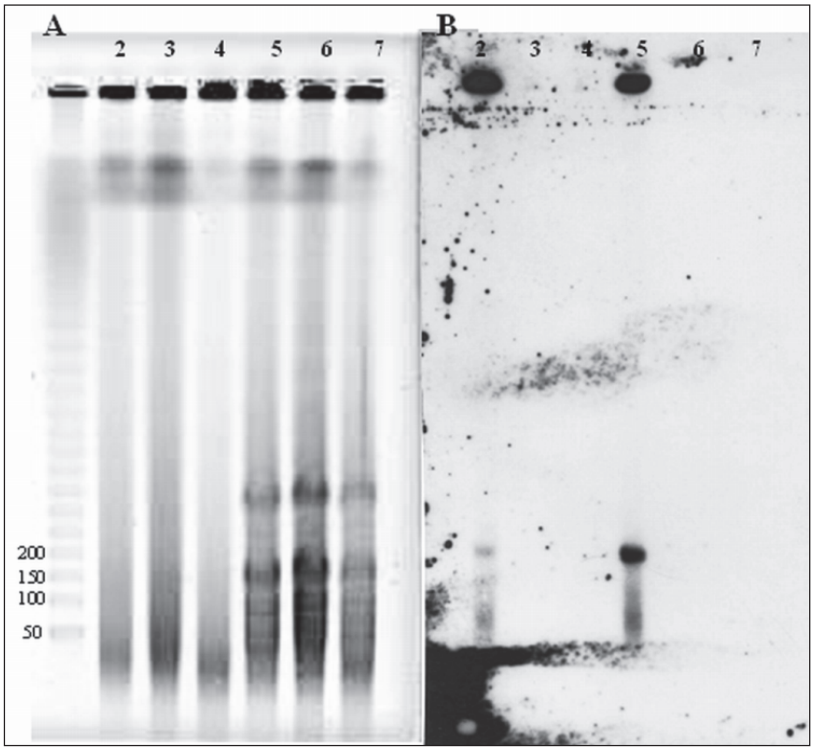

Figure 8. A. Pulse field gel electrophoresis (PFGE) and B. Southern analysis of KTR9 and derived mutant strains. A biotin-labeled 683 bp DNA fragment, specific for pGKT2, was used to probe a PFGE gel of uncut and XbaI digested DNA samples from wildtype and mutant KTR9 strains. Lanes: 2 - uncut KTR9, 3 - uncut deletion mutant #1, 4 - uncut deletion mutant #2, 5 - cut KTR9, 6 - cut deletion mutant #1, 7 - cut deletion mutant #1.

Plasmid-cured KTR9 strains were evaluated for their ability to degrade RDX and utilize RDX as a sole nitrogen source. KTR9 plasmid-cured strains incubated for up to 67 h in LB broth containing 45 μg mL^{-1} RDX did not detectably deplete RDX levels despite achieving optical densities at 600 nm of at least 2.0 (Table 7). In contrast, cultures of wild-type KTR9 depleted RDX to trace levels within 67 h. KTR9 plasmid-cured strains incubated in a minimal salts medium containing RDX as the sole nitrogen source did not degrade RDX and as a result did not grow, while the wild-type KTR9 strain grew and completely degraded the RDX within 48 h (Table 7).

Table 7. RDX degradation studies in KTR9 and mutant strains lacking pGKT2.

	RDX Concentration (μg ml^{-1})[1]	
Bacterial Strains	Rich Medium (LB)	Minimal Medium
Gordonia sp. KTR9 wild-type	1.5 ± 0.2	0.0 ± 0.0
Gordonia sp. KTR9 mutant 1	44.6 ± 0.6	44.8 ± 1.4
Gordonia sp. KTR9 mutant 2	44.2 ± 0.2	44.2 ± 1.2

[1] Wild-type and plasmid cured KTR9 strains were grown for 67 h in LB medium containing 45 ppm RDX, and a minimal medium containing RDX as the sole nitrogen source. Results represent the average and standard deviation of triplicate samples.

Conclusions

Overall, the annotation of the KTR9 genome indicates that the strain has significant metabolic diversity (Figure 5 and Table 3), which could be exploited in the fields of remediation and bioproducts. The annotation also revealed that plasmid pGKT2 encodes an XplA homolog that shares 97% to 99% amino acid sequence identity with characterized XplA cytochrome P450s from *R. rhodococcus* 11Y and *Rhodococcus* sp. DN22. In addition to XplA being highly conserved, it was demonstrated to be both essential and sufficient for RDX degradation via the denitration pathway to NDAB. Plasmid pGKT2 was able to be successfully transferred into other species of actinomycetes, suggesting a role of horizontal gene transfer for the global distribution of the *xplAB* genes. Collectively, these attributes indicated that *xplA* may be an excellent biomarker for predicting RDX degradation.

Proteomic analysis of KTR9 RDX Biodegradation

Introduction

In parallel with KTR9 genome sequencing and annotation efforts, a proteomics approach was initially chosen in order to facilitate the

identification of novel proteins in KTR9. Proteomics is the study of the complete protein complement of a cell and is a powerful tool for understanding the mechanisms by which cells biochemically respond to stimuli. Proteomic studies have been applied to determine xenobiotic transformation pathways and to understand the physiological responses of microorganisms to toxic or inhibitory xenobiotic compounds (Benndorf and Babel 2002, Denef et al. 2005, Kim et al. 2004, Navarro-Llorens et al. 2005, Patrauchan et al. 2005, Segura et al. 2005). Xenobiotics that serve as substrates for growth not only induce the related biodegradative enzymes, but may also induce stress proteins in order to maintain activity and survival of the bacterium. For example, TNT and RDX have been shown to induce stress proteins in the TNT-degrading strain, *Stenotrophomonas* sp. OK-5, and RDX-degrading strain, *Pseudomonas* sp. HK-6, respectively (Chang et al. 2004, Ho et al. 2004).

To further the basic understanding of RDX metabolism, the proteome of strain KTR9 was characterized by comparison of RDX- and nitrite-grown KTR9 cultures. Proteins that were up-regulated in the presence of RDX or unique to the RDX growth condition were selected as potential proteins related to metabolism of RDX. Such proteins may be involved in the recognition (binding and transport) and catalysis of RDX, and the regulation of RDX metabolism. Growth of KTR9 on nitrite was chosen as a control condition to compare with growth on RDX, since degradation of RDX mediated by XplA produces nitrite for growth of KTR9.

Methods

KTR9 growth conditions

In order to obtain enough biomass for differential protein analysis, it was necessary to grow several subcultures of increasing volume of strain KTR9. The initial KTR9 inoculum on Trypticase Soy agar (TSA) plates was started from glycerol stocks (50% v:v). The plates were incubated at 30 ^{o}C for 5 to 7 days to permit colony formation and then two colonies were inoculated into 100 ml of mineral salts medium (MSM (in g/L^{-1}): K_2HPO_4, 0.38 g; $MgSO_4 \cdot 7H_2O$, 0.2 g; $FeCl_3 \cdot 6H_2O$, 0.05 g, pH 7.0; (Thompson et al. 2005)) supplemented with 5 mM sodium succinate and 180 µM RDX. Acetone from an RDX stock solution (135 mM) was allowed to evaporate before the addition of sterile MSM and sodium succinate. This culture was incubated for 2 to 3 days at 30^{o}C with shaking (150 rpm) until the culture reached an

optical density at 600 nm (OD_{600}) of between 0.25 and 0.4 (mid-logarithmic phase) and the RDX concentration was less than 22.5 μM.

Each of the cultures was collected by centrifugation (8,000 rpm for 15 min; GSA rotor), washed once in MSM (without succinate and RDX), and concentrated to an OD_{600} of 3.0 in MSM. The wash step was included since it allowed for more consistent growth of strain KTR9 following subculturing. The cell suspension was then used to inoculate 300 mL of MSM plus 5 mM sodium succinate and 180 μM RDX to an OD_{600} of 0.05. The RDX in these cultures was dissolved from crystalline RDX while stirring the medium for 2 to 3 days in the dark at room temperature. The MSM plus RDX was filter-sterilized prior to use through a 0.45 μm polysulfone filter and the RDX concentration confirmed by HPLC prior to use. This culture was grown for 24 to 36 h as above to an OD_{600} of 0.25 to 0.35 prior to collection, centrifugation, washing with MSM, and concentration in MSM to an OD_{600} of 3.0. This concentrated cell suspension was then used to inoculate three flasks of 300 mL of MSM plus succinate and RDX (180 μM; directly dissolved) and grown for 24 to 36 h as above to the mid-logarithmic phase.

Each of the three 300-mL cultures was collected by centrifugation and the cell pellets were washed twice with MSM. The cultures were pooled in 25 mL of MSM, transferred to a 50-mL polypropylene centrifuge tube, and the cells were collected by centrifugation at 10,000 rpm (SS-34 rotor) and 15 °C. The supernatant was discarded and the cell pellet was immediately frozen in liquid nitrogen. The cell pellet was stored at -80 °C prior to shipment on dry ice to the University of British Columbia.

Strain KTR9 was also grown in MSM plus 5 mM sodium succinate and 4 mM sodium nitrite as a comparison to growth on RDX as the sole nitrogen source. One to two colonies of KTR9 were inoculated into 100 mL of medium and allowed to grow at 30 °C with shaking (150 rpm) for 2 days. This culture was collected by centrifugation and concentrated in MSM to an OD_{600} between 1.5 and 2.0. The concentrated cell suspension was used to inoculate 300 mL of nitrite medium to an OD_{600} of 0.01 and grown for 24 h, at which point the OD_{600} was around 0.35 and the cells were in mid-logarithmic phase. This culture was collected by centrifugation and washed once with MSM prior to concentration to an OD_{600} of 1.5. Two 300-mL flasks were inoculated to an OD_{600} of 0.01 and incubated for 24 to 26 h at which time the OD_{600} was about 0.3 and the cultures were collected by centrifugation, washed twice with MSM, and then pooled into 25 mL of

MSM. The cell pellet was collected (as above), immediately frozen in liquid nitrogen, and stored at -80°C prior to shipment on dry ice to the University of British Columbia.

Three biological replicates of strain KTR9 grown on RDX or sodium nitrite as the sole nitrogen source were prepared at different times from three separately inoculated TSA plates. Quantitative differential protein analyses were performed as described for the related strain, *R. jostii* RHA1 using 2D gel electrophoresis and peptide mass fingerprinting (Patrauchan et al. 2005). Briefly, cells were disrupted by bead beating in a lysis buffer appropriate for the recovery of proteins. The first-dimensional separation was carried out using nonlinear immobilized pH gradient (IPG) strips (24 cm, pH 3 to 7) using the ETTAN IPGphor system (Amersham Biosciences, Baie d'Urfé, Canada). The IPG strips were then equilibrated and run into 12% sodium dodecyl sulfate (SDS)-polyacrylamide gels (24 by 20 cm) using the ETTAN DALT twelve System (Amersham Biosciences) for the second dimension. Broad range molecular mass markers (Invitrogen) were run on each side of the gel. Protein was detected with Sypro Ruby and the stained gels were imaged using a variable mode imager Typhoon 9400 (excitation 488 nm, emission 610 nm; Amersham Biosciences).

Quantitative differential protein expression analysis and peptide mass fingerprinting

Two-dimensional protein gels were screened for suitability of inclusion for quantitative analysis using Progenesis PG240 software (Nonlinear Dynamics, Durham, NC). A total of three replicate protein gels were run for each nitrogen source. Protein spots were selected for identification, excised from the gels, digested with trypsin, and analyzed using a Voyager DESTR matrix-assisted laser desorption ionization-time of flight (MALDI-TOF; (Patrauchan et al. 2005). The obtained mass spectra were processed using *Data Explorer* program tools. The MALDI-TOF spectra were internally calibrated using trypsin autolysis peaks, and processed for noise removal and baseline correction. The resulting spectra peaks were submitted to the Mascot search engine (www.matrixscience.com), and searched against a genome database generated from the KTR9 genome. This KTR9 database was generated by *in silico* digestion of the KTR9 proteome predicted from the genome assembly of KTR9. If no significant result was obtained with the KTR9 database, a search was executed against the NCBI-nr database (http://www.NCBI.NLM.NIH.gov/RefSeq/). Searches were performed allowing for the following modifications: carbamido-methylation of cysteine, partial

oxidation of methionine residues, and up to one missed trypsin cleavage. Proteins were considered identified when the calculated Mascot score was equal to or greater than the threshold for the searched database (in this case, 50). The Mascot score describes the significance of the search result. A score over the threshold indicates a less than 5% chance that the result is a false positive. The threshold for the KTR9 was 50, while the threshold for the NCBI-nr Mascot database was 78. In the case of protein spots with more than one good match, preference was given to protein that had been experimentally verified in the literature. The E-value (Expectation value) associated with the identification of each protein spot is a statistic indicating the probability that two proteins are homologous. Low E-values indicate that the match is not due to chance alone and that the identification is considered statistically significant (http://www.ncbi.nlm.nih.gov/BLAST/tutorial/Altschul-1.html#head2).

Results and discussion

Three replicate 2-D electrophoresis protein gels were run to compare the proteome of strain KTR9 grown on either nitrite or RDX as the nitrogen source. The three gel images were then averaged to determine the number of resolved protein spots per proteome. In the averaged gels, 1120 protein spots were resolved for the nitrite-grown cells and 1012 were resolved in the RDX-grown cells. Comparing the averaged gels between each growth condition revealed 330 spots to be unique to the nitrite-grown cells and 222 to be unique to the RDX-grown cells. Moreover, on gels of RDX-grown cells, 77 protein spots had a normalized volume that had increased by at least two-fold and 112 proteins had a normalized volume that had decreased by at least two-fold. Thirty-five protein spots were selected for identification by peptide mass fingerprinting (Table 8; Figure 9). Selection was based on spot intensity and differential abundance to maximize identification of relevant proteins and pathways. Of these 35 protein spots, 15 had a normalized spot volume that increased between three- and ten-fold and the remaining protein spots were unique to the RDX growth condition (Table 8). The molecular weight and pI range of these 35 proteins was 17 to 97.7 kDa and 3.9 to 5.4, respectively.

Seventeen protein spots yielded Mascot scores above the threshold of the KTR9 database and three that had no significant scores using the KTR9 database had scores above threshold using the NCBI-nr database (Table 9). Two protein spots with statistical significance were identified as nitrite reductase and the XplA cytochrome P450 protein. Both of these protein

Table 8. *Gordonia* sp. KTR9 two-dimensional gel electrophoresis protein spots selected for peptide mass spectrometry analysis.

Spot Number	pI	Molecular Weight (kDa)	Signal Intensity on Nitrite Average Gel	Signal Intensity on RDX Average Gel	Fold Increase
3549	3.9	23.4	0.024	0.072	3.03
3553	4.0	22.5	0.018	0.062	3.43
3936	4.4	17.0	0.016	0.059	3.62
2545	4.3	40.0	0.156	0.583	3.75
931	5.6	97.7	0.009	0.033	3.81
2574	4.8	39.7	0.006	0.025	3.96
2364	4.4	44.4	0.035	0.158	4.49
2541	4.2	40.3	0.029	0.166	5.75
3227	4.1	28.8	0.015	0.088	5.89
1521	3.9	67.6	0.531	3.384	6.37
1059	4.5	90.3	0.021	0.137	6.40
2279	4.2	45.9	0.040	0.300	7.41
2679	4.1	37.7	0.010	0.093	9.42
3849	4.5	18.0	0.004	0.040	9.47
2942	5.4	33.8	0.007	0.077	10.87
965	4.1	96.5	ND[1]	0.069	n/a[2]
1672	4.2	62.4	ND	0.046	n/a
1708	5.1	60.8	ND	0.030	n/a
1773	4.5	57.9	ND	0.609	n/a
1974	5.0	53.0	ND	0.012	n/a
2087	4.6	49.0	ND	0.024	n/a
2091	4.8	49.1	ND	0.088	n/a
2131	4.6	48.4	ND	0.060	n/a
2496	4.6	41.1	ND	0.021	n/a
2598	4.1	39.2	ND	0.022	n/a
2960	5.1	33.6	ND	0.039	n/a
2973	4.8	33.1	ND	0.023	n/a
3198	4.8	29.0	ND	0.055	n/a
3238	4.5	28.6	ND	0.021	n/a
3374	4.4	26.5	ND	0.022	n/a

Spot Number	pI	Molecular Weight (kDa)	Signal Intensity on Nitrite Average Gel	Signal Intensity on RDX Average Gel	Fold Increase
3586	5.4	22.1	ND	0.026	n/a
3617	4.7	21.7	ND	0.026	n/a
3651	5.9	21.7	ND	0.013	n/a
3744	5.9	19.6	ND	0.019	n/a
5077	4.7	43.9	ND	0.982	n/a

[1] Not detected on Nitrite gel.

[2] Fold increase was calculated by dividing the signal intensity from gels of RDX-grown cells by the signal intensity of the corresponding spot from gels of nitrite-grown cells. Therefore, it is not directly applicable for protein spots not detected on nitrite gels.

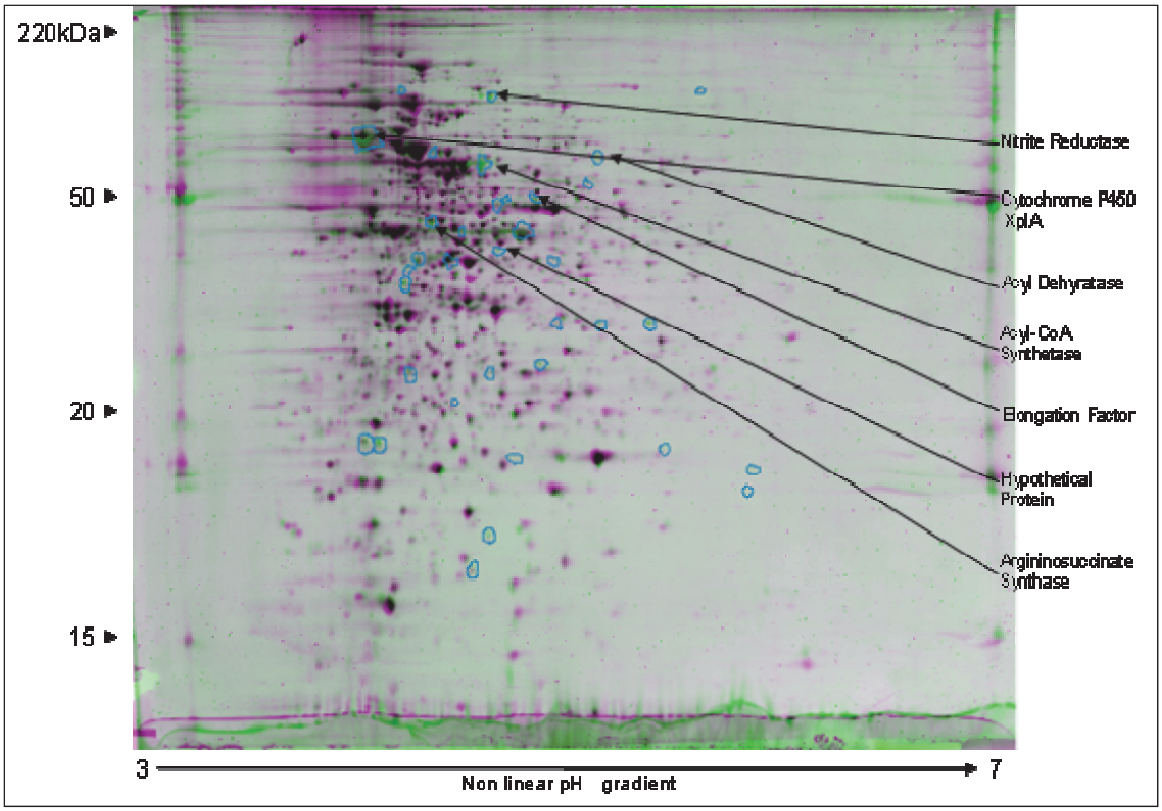

Figure 9. Two-Dimensional (2-D) protein gel electrophoresis of the proteome of *Gordonia* sp. KTR9. The 2-D gel image of nitrite-grown cells is overlaid on the 2-D gel image of RDX-grown cells. Protein spots originating from the nitrite gel are shown in purple; those originating from the RDX gel are shown in green; regions of overlay appear black. The 35 spots that were selected for mass spectrometry analysis are outlined in blue. The locations of seven example proteins that were identified following the Mascot search are also indicated (see Table 8 for Mascot scores).

Table 9. Identification of *Gordonia* sp. KTR9 proteins with Mascot scores above the threshold value of 50. The search was done using the database generated from the KTR9 genome and the NCBI-nr database.

Spot #	Mascot Score	No. of Peptides	Sequence Coverage	Best Match with Proteins in Database	E-value
965[1]	84	14	35	Flagellar protein export ATPase FliI	0.015
1059	80	13	17	Nitrite reductase	0.0
1521	80	5	64	XplA (cytochrome P450)	3.00E-16
1708	56	10	12	Helicase	0.0
1773	174	12	26	Acyl-CoA synthetase	0.0
2091	69	15	51	Elongation factor Tu	0.0
2279	131	16	48	Argininosuccinate synthase	0.0
2364	48	6	36	Hypothetical protein	4.00E-42
2496	55	10	38	Hypothetical protein	4.00E-05
2541	55	10	38	Alcohol dehydrogenase	1.00E-143
2574	64	10	54	Transcriptional regulator	8.00E-48
2598	50	6	45	Hypothetical protein	5.00E-58
2679	53	6	51	No COG hit	n/a
2942	54	9	28	Glycoside hydrolase	0.0
3198	62	8	43	3-oxoacyl-[acyl-carrier-protein] reductase	5.00E-117
3227	54	7	32	ATPase	5.00E-104
3238[1]	80	7	38	2-oxoisovalerate dehydrogenase subunit alpha	0.037
3549	63	7	23	Hypothetical protein	0.22
3849[1]	84	6	38	Hypothetical protein	0.032
5077	69	6	37	Cytochrome P450	2.00E-61

[1] Strain KTR9 protein spots, which were identified by the NCBI-nr database, with a threshold value of 78.

spots were upregulated at least six-fold in the presence of RDX. Nitrite reductase has a role in nitrogen assimilation in most bacteria, and in strain KTR9, this enzyme probably participates in the uptake of nitrite generated from RDX degradation by XplA.

Conclusions

In parallel with KTR9 genome sequencing and annotation efforts, a proteomics approach was initially chosen in order to facilitate the identification of novel proteins in KTR9 associated with RDX degradation. Nitrite was chosen as the control condition in comparison to RDX since degradation of RDX mediated by XplA generates nitrite, which is subsequently

used as the nitrogen source for growth by strain KTR9 and the other aerobic actinomycte RDX-degrading bacteria. The results from this effort are significant, as they indicate that XplA nitrogen assimilation proteins, and transcriptional regulatory proteins are induced in the presence of RDX. Collectively this would suggest that KTR9 can sense the presence of RDX, and respond by the up-regulation of necessary genes to metabolize RDX as a nitrogen source for growth.

Regulation of RDX biotransformation and gene expression in *Gordonia* sp. KTR9

Introduction

The observation that expression of *xplA* is up-regulated in the presence of RDX may indicate that expression of XplA is regulated by the nitrogen status of the cell and the environment. This has implications for the role of *xplA* as a biomarker of RDX degradation, as it may be necessary for bioremediation site managers to monitor inorganic nitrogen sources to ensure effective RDX degradation. Understanding the subtleties that can affect biomarker dynamics has the potential to improve predictability of treatment schemes that incorporate a biomarker monitoring component. Since RDX serves as a nitrogen source for growth in actinomycete bacteria that degrade RDX, it is plausible that alternate inorganic or organic nitrogen sources may compete with RDX as sources of nitrogen for cell growth. Physiological experiments were conducted in this study to test this hypothesis, with the following alternate substrates: glutamate, glutamine, nitrite, nitrate, and ammonium.

Nitrate and ammonium are most likely to be encountered in groundwater due to agricultural fertilizers and both human and animal wastes. In addition, nitrate can be present in groundwater beneath explosive production facilities due to the use of nitric acid. Nitrite rarely accumulates in terrestrial ecosystems and should not be a major factor inhibiting aerobic RDX biodegradation in soil and groundwater. With regards to the aerobic RDX-degrading bacteria, nitrate and ammonium concentrations greater than 100 to 250 mg/L (1.5 to 8 mM) inhibit the rate and extent of RDX degradation (Bernstein et al. 2011; Coleman et al. 1998; Indest et al. 2010). Thus, site characterization should include measurements of the concentrations of nitrate and ammonium in combination with *xplA* gene copy numbers in order to determine whether aerobic RDX biodegradation is a possible treatment option.

Methods

Effect of inorganic nitrogen sources on RDX degradation and gene expression

Strain KTR9 was grown in MSM containing 5 mM glucose, 5 mM succinate, and 10 mM glycerol (C), and 180 μM RDX as the sole nitrogen source. Once the culture grew to the late exponential phase, it was transferred into each of the following media: MSM + C + RDX; MSM + C + $(NH_4)_2SO_4$ (4 mM) + RDX; MSM + C + KNO_2 (4 mM) + RDX; or MSM + C + KNO_3 (4 mM) + RDX. Growth of KTR9 (OD_{600}) and concentrations of RDX were monitored over the course of 68 h. To examine the effects of competing nitrogen sources on the expression of the *xplA* operon, aliquots of the KTR9 cultures were collected after 24 h of growth for isolation of RNA followed by qPCR analysis of *xplA*, *glnAxplB*, *xplR*, and *cyp151C*.

Total RNA was isolated using the Qiagen RNeasy Mini Kit (Valencia, CA) according to the manufacturer's instructions for Gram positive bacteria. Bacterial Protect Reagent (Qiagen) was added to bacterial cell pellets prior to the pellets being stored at -80°C. A 10 min proteinase K treatment (300 μg) step was added to the protocol to enhance RNA recovery. RNA samples were treated with DNase (43 U, Qiagen) for 15 min preceding final purification. RNA samples were run on an Agilent 2100 Bioanalyzer to verify quality and quantity of RNA samples. Total bacterial RNA (up to 2 μg) was reverse-transcribed to cDNA using SuperScript™ III reverse transcriptase (Invitrogen) with random primers (250 ng) according to the manufacturer's instructions. All real-time PCR amplification reactions were performed using the Applied Biosystem 7900HT Fast Real-Time PCR System (Foster City, CA). Quantitative PCR of *xplA* was conducted in 20 μL volumes in 384-well reaction plates using 1×SYBR Green PCR Master Mix (Applied Biosystems). Primer pairs specific for *xplA,* the *glnAxplB* gene fusion, *cyp151C* and *xplR* (Table 10) were diluted to 500 nM final concentration, and template cDNA was diluted 10-fold prior to PCR analysis. Amplification conditions consisted of a single step at 95 °C for 10 min followed by 50 cycles at 95 °C for 20 s, 55 °C for 20 s, and 72 °C for 30 s. The PCR data were analyzed using the accompanying Applied Biosystems 7900HT analysis software with threshold determinations automatically performed by the instrument and then manually optimized. Starting mRNA concentrations and PCR efficiencies were calculated using LinRegPCR (Ramakers et al. 2003). The mRNA concentrations were normalized to 16S rRNA PCR output.

Table 10. DNA primers used in SYBR Green Quantitative PCR Analysis of *xplA*, *glnAxplB*, *xplR*, and *cyp151C* genes.

Real-time PCR Primers	Sequence (5' – 3')
xplaFm2239	GATGACCGCTGCGTCCATCGAT
xplaR2333	CCTGTTGCAGTCGCCTATACC
xplR518F	CAGAGATGTGCCGGATGCT
xplR568R	CGGTCACCGTGCTCATCAC
Cyp151C678F	TGATGAGCTGCGTGATGTGA
Cyp151C728R	GTGTCGTATCCGCCGAAGAT
Glutamine68F	TCGACGCGATCAAGCAGTAC
Glutamine11R	TCACGGCCTGGAAGTCGACG
xplB175F	CAGGGCACGAAGAACGTGAT
xplB225R	CCGATCGTCGAATACCCG

XplR regulator and GlnAXplB fusion protein function

Since the *xplR* gene and the *glnAxplB* fusion gene cluster with the *xplA* gene, it was hypothesized that (a) the XplR protein may regulate expression of the *xplA* gene in an RDX-dependent manner; and (b) that the GlnAXplB fusion protein may retain the XplB reductase function. Therefore, the functions of these proteins were characterized to establish their involvement in RDX biodegradation. In order to generate the quantity of protein needed for characterization, these proteins were heterologously produced in *E. coli*, as follows. These two genes were PCR-amplified, cloned into a pET-28a expression vector, and used to produce the encoded products as polyhistidine-tagged proteins in *E. coli*. Soluble proteins were purified using immobilized metal affinity chromatography (IMAC; Ni-NTA column).

Physiological characterization of xplR deletion mutants

As an alternative to the above approach for *xplR* gene deletion, the following approach was also attempted. The *xplR* gene was targeted for homologous recombination and insertion of a kanamycin resistance (Km^r) marker (NP_478145.1). This site is approximately 1 kb upstream from the *xplAB* gene complex. A DNA construct in which the Km^r gene was inserted near the middle of the *xplR* gene, flanked by ~350 bp, was synthesized by Celtek Biosciences, LLC (Nashville, TN) into a pCR2.1 vector (Invitrogen, Carlsbad, CA). The Km^r construct containing the *xplR* flanking regions (1.6 kb total)

was liberated from the plasmid by digestion with BamHI (New England BioLabs, Inc., Ipswich, MA) and gel purified with a Wizard SV Gel and PCR Clean-up System Kit (Promega, Madison, WI). The purified 1.6 kb fragment was ligated into a BamHI-restricted mobilizable vector, pK18*mobsacB* (Schäfer et al. 1994, van der Geize et al. 2001), and transformed into One Shot Top10 Chemically Competent *E. coli* cells (Invitrogen) that were selected on LB plates with 50 μg mL^{-1} kanamycin.

Recombinant pK18*mobsacB* was introduced from Top10 *E. coli* cells into *Gordonia* sp. KTR9 based on the conjugation strategy presented by (van der Geize et al. 2001). Double crossover transconjugants of the Km^r marker from pK18*mobsacB* into pGKT2 via homologous flanking regions were selected on LBP plates with 50 μg mL^{-1} kanamycin and 10% (w/v) sucrose. Each step was screened by PCR targeting the Km^r construct and various locations on the pGKT2 and pK18*mobsacB* plasmids. This was necessary to confirm the presence or, in the case of pK18*mobsacB*, its absence as described previously (Jung et al. 2011). Additional PCR primers, 5'ATGCAGATCGGAAGCATCTCC3' (xplR_knockout_F) and 5'AACACTGCCAGCGCATCAAC3 (xplR_knockout_R), were developed that annealed to the N-terminal portion of *xplR* and the *kan* gene such that only double-cross recombinants between pGKT2 and the *xplR-kan* construct would be detected. PCR primers 5'CGGTCACCGTGCTCATCAC3' (xplR_568R) and 5'CGTGCTCATCACCTGTGGAA3' (121109xplR_R) that flank the *kan-xplR* insertion site were also developed as a way of verifying that the size of the *xplR* amplification product had increased by the size of the *kan* gene in the insertion mutants. PCR amplification conditions consisted of a single step at 94 °C for 5 min followed by 30 cycles at 94 °C for 30 s, annealing for 30 s at 55 °C (58 °C for primer xplR_knockout_R), 72 °C for 60 s, and a final step at 72 °C for 5 min.

The ability to utilize RDX as a sole nitrogen source was evaluated in *xplR* mutant strain 3c and compared to the KTR9 wild type strain. The KTR9 strains were grown in MSM with 5 mM sodium succinate, 10 mM glycerol, 5 mM glucose, and 180 μM RDX until the late exponential phase. The cultures were washed twice with MSM and transferred to MSM for a 24-h starvation period. The cells were then inoculated into MSM supplemented with 5 mM succinate, 5 mM glucose, 10 mM glycerol and 180 μM RDX at an initial OD_{600} of 0.02. KTR9 wild-type and mutant cultures for resting cell assays were grown to mid-log phase in minimal media with added carbon and RDX as described above, collected by centrifugation, washed with MSM, and resuspended in cold 0.25 mM phosphate buffer, pH 7.0,

containing 112.6 μM RDX to an OD_{600} of 0.6). RDX degradation in resting cell assays was normalized against total protein as determined by the Bradford assay. All KTR9 cultures were incubated at 30 °C with shaking at 150 rpm. Degradation studies and resting cell assays were performed in triplicate.

Differential gene expression analysis of KTR9

Strain KTR9 was grown in 300 mL MSM with glucose (5 mM), succinate (5 mM), and glycerol (10 mM) (GSG) as the carbon sources, and sodium nitrite (4 mM). This culture was collected by centrifugation, washed in MSM medium, and used to inoculate MSM medium plus GSG (50 mL) at an OD_{600} of 0.08. The following amendments were used to investigate gene expression as a result of nitrogen source: (i) RDX (40 ppm); (ii) ammonium sulfate (AS; 4 mM); and (iii) AS (4 mM) + RDX (40 ppm). All cultures were inoculated in triplicate and grown for 24 h, at which time the cells were collected for RNA extraction.

Total RNA was extracted from KTR9 cells using the Qiagen RNeasy kit. Prior to extraction, an enzymatic lysis/mechanical disruption step was added to the protocol, whereby the cell pellet was resuspended in 100 μL TE buffer and 200 μL of lysozyme (20 mg/mL), transferred to an MP Biomedicals Lysing Matrix B tube, and vortexed for 1 min. An optional on-column DNA digestion using the Qiagen RNase-Free DNase Kit was performed to remove any remaining DNA. The quantity and quality of RNA was assessed with the Agilent 2100 Bioanalyzer using the Agilent RNA 6000 Kit. cDNA for microarray analysis was generated using the Invitrogen Superscript II Double-Stranded cDNA Synthesis Kit and the quality of the cDNA was confirmed using the Agilent 2100 Bioanalyzer and Agilent DNA 1000 Kit. The cDNA was Cy3-labeled with the NimbleGen One-Color DNA Labeling Kit. Two micrograms of the labeled cDNA was used for hybridization to a Nimblegen Bacterial Gene Expression Arrays using a custom *Gordonia* sp. KTR9 12×135K array. The arrays were hybridized for 18 h at 42 °C in a Nimblegen Hybridization system and subsequently washed using the Nimblegen Wash Buffer Kit. Washed arrays were scanned using the Agilent Microarray Scanner and images were analyzed using Nimblescan v2.5.26 software and ArrayStar v4.0.0 software. Expression data were log2 transformed and statistical significance was determined using a moderated t-test for binary transcriptome comparisons (i.e. RDX vs. ammonium sulfate). The P-value was set at 0.05 with an FDR correction. Only genes that were induced or repressed at least 3-fold were considered in this report.

For pairwise analysis of gene induction and repression patterns across all transcriptomes, significant gene sets were identified by ANOVA analysis (P value 0.05, 3-fold induction) and overlapping gene sets were identified via Venn diagrams.

Results and discussion

Effect of inorganic nitrogen sources on RDX degradation and gene expression

The effects of ammonium, nitrite, and nitrate on the ability of KTR9 to degrade RDX were investigated. KTR9 degraded RDX most rapidly when this compound was present in liquid cultures as the sole nitrogen source (Figure 10A), with approximately 93% of the RDX degraded within 24 h of inoculation. In contrast, only 21% to 34% of the RDX was transformed after 24 h in the presence of a competing nitrogen source. Even after 68 h of incubation, significant concentrations of RDX remained in cultures containing $(NH_4)_2SO_4$ (63%), KNO_2 (42%), or KNO_3 (13%).

The organization of the *xpl* gene cluster suggests that it may constitute an operon that is regulated by XplR. Bioinformatic analysis of this region indicates that putative bacterial promoter elements (-10 and -35 regions) can be found directly upstream of *xplR* and *cyp151C* (Figure 11). A putative GntR binding site (TnGTnnnACnA) of the FadR subtype was also found within 5 bp of the -35 promoter region of *cyp151C* (Vindal et al. 2007), further implying that XplR could regulate transcription of *cyp151C*. The absence of Rho independent terminator sequences in *cyp151C* and the short intergenic space between this gene and *glnAxplB* also suggests that *cyp151C*, *glnAxplB* and *xplA* are transcribed as a single cistron.

The expression of *xplR, cyp151C*, *glnAxplB*, and *xplA* were compared in KTR9 cells after 24 h of growth in the cultures described above. RNA samples were analyzed by quantitative PCR analysis and relative gene expression data were normalized to the quantity of the 16S rRNA gene. When KTR9 was grown on RDX in the presence of a competing nitrogen source, the expression of all four genes was reduced from 48% to 80% compared to growth on RDX alone (Figure 10B). These results correlated well with the inhibition of RDX degradation (Figure 10A). Specifically, expression of the *xplA* was inhibited by 73% in cultures containing ammonium. These same cultures experienced a 79% reduction in the degradation of RDX. Similarly, expression of the *xplA* gene was inhibited by 75% and 56% in the presence of nitrite and nitrate, resulting in 76% and 66% reductions in the degradation of RDX, respectively.

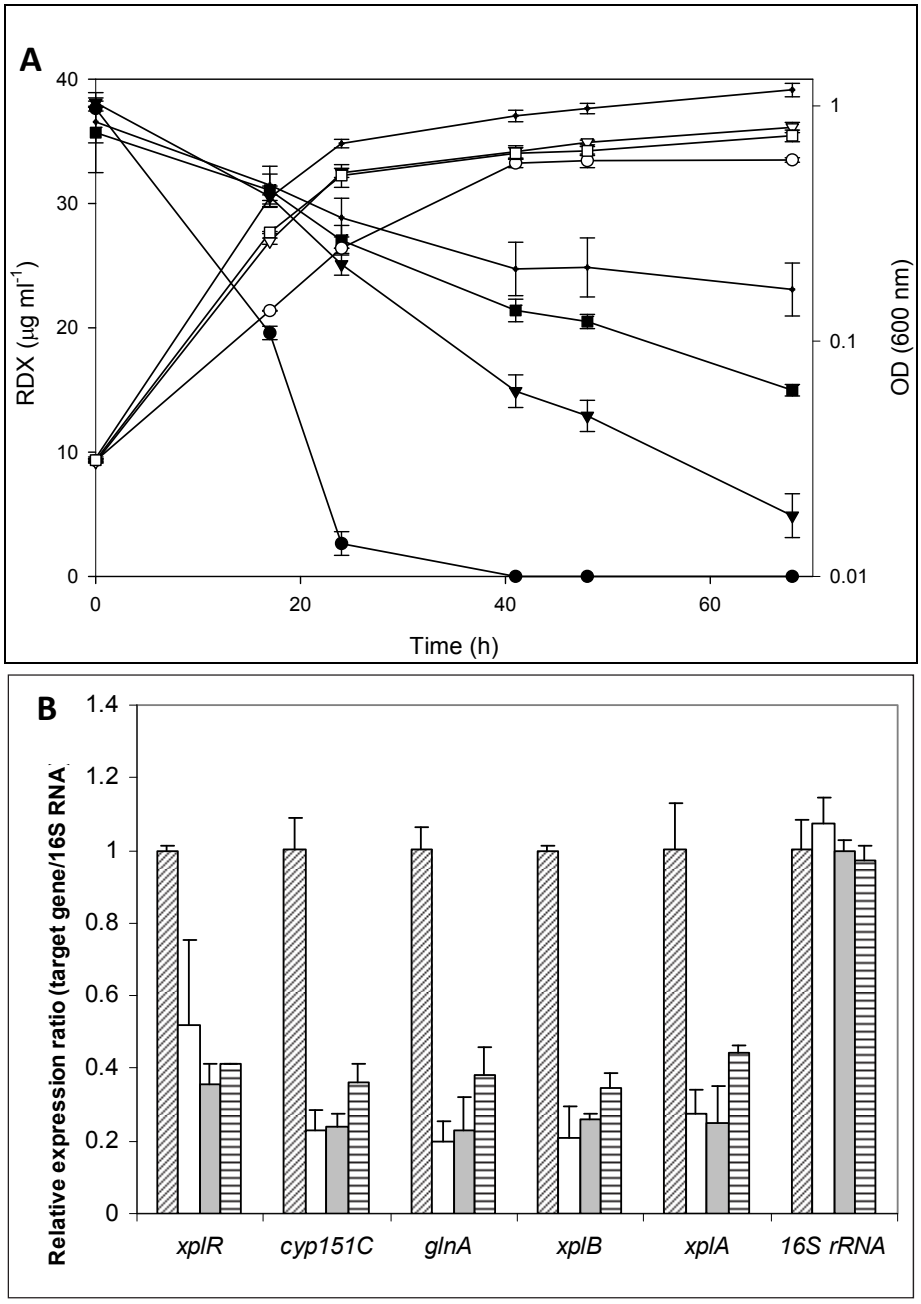

Figure 10. A. The effects of various inorganic nitrogen sources on the RDX-degradation activity and growth of KTR9. Four mM of $(NH_4)_2SO_4$ (dash), KNO_3 (closed triangle), or KNO_2 (closed square) were included as competing nitrogen sources compared to RDX alone (closed circle). Error bars are the standard error of three samples. B. RT qPCR expression analysis using probes for each of *xplR, cyp151C, glnA, xplB,* and *xplA*. RNA was harvested from KTR9 cells grown for 24 h on media containing the indicated nitrogen sources: RDX alone (diagonal lines), RDX + $(NH_4)_2SO_4$ (blank bars), RDX + KNO_2 (shaded bars), RDX + KNO_3 (horizontal lines). Taken from Indest et al. (2010).

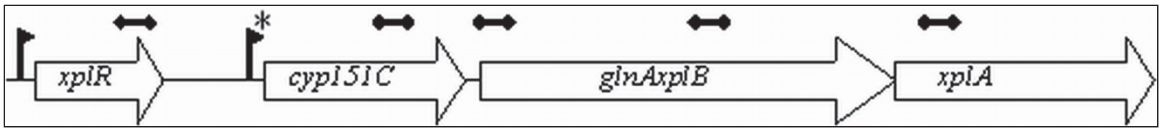

Figure 11. The *xpl* gene cluster. Putative promoter regions (-10 and -35 regions) were found upstream of the *xplR* ORF (156809-157548 bp) at positions 156741-156761bp and the *cyp151C* ORF (158328-159527) at positions 158272-158290 bp. A GntR binding site (*) (TnGTnnnACnA) was found 5 bp upstream of the promoter region for *cyp151C*. Regions targeted by real-time PCR are designated by barbell lines about the gene boxes (Indest et al. (2010).

XplR regulator and GlnAXplB fusion protein function

The annotation revealed two genes that cluster with *xplA* and might be involved in RDX degradation: x*plR,* which is predicted to encode a GntR-type transcriptional regulator and a gene that appears to be a fusion of *glnA* and *xplB*, predicted to encode a glutamine synthetase (GlnA) and the reductase (XplB) for XplA, respectively. Both *glnA* and *xplB* are close to full length. The fusion gene might therefore encode a bifunctional protein. It is hypothesized (a) that XplR may regulate *xplA* expression in an RDX-dependent manner; and (b) that GlnAXplB may reduce XplA or catalyze the transformation of an RDX degradation product.

A clone carrying *xplR* (without mutation) was transformed into *E. coli* to produce recombinant protein for use in binding studies. Most of the obtained protein was insoluble. However, a significant portion could be solubilized using a 0.1-M potassium phosphate buffer, pH 8.0, containing 8 M urea, and 10 mM β-mercaptoethanol. The denaturated sample was refolded on a nickel column. The column was washed with four column volumes of 0.1 M potassium phosphate buffer, pH 8.0, 10 mM β-mercaptoethanol, and decreasing amounts of urea (8 M, 6 M, 4 M, 2 M, 1 M, 0 M) before eluting with two column volumes of 0.1 M potassium phosphate buffer, pH 8.0 and 150 mM imidazole. The refolded XplR was then eluted with four bed volumes of 0.1 M potassium phosphate buffer, pH 8.0 containing 300 mM imidazole. The elution was concentrated and buffer exchanged into 0.1 M potassium phosphate buffer, pH 8.0 using ultrafiltration. As the protein remained soluble, it was assumed to be refolded. The refolded protein could bind to a 100-bp DNA fragment, which contained the promoter region upstream of *cyp151C,* but could bind to other DNA fragments as well. Therefore, the DNA-binding ability of this renatured protein did not appear to be very specific for the *xplA* operon.

The GlnAXplB fusion protein was produced as a soluble protein. Approximately 9.3 mg of protein was obtained from 1 L of bacterial cell culture. One

μg of purified protein was incubated at 30 °C overnight in the presence of 6 mM glutamine, 15 mM $MgCl_2$, 20 mM NH_4Cl, 16 mM ATP, and 200 mM Tris-Cl at pH 7.4 in a total volume of 10 μL. In preliminary assays, the recombinant fusion protein did not possess glutamine synthetase activity. The expected product, glutamate, could not be detected by thin layer chromatography in the reaction mixture (solvent: butanol: acetic acid: water= 7.5:3:2).

Effects of an xplR mutation on RDX degradation

A kanamycin resistance marker (Km^r) was inserted, via a targeted, site-specific recombination event within the middle of the *xplR* coding region (KTR9_4921) approximately 1 kb downstream of the *xplAB* gene locus. Recombinational insertion of the Km^r marker in the pGKT2 was confirmed via PCR with a unique primer set that primes within the *xplR* locus and the Km^r gene such that an amplification product is only observed if a double crossover event has occurred (Figure 12 A, lanes 1-3). Additional primer sets that amplify within the *xplR* gene flanking the insertion site show an increased size that is equivalent to the size of the Km^r gene (Figure 12, B and C, lanes 1-3), further indicating that Km^r gene insertion has occurred.

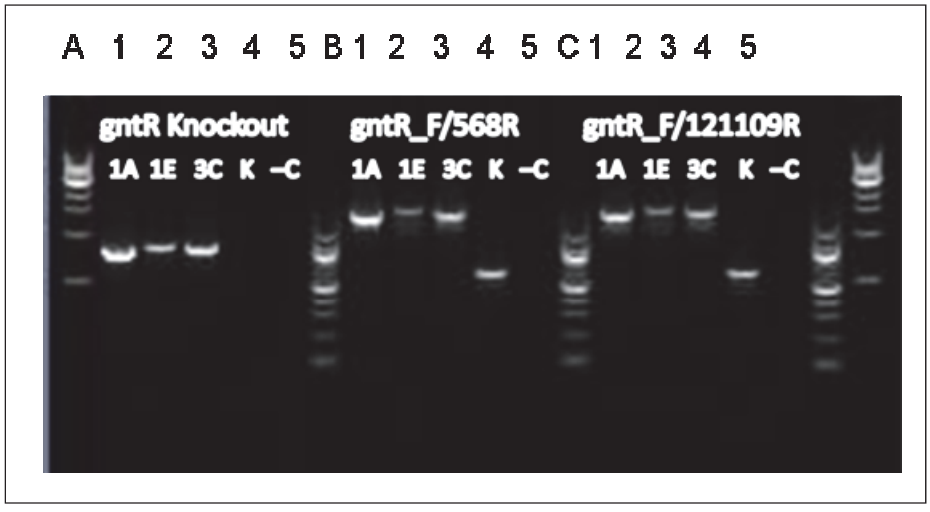

Figure 12. PCR analysis of wild-type and xplR mutants.

The ability to utilize RDX as a sole nitrogen source was evaluated in *xplR* mutant strain 3c compared to the wild-type strain. While the mutant strain was able to degrade RDX, it did so at a slower rate than the wild-type strain (Figure 13). In general, *xplR* mutants tended to clump, thereby complicating absorbance measurements and, as a result, growth estimates.

To compensate for differences in growth (and clumping issues) between the parent and mutant strains, resting cell assays were conducted to determine if RDX degradation rates were diminished in the *xplR* mutant. No significant differences were observed in the rate of RDX degradation between the wild-type and *xplR* mutant strain (Figure 14). Similarly, no significant differences in RDX degradation rates were observed over 70 h when the wild-type and *xplR* mutant strain were incubated in the presence of 4 mM ammonium sulfate and RDX (Figure 15).

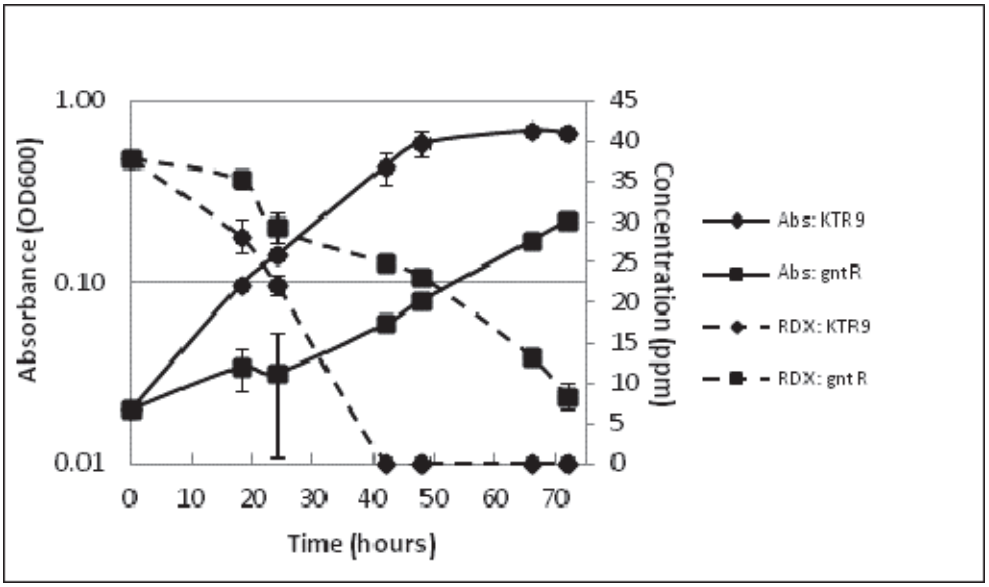

Figure 13. Growth of KTR9 and KTR9 *xplR* 3c mutant on RDX as a sole nitrogen source.

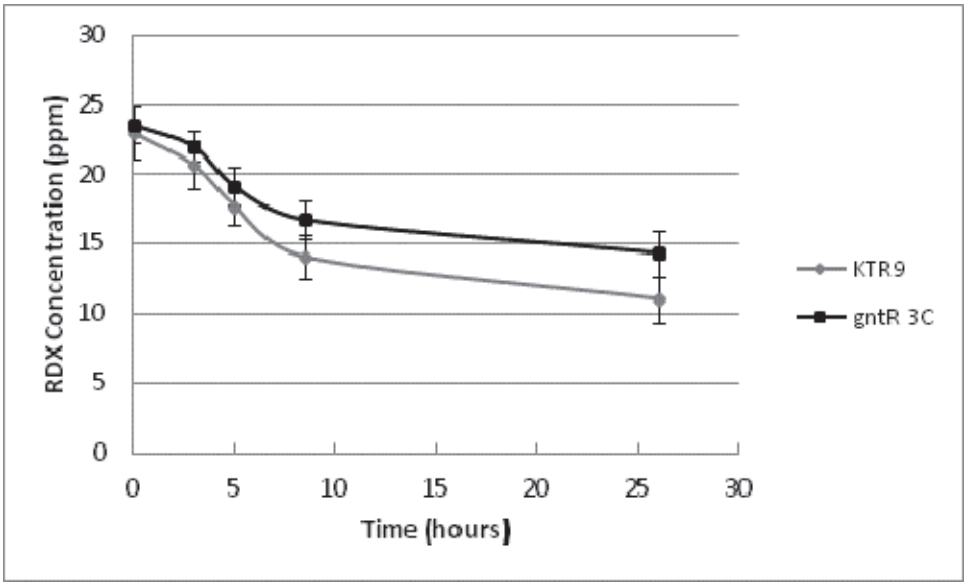

Figure 14. RDX degradation in resting cell assays of KTR9 and *xplR* 3c mutant.

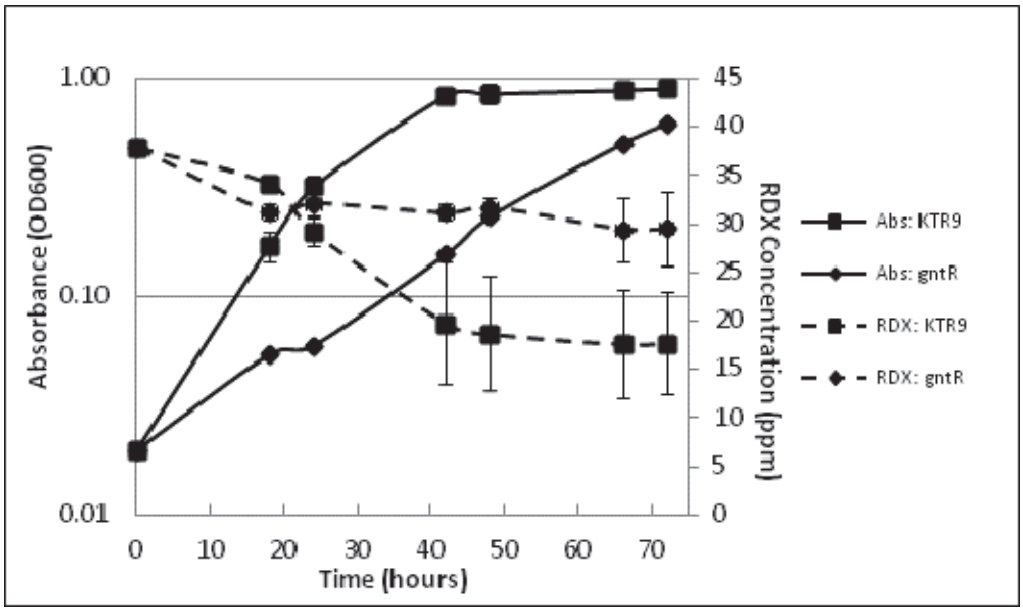

Figure 15. The effects of 4mM ammonium sulfate on RDX degradation in wild-type and *xplR* 3c KTR9.

Differential gene expression analysis

It has previously been shown that RDX degradation is significantly inhibited in the presence of ammonium in *Gordonia* sp. KTR9 (Indest et al. 2010, Thompson et al. 2005). To further investigate this observation, microarray analysis of strain KTR9 was conducted with cultures of KTR9 grown on a combination of nitrogen sources, which included (a) 40 ppm RDX, (b) 4 mM ammonium sulfate, and (c) 40 ppm RDX-and-4 mM ammonium sulfate. Cultures for transcriptome analysis were harvested during mid-log phase when RDX concentrations were determined to be 1.1 ppm (97% loss) for those cultures growing on RDX and 35.5 ppm (11% loss) for those cultures growing on RDX-and-4 mM ammonium sulfate (Figure 16). Transcriptome analysis of KTR9 cultures grown in the presence of RDX compared to those grown on 4 mM ammonium sulfate as a control identified 260 gene targets that were differentially expressed by at least 3-fold. Of these gene targets, 180 were upregulated in the presence of RDX, whereas the remaining 80 gene targets were downregulated. A select number of these gene targets are presented in Tables 11 and 12, respectively.

The majority of genes up-regulated in the presence of RDX are involved in transport, nitrogen assimilation, nucleic acid/amino acid catabolism/fatty acid catabolism, stress/redox imbalance, RDX degradation, or gene regulation and rearrangement (Table 11). Collectively, these functions suggest

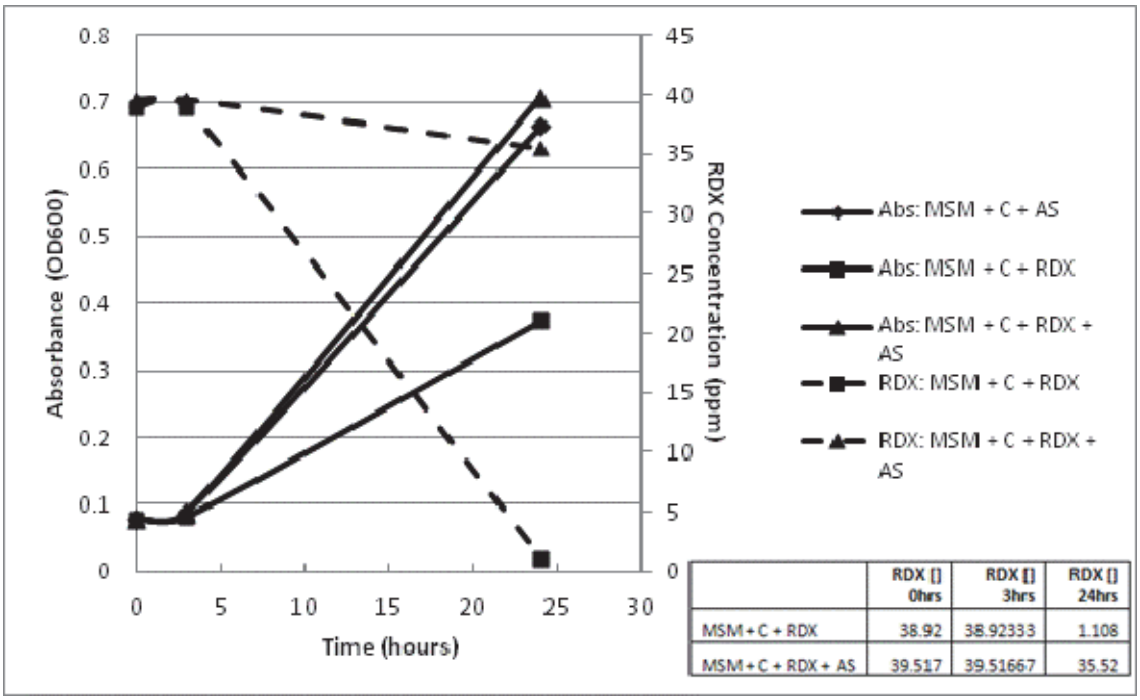

Figure 16. Growth of *Gordonia* sp. KTR9 and degradation of RDX in MSM + C + RDX or MSM + C + RDX + ammonium sulfate (AS).

Table 11. Genes up-regulated in KTR9 during growth on RDX.

Locus	Function	Fold change
	Transport	
KTR9_1425	Nitrate/nitrite transporter	109.586
KTR9_1947	ABC-type nitrate/sulfonate/bicarbonate transport system, permease component	72.958
KTR9_4688	Ammonia permease	53.726
KTR9_1948	ABC-type nitrate/sulfonate/bicarbonate transport systems, periplasmic components	42.89
KTR9_1300	Branched-chain amino acid ABC-type transport system, permease components	32.201
KTR9_1715	Amino acid transporters	27.794
KTR9_0322	Predicted flavoprotein involved in K+ transport	27.591
KTR9_1608	Cytosine permease /uracil permease /thiamine permease /allantoin permease	26.207
KTR9_1301	ABC-type branched-chain amino acid transport systems, periplasmic component	26.03
KTR9_3984[1]	MspA family protein	21.991
KTR9_1302	Formate/nitrite family of transporters	20.478
KTR9_1946	ABC-type nitrate/sulfonate/bicarbonate transport system, ATPase component	12.138
KTR9_4364	Major facilitator superfamily permease	10.21
KTR9_4612	Na+/H+-dicarboxylate symporters	9.899

Locus	Function	Fold change
KTR9_0664	ABC-type branched-chain amino acid transport system, permease component	8.928
KTR9_3512	ABC-type transport system involved in cytochrome bd biosynthesis, ATPase and permease components	8.816
KTR9_0667[1]	ABC-type branched-chain amino acid transport systems, periplasmic component	8.282
KTR9_0666	ABC-type branched-chain amino acid transport systems, ATPase component	7.873
KTR9_3513	ABC-type multidrug transport system, ATPase and permease components	7.639
KTR9_0665	ABC-type branched-chain amino acid transport systems, ATPase component	7.336
KTR9_1298	Uncharacterized ABC-type transport system, ATPase component	7.245
KTR9_1897[1]	Permeases, MFS superfamily	7.063
KTR9_1481	Xanthine/uracil permeases	6.32
KTR9_0663[1]	Branched-chain amino acid ABC-type transport system, permease components	6.095
KTR9_4492	ABC-type multidrug transport system, permease component	5.585
KTR9_2255	Xanthine/uracil permeases	5.541
KTR9_1297	ABC-type branched-chain amino acid transport systems, ATPase component	4.857
KTR9_3418[1]	Permease, MFS superfamily	4.013
pGKT1_0025[1]	Outer membrane adhesin like protein	3.694
KTR9_2427[1]	ABC-type multidrug transport system, ATPase and permease components	3.431
KTR9_2935[1]	ABC-type polysaccharide/polyol phosphate export systems, permease component	3.308
KTR9_2649[1]	Preprotein translocase subunit YidC	3.016
Nitrogen Assimilation		
KTR9_3974	NAD(P)H-nitrite reductase	58.659
KTR9_3975	Ferredoxin subunits of nitrite reductase and ring-hydroxylating dioxygenases	54.866
KTR9_3976	Putative nitrate reductase / sulfite reductase	48.565
KTR9_1424	NAD(P)H-nitrite reductase	41.192
KTR9_1423	Ferredoxin subunits of nitrite reductase and ring-hydroxylating dioxygenases	35.391
KTR9_1891	4-aminobutyrate aminotransferase and related aminotransferases	34.728
KTR9_3894	Glutamine synthetase, type III	26.813
KTR9_1308	Cyanate lyase	18.682
KTR9_2566	Glutamate synthase domain 1	18.205
KTR9_0832	Glutamate synthase (ferredoxin)	13.136
KTR9_2565	Glutamate synthase domain 3	12.422
KTR9_0830	Glutamate synthase, NADH/NADPH, small subunit	12.264
KTR9_1900	Asp-tRNAAsn/Glu-tRNAGln amidotransferase A subunit and related amidases	11.942

Locus	Function	Fold change
KTR9_2564	ferredoxin-dependent glutamate synthase	7.946
KTR9_2568	Glutamine synthetase, type III	6.746
	Stress/Redox	
KTR9_4657[1]	Protease subunit of ATP-dependent Clp proteases	9.998
KTR9_4656[1]	Protease subunit of ATP-dependent Clp proteases	9.204
KTR9_2423[1]	Predicted iron-dependent peroxidase	7.027
KTR9_0966[1]	Heme oxygenase	6.87
KTR9_3263[1]	Chaperonin GroEL (HSP60 family)	6.825
KTR9_0037	Alkylhydroperoxidase, AhpD family	5.824
KTR9_2060[1]	Molecular chaperone	4.839
KTR9_0038[1]	Alkyl hydroperoxide reductase/ Thiol specific antioxidant/ Mal allergen	4.643
KTR9_4738[1]	Mycothione/glutathione reductase	4.227
KTR9_3166[1]	Predicted redox protein, regulator of disulfide bond formation	4.12
KTR9_2642[1]	Thiol-disulfide isomerase and thioredoxins	3.726
	RDX Degradation Cluster	
KTR9_5233	Hypothetical protein	166.206
KTR9_5232	Hypothetical protein	60.264
KTR9_5234	Hypothetical protein	59.604
KTR9_5229	Cytochrome P450	37.94
KTR9_5230	GlnA-XplB fusion protein,glutamine synthetase, GlnA, flavodoxin reductase, XplB	34.188
KTR9_5235	Hypothetical protein	25.628
KTR9_5231	Flavodoxin-cytochrome P450 XplA	22.585
KTR9_5236	Hypothetical protein	11.297
KTR9_5226	Hypothetical protein	8.365
KTR9_5228	Transcriptional regulators	5.182
	Nucliec Acid /Amino Acid Catabolism	
KTR9_1894	Xaa-Pro aminopeptidase	39.78
KTR9_3888	Proline dehydrogenase	20.621
KTR9_1712	Allophanate hydrolase subunit 2	12.273
KTR9_1952	Cytosine deaminase and related metal-dependent hydrolases	9.642
KTR9_1950	Putative amidase	9.159
KTR9_1951	Pyridoxamine-phosphate oxidase	9.11
KTR9_1896	Putative acetylornithine deacetylase	5.67

Locus	Function	Fold change
KTR9_0531	Urea amidohydrolase (urease) gamma subunit	5.344
KTR9_0529	Urea amidohydrolase (urease) alpha subunit	4.671
KTR9_3423[1]	Aspartyl aminopeptidase	4.028
KTR9_0611	Acetylglutamate kinase	3.925
KTR9_0610	Acetylornithine aminotransferase	3.574
	Fatty Acid Catabolism	
KTR9_2575	Ethanolamine utilization protein-like protein	14.636
KTR9_0828	Acyl-CoA thioesterase	9.5
KTR9_4611	Ceramidase	3.599
	Recombination	
KTR9_1265[1]	Integrase	6.567
KTR9_2592	Transposase, IS4 family protein	5.104
KTR9_0015[1]	Regulatory protein RecX	4.664
pGKT2_0080[1]	Putative recombinase	3.941
	Regulators	
KTR9_1309	Transcriptional regulator (PucR)	7.232
KTR9_1895	Transcriptional regulators (GntR)	6.707
KTR9_1131[1]	Transcription regulator, AsnC-type-like protein	5.229
KTR9_4194	Transcriptional regulator (TetR)	4.965
KTR9_4690	UTP:GlnB (protein PII) uridylyltransferase	4.424
KTR9_1635[1]	Regulatory protein TetR	4.113
KTR9_0936[1]	Transcriptional regulators (AsnR)	3.429
KTR9_1429[1]	Transcriptional regulator (TetR)	3.348

[1] Differentially expressed gene targets identified in a pairwise analysis that are common to the transcriptomes of cells grown on ammonium sulfate versus RDX with cells grown on the RDX versus RDX and ammonium.

Table 12. Genes Down-regulated in KTR9 During Growth on RDX

Locus	Function	Fold change
	Transport	
KTR9_3040	Permease, MFS superfamily	42.675
KTR9_0778	Glycerol uptake facilitator and related permeases (Major Intrinsic Protein Family)	13.987
KTR9_0871	ABC-type transport system involved in resistance to organic solvents, periplasmic component	6.308
KTR9_0458	2-keto-3-deoxygluconate permease	5.9
KTR9_0870	ABC-type transport system involved in resistance to organic solvents, periplasmic component	5.784
KTR9_3667	ABC-type transport system involved in resistance to organic solvents, periplasmic component	5.283
KTR9_3249	Predicted symporter	5.206
KTR9_3662	ABC-type transport system involved in resistance to organic solvents, permease component	5.18
KTR9_0869	ABC-type transport system involved in resistance to organic solvents, periplasmic component	5.054
KTR9_0872	ABC-type transport system involved in resistance to organic solvents, periplasmic component	4.897
KTR9_0868	ABC-type transport system involved in resistance to organic solvents, periplasmic component	4.755
KTR9_2327	ABC-type molybdate transport system, permease component	4.077
KTR9_4472	ABC-type sugar transport systems, permease components	4.031
KTR9_3818	Amino acid transporters	3.682
KTR9_0873	ABC-type transport system involved in resistance to organic solvents, permease component	3.664
KTR9_2328	ABC-type molybdate transport system, periplasmic component	3.63
KTR9_3663	ABC-type transport system involved in resistance to organic solvents, permease component	3.022
	Oxidreductase	
KTR9_4237	Coenzyme F420-dependent N5,N10-methylene tetrahydromethanopterin reductase and related flavin- dependent oxidoreductases	11.916
KTR9_1929	Cytochrome P450	4.452
	Transcriptional Regulation	
KTR9_2225	Transcriptional regulator, AraC family	7.352
KTR9_1470	Transcriptional regulator containing PAS, AAA- type ATPase, and DNA-binding domains	6.315
KTR9_2221	Transcriptional activator of acetoin/glycerol metabolism	4.46
KTR9_2746	Transcriptional regulator	4.039
KTR9_0030	Transcriptional regulators of sugar metabolism	3.841

that, from the global metabolic perspective, RDX-exposed KTR9 cells are starved for nitrogen. For example, there are a number of genes that are up-regulated whose function is to transport nitrogen containing molecules like ammonia, nitrate, nitrite, amino acids, and nucleic acids into the cell. These are both active transporters that couple transport with an energy source (ABC-type) as well as passive transporters, like permeases and symporters. In addition to acquiring nitrogen from its environment, the KTR9 transcriptome response suggests that cells growing on RDX also need to scavenge endogenous nitrogen sources as implied by a number of up-regulated genes that are involved in the catabolism of nucleic acids, amino acids, and fatty acids. In addition to increasing the transport and catabolism of nitrogen containing compounds, genes involved in nitrogen assimilation, such as nitrite reductase, glutamine synthetase, and glutamate synthase, are heavily induced by KTR9 when growing on RDX. These genes likely assimilate the nitrite released from the transformation of RDX into glutamine and glutamate which, through the subsequent action of various transaminases, can be used for the synthesis of amino acids, nucleic acids, and other nitrogen containing molecules.

There are also a number of genes up-regulated in the presence of RDX that suggest a redox imbalance and/or stress response. These genes include various chaperonins, as well as proteases, reductases, and thioredoxins. This combination of gene targets suggests that the transient presence of RDX as it is metabolized may generate reactive nitrogen/oxygen species that result in protein damage subsequently triggering chaperonin and protease activity. Interestingly, two of the genes in this category, alkyhydroperoxidase and alkyhydroperoxide reductase, have been associated with reactive nitrogen intermediates like nitrite, which is an RDX transformation product. In contrast to what is observed when RDX is actively metabolized, when KTR9 is grown on RDX-and-ammonium sulfate, RDX remains in the medium resulting in the significant up-regulation of genes involved in redox imbalance, protein damage, and monooxygenase activity (Table 13). Despite the induction of these genes, RDX levels remain constant and cell growth is similar to growth in the presence of ammonium sulfate.

Perhaps the most significant group of genes up-regulated in the presence of RDX are those shown to be directly involved in RDX degradation, namely the XplA and XplB proteins. More intriguing is the observation that a cluster of at least 10 hypothetical genes contiguous with the *xplAB* gene locus are upregulated, some of which are greatly induced (KTR9_5228-5236), but

Table 13. Genes up-regulated in KTR9 during growth on ammonium sulfate and RDX. Gene targets that are upregulated in the presence of RDX + ammonium sulfate (control condition: ammonium sulfate) minus those targets that upregulated in the presence of RDX (control condition: ammonium sulfate).

Locus	Function	Fold change
	Transport	
KTR9_0722	ABC-type branched-chain amino acid transport system, permease component	10.397
KTR9_0200	ABC-type transport system involved in Fe-S cluster assembly, ATPase component	10.232
KTR9_0198	ABC-type transport system involved in Fe-S cluster assembly, permease component	7.465
KTR9_2967	Sulfate permease and related transporters, MFS superfamily	6.851
KTR9_0721	ABC-type branched-chain amino acid transport systems, ATPase component	6.245
KTR9_0720	ABC-type branched-chain amino acid transport systems, ATPase component	6.117
KTR9_0723	ABC-type branched-chain amino acid transport systems, periplasmic component	5.177
KTR9_0199	ABC-type transport system involved in Fe-S cluster assembly, permease component	5.057
KTR9_4137	ABC-type proline/glycine betaine transport systems, permease component	4.975
KTR9_3348	TRAP-type C4-dicarboxylate transport system, periplasmic component	3.236
KTR9_1698	ABC-type nitrate/sulfonate/bicarbonate transport systems, periplasmic components	3.165
KTR9_1764	ABC-type transport system involved in resistance to organic solvents, periplasmic component	3.154
KTR9_0068	K+ transport systems, NAD-binding component	3.132
KTR9_4136	ABC-type proline/glycine betaine transport systems, ATPase components	3.077
	Stress/Redox Inbalance	
KTR9_1469	Chaperonin GroEL, HSP60 family	525.211
KTR9_0480	Catalase (peroxidase I)	107.594
KTR9_3333	Thioredoxin reductase	27.735
KTR9_3334	Methyltransferase type 11	24.038
KTR9_1938	Catalase (peroxidase I)	18.774
KTR9_4327	Co-chaperonin GroES (HSP10)	16.332
KTR9_4328	Chaperonin GroEL (HSP60 family)	14.86
KTR9_3611	Molecular chaperone (small heat shock protein)	7.88
KTR9_2026	Peptide methionine sulfoxide reductase A	6.861
KTR9_2027	Peptide methionine sulfoxide reductase B	5.31
KTR9_4648	DsbA oxidoreductase	5.077
KTR9_1202	Coenzyme F420-dependent N5,N10-methylene tetrahydromethanopterin reductase and related flavin- dependent oxidoreductases	4.894
KTR9_4237	Coenzyme F420-dependent N5,N10-methylene tetrahydromethanopterin reductase and related flavin- dependent oxidoreductases	4.775

Locus	Function	Fold change
KTR9_3032	Thiol-disulfide isomerase and thioredoxins	4.701
KTR9_2555	Coenzyme F420-dependent N5,N10-methylene tetrahydromethanopterin reductase and related flavin- dependent oxidoreductases	4.283
KTR9_2641	Thioredoxin reductase	3.986
KTR9_3420	Glutathione peroxidase	3.111
KTR9_3380	Predicted oxidoreductases (related to aryl- alcohol dehydrogenases)	3.022
Monooxgenase Activity		
KTR9_1467	Conserved hypothetical protein, DUF59 superfamily	222.869
KTR9_1468	Zn-dependent alcohol dehydrogenases	187.59
KTR9_1466	Predicted metal-dependent hydrolase	177.735
KTR9_1463	2-polyprenylphenol hydroxylase and related flavodoxin oxidoreductases	142.8
KTR9_1464	Monooxygenase hydroxylase	68.818
KTR9_1465	Monooxygenase component MmoB/DmpM	62.05
KTR9_1462	Methane monooxygenase	47.931
KTR9_0741	Cytochrome P450	6.641

their function is currently unknown. A number of putative transcription regulators are also induced in the presence of RDX as well as a few transposon-related genes, some of which are located on the *xplAB* pGKT2 plasmid. Of particular interest is the up-regulation of an UTP:GlnB (protein PII) uridylyltransferase, which is a critical component of the nitrogen signal cascade in *C. glutamicum* and *Streptomyces* species that is up-regulated during times of nitrogen limitation. This protein, in combination with a TetR regulator known as AmtR/GlnR, is a global repressor responsible for regulating various cellular processes including ammonium uptake and signal transduction, ammonium assimilation, urea uptake and metabolism, and creatinine uptake and metabolism. A number of TetR regulators have been identified that are upregulated in the presence of RDX and may have a role similar to AmtR/GlnR in combination with the UTP:GlnB (protein PII) uridylyltransferase.

Additional comparisons between gene targets up-regulated in the presence of RDX-and-ammonium sulfate with genes up-regulated in the presence of RDX (ammonium sulfate as the control condition in both cases) revealed 125 gene targets induced in the RDX-and-ammonium sulfate condition, a condition in which the RDX persists in the media (Figure 17, Table 13).

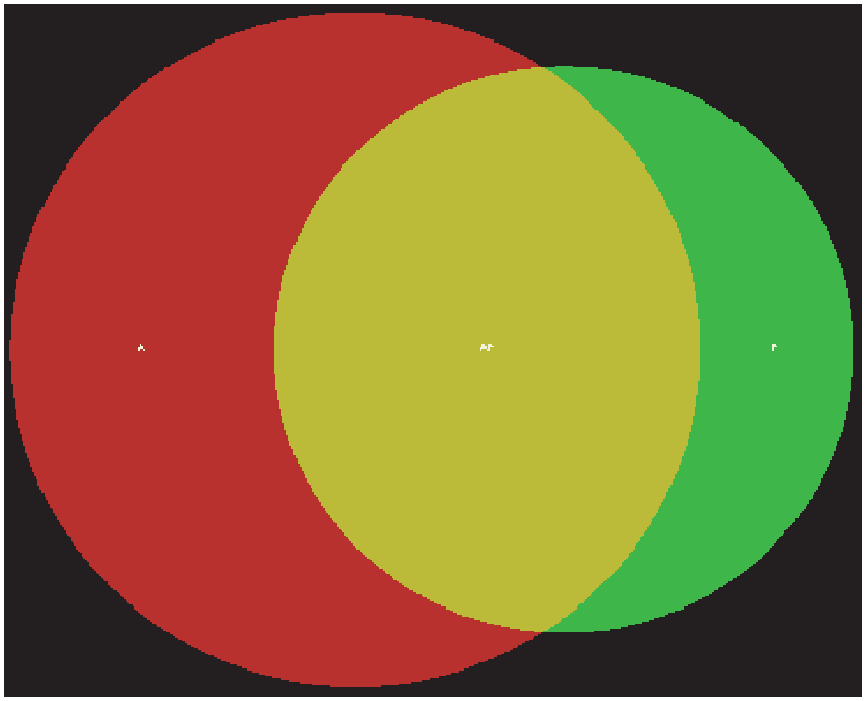

Figure 17. Venn diagram illustrating 169 (out of 587) differentially expressed genes common to the transcriptomes of cells grown on ammonium sulfate versus RDX (red) with cells grown on the RDX versus RDX-and-ammonium (green).

Interestingly, gene targets that make up this group are involved in transport, redox imbalance/stress, and monooxygenase activity. A pairwise analysis of gene induction and repression patterns across the three transcriptomes identified 169 (out of 587) differentially expressed genes common to the transcriptomes of cells grown on ammonium sulfate versus RDX with cells grown on the RDX versus RDX-and-ammonium (Figure 17). Interestingly, most of the genes listed in Table 11 (those without an asterisk) were identified as common to these transcriptomes. These include transport, nitrogen assimilation, amino acid/nucleic acid/fatty acid catabolism, RDX degradation, and transcriptional regulation.

Conclusion

The qPCR data presented herein indicate that the entire *xpl* cluster is transcriptionally regulated in such a fashion inasmuch as inorganic nitrogen sources repressed *glnAxplB-xplA* transcript levels to a degree that correlated well with inhibition of RDX degradation. The functional characterization of XplR *in vitro* and via *xplR* gene knockouts indicated that XplR does not have a role in regulating RDX degradation. A

functional role for the GlnAXplB protein was not established based on *in vitro* studies. KTR9 transcriptome studies indicate that growth on RDX results in a nitrogen limitation response and that this response may be mediated by GlnR. In addition, other genes involved in RDX degradation were implied by their proximity and having an expression pattern similar to the *xplAB* gene cluster.

Role of nitrogen limitation and GlnR on RDX degradation

Introduction

Transcriptome analysis of KTR9 grown on RDX suggests that the transcriptome response to RDX is likely a reaction to nitrogen limitation rather than a response to RDX. To investigate this further, in-depth physiological experiments were conducted with KTR9, looking at a range of nitrogen sources and concentrations. Time course studies were performed to determine the existence of correlations between nitrogen substrate removal, *xplA* gene expression, and RDX degradation. The role of GlnR, a global regulator in nitrogen assimilation, on RDX degradation was also evaluated in mutant *glnR* KTR9 strains.

Methods

Expression of the xplA gene in N-limited and C-limited KTR9 cells

The earlier studies on inorganic nitrogen effects on RDX degradation and XplA activity were not associated with the amount of inorganic nitrogen remaining in the medium and were only concerned with inhibitory concentrations of inorganic nitrogen. The effects of different concentrations of inorganic nitrogen (NH_4Cl and $NaNO_2$) and carbon (succinate) on the growth physiology of strain KTR9, degradation of RDX, and expression of the *xplA* gene were investigated. For these experiments, KTR9 was inoculated from frozen stocks into M9 medium supplemented with Goodies 20 mM succinate as the carbon source, and either (a) 0.3 mM RDX; (b) 0.3 mM RDX plus 1.8 mM NH_4Cl; (c) 0.3 mM RDX plus 6 mM NH_4Cl; (d) 0.3 mM RDX plus 1.8 mM $NaNO_2$; or (e) 0.3 mM RDX plus 4 mM $NaNO_2$ as the nitrogen sources. Carbon limitation in KTR9 was examined using M9 Goodies containing 2 mM NH_4Cl (a non-nitrogen limiting concentration) and various concentrations of succinate at 2.5, 5, 10 or 15 mM. In all cases, RDX concentration was measured by HPLC and growth was monitored by OD_{600} measurements.

After nitrogen and carbon-limiting conditions were established, the effect of these conditions on the expression of *xplA* was quantified by RTqPCR using the *xplA* TaqMan assay. For the N-limited treatment (0.9 mM NH_4Cl), KTR9 cells were collected at early log phase (20 h), middle log phase (29 h) and late log phase (44 h). For the C-limited treatment (3 mM NH_4Cl and 8 mM succinate) KTR9 cells were collected at early log phase (20 h), middle log phase (30 h), and late log phase (39 h). The RTqPCR reactions used a TaqMan universal PCR master mix (Applied Biosystem) and a Mx3000P (Stratagene) instrument. RNA levels are expressed relative to that of the reference gene, *sigA*. The expression of the *sigA* gene is fairly constant under varying growth conditions so that it can be used as an internal standard (Capyk et al. 2009). Ammonium concentrations were determined by the sodium salicylate-hypochlorite method. The range of this assay is 0.5 - 25 ppm of NH_3 nitrogen (equivalent to 0.04 - 1.78 mM). All experiments were performed in triplicate.

GlnR regulation

GlnR is an OmpR-type transcriptional regulator that has been shown to play a central role in regulating nitrogen uptake and metabolism in actinomycetes (Tiffert et al. 2008, Amon et al. 2008). As *Gordonia* sp. KTR9 is also an actinomycete, it is hypothesized that GlnR is involved in regulating RDX degradation, including processes other than those catalyzed by XplA, such as uptake. MEME, a sequence analysis software tool, was used to predict GlnR binding in KTR9 based on known binding sites in *Streptomyces coelicolor* (http://meme.sdsc.edu/meme4_4_0/intro.html). A recombinant form of GlnR fused to an N-terminal His-tag was produced in *E. coli* and purified using IMAC. The His-tag is a series of residues, including at least six successive histidine residues, which can be fused to the N- or C-terminus of a protein. Such tags are used to facilitate the purification of the tagged protein. Fragments of 150 bp containing predicted GlnR-binding sites were amplified from upstream of the following RDX- and N-catabolic genes: KTR9_1207, glutamine synthetase; KTR9_1987, ammonium permease; KTR9_1290, nitrate reductase; and KTR9_4922, XplA cytochrome P450. The binding of GlnR to the upstream region of nitrite reductase (KTR9_3114) was very weak. Thus, this group was excluded after initial screening. Each amplicon was tested for interactions with GlnR in a gel mobility shift assay using 30 ng of template DNA in a total volume of 20 µL.

Phenotypic studies of the KTR9 glnR deletion mutant

To further examine the role of GlnR in regulating nitrogen and RDX metabolism in strain KTR9, homologues of *glnR* were identified and deleted in both *Gordonia* sp. KTR9 and *Rhodococcus jostii* RHA1. The *glnR* gene was deleted in KTR9 using the *sacB* counterselection system that has been used in several rhodococcal strains (van der Geize et al. 2001). In order to verify the genotype of the *glnR* mutant, two sets of primers, one pair flanking the gene and one pair flanking (upstream) and internal (within the gene) were used to amplify the *glnR* gene in KTR9 and *glnR* mutant cells, respectively. To determine the phenotypic effect of the *gln*R deletion on N utilization, the KTR9 wild-type and the *glnR* mutant were grown in M9 Goodies with succinate and different inorganic and organic nitrogen sources (NH_4Cl, glutamine, urea, cytosine, valine, $NaNO_2$, KNO_3, and RDX). The *gln*R mutant cells clumped extensively in liquid culture such that monitoring growth by optical density required the addition of Tween 80 to the medium.

Degradation of RDX and xplA gene expression by the glnR mutant in N-limiting conditions

Both the KTR9 wild-type and *glnR* mutant strains were grown in M9 supplemented with Goodies plus 20 mM succinate and 18 mM NH_4Cl. When the cultures reached the mid-exponential phase, they were harvested and washed twice using M9 medium without any nitrogen source. The washed culture suspensions were each equally divided at the same cell density (OD_{600} ~ 1.2) among 4-5 flasks of M9 supplemented with Goodies plus 20 mM succinate and various nitrogen sources. Media for growth of the wild-type strain of KTR9 contained (a) no nitrogen source; (b) 0.9 mM NH_4Cl; (c) 0.3 mM RDX; (d) 0.9 mM NH_4Cl plus 0.3 mM RDX; and (e) 0.9 mM $NaNO_2$. Media for the glnR mutant contained (a) no N source, (b) 3 mM NH_4Cl, (c) 0.3 mM RDX or (d) 3 mM NH_4Cl plus 0.3 mM RDX. Cell suspensions were incubated at 30 ºC with shaking and samples were collected at 0, 1, 2, 4, 6, and 8 h for quantification of the *xplA* gene by RTqPCR. In addition, ammonium concentrations were determined as above for those flasks containing ammonium. RDX removal was further analyzed by HPLC in *glnR* mutant cell suspensions for the two treatments containing RDX. Some growth occurred in these treatments, with approximately one doubling of OD in all treatments with added N sources.

Expression of KTR9_0967 permease/transporter protein

Degradation of RDX by KTR9 is likely to involve transport of RDX into the cell. Several transport genes were observed to be differentially expressed by growth of KTR9 on RDX compared to ammonium. Some of these genes were highly up-regulated, and one gene region in particular was considered as encoding a protein for the transport of RDX. Artemis software was used to view KTR9_0966, 0967, and 0968 genes. The KTR9_0967 amino acid sequence was used as a query sequence in NCBI. Expression of KTR9_0967 was measured using RTqPCR. Cells were harvested at different growth stages for RNA isolation: Lag-phase: 39 h RDX; Early log-phase: 48 h RDX, 24 h NH_4Cl and $NaNO_2$; Mid-log phase: 65 h RDX, 36 h NH_4Cl and $NaNO_2$; Late log-phase: 48 h NH_4Cl and 42 h $NaNO_2$.

Deep sequencing transcriptomic analysis

Deep-sequencing transcriptomic data were used to further refine the genome annotation and to provide a complementary analysis to the microarray gene expression data. For these analyses, strain KTR9 was grown in M9 supplemented with Goodies plus 20 mM succinate and either 0.9 mM NH_4Cl or 0.3 mM RDX as the nitrogen source. Total RNA was extracted using the RiboPure-Bacteria Kit (Ambion) in combination with Turbo-DNase, to remove trace amounts of contaminating genomic DNA. RNA samples yielded no bands when used as a template for PCR, indicating an absence of contamination with genomic DNA in the RNA samples. Moreover, the OD_{260}/OD_{280} and OD_{260}/OD_{230} ratios of the samples exceeded 2.0, indicating a lack of contamination from proteins and chemicals. Pooled RNA samples (n=3) from each of the two treatments were submitted to the Genome Science Centre, Vancouver, for whole transcriptome shotgun sequencing. The services provided included rRNA depletion, library construction, and paired-end ditag sequencing with the Illumina Genome Analyzer IIx system.

Results and discussion

Expression of the xplA gene in N-limited and C-limited KTR9 cells

Degradation of RDX by aerobic RDX-degrading actinomycete bacteria is known to be inhibited by inorganic nitrogen sources (Coleman et al. 1998, Indest et al. 2010, Nejidat et al. 2008, Thompson et al. 2005). However, the effect of lower amounts of inorganic nitrogen on RDX degradation rates and *xplA* gene expression has not been studied. A comparison of the

loss of ammonium (1.8 mM) or nitrite (1.8 mM) and RDX in cultures of strain KTR9 indicated that RDX removal began a few hours after depletion of the inorganic nitrogen (Figures 18A and 18B). This suggests that the inorganic N sources are preferentially used by KTR9. Interestingly, RDX degradation was inhibited even after removal of 6 mM NH_4Cl (Figure 18C). It is hypothesized that the higher NH_4Cl concentration caused cells to store excess N and not to experience N limitation. Additional KTR9 growth curves, RDX removal, and inorganic nitrogen concentrations for cultures grown on different concentrations of nitrogen are shown in Appendix A.

Growth of strain KTR9 was linearly correlated to concentrations of succinate, indicating that all cultures were limited for carbon under these conditions (Figure 19). In previous experiments, the maximum OD of KTR9 cultures grown in the N-limited condition (0.9 mM NH_4Cl) was approximately 1.2. In order to have a similar maximum OD to test the effect of C-limited conditions on gene expression, the concentration of succinate must be approximately 8 mM (Figure 19). To ensure that there is no N starvation in the C-limited medium, KTR9 was grown on N-limited medium (Figure 20A) and at three different concentrations of NH_4Cl (2 mM, 3 mM, and, 4 mM). The depletion of NH_4^+ was measured in all cell suspensions. Ammonia was totally depleted after 40 h of growth in cultures supplemented with 2 mM NH_4Cl (Figure 20B). However, when 3 or 4 mM NH_4Cl was added to the cultures, ammonia could still be detected in the stationary phase (Figures 20C and 20D), indicating that there was no N starvation in these treatments. Thus, it was decided to test gene expression in a medium containing 8 mM succinate and 3 mM NH_4Cl.

The expression of the *xplA* gene was measured at different stages of growth and RDX removal for strain KTR9. When RDX was present in the medium (39 h, ~ 72% remaining; and 48 h, ~ 26% remaining) the transcript level of *xplA* was relatively low (Figure 21). However, the abundance of *xplA* transcripts increased roughly four-fold in the late-exponential phase (65 h) when RDX was completely degraded (Figure 21), suggesting that depletion of N may be involved in up-regulation of *xplA* expression. Similar expression patterns were found in KTR9 cultures grown only in the presence of NH_4Cl and $NaNO_2$ (Figure 21): transcript levels were very low at the early-exponential phase (24 h), peaked at the mid-exponential phase (36 h), and then dropped dramatically at the late-exponential phase (48 h for NH_4Cl or 42 h for $NaNO_2$) (Figure 21). These results suggest that the concentration of

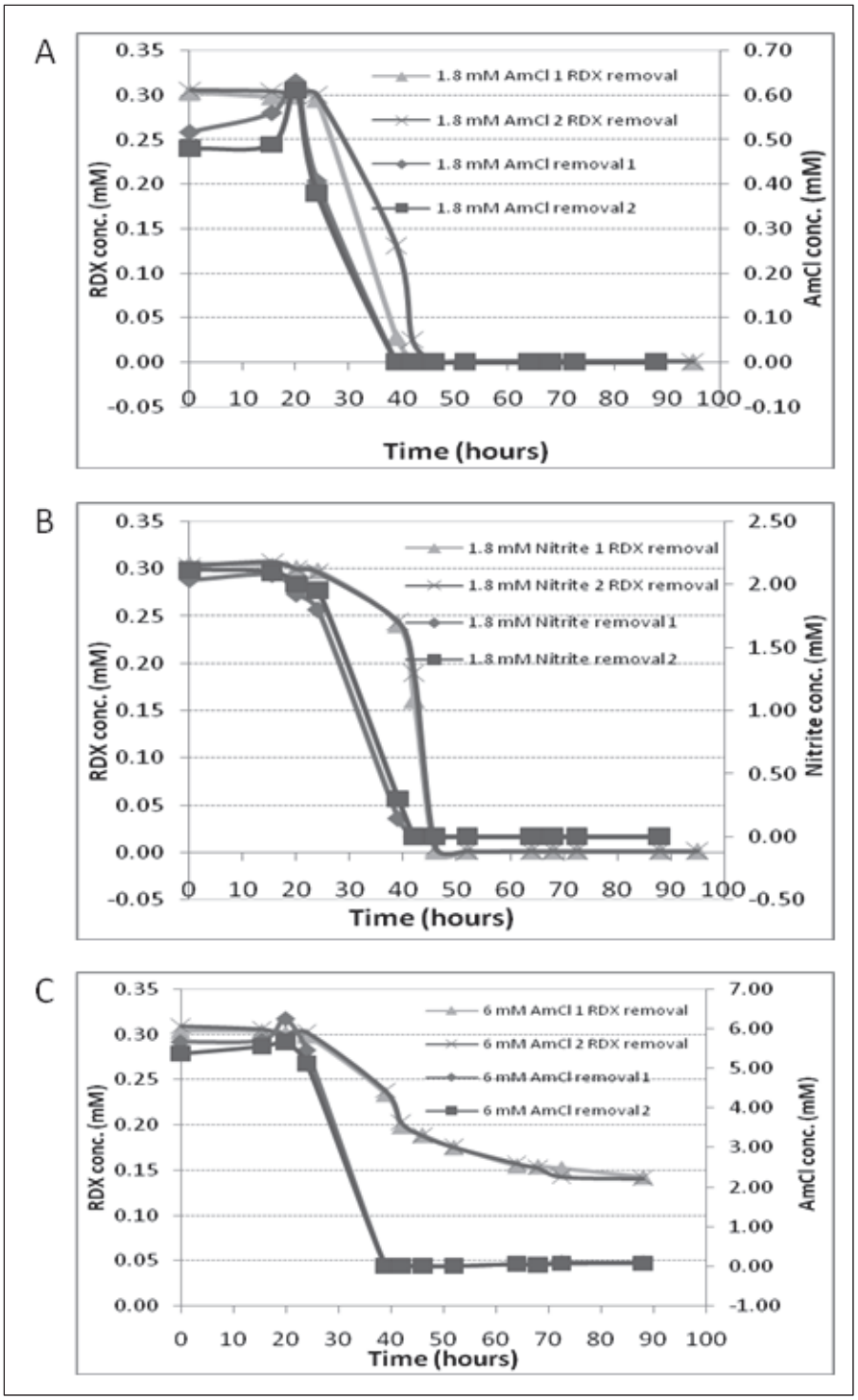

Figure 18. Depletion of RDX and inorganic N in KTR9 cultures grown on (A) 0.3 mM RDX and 1.8 mM NH_4Cl, (B) 0.3 mM RDX and 1.8 mM $NaNO_2$, and (C) 0.3 mM RDX and 6 mM NH_4Cl.

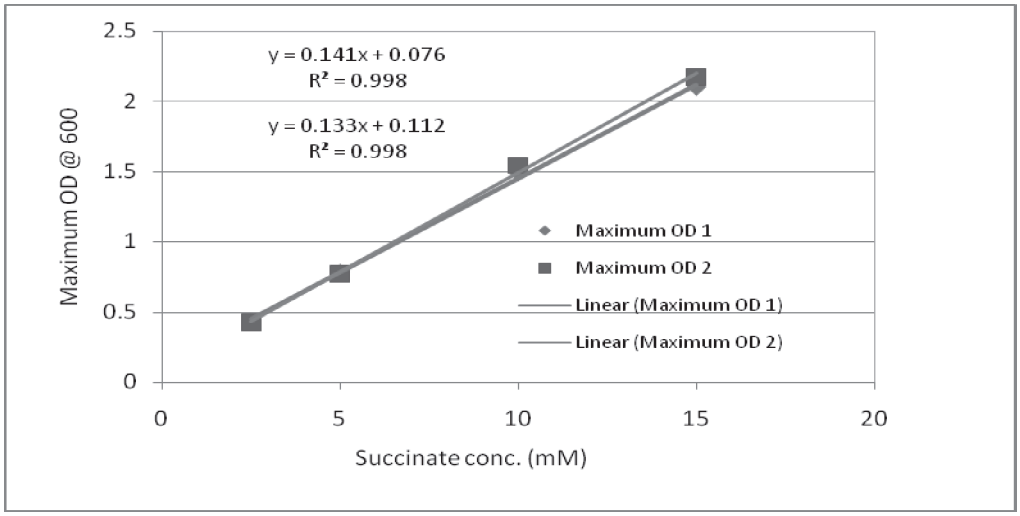

Figure 19. Correlation between maximum OD_{600} and succinate concentration in medium (n=2).

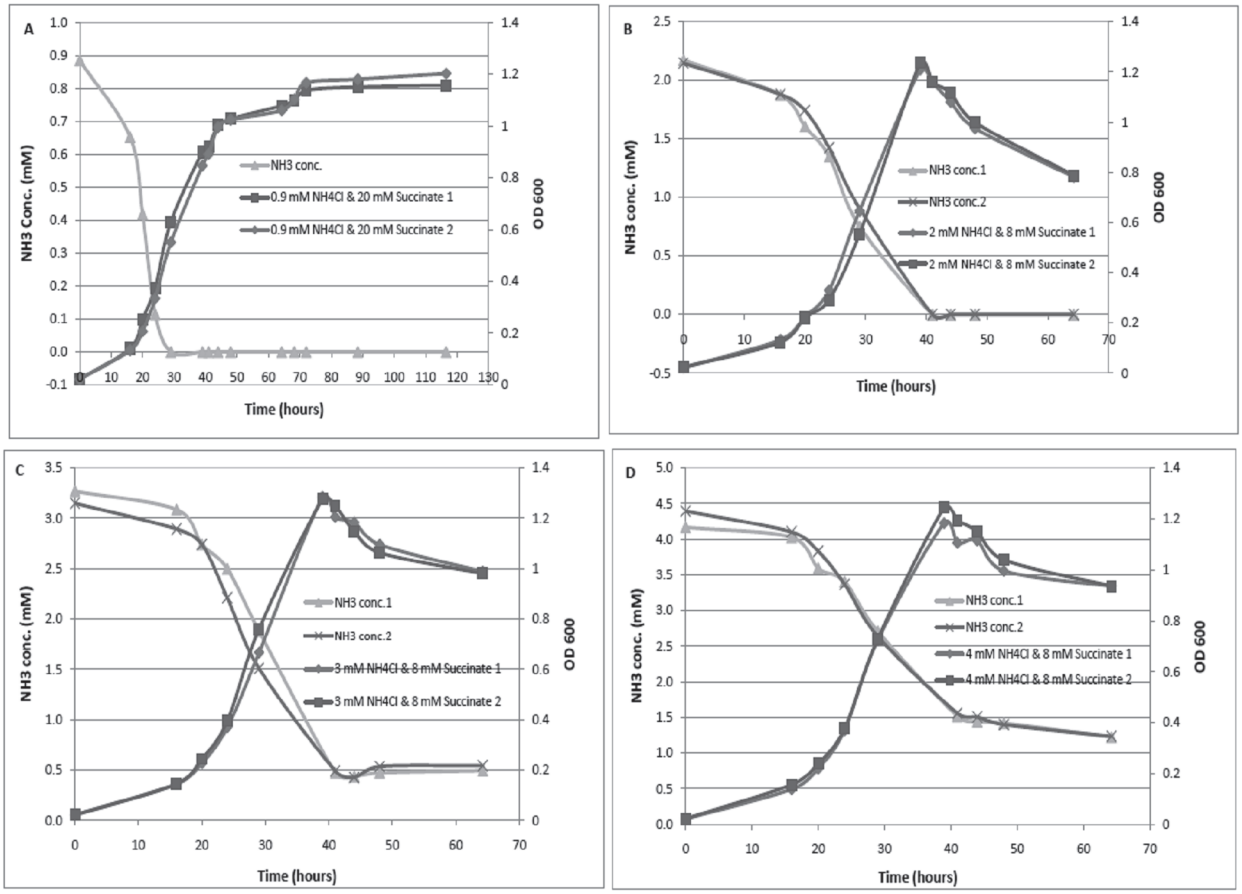

Figure 20. Ammonium concentration and KTR9 growth in N-limited cultures (A) and in three C-limited cultures (B, C, D).

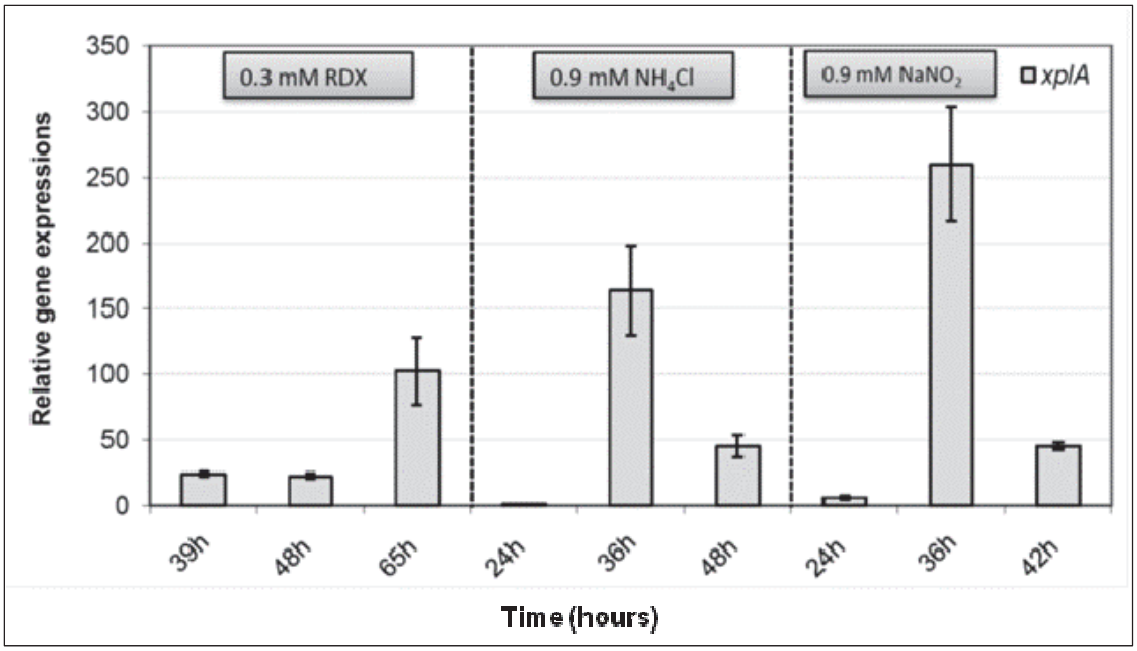

Figure 21. *xplA* relative gene expression at different growth stages of KTR9 grown on RDX, NH_4Cl, and $NaNO_2$ using qPCR. Expression levels are normalized to *sigA* expression, and a value of 1.0 was assigned to the lowest value measured.

ammonia or nitrite in the cell medium may play a role in the expression of *xplA*. Indeed, the presence of either N source appeared to repress *xplA* expression (expression approximately 25-fold lower than during growth on RDX), and depletion of either appeared to lead to *xplA* induction (more than 100-fold).

Since nitrogen levels appeared to regulate *xplA* expression and RDX removal, the expression of the *xplA* gene was measured during growth of KTR9 under N-limiting conditions. Similarly, C-limiting conditions were examined. The *xplA* gene was highly induced as cultures became N-limited. However, the expression level of the *xplA* gene was low in C-limited conditions (Figure 22). These data suggest that N limitation in KTR9 induces *xplA* to levels much higher than when RDX is used as an N source. Indeed, *xplA* expression may be driven principally by N-limitation and not by RDX presence.

GlnR regulation

GlnR is a central regulator of nitrogen uptake and metabolism in actinomycetes related to *Gordonia*. More specifically, it controls the expression of genes responsible for the utilization of alternate N sources, up-regulating these genes under conditions of N limitation. It is therefore hypothesized

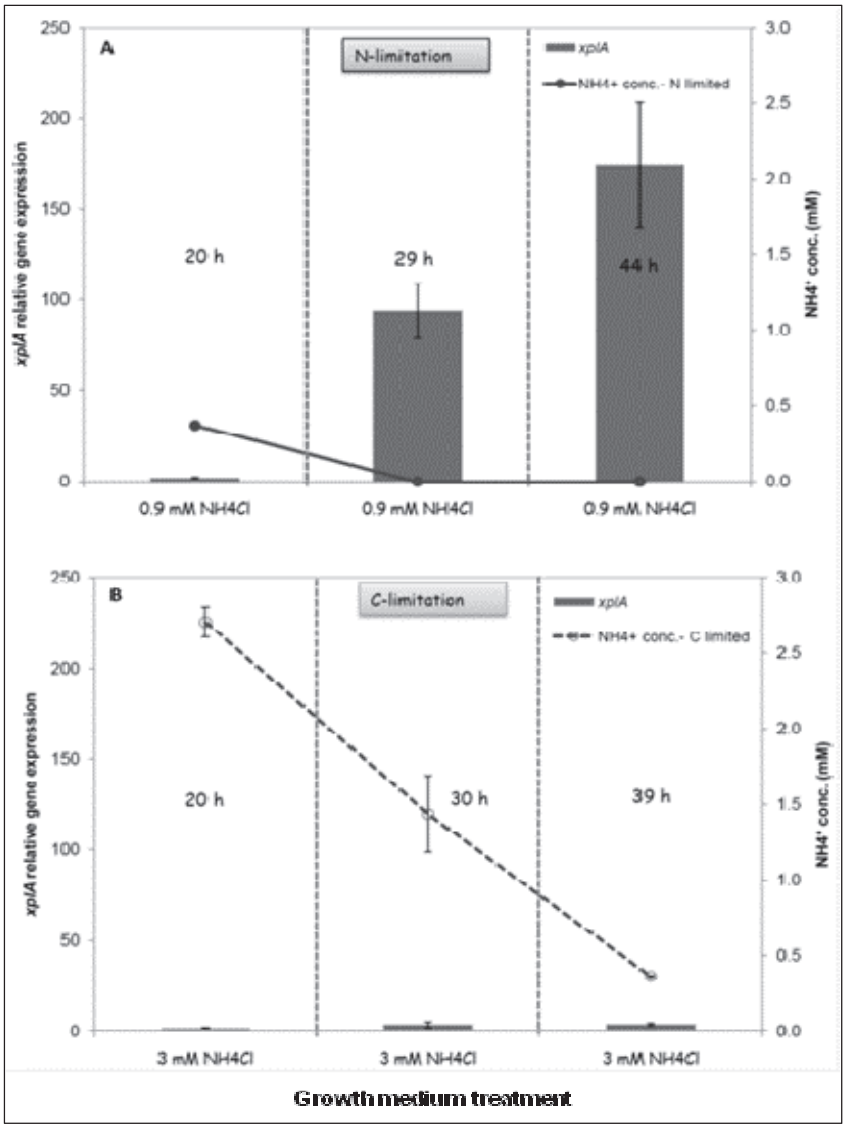

Figure 22. Gene expression of *xplA* and ammonia concentration at different growth stages of KTR9 grown on N-limited and C-limited conditions (n =3).

that GlnR plays a role in regulating RDX degradation in KTR9. Consistent with this hypothesis, a *glnR* disruption mutant did not use RDX as a sole N source (below). Using MEME and the GlnR binding sequence from *Streptomyces coelicolor*, GlnR binding sequences were predicted to occur upstream of several N-utilization genes including a high affinity site upstream of KTR9_1987 (ammonium permease). However, no significant GlnR binding site was predicted to occur upstream of the *xpl* operon. In gel mobility shift assays, 150 bp amplicons containing predicted binding sites showed weak binding except for that associated with the nitrate reductase gene (KTR9_1290). In these experiments, up to 2 µg of protein was used. Interestingly, strong binding was observed between GlnR and the region

upstream of KTR9_1290 when GlnR was reduced to 0.7 µg and 10 mM (460 mg/L) nitrite was added into the protein-DNA mixture before it was loaded to the gel. This result suggests that the presence of the nitrite ion might alter the affinity of GlnR to certain DNA regions.

Nitrite is generally rapidly transformed to nitrate in soil and nitrite rarely accumulates. Nitrite-oxidizing bacteria can be inhibited by high levels of free ammonia (NH_3) that might occur in alkaline soils with pH values greater than 9.2 (Smith et al. 1997). Temporary increases in the rate of ammonium oxidation compared to the rate of nitrite oxidation can lead to the accumulation of nitrite in soil. This has been observed in a semi-arid soil at the beginning of the wet season but the levels of nitrite (1.74 ± 0.9 µg/g sdw; Gelfand and Yakir 2008) were less than the concentration of nitrite that bound to GlnR. Soils collected from two military ranges with a semi-arid climate (Ft. Polk, LA and Ft. Bliss, TX) contained NO_3-N concentrations between 2 and 10 mg/kg sdw and NH_4^+-N concentrations from < 17 to 20 mg/kg sdw (Crocker et al. 2005). Thus, inorganic nitrogen concentrations in surface soils on ranges that will be exposed to RDX are not expected to inhibit aerobic RDX biodegradation or affect the binding of GlnR to DNA.

Phenotypic studies of the KTR9 glnR deletion mutant

To confirm that the *sacB* counterselection system succeeded in gene deletion in KTR9, the genotype of the *glnR* mutant was verified by PCR. The *glnR* region was amplified in mutant and wild type cells (Figure 23). The size of the resulting amplicons was in accordance with the expected size (Table 14, Figure 23), confirming that *glnR* was indeed deleted in the mutant strain. Consistent with the central role of GlnR in N metabolism, an RHA1 *glnR* deletion mutant was unable to grow on urea, nitrate, or acetonitrile as the N source and showed impaired growth on ammonium (data not shown). Growth of the KTR9 *gln*R mutant was observed on 18.7 mM NH_4Cl, 10 mM glutamine, and 20 mM urea (data not shown). Both mutants were strongly impaired for growth on 2 mM cytosine, 10 mM valine, and 10 mM nitrate (data not shown). When growth experiments were executed at N concentrations equivalent to that of 0.3 mM RDX, growth of the KTR9 mutant on 0.9 mM NH_4Cl, glutamine, urea, and cytosine was impaired relative to that of the wild-type (Appendix A). The mutant strain was unable to grow on 0.3 mM RDX (Figure 24A), 2 mM nitrite, and 2 mM nitrate (Figure 24B). These results suggest that GlnR is involved in the regulation of nitrate or nitrite assimilation processes.

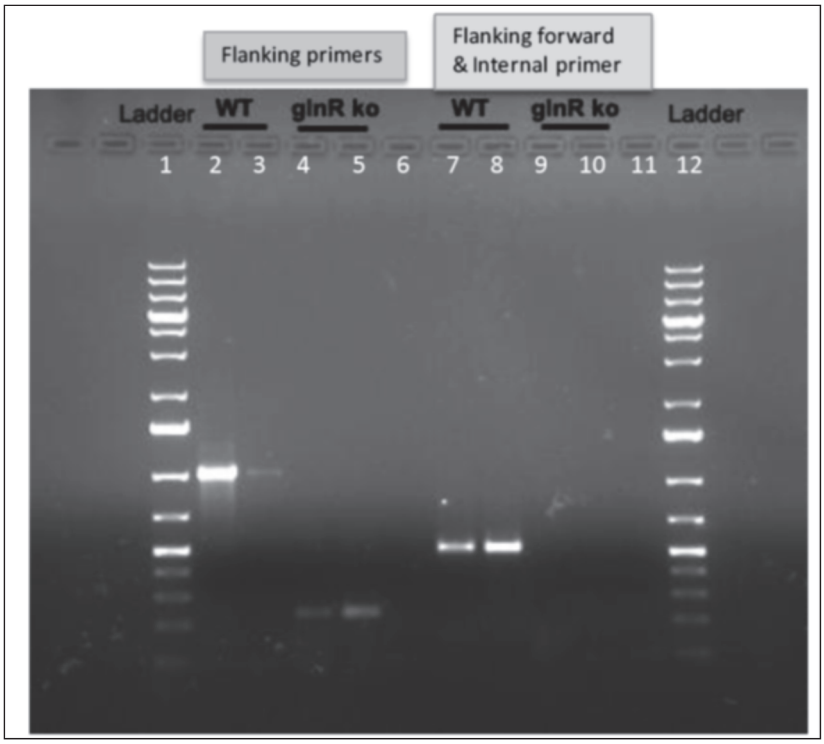

Figure 23. PCR amplification products of the *glnR* region in KTR9 wild-type and the *glnR* mutant strains. Flanking primers (forward and reverse primers located 250 bp upstream and downstream of *glnR* gene) were used for lanes 2-5. Flanking forward primer (250 bp upstream of the *glnR* gene) and internal primer (within the ORF of *glnR* gene) were used for lanes 7-10. Lanes 1 and 12 represent the DNA ladder.

Table 14. Expected PCR product sizes of the *glnR* gene when using different set of primers in KTR9 wild type cells and *glnR* mutant cells. Lane numbers refer to Figure 23.

PCR Primers	KTR9	KTR9 ΔglnR mutant
Two flanking primers	1004 bp (lanes 2 & 3)	< 300 bp (lanes 4 & 5)
Flanking + internal primers	506 bp (lanes 7 & 8)	-- (lanes 9 & 10)

Degradation of RDX and xplA gene expression by the glnR mutant grown on different N sources

The *glnR* mutant is incapable of utilizing RDX as a nitrogen source for growth, most likely because the mutant also cannot use nitrite as a nitrogen source for growth. Despite this fact, it is important to determine if the glnR mutant transforms RDX and if the mutant expresses the *xplA* gene when grown on different nitrogen sources. First of all, the greatest *xplA* gene expression in the KTR9 wild-type strain occurred whenever ammonium, nitrite, or RDX was depleted from the medium. After the addition of 0.9 mM NH_4Cl or 0.9 mM $NaNO_2$ (Figure 25A), the expression

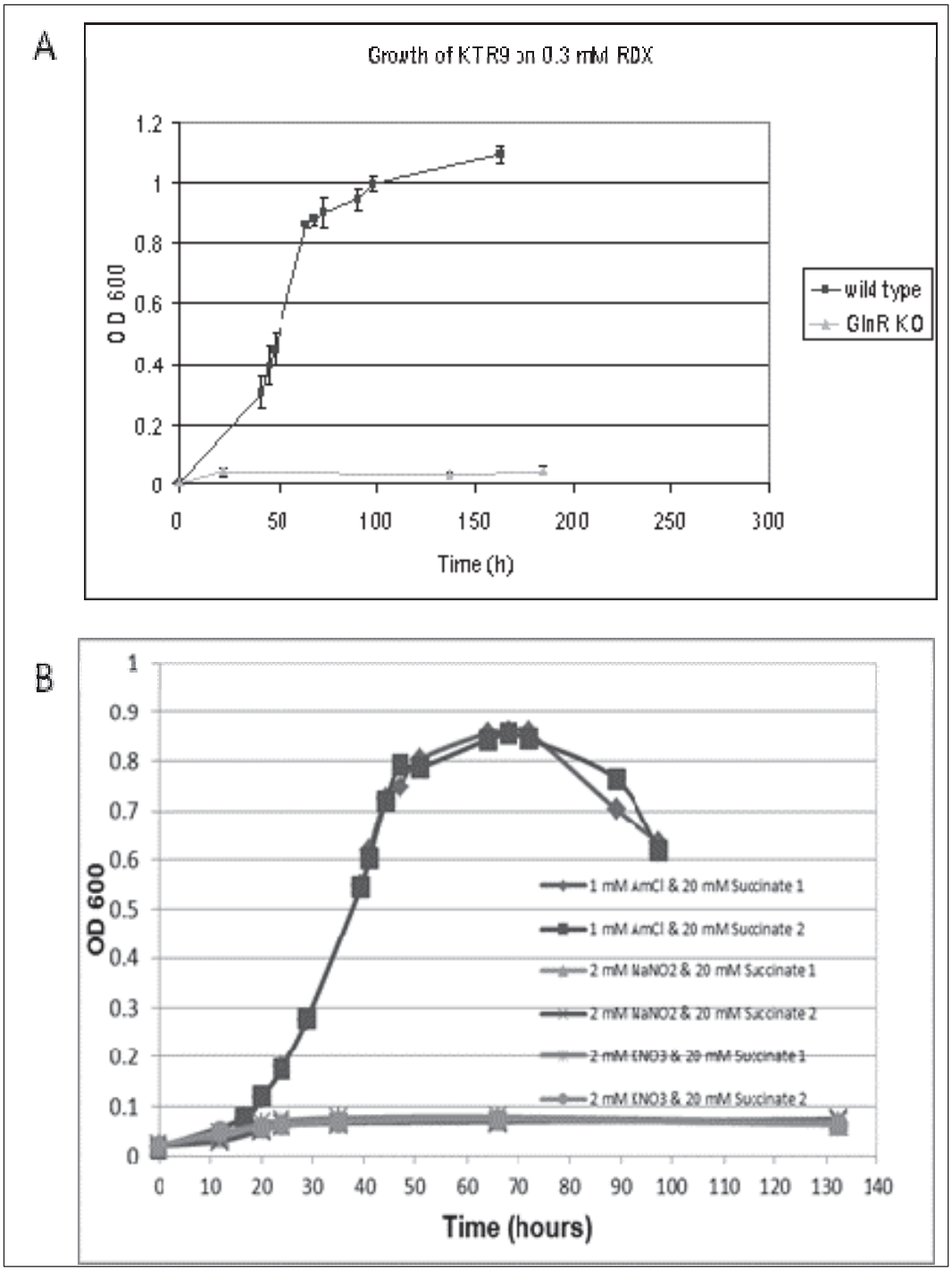

Figure 24. Growth of KTR9 wild-type (-■-) and *glnR* deletion mutant (-▲-) in M9 supplemented with Goodies, 20 mM succinate, and 0.3 mM RDX (A); or growth of the KTR9 *glnR* deletion mutant in M9 supplemented with Goodies, 20 mM succinate, and 1 mM NH_4Cl (♦,■), 2 mM $NaNO_2$ (▲, ×), or 2 mM KNO_3 (∗, •) (B).

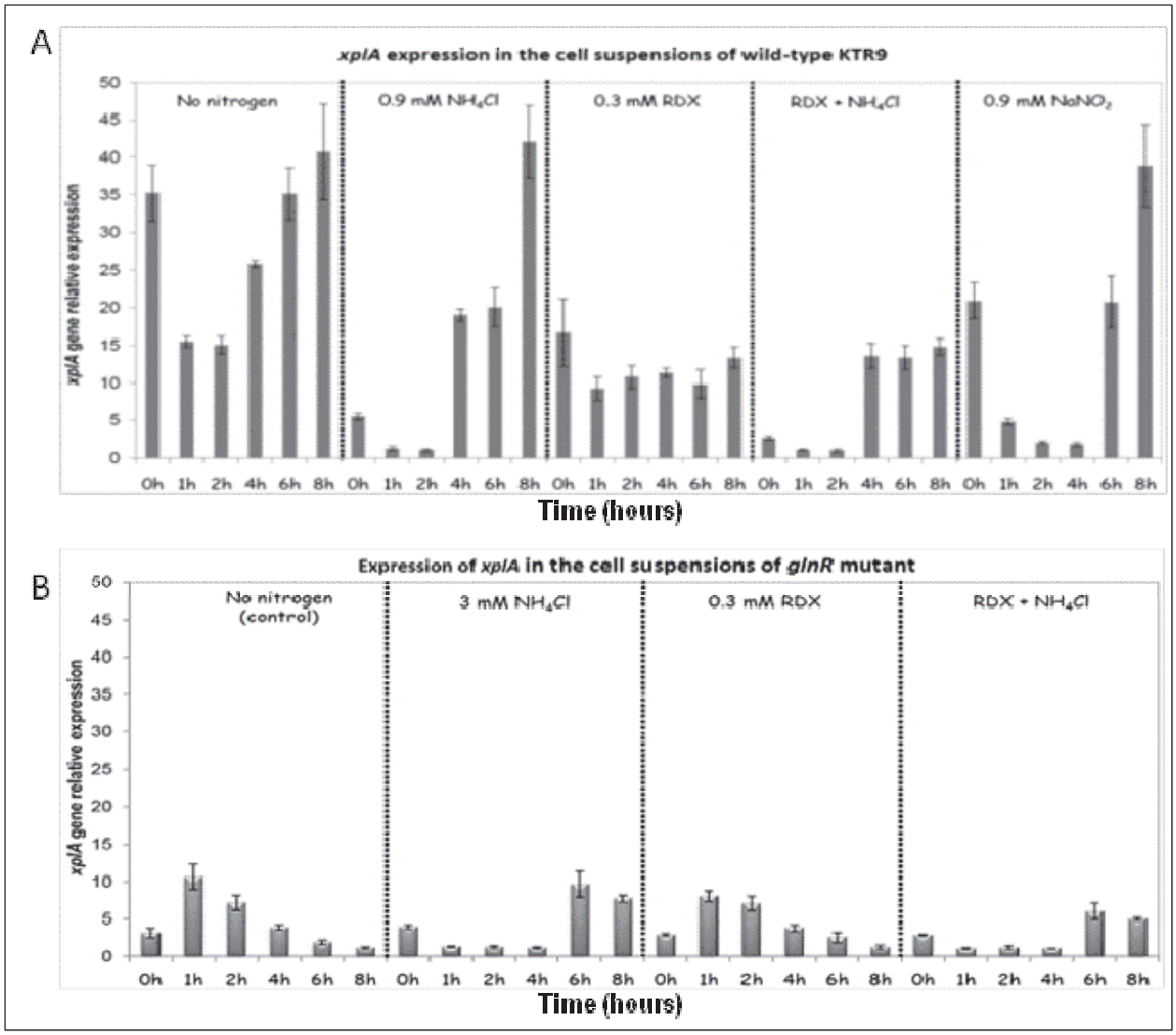

Figure 25. The relative expression of *xplA* in cell suspensions of the KTR9 (A) wild-type, and (B) *glnR* mutant and incubated with various N sources.

of *xplA* was repressed approximately 20- to 30-fold within the first 2 to 4 h relative to the treatment without added nitrogen. However, after 6 to 8 h of incubation with NH_4Cl or $NaNO_2$, the *xplA* gene was up-regulated and its expression level was similar to that observed in the no nitrogen treatment (Figure 25A). These results suggested that these cultures may be limited for nitrogen by this time, and that the *xplA* gene may be highly up-regulated in conditions of nitrogen limitation. Interestingly, the expression level of the *xplA* gene did not change much during 8 h of incubation with RDX, suggesting that RDX or some of its degradation product(s) is able to stabilize *xplA* expression (Figure 25A). Similarly, *xplA* was up-regulated in the *glnR* mutant whenever ammonium levels were depleted (after 6 h) in cultures grown with 3 mM NH_4Cl or 3 mM NH_4Cl plus 0.3 mM RDX

(Figure 25B), suggesting that the induction of the *xplA* gene is regulated by N limitation in both *glnR* mutant and wild-type cells. Thus, the repression of *xplA* expression by ammonium and nitrite is not dependent on GlnR.

While RDX was almost completely removed in the wild-type cell suspensions, only 20%-30% of the RDX disappeared from the *glnR* mutant cell suspensions after 8 h (Figure 26A), indicating that RDX is not efficiently degraded by the *glnR* mutant. Small amounts of nitrite accumulated in suspensions of the *glnR* mutant in treatments amended with 0.3 mM RDX or 0.3 mM RDX plus 3 mM NH_4Cl (Figure 26B), showing that denitration occurred when RDX was partially degraded in the *glnR* mutant. Since *xplA* is expressed in the *glnR* mutant, these data suggest that transport of RDX into the cell may depend on GlnR. A search was conducted to see if some of the up-regulated genes in the transcriptomic database would correspond to a transporter.

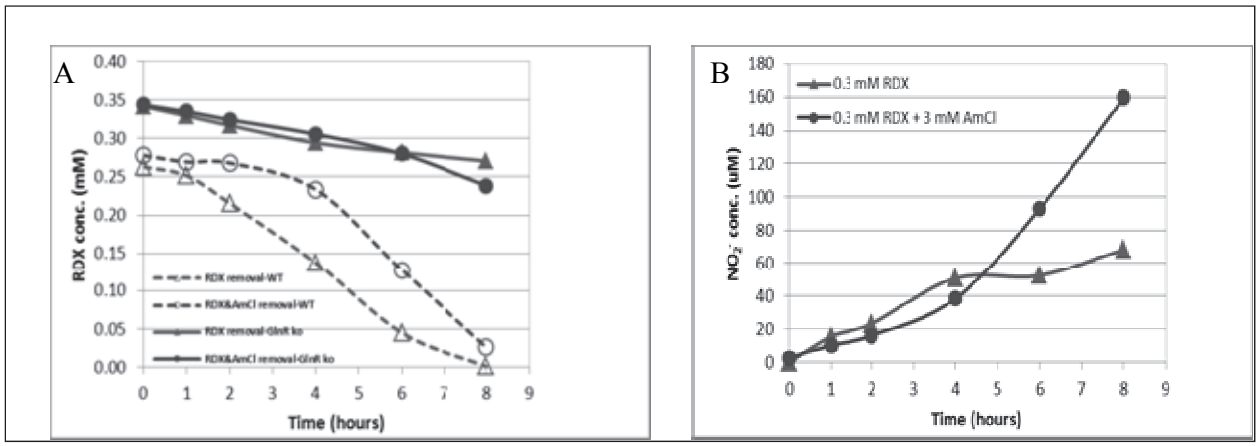

Figure 26. (A) RDX concentration in the cell suspensions of *glnR* mutant (solid lines) and KTR9 wild-type (dotted lines). (B) Nitrite accumulation in the medium of *glnR* mutant cell suspensions for treatment with 0.3 mM RDX and treatment with both RDX and NH_4Cl.

Expression of KTR9_0967

Genes *KTR9_0966*, *0967,* and *0968* were first noticed in Illumina transcriptomic data because they were the most up-regulated (up to 80-fold increase) among all expressed genes in RDX grown cultures compared to the NH_4Cl grown cells (Tables 15 and 16). These three genes are all located in an apparent operon on the KTR9 chromosome (data not shown). When the KTR9_0967 amino acid sequence was compared to known sequences in the NCBI nr database, a conserved domain search showed two possible identities. The first one consists of a sodium solute symporter family (SSF superfamily) and the second one, a CodB protein annotated as a

Table 15. Selected up-regulated genes in cells grown on RDX relative to cells grown on NH_4Cl.

Feature ID	Description	Proportions Fold Change	P-value
KTR9_0966	Hypothetical protein	10.1	$< 10^{-16}$
KTR9_0967	Permease for cytosine/purines, uracil, thiamine, allantoin transporter	86.1	$< 10^{-16}$
KTR9_0968	N-methylhydantoinase B / acetone carboxylase, alpha subunit	87.1	$< 10^{-16}$
KTR9_0969	N-methylhydantoinase A / acetone carboxylase, beta subunit	80.2	$< 10^{-16}$
KTR9_1738	Large subunit of ring-hydroxylating dioxygenase	4.3	$< 10^{-16}$
KTR9_1745	Permease, MFS superfamily	4.3	$< 10^{-16}$
KTR9_1746	FMN-binding protein	4.7	$< 10^{-16}$
KTR9_3137	Esterase / lipase	4.1	$< 10^{-16}$

Table 16. Selected down-regulated genes in cells grown on RDX relative to cells grown on NH_4Cl.

Feature ID	Description	Proportions Fold Change	P-value
KTR9_0380	Permease, MFS superfamily	-4.3	$< 10^{-16}$
KTR9_0593	Chaperonin GroEL (HSP60 family)	-4.2	$< 10^{-16}$
KTR9_1819	Membrane protein	-5.1	$< 10^{-16}$
KTR9_2448	Peptidase_M23 superfamily	-4.5	$< 10^{-16}$
KTR9_3381	Trypsin-like serine proteases	-15.7	$< 10^{-16}$
KTR9_3947	4-aminobutyrate aminotransferase and related aminotransferases	-27.3	$< 10^{-16}$
KTR9_3948	FAD/FMN-dependent dehydrogenases	-46.9	$< 10^{-16}$
KTR9_3949	Succinate-semialdehyde dehydrogenase	-54.3	$< 10^{-16}$

purine-cytosine permease. In *E.coli* the CodB protein is a cytosine permease and its transcript level is regulated by nitrogen (Danielsen et al. 1992; Muse et al. 2003). The *codB* gene showed 3-fold up-regulation in nitrogen-limited medium compared to a nitrogen rich medium in *E. coli*. Since *KTR9_0966* was highly up-regulated in RDX grown cultures, it may be a transporter for RDX in KTR9. Therefore, *KTR9_0966* gene expression was measured in growing KTR9 cells. The *KTR9_0966* gene was most highly up-regulated in the mid exponential phase of RDX grown cultures in comparison with

cultures grown on inorganic nitrogen sources such as NH_4Cl or $NaNO_2$ (Figure 27). In RDX grown cultures, the *KTR9_0966* expression level was quite low in the early growth stage (39 and 48 h) when RDX was present in the cultures. However, the abundance of the *KTR9_0966* transcript showed a dramatic increase at the mid-log phase when RDX was depleted. Although this pattern of expression does not strongly suggest that *KTR9_0966* is involved in the RDX transport, this remains a possibility. Alternatively, this gene could be responsible for the efflux of expected RDX metabolites such as NDAB. Nevertheless, the current data do not rule out the possibility that this gene is only controlled by nitrogen level and is not involved in the transport of RDX or its metabolites.

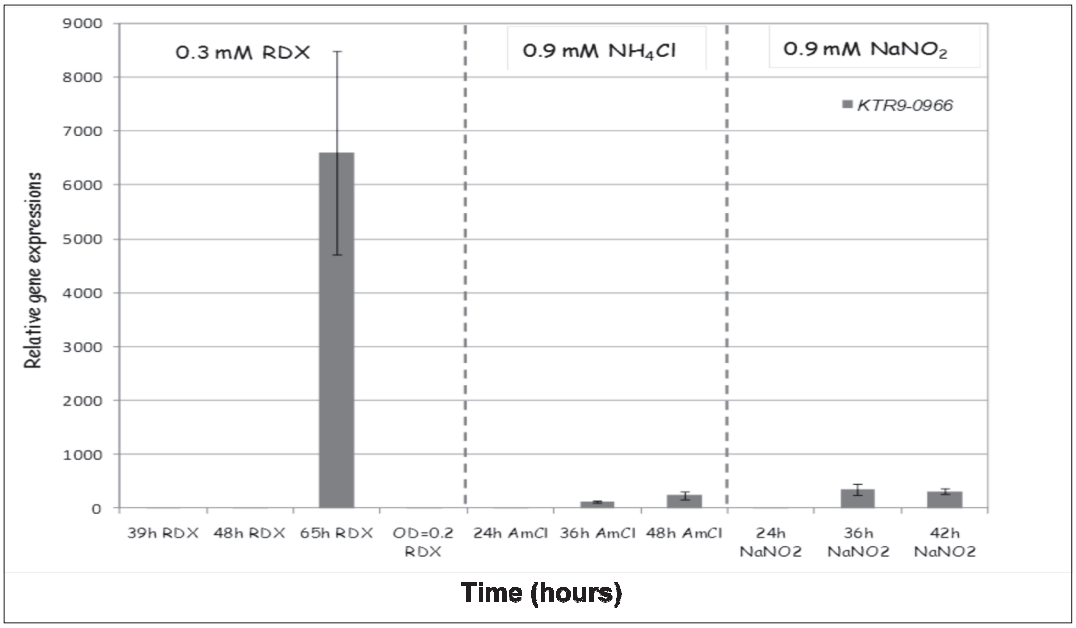

Figure 27. Expression of *KTR9_0966* in KTR9 cells grown using different N-sources. Cells were harvested at the following growth stages: lag-phase (39 h RDX); early log-phase (48 h RDX, 24 h NH_4Cl and $NaNO_2$); mid-log phase (65 h RDX, 36 h NH_4Cl and $NaNO_2$); and late log-phase (48 h NH_4Cl and 42 h $NaNO_2$).

Deep sequencing transcriptomic analysis

Transcriptomic sequencing yielded ~58 million reads from cells grown on either NH_4Cl or RDX. The longest reads were 76 bp for both treatments (Table 17). When these reads were aligned with the KTR9 genome, approximately 20 million reads were mapped to the 5076 annotated ORFs. Many of the reads aligned with tRNA genes, which are not included in the coded gene annotation. Reads aligning to rRNA genes were excluded from the dataset.

Table 17. Number of total reads (pair-ended tag sequencing) from Illumina sequencing.

Reads	RDX Treatment	NH_4Cl (Control)
Total	57,947,276	58,167,452
Mapped	20,162,560	20,492,241
Uniquely	17,071,161	17,922,366
Non specifically	3,091,399	2,569,875
Unmapped	37,784,716	37,675,211
Longest	76 bp	76 bp

Of the 5076 mapped reads, 267 genes showed differential expression in the RDX treatment versus the NH_4Cl treatment. The difference in expression of these genes was more than two-fold with a cutoff P value below 0.05 (Z test). Of these, 116 genes were upregulated and 151 genes were downregulated on RDX. Selected up- and down-regulated genes are listed in Tables 15 and 16. In several cases, consecutive locus tags indicate groups of co-regulated genes (operons). However, this transcriptomic experiment was not as informative about genes expressed during the degradation of RDX, because the RDX was depleted by the time the cells were harvested.

Conclusions

An in-depth physiological characterization of the correlation between nitrogen and carbon substrate growth conditions, *xplA* gene expression, and RDX degradation indicated that *xplA* expression may be driven principally by nitrogen limitation and not by the presence of RDX. The presence of ammonium or nitrite at concentrations above 4 mM repressed *xplA* expression (expression approximately 25-fold lower than during growth on RDX), and depletion of either appeared to lead to *xplA* induction (more than 100-fold). This repression of *xplA* and RDX removal did not appear to be regulated by the global nitrogen regulator, GlnR. The transcriptomic sequencing generally supported the earlier differential gene expression studies (Section titled "Regulation of RDX Biotransformation and Gene Expression in *Gordonia* sp. KTR9") in that potential transporter and permeases were apparently up-regulated in the presence of RDX. However, the transcriptomic and subsequent gene expression study with a possible permease did not conclusively prove a role of the permease in RDX transport into strain KTR9. Thus, only *xplA* met the biomarker criteria of (1) being specific to RDX degradation via denitration to NDAB, (2) a global distribution at RDX contaminated sites, and (3) high sequence homology among the known *xplA* gene sequences.

4 Determination of RDX Biodegradation Pathways in *Shewanella oneidensis* MR-1

Introduction

A diversity of bacteria can degrade RDX anaerobically, including strict anaerobic species, *Clostridium* and *Desulfovibrio*, and facultative anaerobes *Geobacter*, *Shewanella*, and genera within the *Enterobacteriaceae*. RDX-degrading *Shewanella* strains have been isolated from cold marine sediment (Zhao et al. 2005, 2006). Among these isolates, *S. halifaxensis* was shown to degrade RDX anaerobically, under trimethylamine *N*-oxide (TMAO)-respiring conditions, via a major route consisting of the sequential reduction of the $N\text{-}NO_2$ groups to produce the corresponding nitroso derivatives MNX, DNX, and TNX (Figure 2B) and a minor route involving denitration followed by ring cleavage (Figure 2B) to produce methylenedinitramine (MEDINA) and its decomposition products HCHO and N_2O (Halasz et al. 2002). Furthermore, *S. halifaxensis* and *Shewanella sediminis* are well-adapted to explosives since they also transform TNT, 2,4-dinitrotoluene, and perchlorate (Zhao et al. 2010). Other species of *Shewanella* share this trait but transform the explosives at much slower rates (Zhao et al. 2010). Since *Shewanella* species use both the nitroso route and denitration route for RDX degradation, RDX-degrading *Shewanella* were an attractive choice in this project in order to identify genes and enzymes involved in anaerobic RDX catabolism. The freshwater strain, *Shewanella oneidensis* strain MR-1, was chosen as the model strain for the anaerobic work as it was more applicable to terrestrial groundwater environments than the marine *Shewanella* strains.

S. oneidensis is very well characterized physiologically and biochemically due to its ability to transform a variety of toxic metals and other contaminants. In addition, the genome of strain MR-1 has been sequenced and annotated so that gene microarrays are commercially available for gene expression studies. The objectives of this task were:

1. To investigate the physiology and metabolic pathways used by MR-1 to transform RDX.
2. To determine whether induction or up-regulation of RDX activity occurred in the presence of RDX.

3. To use differential gene expression studies with MR-1 to determine genes associated with the transformation of RDX by strain MR-1.
4. To generate transposon insertion mutants of MR-1 and functionally and genetically characterize the mutants with respect to RDX transformation.

Growth physiology of *Shewanella oneidensis* MR-1 on RDX as a carbon or nitrogen source or electron acceptor

Introduction

The actual mechanism(s) of RDX biodegradation in strain MR-1 was not known at the beginning of this project. Initial studies with MR-1 were designed to determine the physiology and mechanism(s) of RDX transformation when MR-1 was grown in the presence of RDX. The ability of strain MR-1 to use RDX as a carbon or nitrogen source, or an electron acceptor for growth, was determined using growth studies. Resting cell assays were used to establish the mechanism(s) of RDX transformation. It was also important to determine whether an up-regulation or induction of RDX activity occurred in MR-1 during growth in the presence of RDX. This latter information is important to the interpretation of differential gene expression studies with strain MR-1.

Methods

Bacterial growth conditions

Shewanella oneidensis strain MR-1 was purchased from the American Type Culture Collection (*ATCC* 700550). Strain MR-1 was cultivated with RDX in the minimal medium MMR2 (Tang et al. 2007) and consisted of (per L of distilled water): 1.34 mM KCl, 5 mM NaH_2PO_4, 0.7 mM Na_2SO_4, 1 mM $MgSO_4 \cdot 7H_2O$, 0.2 mM $CaCl_2 \cdot 2H_2O$, 50 mM NaCl, 20 mM PIPES, a vitamin mixture (1 L of medium contains 0.02 mg biotin, 0.02 mg folic acid, 0.1 mg pyridoxine-HCl, 0.05 mg thiamine-HCl, 0.05 mg riboflavin, 0.05 mg nicotinic acid, 0.05 mg DL-pantothenic acid, 0.05 mg *p*-aminobenzoic acid, 0.05 mg lipoic acid, 2 mg choline chloride, 0.01 mg vitamin B12), and trace elements (1 L of medium contains 10 mg $FeCl_2 \cdot 4H_2O$, 5 mg $MnCl_2 \cdot 4H_2O$, 3 mg $CoCl_2 \cdot 4H_2O$, 2 mg $ZnCl_2$, 0.5 mg $Na_2MoO_4 \cdot 4H_2O$, 0.2 mg H_3BO_3, 1 mg $NiSO_4 \cdot 6H_2O$, 0.02 mg $CuCl_2 \cdot 2H_2O$, 0.06 mg $Na_2SeO_3 \cdot 5H_2O$, 0.08 mg $Na_2WO_4 \cdot 2H_2O$). The medium was supplemented with 28 mM NH_4Cl and 20 mM sodium lactate as the nitrogen and carbon source, respectively. Either trimethylamine N-oxide (TMAO; 30 mM) or fumarate (23 mM) was

used as the electron acceptor. The pH was adjusted to 7.0 before filter sterilization.

Growth assays with RDX as the sole carbon, nitrogen, or terminal electron acceptor

The ability of strain MR-1 to use RDX as a sole nitrogen or carbon source or as a terminal electron acceptor was assessed in the minimal medium MMR2 under anaerobic conditions. Ammonium chloride (NH_4Cl) was omitted from the medium when RDX was tested as the sole nitrogen source for growth; lactate was omitted when RDX was tested as the sole carbon source; TMAO and fumarate were omitted as the electron acceptor when RDX was tested for its ability to support anaerobic respiration. The growth of MR-1 on RDX was evaluated by optical density (OD_{600}), dry weight, and protein content (BCA Protein Assay kit, Pierce, Rockford, IL). Transformation of RDX by strain MR-1 was also examined in the rich LB medium, and in MMR2 supplemented with peptone plus yeast extract (both at 0.2 % w:v).

Induction of RDX activity in Shewanella oneidensis MR-1

The nature of the regulation of RDX degradation was investigated in strain MR-1 using protein synthesis inhibitors. Strain MR-1 was grown to the exponential phase in MMR2 medium with NH_4Cl as the nitrogen source. The cells were harvested by centrifugation at 18 000 x *g* for 20 min at 4 °C, washed, and resuspended in 25 mM phosphate buffer (pH 7.0). All the reaction mixtures for the resting cells contained the cell suspensions (final OD_{600} of 1.0) and 20 ppm RDX. The protein synthesis inhibitors chloramphenicol (150 µg/mL) and rifampicin (100 µg/mL) were individually added to one part of the cells, while a third part was left free of inhibitors. Resting cells were incubated anaerobically, at room temperature, in the dark, with mixing at 150 rpm. At defined incubation times, triplicate vials were sacrificed and the concentration of RDX in the samples was analyzed by HPLC.

In a second experiment, induction of RDX-related enzymes was determined by comparing the loss of RDX in MR-1 cultures that had been grown in the presence or absence of RDX. Strain MR-1 was cultivated in three 500-mL serum bottles containing 350 mL of MMR2. At mid exponential phase, one bottle received 5 ppm RDX (from an acetone stock) and 15 µg/mL chloramphenicol (in 95% ethanol), one bottle received 5 ppm RDX, and the third

bottle was not amended with RDX or chloramphenicol. An equal volume of ethanol or ethanol plus acetone was added to the second and third bottles, respectively, to account for the solvents added from the RDX and chloramphenicol stocks (Table 18). The MR-1 cultures were incubated for an additional 3 h and then the cells were harvested by centrifugation (as above), washed, and resuspended in 25 mM phosphate buffer (pH 7.0). The reaction mixtures for the resting cell assays consisted of the cell suspensions (final OD_{600} of 1.2) and 20 ppm RDX. Triplicate samples were analyzed for RDX at defined incubation times.

Table 18. *Shewanella oneidensis* MR-1 RDX and chloramphenicol incubation conditions.

Treatment	Addition of			
	RDX	Chloramphenicol[1]	Ethanol	Acetone
Control	No	No	Yes[2]	Yes[3]
RDX[6]	Yes	No	Yes	Yes[4]
RDX + Chloramphenicol	Yes	Yes	Yes[5]	Yes

[1]Chloramphenicol added at 15 μg mL^{-1}.

[2]Added as an equal volume to chloramphenicol addition.

[3]Added as an equal volume to RDX addition.

[4]Added due to RDX addition.

[5]Added due to chloramphenicol addition.

[6]RDX added at 5 mg mL^{-1}.

RDX degradation by actively growing MR-1 cultures

Bacterial growth and RDX degradation were followed in MMR2 medium supplemented with lactate, TMAO, and RDX at 90 μM. The medium was distributed in sterile glass serum bottles sealed with rubber septa and aluminum crimp caps. The bottles were made anaerobic by degassing for 30 min and then performing five cycles of degassing and recharging with argon. Bacterial cells were inoculated at an initial OD_{600} of 0.04. Abiotic controls containing RDX in non-inoculated culture medium and controls containing bacteria in medium without RDX were conducted in parallel. The bottles (in triplicate) were incubated for a period of 72 h in the dark at 25 ^{o}C with agitation at 150 rpm. Growth was followed by optical density (OD_{600}). Samples were collected for analysis of RDX and its products.

Resting cell assays for metabolic studies

For time course experiments, cells grown anaerobically in MMR2 with lactate, TMAO, and 22.5 μM RDX were harvested at the late exponential phase, washed in a cold 25-mM sodium phosphate buffer (pH 7.0), and resuspended at a concentration of 2 mg protein mL^{-1} in the same buffer but containing ~90 μM RDX. The reactions were performed in serum bottles that were sealed and made anaerobic by briefly degassing (1 min) and then purging with argon for 10 min at 5 psi. The bottles were incubated at 25 ^{o}C in the dark. Non-inoculated controls and controls without RDX were conducted in parallel. At selected times, aliquots of the cell suspensions were collected, centrifuged at 16,000 x *g* for 10 min and the supernatant was used for chemical analysis of RDX and its breakdown products. The results are presented as the mean of triplicate assays with the standard errors (SE). Protein concentration was determined by the bicinchoninic acid method using the BCA Protein Assay kit. Some microcosms were spiked with L-[U-^{14}C]RDX (0.038 μCi) to measure mineralization (liberated as $^{14}CO_2$) with a Tri-Carb 4530 liquid scintillation counter (model 2100 TR; Packard Instrument Company) as described previously (Zhao et al. 2002).

RDX and metabolite analyses

RDX, MNX, DNX, and TNX were analyzed by reverse phase HPLC. The HPLC was connected to a photodiode array detector set at 254 nm. Samples (50 μL) were injected into a Supelcosil LC-CN column (inside diameter, 4.6 mm; length, 25 cm; Supelco, Oakville, Ontario, Canada), and the analytes were eluted by using a methanol-water gradient at a flow rate of 1.5 mL/min (Halasz et al. 2002). RDX ring-cleavage products, NDAB and MEDINA, were analyzed as previously reported using a Waters HPLC system with an AnionSep Ice-Ion-310 Fast organic acids column (St. Louis, Missouri, USA) maintained at 35°C (Bhushan et al. 2003). The mobile phase was acidified water (pH 2.0) at a flow rate of 0.6 mL/min. Chromatograms were taken at a wavelength of 225 nm.

Nitrous oxide (N_2O) was analyzed in the headspace of collected samples using an Agilent 6890 gas chromatograph equipped with an electron capture detector (ECD). Headspace gas samples were manually injected with a gastight syringe on a 3.65-m x 3-mm Chromosorb 102 column (60-80 mesh) maintained at 50°C for 5 min. Helium at 30 mL/min was the carrier gas and the injector and the detector were maintained at 125 °C and 350 °C, respectively.

Nitrite (NO_2^-) and nitrate (NO_3^-) were analyzed by ion chromatography according to EPA Method 300.0 (EPA) using a Dionex DX 120 ion chromatograph (Sunnyvale, California, USA) equipped with a 4-mm x 50-mm AG18 guard column and a 4-mm x 250-mm AS18 analytical column. NO_2^- and NO_3^- were eluted from the column with 30.4 mM KOH and quantified by suppressed conductivity detection. Other RDX metabolites, such as formamide, ammonium, formaldehyde, and formic acid, were analyzed as described previously (Fournier et al. 2002, Halasz et al. 2002).

Results and discussion

Growth assays with RDX as the sole carbon, nitrogen or terminal electron acceptor

Shewanella oneidensis MR-1 can rapidly degrade RDX under anaerobic conditions when provided with other substrates that support growth (Figure 28). Significant growth of MR-1 within 20 h was observed in MMR2 medium supplemented with 0.2% peptone plus 0.2% yeast extract. During this time, approximately 50% of the RDX added was degraded by MR-1 with all of the RDX being consumed after 60 h of incubation. Similarly, it was observed that growth and viability of strain MR-1 in rich LB medium was enhanced by the addition of RDX (Figure 29). These results are consistent with an enhancement in the viability of *S. halifaxensis* by RDX, suggesting that RDX may be a weak electron acceptor in both strains (Kwon and Finneran 2008b; Zhao et al. 2010). However, anaerobic growth of MR-1 in mineral salts medium MMR2 was not supported by the addition of RDX as the sole nitrogen source, carbon source, or electron acceptor (data not shown). Thus, it appears as if the anaerobic degradation of RDX by strain MR-1 is most likely co-metabolic, with alternate substrates providing carbon, nitrogen, and energy for growth. This conclusion does not exclude the possibility that nitrogen produced from the degradation of RDX can be utilized for growth by MR-1.

Induction of RDX activity in Shewanella oneidensis MR-1

The results of duplicate induction assays demonstrated that RDX induced the expression of RDX degrading genes to some extent. Figure 30 shows the effect of the protein synthesis inhibitors chloramphenicol and rifampicin on the degradation rates of RDX by resting cell suspensions of strain MR-1. In the presence of rifampicin, RDX degradation was completely inhibited, while the addition of chloramphenicol inhibited the rate of RDX

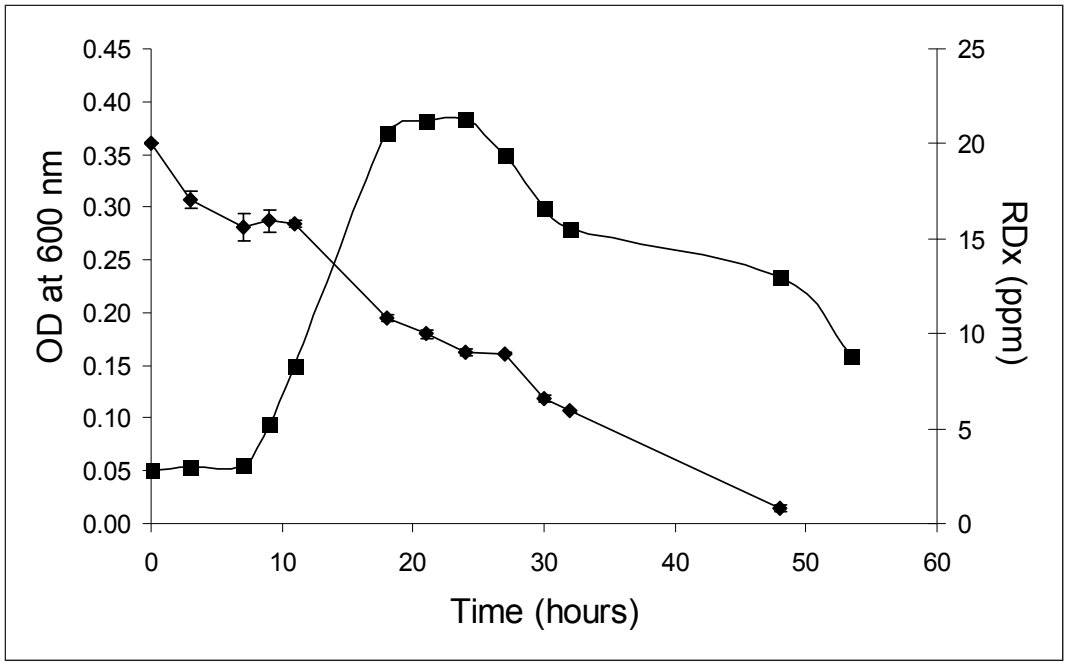

Figure 28. Anaerobic growth (■) and RDX removal (◆) by *Shewanella* MR-1 in minimal medium MMR2 supplemented with 0.2% peptone and yeast extract.

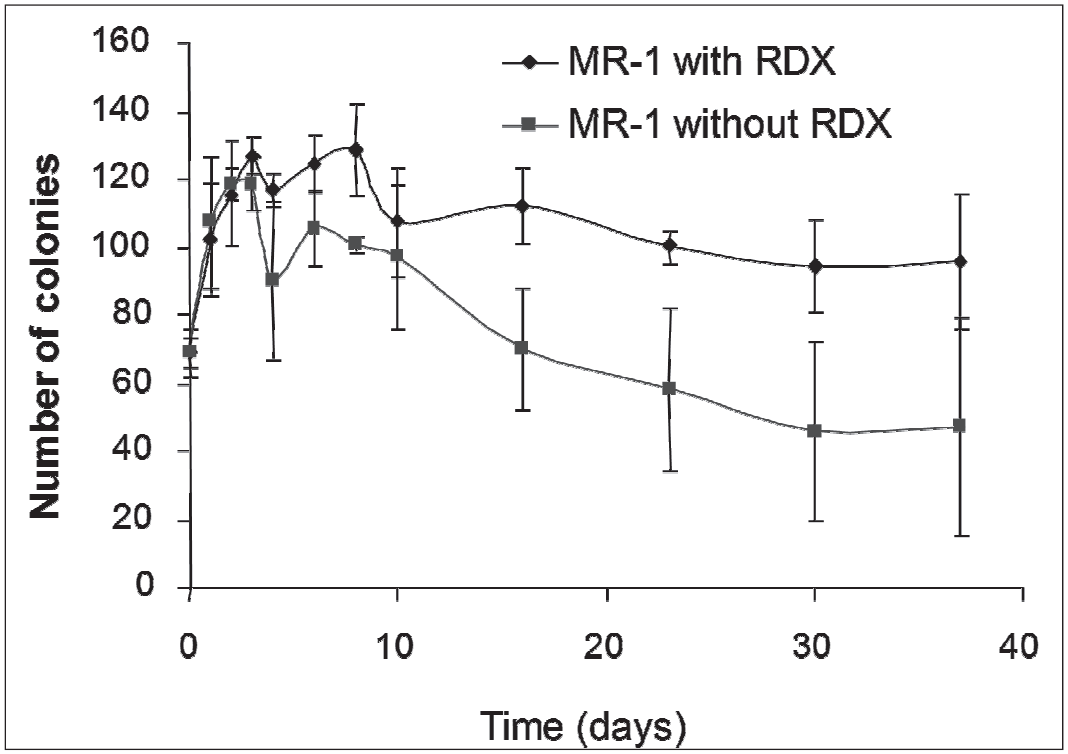

Figure 29. Plate counts for MR-1 incubated in LB medium oversaturated with RDX. The error bars represent the standard deviations of triplicate cultures.

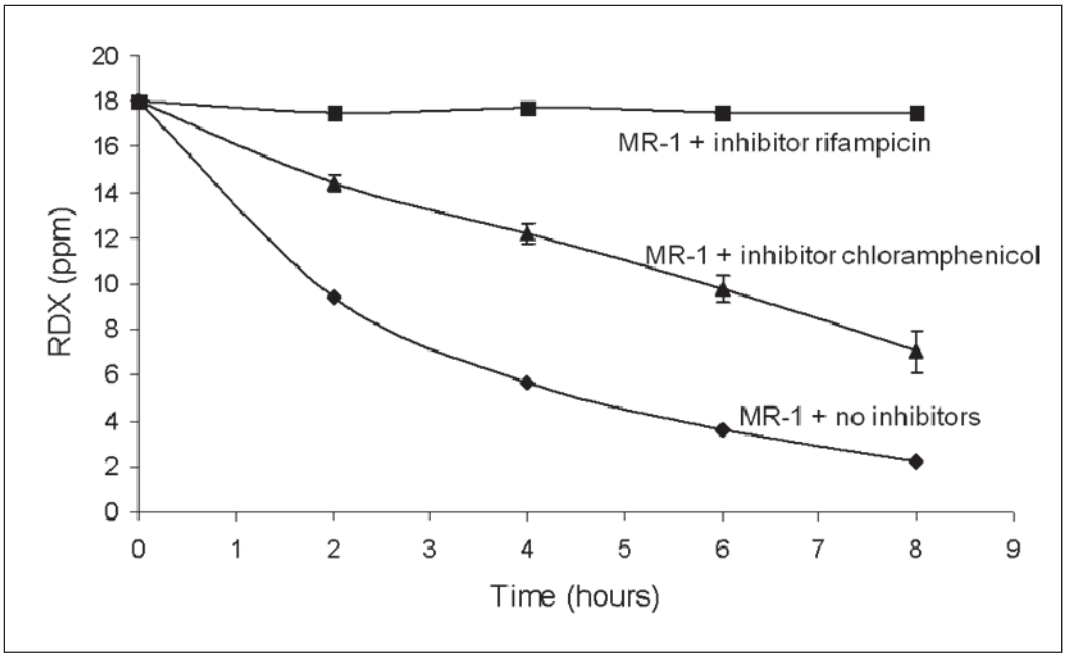

Figure 30. Effect of protein synthesis inhibitors chloramphenicol and rifampicin on RDX degradation by resting cell suspensions of MR-1. The error bars indicate the standard deviations.

degradation. Figure 31 shows that actively growing cultures pre-incubated for 3 h with RDX degraded RDX at a rate of 9.6 ppm/h, which is 1.6 times greater than that of the cultures not pre-incubated with RDX (6.0 ppm/h). Only negligible degradation of RDX was observed (0.8 ppm/h) by cells pre-incubated with RDX and chloramphenicol.These results indicated that RDX degradation in MR-1 is inducible or up-regulated by RDX. Thus, differential gene expression studies could be utilized to identify genes related to biotransformation of RDX by strain MR-1.

RDX transformation in MR-1

RDX degradation by strain MR-1 in MMR2 medium was studied using growing and resting cell cultures. Growth of MR-1 was accompanied by the degradation of RDX at a rate of 4.3 μmol L^{-1} h^{-1}. After 12 h of incubation, ~50% of RDX was degraded, producing mostly the three nitroso derivatives MNX (72%), DNX (4%) and TNX (trace). Other degradation products such as MEDINA and NDAB could not be analyzed for because of interference from the medium. Resting cells of MR-1 in phosphate buffer (2 mg protein mL^{-1}) degraded RDX at a rate of 3.54 μmol h^{-1} g^{-1}. The disappearance of RDX was accompanied by the sequential formation of the three nitroso derivatives MNX (47.8%), DNX (38.5%), TNX (7.4%), and the degradation products MEDINA (1.1%), NDAB (0.4%), HCHO (2.2%), N_2O (0.3%) and

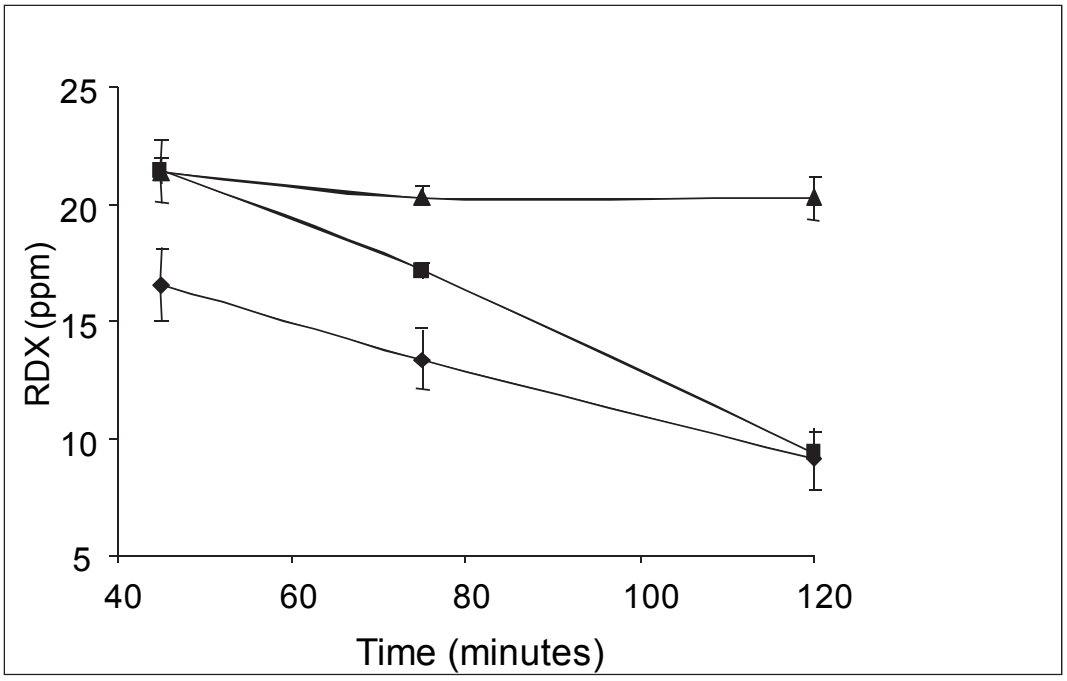

Figure 31. RDX removal by resting cells of strain MR-1 pre-incubated for 3 h without RDX (■); with RDX (◆); or with RDX plus chloramphenicol (▲). The error bars indicate the standard deviations.

ammonia (5.5%) (Figure 32). The C- and N-mass balances were calculated at 97% and 101%, respectively (Table 19). Thus, MR-1 degrades RDX via two anaerobic metabolic pathways as illustrated in Figure 2B: (1) a major route represented by the sequential reduction of the nitro groups (N-NO_2) to nitroso groups (N-NO) to produce MNX, DNX, and TNX; and (2) a minor route involving initial denitration followed by ring cleavage as demonstrated by the detection of key products such as MEDINA, NDAB, N_2O and HCHO. The present finding was in line with what was observed during degradation of RDX with the marine strain *S. halifaxensis* (Zhao et al. 2008).

Conclusions

Members of the genus *Shewanella* are known to exist in terrestrial and marine soils, waters, and sediments and for their nutritional diversity and ability to use numerous electron acceptors. Several *Shewanella* species have now been shown to transform RDX under anaerobic conditions (this study; (Zhao et al. 2010)). The transformation of RDX in strain MR-1 is apparently co-metabolic in that growth of MR-1 requires the presence of carbon, nitrogen, and electron acceptor sources other than RDX. However, the growth of strain MR-1 is slightly increased when RDX is present, which suggests that RDX may supply some nitrogen for growth (from the ring

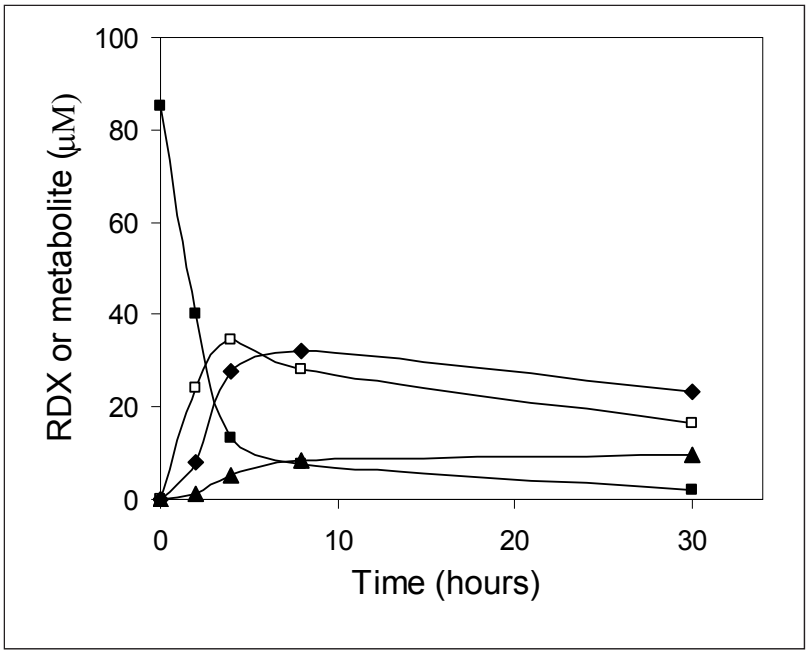

Figure 32. Anaerobic transformation of RDX (~90 μM) at 25 °C in 25 mM sodium phosphate buffer pH 7.0 by MR-1 cells pre-grown in MMR2 medium. The cell protein concentration was 2 mg ml^{-1}. RDX ■; MNX □; DNX ▼; TNX ▲.

Table 19. Stoichiometry of nitrogen and carbon during RDX degradation by MR-1. Calculations are based on the percentage of RDX degraded using the total theoretical numbers on N and C atoms.

End Product	N-mass %	C-mass %
MNX	0.9	0.9
DNX	21.7	21.7
TNX	71.9	71.9
MEDINA	1.1	0.5
NDAB	0.0	0.0
Nitrate	0.0	NA[1]
Nitrite	0.0	NA
Ammonium	5.5	NA
Nitrous oxide	0.3	NA
Formaldehyde	NA	2.2
Formate	NA	0.0
Total	101.4%	97.2%

[1]NA – not applicable

cleavage product ammonium). In addition, induction or up-regulation of RDX degradation in MR-1 was observed so that differential gene expression studies were possible (see below). The adaptation of *Shewanella* species to many different environments and geochemical conditions suggests that these bacteria make up one of the dominant populations responsible for the anaerobic transformation of explosives.

Gene disruption and characterization of RDX pathways in mutant strains

Introduction

Only a few genes and enzymes responsible for anaerobic biodegradation of RDX have been identified. NsfI, a type I nitroreductase from *Enterobacter cloacae* strain 96-3, was the first enzyme presumed to catalyze the two-electron reduction of RDX to nitroso-intermediates. A cytochrome c552 purified from *S. halifaxensis* was recently reported to catalyze RDX degradation anaerobically via initial denitration followed by ring cleavage to produce MEDINA (Zhao et al. 2008). By analyzing the genomes of 15 *Shewanella* strains, Zhao et al. (2010) observed that the RDX-degrading strains had a higher number of genes for cytochromes and nitrate/nitrite reductases. Despite progress made towards understanding the anaerobic degradation routes of RDX, the genetic determinants dictating the fate of RDX under anaerobic conditions are still unclear. Random transposon mutagenesis of strain MR-1 was undertaken to identify genes involved in the anaerobic metabolism of RDX. One of the advantages of transposon mutagenesis is that the transposon serves as a marker that can be used to clone and sequence the region of genomic DNA that has been disrupted. Transposon insertion mutants of MR-1 that were isolated had reduced rates of RDX transformation compared to the wild type MR-1 strain. The genes that were interrupted by the transposon insertion were determined as well as the rates of RDX transformation and product distribution in these mutants.

Methods

Construction and screening of the transposon library

A transposon library of MR-1 was generated by random mutagenesis using the EZ-Tn5™ <R6Kγori/KAN-2>Tnp Transposome™ Kit (Epicentre, Madison, Wisconsin) according to the manufacturer's instructions. Freshly grown MR-1 cells were transformed with 1 µl of the Tnp transposome.

Transformants were initially selected on LB agar containing 50 μg kanamycin mL^{-1} (Kan 50) and then grown aerobically overnight in 96-well plates containing 1 mL of LB Kan 50. For phenotypic screening of RDX transformation, a MULTI-BLOT™ Replicator (V&P Scientific) was used to transfer culture inocula to a new 96-well plate filled with 1.5 mL of LB supplemented with 90 μM RDX. Controls consisted of two wells inoculated with the wild-type MR-1 and two uninoculated wells. The plates were sealed with sterile breathable membranes and placed in anaerobic jars. The jars were purged with oxygen-free N_2 and incubated for 48 h at 30 °C in the dark. After centrifugation at 4,000 x *g* for 10 min, the supernatants were transferred in 1-mL glass vials for RDX quantification by HPLC. Kanamycin-resistant MR-1 strains with reduced RDX degradation activities were further characterized by identification of the disrupted gene, RDX degradation rates, and product distribution.

Determination of transposon insertion sites

Genomic DNA was extracted from the selected mutants using the QIAGEN DNeasy Blood & Tissue Kit. Five micrograms of purified DNA was added to 100 μL of Tris-EDTA (pH 8.0) and submitted to 200 passages through a 30-gauge hypodermic needle. DNA fragments 6 to 8 kb in length were purified from an agarose gel using the illustra™ GFX™ PCR DNA and Gel Band Purification Kit (GE Healthcare) and eluted in water. One microgram of purified DNA was blunt ended and 5'-phosphorylated using the End-it DNA End-Repair Kit (Epicentre). The repaired DNA was self-ligated at 14 °C overnight with the T4 DNA ligase (Promega). Ligation products were transformed into freshly prepared electrocompetent *E. coli* EC100D *pir*-116 (Epicentre) and plated on LB agar Kan 50. The transposon insertion sites from a number of kanamycin-resistant rescue clones were amplified by PCR using the transposon-specific primers KAN-2 FP-1 and R6KAN-2 RP-1 (Epicentre). Sequencing of the amplicons was performed at the McGill University Genome Quebec Innovation Centre (Montreal, Canada). The identity of the DNA sequences was determined by a search of the NCBI non-redundant database using DNA-DNA BLAST (blastn). The search was limited to records matching the genome of *S. oneidensis* MR-1 (genome AE014299, taxid 211586).

Southern blot hybridization

Southern blot hybridization was performed to confirm the insertion site of the transposons. The genomic DNA from the mutants and the wild-type

strains was digested with three restriction enzymes (*BstB*I, *EcoR*V and *Nco*I) and the resulting digested DNAs were separated by electrophoresis on a 0.5% agarose gel. DNA was transferred on a positively charged nylon membrane. The membrane was hybridized with a DIG-labeled probe targeting the Kan^r gene of the transposon (Roche PCR DIG Probe Synthesis Kit). Detection was performed by chemiluminescence. The expected sizes of the transposon-containing DNA bands were calculated using the web-based program Webcutter 2.0.

Growth physiology and RDX degradation mechanisms in MR-1 transposon mutants

Growth and RDX degradation by the transposon mutants of strain MR-1 was followed in MMR2 medium supplemented with 90 μM RDX and TMAO as the electron acceptor. In addition, the ability of the transposon mutants to utilize fumarate, nitrate, and Fe(III) as electron acceptors was determined using growth assays in MMR2 containing lactate, NH_4Cl, and the various electron acceptors (15 mM).

Complementation of transposon mutants of MR-1

Gene complementation of mutant C9 was performed to ensure that the phenotype observed was caused by disruption of the *cymA* gene. The complete *cymA* gene, plus 97 and 120 nucleotides of the upstream and downstream regions, respectively, was PCR-amplified from the wild-type MR-1 using the primers C9v2F_EcoRI (5'CGGCATTTTTAGGCTTGAATCCAAACTTCT3') and C9v2R_BamHI (AATCGCCCTTAGCGCCGGATCCCGCAGAG). The 783-bp *Eco*RI-*BamH*I fragment was cloned directionally into pBBR1MCS-5, a broad-host-range cloning vector with gentamycin resistance (Kovach et al. 1995), resulting in plasmid pB14. The pB14 plasmid was electroporated into *E. coli* DH10B and the colonies were selected on LB plates with gentamycin at 20 μg/ml. The plasmid was then purified with the QIAprep Spin Miniprep kit and the proper cloning orientation was confirmed by sequencing. Plasmid pB14 was finally electroporated into mutant C9 and growth of the complemented C9 mutant with fumarate as the electron acceptor was assessed. In addition, the ability to transform RDX in the complemented C9 mutant was compared to mutant C9 containing pBBR1MCS-5 (without the *cymA* insert) as a control.

Results and discussion

Screening the transposon library for RDX-defective mutants and identification of the disrupted genes

A transposon library of MR-1 was constructed to understand the genes responsible for initiating RDX degradation. Random insertion mutagenesis generated ~2,500 transformants (mutants), which were subjected to phenotypic screening for RDX removal. After 48 h of incubation in LB amended with RDX, the cultures of five mutants had remaining concentrations of RDX similar to the concentration observed in uninoculated controls. These mutants were submitted to three additional rounds of screening to confirm the RDX-defective physiology. To exclude the possibility that the RDX-defective phenotype might be a result of severe growth defects, the growth of mutants in LB plus RDX was monitored. Five mutants (B4, B9, C9, D6, and E7) retained the RDX-defective phenotype after three rounds of screening while their growth was similar to or slightly lower than that of the wild type (data not shown).

Three distinct transposon-interrupted genes were sequenced and identified from the mutant strains (Table 20). Two of the genes are involved in quinone biosynthesis, i.e. a chorismate synthase gene (SO_3078.2; mutants B4 and B9) and the naphthoate synthase gene *menB* (mutant D6). The third gene, *cymA* (mutant C9), encodes a tetraheme cytochrome c. Southern blots showed the presence of single insertions of the Km^r gene in the genomic DNA of the mutants, as well as its absence in the MR-1 wild-type strain. The sizes of the bands in *BstB*I, *EcoR*V, and *Nco*-digested genomic DNAs were consistent with the expected bands (data not shown). The transposon insertion site was mapped to a putative transposase in mutant E7 and the reduction in the RDX degradation rate is likely due to unknown physiological effects caused by the insertion. Growth in the rich LB medium probably masked these physiological effects. Since the transposon mutation was not specific to RDX degradation, this mutant was no longer studied.

Growth physiology and RDX degradation mechanisms in MR-1 transposon mutants

The four mutants grew in MMR2 with TMAO as the electron acceptor reaching an OD_{600} of ~0.27 - 0.35. Growth of mutant strains B4, B9, and D6 was not associated with significant RDX degradation during 72 h of

Table 20. RDX-defective *Tnp* strains of *Shewanella oneidensis* MR-1.

Strain	RDX Degradation Rate (μmol g^{-1} h^{-1})[1]	Disrupted ORF[2]	Function
Wild type	3.54 ± 1.22	n/a	n/a
B4, B9	<0.1	SO_3078.2	Chorismate synthase; shikimate pathway
D6	0.11 ± 0.02	*menB*	Naphthoate synthase; menaquinone biosynthetic pathway
C9	0.32 ± 0.07	*cymA*	*c*-type cytochrome
E7	0.7 ± 0.16	SO_3039	Putative transposase

[1]in resting cells pre-grown in MMR2 with TMAO and RDX.

[2]n/a = not applicable.

incubation. Mutant strain C9 started to transform RDX at a rate of 0.75 after the cells reached the stationary phase at an OD_{600} of 0.35 (data not shown). Growth or RDX degradation did not occur in the uninoculated controls. Mutants D6 and C9 did not grow under fumarate-, nitrate-, or Fe(III)-respiring conditions. Mutants B4 and B9 retained the ability to grow anaerobically with fumarate, nitrate, or Fe(III) as the sole terminal electron acceptor. Similarly, other studies have shown that MR-1 strains containing a deleted *menB* gene are defective in the reduction of several substrates including Fe(III), Mn(IV), fumarate, and nitrate (Myers and Myers 1993, Myers et al. 2004, Saffarini et al. 2002). It has also been demonstrated that the absence of *cymA* significantly impedes the ability of MR-1 (i.e. 80–100%) to use a range of substrates as terminal electron acceptors, including Fe(III)/Mn(IV) oxides, fumarate, nitrate, nitrite, and (Myers and Myers 1997, Schwalb et al. 2003) dimethylsulfoxide.

The RDX degradation products were identified in resting cells of strains D6 and C9 (Figures 33B and 33C, Table 21). Strains B4 and B9 were excluded from further study due to insufficient RDX degradation. Degradation of RDX by strain D6 was similar to that of the wild-type (Figure 33A) regarding the initial reduction of RDX to MNX (74% of initial RDX degradation) but occurred at a drastically reduced rate (0.11 μmol g^{-1} h^{-1} compared to 3.54 μmol g^{-1} h^{-1}; Table 21). As for MNX, the product disappeared gradually without producing DNX or TNX (Figure 33B). Although MEDINA could not be detected, its two marked decomposition products (HCHO and N_2O) were observed. An additional degradation assay was performed using MNX as the substrate, and DNX or TNX were not produced (data not shown). RDX degradation by C9 occurred at a rate of 0.32 μmol h^{-1} g^{-1}

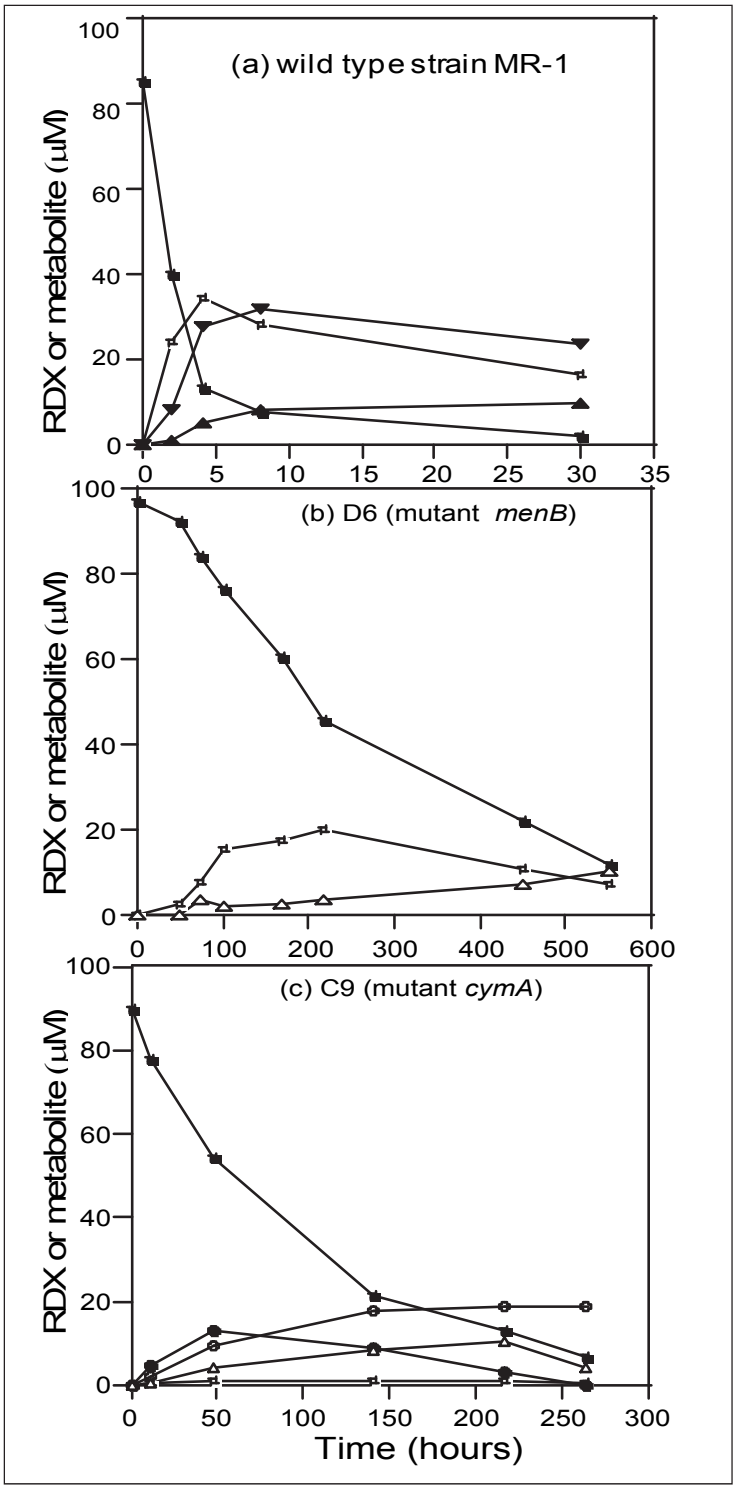

Figure 33. Anaerobic transformation of RDX (~90 μM) by resting cell suspensions of MR-1 wild-type (a) and transposon mutants D6 (b) and C9 (c). Cultures pre-grown in MMR2 medium and then suspended in 25 mM sodium phosphate buffer, pH 7.0 at a cell protein concentration of 2 mg mL^{-1}. ■ RDX;□ MNX; ▼DNX;▲TNX; ● MEDINA; ○ NDAB;Δ HCHO

Table 21. Stoichiometry of nitrogen after degradation of ~45 µM RDX by resting cells of MR-1 wild-type and transposon mutants, D6 and C9. Numbers were calculated based on the percentage of RDX removed using total theoretical numbers of N atoms.

Metabolite	MR-1 (%)	D6 (%)	C9 (%)
MNX	47.8 (±0.3)	74.3 (±3.3)	2.7 (±0.6)
DNX	38.5 (±0.7)	BDL	BDL
TNX	7.4 (±0.2)	BDL	BDL
MEDINA	1.1 (±0.1)	BDL	21.0 (±0.2)
NDAB	0.4 (±0.2)	BDL	14.3 (±0.2)
NO_2^-	0.0 (±0.0)	BDL	3.4 (±0.6)
NH_4^+	5.5 (±0.4)	ND	42.4 (±2.1)
N_2O	0.3 (±0.1)	0.3 (±0.1)	12.5 (±3.1)
Total (%)	101.0	74.3	96.3

BDL = below detection level; ND = not determined.

(Table 21). RDX was degraded mostly via initial denitration leading to ring cleavage and decomposition to MEDINA (21.0%), NDAB (14.3%), NO_2^- (3.4%), N_2O (12.5%), and ammonia (42.4%) (Figure 33C, Table 21). Traces of MNX were also detected. MEDINA declined over time as it decomposed to HCHO (12% of the C) and N_2O. For mutant C9, the N- and C- mass balances were 96% and 36%, respectively. The C-mass balance was finalized by incubations with uniformly labelled ^{14}C-[RDX]: 63% of $^{14}CO_2$ was recovered for a C-mass balance of 99% (data not shown).

Complementation of transposon mutants of MR-1

Plasmid pB14 containing the wild-type, uninterrupted *cymA* gene was successfully transferred into MR-1 transposon mutant C9 by electroporation. The vector plasmid without this insert, pBBR1MCS-5, was also successfully transferred into mutant C9. Growth of mutant C9 in MMR2 with fumarate as the electron acceptor was restored by complementation with the wild-type *cymA* gene (Figure 34b). The rate of RDX transformation by the *cymA*-complemented C9 mutant (C9:pB14) also occurred at nearly the same rate as the MR-1 wild-type strain (Figure 34a). In contrast, mutant C9 containing pBBR1MCS-5 without the *cymA* gene was unable to grow under fumarate-respiring conditions and the rate of RDX degradation did not change from that observed with C9 (Figure 34). Complementation of mutant D6 with the wild-type, uninterrupted *menB* gene was unsuccessful (data not shown), which suggested that the transposition affected other unknown gene/protein activities in MR-1.

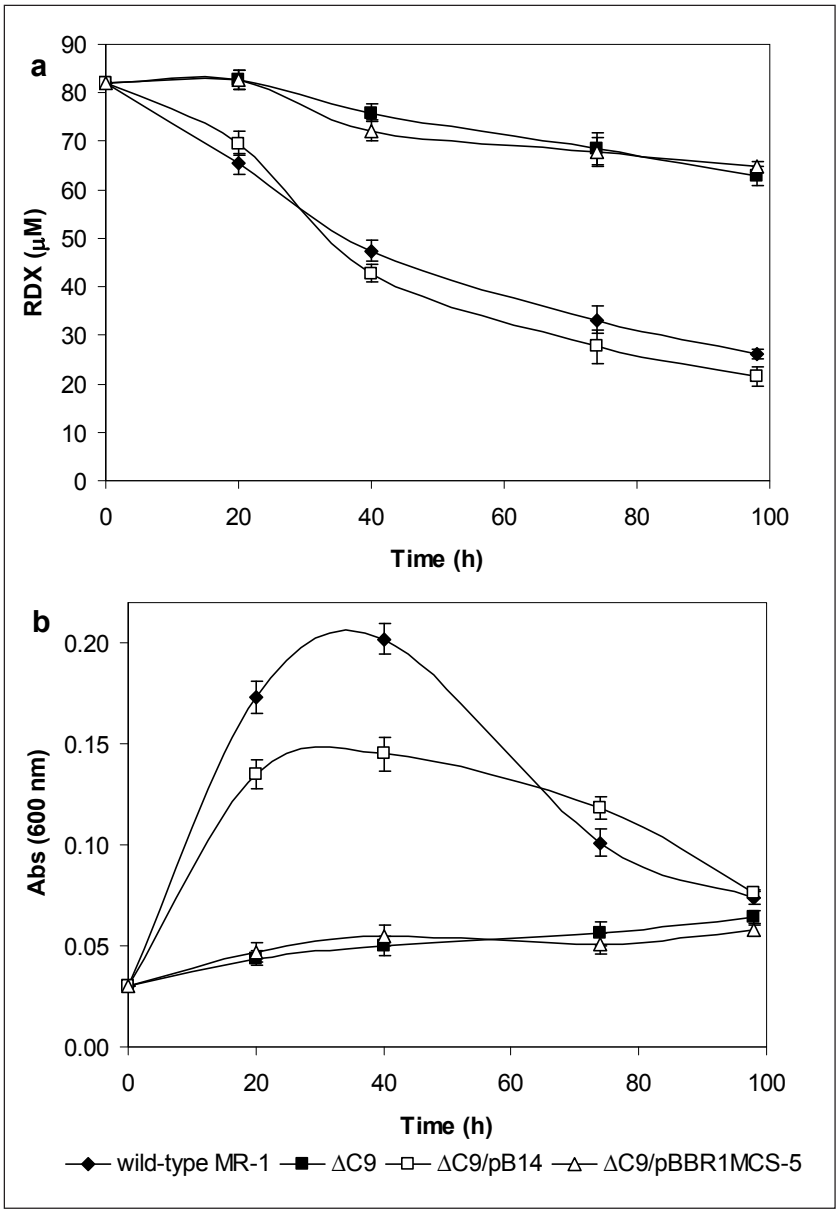

Figure 34. Complementation of mutant C9 with the plasmid pB14. a) RDX removal during a growing cell assay in MMR2; b) Bacterial growth of wild-type, mutant C9, and mutant C9 with complementation plasmids. Medium : MMR2 with fumarate as the sole electron acceptor.

Disruption of the chorismate synthase gene, *menB* gene, and *cymA* gene significantly reduced the rates of RDX degradation by MR-1 (Table 20). The role of chorismate synthase is to catalyze the last step of the shikimate pathway for the production of various products including menaquinone (MQ), ubiquinone, and aromatic amino acids. Naphthoate synthase (MenB) is an important enzyme in the naphthoquinone (menaquinone and dimethyl-menaquinone) biosynthesis pathway. Ubiquinone and MQ shuttle electrons between the membrane-bound protein complexes in the electron-transport

chain, MQ serving as the major electron carrier during anaerobic growth on several terminal reductases (Taber 1980). The membrane bound *c*-type cytochrome CymA was also shown to act as an electron transfer intermediate, this time between MQ of the inner membrane and various periplasmic terminal reductases (Schwalb et al. 2003). In general, mutants D6 and C9 had similar phenotypes, being unable to use fumarate, nitrate, and nitrite as electron acceptors for growth. However, the end products of RDX degradation in the two mutants were significantly different (Table 21).

Conclusions

Results suggest that electron transport components have a role in the anaerobic metabolism of RDX by MR-1. Mutants C9 and D6 had reduced abilities to degrade RDX in comparison to the wild-type. Specifically, the reduction of the N-NO_2 groups of RDX to the corresponding N-NO derivatives were affected by disruption of *cymA* and *menB* genes (Table 21). On the other hand, denitration of RDX to MEDINA and NDAB was not affected by the absence of CymA, but was affected by the absence of MenB (Table 21). Although RDX transformation was greatly repressed in mutants C9 and D6 compared to the wild, it was not completely inhibited. Since *Shewanella* species have on the order of 40 *c*-type cytochromes (Fredrickson et al. 2008), this versatility could be exploited in the MR-1 mutants for the reduction of RDX by different routes. However, how MR-1 may regulate or catalyze RDX transformation is still unknown due to the robust electron transport system and cytochrome pool in *Shewanella*. The downstream components involved in RDX transformation by MR-1 are also unknown since CymA can couple to multiple terminal reductases and periplasmic electron transfer proteins (Zhao et al. 2010). The screening of 2,500 transposon mutants certainly did not identify the totality of the genes involved in the RDX metabolism by MR-1. However, the identification of the *cymA* gene provided evidence that electron transport components have a role in the anaerobic metabolism of RDX by MR-1.

The anaerobic transformation of RDX to MNX, DNX, and TNX preserves the nitramine ring structure and all of the carbon and nitrogen atoms. These nitroso products are toxic to many organisms, reducing fecundity, causing death, and inducing DNA damage (Pan et al. 2007; Zhang et al. 2006). Mutant C9 primarily degraded RDX by denitration to MEDINA and NDAB, which represents a more environmentally benign approach for the remediation of RDX-contaminated sites. The ring cleavage product MEDINA is unstable and decomposes to HCHO or CO_2 and N_2O. Both HCHO and

NDAB can be degraded and mineralized by other microorganisms in soil and groundwater, including *Methylobacterium* and *Phanerochaete chrysosporium*. A better understanding of the biological components that determine the fate of RDX and the cooperation of bacterial consortia *in situ* will help to improve bioremediation strategies for RDX.

Transcriptomic analysis of MR-1 RDX biodegradation

Introduction

While much progress has been made in identifying the genes and associated pathways by which some bacterial genera transform RDX under aerobic conditions, little is known about the genes involved in the anaerobic transformation of RDX. The transposon mutagenesis of strain MR-1 indicated that CymA, a cytochrome c, is involved in either transferring electrons directly to RDX or indirectly to reductase(s) that subsequently reduce RDX. However, this random mutagenesis approach did not produce mutations within potential reductases. Differential gene expression analysis of MR-1 cultures was used in order to determine if reductases or other genes participate in RDX transformation in MR-1.

Methods

RNA extraction, labeling, and microarray experimentation

For microarray studies, *Shewanella* MR-1 was grown under anaerobic conditions in LB broth and LB broth with RDX (40 ppm). The anaerobic LB medium was prepared by boiling and incubation overnight in GasPak EZ Anaerobe Pouch Systems (BD Diagnostics). Duplicate cultures with a resazurin indicator (0.0002%) were used to ensure the method described produced anaerobic culture conditions. Anaerobic cultures were inoculated at an initial OD_{600} of 0.01 from an overnight culture of MR1 that was grown in LB under aerobic conditions. Inoculated serum bottles were incubated in fresh GasPak pouches (two bottles per bag) at 30 ^{o}C with shaking at 150 rpm.

Total RNA was extracted from *Shewanella* MR-1 cells using the Qiagen RNeasy kit. Prior to extraction, an enzymatic lysis/mechanical disruption step was added to the protocol, whereby the cell pellet was resuspended in 100 µl TE buffer and 200 µl lysozyme (20 mg/ml), transferred to an MP Biomedicals Lysing Matrix B tube, and vortexed for 1 min. An optional on-column DNA digestion using the Qiagen RNase-Free DNase Kit was

performed to remove any remaining DNA. The quantity and quality of RNA was assessed with the Agilent 2100 Bioanalyzer using the Agilent RNA 6000 Kit. The cDNA for microarray analysis was generated using the Invitrogen Superscript II Double-Stranded cDNA Synthesis Kit and the quality of the cDNA was confirmed using the Agilent 2100 Bioanalyzer and Agilent DNA 1000 Kit. The cDNA was Cy3-labeled with the NimbleGen One-Color DNA Labeling Kit. Two micrograms of the labeled cDNA was used for hybridization to a Nimblegen 4 x 72k *Shewanella oneidensis* MR-1 array (cat# A6706-00-01). The arrays were hybridized 18 h at 42°C in a Nimblegen Hybridization system and washed using the Nimblegen Wash Buffer Kit. Washed arrays were scanned using the Agilent Microarray Scanner and images were analyzed using Nimblescan v2.5.26 and ArrayStar v4.0.0 software. Expression data were log2 transformed and statistical significance was determined using a moderated t-test for binary transcriptome comparisons. The P-value was set at 0.05 with an FDR correction being applied and only those genes induced or repressed by at least two-fold were considered in this report.

Regulatory network inference

Regulatory effects of genes can be inferred using algorithms that perform statistical inferences from observational data. This study applied a mutual information based method, the Context Likelihood of Relatedness (CLR) algorithm (Beliaev et al. 2002) to reconstruct a regulatory network for RDX transformation in MR-1. Mutual information (MI) is a general measurement of dependencies between pairs of variables (genes, proteins, or physiological measurements). The higher the MI score between the two variables, the greater the information that can be derived on the states of one variable from the pattern of states of the other variable. High scoring MI–derived interactions between gene pairs can be used to formulate trial structures of underlying regulatory networks, as guidance for further exploration.

Although estimation of the MI score is not based on any assumptions about the distribution of variables, it does require a relatively large number of data points (>50) on the state of each node (Faith et al. 2007; Margolin et al. 2006). Once the set of MI values is estimated, the algorithm generates a network by using gene-to-gene comparisons (edges) whose raw or adjusted MI-based scores pass a user-defined cutoff, which is set empirically or on the basis of statistical significance (Margolin et al. 2006). The algorithm generates a pair-wise matrix of MI-based values, and the significance of the

MI score between genes X and Y is estimated by comparing the MI score with a background distribution of MI values. The background distribution is created anew for each pair of genes and estimated by a joint normal distribution of the combined set of MI values of all the possible incoming and outgoing edges for each gene of the pair (Faith et al. 2007).

Results and discussion

RDX transformation by MR-1 was studied in LB broth supplemented with 40 ppm RDX. After 20 h of incubation, ~66% of RDX was degraded (Figure 35). Products of RDX transformation were identified as MNX, DNX, and TNX (data not shown). At this time, the cultures were harvested for differential gene expression analysis. The analysis of the transcriptomes of MR-1 cultures grown in the presence of RDX compared to those grown on LB broth without RDX identified 276 gene targets that were differentially expressed by at least 2-fold. In the presence of RDX, 138 of these gene targets were up-regulated, whereas the remaining gene targets were down-regulated. A select number of these gene targets are presented in Tables 22 and 23, respectively.

The majority of genes up-regulated in the presence of RDX are involved in nitrogen metabolism, transport, redox balance, and transcriptional regulation (Table 22). Genes up-regulated in the presence of RDX that suggest a redox imbalance include oxidoreductases and components of the electron transport chain. Among up-regulated genes, there is the strong induction of

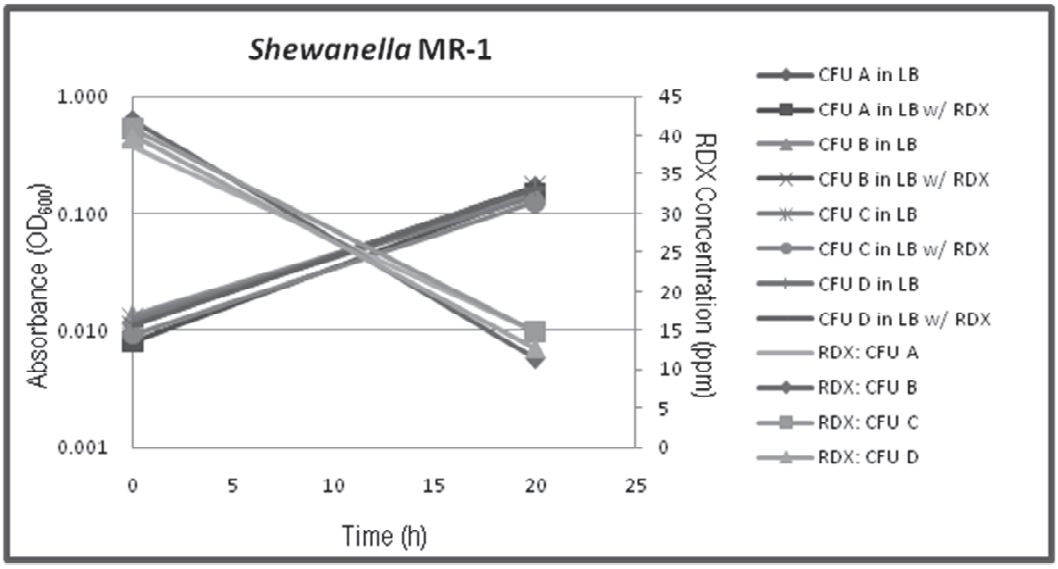

Figure 35. Anaerobic metabolism of RDX in *S. oneidensis* MR-1 grown in LB broth with or without RDX.

Table 22. Identification of genes up-regulated by growth of MR-1 in the presence of RDX.

Locus	Function	Fold change
	Transport	
SO_1043070600000969	amino acid ABC transporter, permease protein	7.765
SO_1044070600000970	amino acid ABC transporter, periplasmic amino acid-binding protein	6.142
SO_3669070600003333	heme transport protein	5.765
SO_0530070600000496	transporter, LysE family	5.322
SO_4081070600003697	amino acid permease	4.79
SO_1042070600000968	amino acid ABC transporter, ATP-binding protein	4.465
SO_4565070600004136	transporter, putative	3.345
SO_2555.1070600002314	outer membrane protein OmpA weak homolog	2.986
SO_3673070600003337	hemin ABC transporter, periplasmic hemin-binding protein	2.63
SO_0534070600000499	arsenical pump membrane protein, putative	2.398
SO_1336070600001237	Na+/H+ antiporter	2.361
SO_0539070600000503	transporter, putative	2.34
SO_3675070600003339	hemin ABC transporter, ATP-binding protein	2.316
SO_3819.1070600003465	hypothetical ammonia permease	2.131
	Nitrogen metabolism	
SO_1363070600001264	hydroxylamine reductase	23.138
SO_0279070600000260	argininosuccinate lyase	17.499
SO_0276070600000257	acetylglutamate kinase	14.875
SO_0277070600000258	ornithine carbamoyltransferase	13.078
SO_0278070600000259	argininosuccinate synthase	11.014
SO_4245070600003844	N-acetylglutamate synthase	7.76
SO_1324070600001225	glutamate synthase, small subunit	5.031
SO_2767070600002514	asparagine synthetase B	4.916
SO_1325070600001226	glutamate synthase, large subunit	4.626
SO_4344070600003941	threonine dehydratase	2.531
	Redox	
SO_1364070600001265	iron-sulfur cluster-binding protein	15.902
SO_3392070600003091	oxidoreductase, FMN-binding	4.764
SO_A0164070600004459	iron-containing alcohol dehydrogenase	2.699
SO_2269070600002058	ferredoxin, 2Fe-2S	2.427
SO_2501070600002266	radical activating enzyme	2.29
SO_4485070600004069	diheme cytochrome c	2.239
SO_2512070600002275	electron transport complex protein RnfG	2.027

Locus	Function	Fold change
SO_0536070600000501	redox-active disulfide protein 2	2.003
Regulation		
SO_1482070600001372	TonB-dependent receptor, putative	3.962
SO_4052070600003674	transcriptional regulator, MarR family	2.125
SO_2653070600002404	transcriptional regulator, Ner family	2.002
SO_3393070600003092	transcriptional regulator, TetR family	2.011

Table 23. Identification of genes down-regulated by growth of MR-1 in the presence of RDX

Locus	Function	Fold change
Transport		
SO_0313070600000292	putrescine-ornithine antiporter	6.152
SO_0312070600000291	outer membrane porin, putative	5.632
SO_4021070600003647	transporter, putative	2.899
SO_1959070600001786	ABC transporter, periplasmic substrate-binding protein, putative	2.627
SO_1007070600000935	hypothetical Na+/H+ antiporter	2.435
SO_3863070600003506	molybdenum ABC transporter, periplasmic molybdenum-binding protein	2.292
SO_3865070600003508	molybdenum ABC transporter, ATP-binding protein	2.19
SO_3864070600003507	molybdate transport permease protein	2.071
Nitrogen Metabolism		
SO_0314070600000293	ornithine decarboxylase, inducible	5.812
SO_0484070600000452	formate-dependent nitrite reductase, nrfD protein	4.04
SO_2592070600002346	dihydroorotate dehydrogenase	3.933
SO_1276070600001179	4-aminobutyrate aminotransferase	2.001
Electron transport		
SO_0939070600000874	cytochrome c, putative	4.247
SO_2178070600001979	cytochrome c551 peroxidase	2.403
SO_1427070600001324	decaheme cytochrome c	2.619
SO_0902070600000838	Na(+)-translocating NADH-quinone reductase subunit A	2.072
SO_0904070600000840	Na(+)-translocating NADH-quinone reductase subunit C	2.019
SO_3920070600003558	periplasmic Fe hydrogenase, large subunit	2.711
SO_3921070600003559	periplasmic Fe hydrogenase, small subunit	2.857
Redox Stress		
SO_0958070600000892	alkyl hydroperoxide reductase, C subunit	2.023
SO_0956070600000891	alkyl hydroperoxide reductase, F subunit	2.462
SO_3349070600003052	glutathione peroxidase, putative	2.889

Locus	Function	Fold change
SO_0882070600000820	oxidoreductase, GMC family	2.632
Chemotaxis		
SO_4043070600003666	TonB domain protein	2.745
SO_3642070600003312	methyl-accepting chemotaxis protein	2.272
SO_4002070600003628	sensory transduction histidine kinase	2.186
SO_3838070600003484	methyl-accepting chemotaxis protein	2.179
SO_2907070600002634	TonB-dependent receptor domain protein	2.137
SO_2469070600002235	hypothetical TonB-dependent receptor	2.068

an adjacent gene set coding for a hydroxylamine reductase (SO_1363) and an iron-sulfur cluster-binding protein (SO_1364) in the presence of RDX (16- to 23-fold increase). The reductase belongs to a larger protein family known as Hybrid Cluster Proteins (HCP), formerly known as prismane (Moura et al. 1992). These proteins are thought to play a role in nitrogen metabolism but the specific function of this reductase is unknown. Previously, it has been shown in MR-1 that hydroxylamine reductase activity is upregulated during anaerobic growth in the presence of nitrate (Beliaev et al. 2002). Other studies in *Rhodobacter capsulatus* in which the hydroxylamine reductase activity was inactivated demonstrated that this gene was necessary for growth on hydroxylamine as a sole nitrogen source (Cabello et al. 2004). The authors concluded that the *hcp* gene product is likely involved in the detoxification and further assimilation of hydroxyamine. In *Salmonella enterica*, *hcp* transcription was shown to be up-regulated in the presence of acidified nitrite suggesting that reactive nitrogen species was involved in induction (Kim et al. 2003). Collectively, these findings suggest that the results generated in this study are consistent with a scenario in which MR-1 transforms RDX via a sequential nitroreductase activity (SO_2708) into the highly reactive nitroso derivatives MNX, TNX, DNX. The nitroso derivatives in turn are further postulated to degrade into hydroxylamino-derivatives. As a result, the hydoxyamine derivatives are further reduced to ammonia via the hydroxylamine reductase. Interestingly, because the cells are not limited for nitrogen, levels of ammonia likely increase in the cell. Consequently, a number of genes involved in the urea cycle and nitrogen assimilation are up-regulated in the presence of RDX, presumably in response to elevated endogenous pools of ammonia. In contrast, various peroxidases and reductases, as well as components that mediate electron transport, are down-regulated in the

presence of RDX. Some of these gene targets are discussed further in the context of network analysis (Table 23).

A role for c-type cytochromes and RDX denitration pathway(s) has been postulated based on the observation that cytochrome c552 is upregulated when *S. halifaxensis* is grown in RDX minimal media with TMAO as a terminal electron acceptor (Zhao et al. 2010). Interestingly, as part of this study, three transposon mutants with insertions in genes encoding enzymes for quinone biosynthesis (chorismate synthase and naphthoate synthase) as well as a cytochrome c, CymA, were significantly impaired in their ability to transform RDX. While these gene targets were not differentially expressed in the presence of RDX, network inference analysis of transcriptome data suggests significant linkages between a subset of differentially expressed genes and the genes interrupted in these transposon mutants (Figure 36). In particular, a flavocytochrome c flavin subunit served as a first neighbor to both genes involved in quinone biosynthesis as well as multiple genes involved in redox stress including an alkyl hydroperoxide reductase, glutathione peroxidase, Na(+)-translocating NADH-quinone reductase, and a thiol:disulfide interchange protein (Figure 36A). Additional linkages could also be found between chorismate synthase and an alkyl hydroperoxide reductase, a thiol:disulfide interchange protein, and an ATP synthase F1, epsilon subunit via a serine/threonine kinase first neighbor. Similarly, a hypothetical protein with significant homology to pyridoxine 5'-phosphate oxidase (involved in vitamin B6 metabolism) served as a first neighbor to the gene encoding CymA and a number of differentially expressed genes identified by transcriptomics including multiple methyl-accepting chemotaxis proteins, multiple components of a TonB-dependent receptor, an outer membrane porin, a cytochrome c551 peroxidase, a decaheme cytochrome c, and a sensory transduction histidine kinase (Figure 36B). A chemotaxis response can be implied from this analysis in the presence of RDX. Perhaps, in the presence of RDX, the cells respond by changing their migration pattern. Interestingly, chemotaxis-mediated biodegradation of cyclic nitramine explosives RDX, HMX, and CL-20 by *Clostridium* sp. EDB2 has been previously reported (Bhushan et al. 2004).

Conclusions

While the significance of the network associations is largely implied, collectively along with the mutagenesis of the *cymA* gene (this study) and other genomic observations (Fredrickson et al. 2008, Zhao et al. 2010), it is suggested that c-type cytochromes may play an intermediary role in the

fortuitous reduction of RDX. The genus *Shewanella* is classified as an electrogenic bacterium, capable of transferring electrons to various organic and inorganic substrates. These electron transfer processes are largely mediated by a membrane system that has an extensive electron transport chain apparatus with numerous cytochrome components (Fredrickson et al. 2008). In the context of this work, while a functional gene associated with RDX degradation was not identified in strain MR-1, a phylogenetic gene marker targeting this bacterial genus may have some benefit, since a number of species from this genus have been shown transform RDX (Zhao et al. 2010).

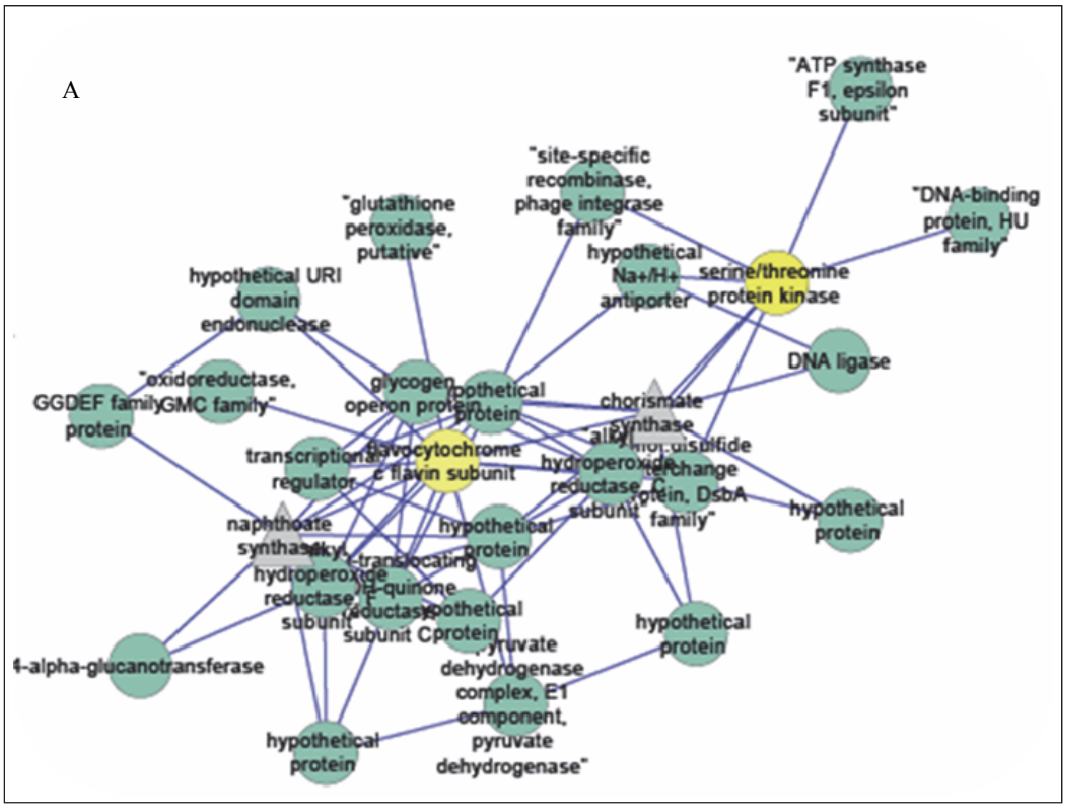

Figure 36. A total of 4296 genes across replicate samples were used to reconstruct a transcriptional network illustrating first neighbor linkages between genes differentially expressed in MR-1 in response to RDX with mutations in genes encoding chorismate synthase and MenB defective in the ability to degrade RDX (A). Similarly, an additional transcriptional network illustrating first neighbor linkages between genes differentially expressed in MR-1 in response to RDX with mutations in a tetraheme cytochrome CymA gene was also generated (B). Differential gene targets are represented as green circles, mutated gene targets are represented as gray triangles, and yellow circles represent first neighbor linkages connecting the groups. A z-score cutoff of 3.5 standard deviations higher than the mean CLR score was used to filter 993 edges between 11172 genes as the most significant interactions. The derived network was investigated using visualization software Cytoscape and represented as a subnetwork of first neighbors using the nodes designed in yellow. Collectively this subnetwork consists of 69 edges and 102 nodes.

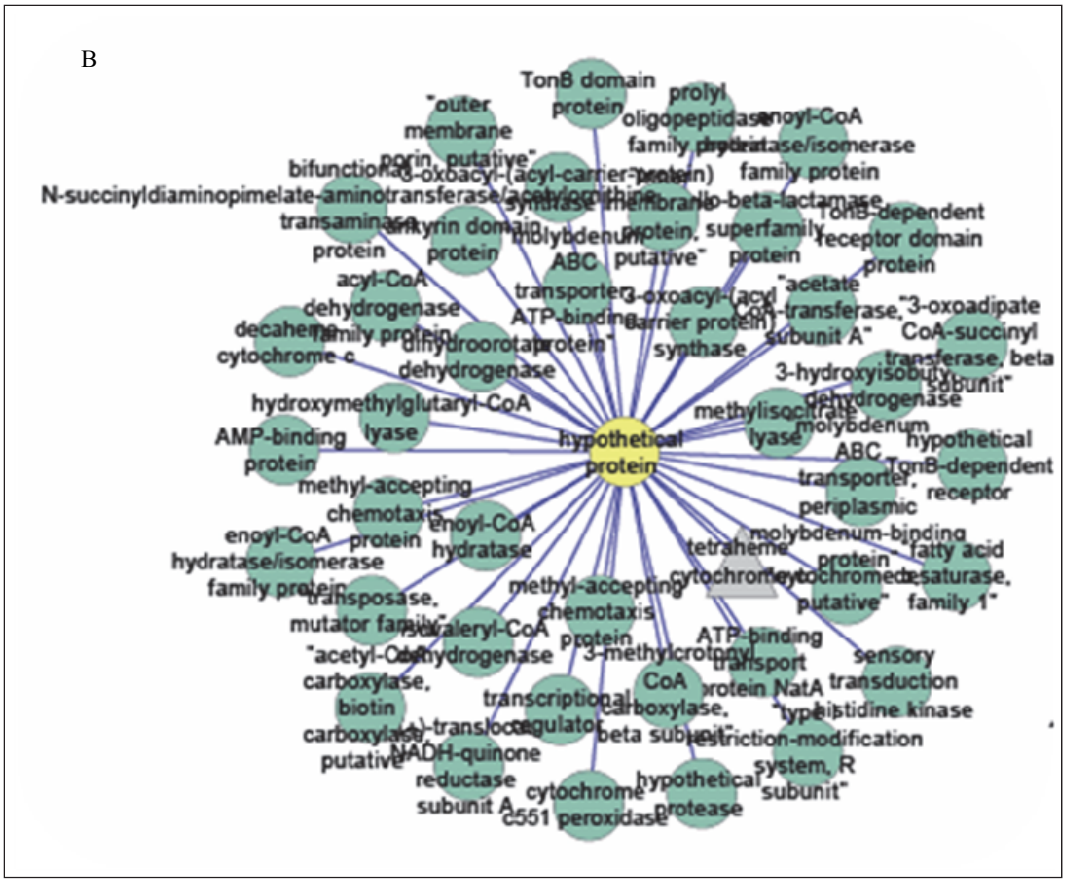

Figure 36. (continued).

5 Development and Validation of the *xplA* Gene Biomarker

Introduction

Currently all aerobic RDX-degrading bacteria that metabolize RDX via denitration to NDAB have been shown to contain the highly conserved *xplA* gene (Bernstein et al. 2011; Indest et al. 2010; Nejidat et al. 2008; Ronen et al. 2008; Seth-Smith et al. 2002). Enzyme studies with purified XplA (Jackson et al. 2007) and gene knockout studies (this study; Indest et al. 2010) have proven that XplA catalyzes the denitration of RDX. In addition, the incorporation of the heavy isotopes of nitrogen and carbon from ^{15}N-labeled RDX into the *xplA* gene was demonstrated by Roh et al. (2009). Quantitative polymerase chain reaction (qPCR) is the dominant molecular method used in environmental microbiology for detecting and monitoring the presence of a specific gene target(s) (Sharkey et al. 2004). Quantitative polymerase chain reaction (qPCR) is a method that can be used to quantify the number of gene copies in the original sample even if they are originally present in low abundance. Several studies have developed quantitative PCR methods for functional genes and correlated the gene expression with field contaminant concentrations and degradative activity in microcosms (Beller et al. 2002, Hosada et al. 2005, Indest et al. 2007, Nyyssonen et al. 2006, Powell et al. 2006).

The proteomics and genomics studies with *Gordonia* sp. KTR9 identified *xplA* as an excellent gene candidate for a qPCR assay based on sequence conservation and the fact that both the gene and protein were up-regulated in the presence of RDX. In addition, two potential regulators of RDX biodegradation, *xplR* and *glnR*, two enzymes for nitrogen assimilation, nitrite reductase and glutamine sythetase (*glnA*), and a potential permease/ transport protein for purines (KTR9-0967) represented candidate genes that possibly have a role in RDX metabolism in KTR9. Nitrite reductase and *glnA* are not specific to RDX degradation and are therefore not suitable as functional gene targets for RDX degradation. The specificity of the role of the other gene candidates with regard to RDX degradation has not been fully determined at this time.

With *S. oneidensis* MR-1, the transposon mutagenesis and differential gene expression studies indicated that a tetraheme cytochrome, CymA,

may have a role in the anaerobic reduction of RDX. The *cymA* transposon mutant not only had a reduced rate of RDX degradation compared to the wild-type strain, but also exhibited a shift in the proportion of end products that were produced. Apparently, CymA is involved in transferring electrons to RDX resulting in reduction of RDX via the two electron reduction route (Figure 2B) as the major mechanism. Complementation of this mutant fully restored reduction of RDX similar to that of the wild-type. The role of napthoate synthase, MenB, in anaerobic RDX denitration could not be confirmed since complementation of mutant D6 was not effective at restoring RDX degradation. The differential gene expression studies, while not directly indicating an up-regulation in *cymA,* did however imply that a cytochrome c acted as a major node affecting several up-regulated genes in MR-1. Unfortunately, CymA is not unique to RDX degradation since it functions as an electron carrier for the reduction of multiple electron acceptors. Thus, *cymA* is not a suitable gene candidate as a biomarker of anaerobic RDX degradation.

Based on this study's findings, *xplA* is the most suitable gene target for development of a TaqMan qPCR assay for the application of monitoring or detecting *in situ* RDX biodegradation. The specificity and sensitivity of this assay were evaluated using a variety of bacterial strains. In addition, the natural abundance of *xplA* in groundwater and soils was determined as well as the ability to correlate the abundance of *xplA* with RDX degradation rates in groundwater and soil microcosms.

Design of the *xplA* TaqMan quantitative PCR assay

Introduction

A TaqMan PCR assay was recently developed, targeting the *xplA* functional gene in *R. rhodochrous* strain 11Y (Indest et al. 2007). This assay was shown to cross react with other aerobic RDX-degrading strains including *Williamsia* sp. KTR4, *Gordonia* sp. KTR9, and *Rhodococcus* sp. DN22. Additional aerobic RDX-degrading strains and *xplA* gene sequences have been identified in the years since this initial research was completed so that it was necessary to redesign the primers and probes.

Methods

In order to find genetic homologues, 18 *xplA* gene sequences that were available from the NCBI genomic database were compared using various

BLAST algorithms (including blastn, tblastn, and tblastx; Altschul et al. 1990). Highly conserved regions that would be suitable for optimizing the TaqMan qPCR primers and probes, targeting the *xplA* gene, were determined from gene alignments using the ClustalW (Thompson et al. 1997) subroutine. The primer and probe sequences were designed using Primer Express software (version 2, Applied Biosystems, Foster City, CA), evaluated *in silico* for their specificity and then manually optimized to improve specificity.

The specificity of the TaqMan PCR primers and probe with genomic DNA from closely related bacterial strains was assessed. *Gordonia desulfuricans*, *Gordonia rubripertincta*, *Gordonia polyisoprenivorans*, *Gordonia nitida*, *Gordonia terrae*, *Gordonia alkanivorans*, *Gordonia amarae*, *Gordonia rhizosphera*, *Gordonia amicalis*, *Gordonia hydrophobica*, *Gordonia hirtusa*, *Williamsia maris*, *Williamsia murale*, and *Rhodococcus rhodochrous* RHA1 did not degrade RDX in a minimal or rich medium. *G. polyisoprenivorans* (*xplA*) and *R. rhodochrous* RHA1 (*xplA*) (Jung et al. 2011) are transconjugant strains that carry pGKT2 from strain KTR9 and are capable of degrading RDX. All strains were grown in Luria Bertani medium at 30 °C prior to isolation of genomic DNA. Genomic DNA was isolated from 1 ml of culture with the Qiagen DNeasy tissue kit according to the manufacturer's protocol for Gram positive bacteria. This protocol included the pre-incubation of the cell pellets at 37 °C for 1.5 h in lysis buffer containing lysozyme and RNaseA. All DNA extracts (200 µL) were concentrated to 30 µl using Amicon Microcon 100 filters. The specificity of the *xplA* TaqMan assay was also evaluated using genomic templates extracted from pure cultures of additional *Rhodococcus* species, and other bacterial species that did not degrade RDX.

All real-time PCR amplification reactions were performed using Applied Biosystems' 7900HT Fast Real-time PCR system (Foster City, CA). PCR was carried out in 50-µL volumes in 96-well reaction plates containing 10-50 ng of genomic DNA. All amplification reactions were optimized using 1× QuantiTect PCR Probe Master Mix (Qiagen, Valencia, CA). The optimal primer/probe concentrations for detection of the *xplA* gene target were as follows: xplA_457f primer (300 nM: 5'CGACGAGGAGGACATGAGATG-3'); xplA_462r primer (300 nM: 5'GCAGTCGCCTATACCAGGGATA-3'); and xplA_TM_479 TaqMan probe (200 nM: 5'-[6-FAM]CCGCTGCGTCCATCGATCGC[Tamra-Q]-3'). Amplification conditions for this reaction consisted of a single step at 95 °C for 12 min

followed by 50 cycles at 95°C for 20 s, 55°C for 20 s, and 72 °C for 30 s. Relative Fluorescent Units (RFU) of each PCR reaction were monitored over the course of the reaction at the beginning of each annealing cycle. Data were analyzed using the accompanying 7900HT analysis software (Applied Biosystems, Foster City, CA). Threshold determinations were automatically performed by the instrument and then manually optimized. The standard curve of the *xplA* TaqMan assay was generated using serial dilutions of an *xplA* containing plasmid (pET11a, Celtek) or genomic DNA isolated from strain KTR9.

Results and discussion

The sensitivity of the *xplA* TaqMan assay was evaluated using serial dilutions of an *xplA* containing plasmid ranging from 0.1 to 1 x 10^8 copies as well as genomic DNA (10 fg to 10 ng) extracted from KTR9. The assay sensitivity was linear over a range of up to seven orders of magnitude with as little as 10 *xplA* copies or 10 fg genomic DNA being detected. Sensitivity is defined based on a cycle threshold value (Ct). The Ct value represents the number of PCR cycles necessary to detect the fluorescent signal above background noise. Once this Ct value is exceeded the exponential accumulation of product can be measured. A no template control (NTC) is included in all reactions so that the limit of detection can be defined. The limit of detection is usually defined to be at least one log (three cycles) fold higher than the Ct value of the NTC (Smith and Osborne 2009). In general, most of the TaqMan qPCR assays that were completed using plasmid pET11a had a sensitivity of between 10 and 100 copies of *xplA*. The Ct values that corresponded with this sensitivity were equivalent to 38 to 40 cycles. Thus, the functional limit of detection for the *xplA* gene with the TaqMan qPCR assay was set to 100 copies per 20 µl PCR reaction.

The specificity of the *xplA* TaqMan assay was tested using genomic template DNA from various RDX-degrading bacteria as well as bacteria that did not degrade RDX. Of the 6 RDX-degraders tested (i.e. *Rhodococcus rhodochrous* 11Y, *Rhodococcus* sp. DN22, *Gordonia* sp. KTR9, *Williamsia* sp. KTR4, *Rhodococcus* sp.YH1, and *Rhodococcus* sp. YY1), all reacted positively with the *xplA* TaqMan assay. Additional *Gordonia* and *Williamsia* species that are unable to degrade RDX did not cross-react with the *xplA* TaqMan assay as observed by Ct values that were slightly higher than the NTC (Table 24). Furthermore, *G. polyisoprenivorans xplA* and *R. jostii* RHA1 *xplA*, which obtained plasmid pGKT2 by conjugation with strain KTR9, were positively amplified with the *xplA* TaqMan assay.

Molecular detection of *xplA* in soil and groundwater

Introduction

The *xplA* TaqMan qPCR assay was shown to be specific for RDX-degrading bacteria containing the *xplA* gene and the sensitivity was found to be reasonable. The next step in validating the use of this biomarker assay for field detection and monitoring of RDX degradation processes is to assess the application of the assay with field-collected samples. The goal of this task is to assess the presence and abundance of the *xplA* gene in soil or groundwater collected from RDX-contaminated sites.

Table 24. Specificity of the *xplA* TaqMan qPCR assay. Ct values were calculated from the standard curve generated from an *xplA* containing plasmid and are the average of duplicate samples. Undetermined samples did not generate Ct values.

Species	Ct	RDX degradation
Gordonia sp. KTR9	17.91	+
Williamsia sp. KTR4	19.15	+
Rhodococcus jostii RHA1 *xplA*	17.75	+
R. rhodochrous 11Y	18.69	+
Rhodococcus DN22	18.52	+
Rhodococcus sp. YH1	20.48	+
Rhodococcus sp. YY1	18.96	+
G. alkanivorans	39.86	-
G. amarae	35.28	-
G. amicalis	37.39	-
G. desulfuricans	36.81	-
G. hirtusa	37.14	-
G. hydrophobica	36.12	-
G. nitada	37.61	-
G. polyisoprenivorans xplA	18.11	+
G. polyisoprenivorans	34.03	-
G. rhizosphera	37.19	-
G. rubropertincta	37.92	-
G. terrae	40.88	-
W. maris	35.00	-
W. murale	35.07	-
No template control	40.15	-

Methods

Groundwater collection and DNA extraction

Groundwater was collected from an RDX-contaminated plume that has migrated outside the confines of the Iowa Army Ammunition Plant (IAAAP) near Burlington, Iowa. Since 2007 the groundwater has been undergoing remediation via injection of sodium acetate. The sodium acetate is being delivered to the plume through a series of permanent injection wells along a linear transect situated to the north of the plume (TetraTech). Groundwater (4-L) was collected in July 2009 from wells MW309 and EMW-02, which are downgradient of the injection wells, shipped on ice overnight to ERDC, and then stored at 4 ^{o}C. One liter of groundwater from each well was filtered through a 0.2-µm filter. The filters were stored at -80^{o}C in sterile Whirl Pak bags prior to DNA extraction using the PowerSoil DNA isolation kit (Mo Bio Laboratories, Inc., Carlsbad, CA). For DNA extraction, each filter was aseptically divided into six equal parts and each piece of filter was added to a separate bead beating tube. The DNA was extracted from the filters essentially following the manufacturer's instructions except that lysis was achieved using a homogenizer set at 5 m/s for 15 s. Following elution of the DNA, three replicate samples were pooled via ethanol precipitation and resuspension in 30 µl of 10 mM Tris buffer, pH 8.0.

Groundwater from the Umatilla Chemical Depot (UMCD), Hermiston, Oregon, was collected on site from the influent spigot of the groundwater treatment system. The UMCD is on the list of military facilities for Base Realignment and Closure (BRAC), but explosive-contaminated soils and groundwater were found at the site in 1990. In 1994, a groundwater pump and treat facility was installed at the site to remove explosives (TNT and RDX) using granular activated carbon (U.S. Army Engineer District, Seattle 2010). However, the removal of explosives from the groundwater has not been very effective in the last 5 -10 years and other means of treating the groundwater are being investigated. The groundwater was collected in February 2010 and shipped overnight on ice and then stored at 4 ^{o}C. The groundwater (1-L) was aseptically filtered through 0.45-µm filters (in triplicate). Each filter was cut into six pieces and extracted separately with the PowerSoil DNA isolation kit as above. Three of the extracts were pooled by centrifugation with Microcon 100 ultrafilters (Millipore) to provide two replicates per 1 L of filtered groundwater (1A, 1B etc.). In addition, groundwater from several wells was filtered on site through Sterivex filters (Millipore Inc.) in September 2010. The filters were aseptically removed

from the cartridge housing and cut into pieces with a sterile razor blade. Several pieces of the Sterivex filter were individually extracted with the PowerSoil DNA isolation kit and subsequently pooled.

Soil collection and DNA extraction

Soil samples were collected in a 10 m by 10 m grid at Grenade Range 2D at Canadian Forces Base (CFB), Petawawa, Ontario in November 2008. The grid was located at the center of the range, which measured approximately 50 m by 40 m. The grid was made of 36 square quadrants of equal dimensions, 1.7 m by 1.7 m (Figure 37). The 36 samples of surface soil weighing a minimum of 50 g were stored immediately at -80 °C and shipped in insulated coolers to Vancouver, British Columbia. Samples were homogenized with a 2-mm sieve to remove gravel and other debris and stored at -80 °C. DNA was extracted from these soil samples using the Ultraclean Soil DNA Isolation Kit (MoBio Laboratories, Inc). Soil was processed in 0.5-g quantities using the kit and DNA was eluted into water or 10 mM Tris, pH 8 for use in sequencing and PCR applications. Samples were incubated in bead tubes at 90 °C for 10 minutes prior to the vortex step, which was increased to 20 min. The protracted elution step was incorporated into the DNA extraction method with the primary goal of maximizing yields of DNA for metagenomic sequencing. DNA was eluted with four rounds of elution using 200 µL of water or Tris buffer and an incubation step at 50 °C prior to centrifugation. Purified DNA was prepared in a final volume of 800 µL. Replicate extractions were needed for PCR and also for sequencing applications.

In addition, soil was collected from Eagle River Flats, an active Army impact range, site LO#3, Ft. Richardson, Alaska. One hundred incremental samples from a 20 m x 20 m area were collected in July 2009. The soil cores were very moist and contained much plant material and many plant roots. Six random incremental samples were immediately stored at -80°C for DNA extraction. The remaining soil cores were air-dried and sieved (2-mm mesh) to remove plant material and homogenize the soil. The composite soil was then stored at 4 °C for microcosm studies. DNA was extracted from thawed soil cores (5 g) using the PowerMax Soil DNA isolation kit (MoBio Laboratories, Inc) according to the manufacturer's directions using heat (65 °C for 30 min) to lyse the cells. The DNA extract (8 ml) was concentrated by ethanol precipitation and resuspension in 500 µl of 10 mM Tris buffer, pH 8.0.

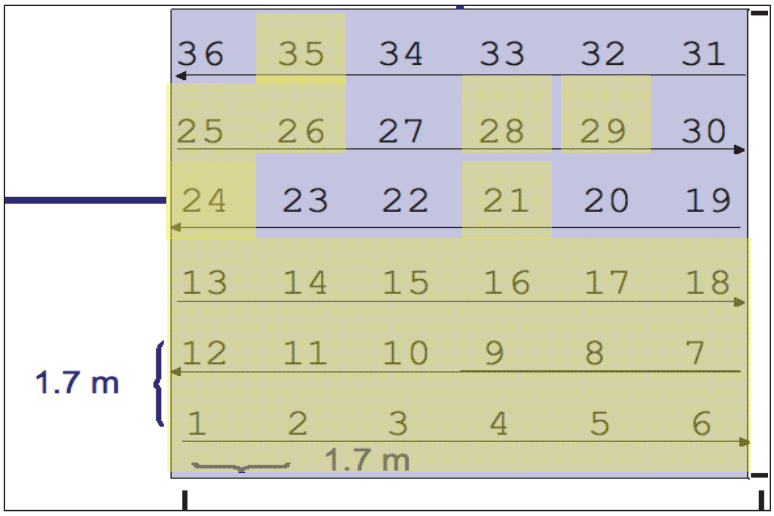

Figure 37. Location of each quadrant numbered 1 to 36 within the 10 m by 10 m grid sampled in Grenade Range 2D at CFB Petawawa. Grey quadrants were selected for subsequent microcosm experiments.

Soil was collected from the drainage lagoon site at UMCD at the same time as the groundwater collection. Since actual collection of aquifer material was not possible at this time, the lagoon soil served as a surrogate for actual groundwater material. Three buckets of soil from this area were collected. Approximately 1 ft of soil was removed from the three locations prior to the sample collection to minimize the amount of vegetative material. The soil had the appearance of basalt rocks of various sizes with sand. In addition, soil was collected from a site near Camp Shelby Joint Forces Training Center, Mississippi, due to lack of access to Camp Shelby JFTC since the start of the Gulf War. Bulk soil was collected in 2008, air-dried, crushed and sieved to remove plant material and large rocks. Six 0.25-g samples of soils were extracted using the Power Soil DNA isolation kit (MoBio Laboratories, Inc.) using bead beating (15 s at 5 m/s in duplicate with a 30-s pause) instead of vortex mixing, and subsequently pooled into two extracts using Microcon 100 filters.

Quantitative PCR analysis of xplA

Quantitative PCR was performed on soil DNA extracts from CFB Petawawa using the SYBR Green approach. A Biorad Opticon qPCR system was used with 96-well plates containing 5 µl of template DNA in a total 25 µl reaction. Biorad IQ SYBR Green supermix was used to set up reactions and bovine albumin was added to each reaction to a final concentration of 0.08 mg/ml. The primer sequences and the thermal cycle profile used were as described

by Indest et al. (2007). Forward and reverse primers were used in the reactions at a final concentration of 300 nM each. A plasmid standard was generated for this assay by cloning a PCR product for the section of the *xplA* gene being amplified in qPCR (sequence of insert: 5' GA TGACCGCTGC GTCCATCGAT CGCGAGCTCG TGCCGTGGTC GGATCCCGAA TTCAGGAACA ACCCCTATCC CTGGTATAGG CGACTGCAAC AGG 3') into a ZERO TOPO Blunt vector (Invitrogen). *Gordonia* sp. KTR9 genomic DNA was used as the template for generating the insert for the PCR standard. The average of two to three replicate experiments was used to obtain average copy numbers ± standard deviation.

TaqMan *xplA* analysis of IAAAP and UMCD groundwater DNA extracts; and UMCD, Camp Shelby, and Ft. Richardson soil DNA extracts was performed as in section VI-1. DNA extracts (1 µl) were mixed with 19 µl of the QuantiTect mix. Duplicate qPCR reactions were analyzed for each sample per PCR plate and quantity of *xplA* was calculated from an average of three separate qPCR assays performed over several days to reduce variability. Each qPCR assay included a standard curve using serial dilutions of pET11a, a positive control (KTR9 genomic DNA), and a no-template control.

Results and discussion

CFB Petawawa

RDX levels were quantified and shown to be heterogeneously distributed across the sampling area (Figure 38). The majority of samples had RDX concentrations below 10 mg/kg. These concentrations were at least eight times greater than the detection limit, which was approximately 0.3 mg/kg. The copy numbers for *xplA* detected in these soil samples indicate that the levels of RDX contamination do not seem predictive of the *xplA* copy numbers in the microbial community (Figure 39). In general, there was a relatively even distribution of *xplA* (within an order of magnitude) across the entire sampling area. The exceptions were quadrants 21, 26, and 18. Quadrants 21 and 26 had similar *xplA* levels but the RDX levels were different at 1035 and 383 mg/kg, respectively. The RDX concentrations may reflect hot spots left behind from recent range activity and the fact that there hasn't been time for bacteria to degrade this quantity of RDX. Quadrant 18 had the highest amount of detectable *xplA* copies, but a low concentration of RDX, which may be due to the presence of active aerobic RDX-degrading bacteria (Figures 38 and 39).

23	13	ND	2.5	7.7	8.9
97	383	83	ND	6.3	
6.3	23	25	1035	18	4.4
4.5	6.3	4.5	6.5	2.5	4.0
3.7	6.9	12	4.3	3.2	3.6
4.4	2.4	3.3	2.7	3.8	2.6

Figure 38. RDX concentrations per quadrant (mg/kg). Values shown are the average of duplicate extractions. ND = not detected.

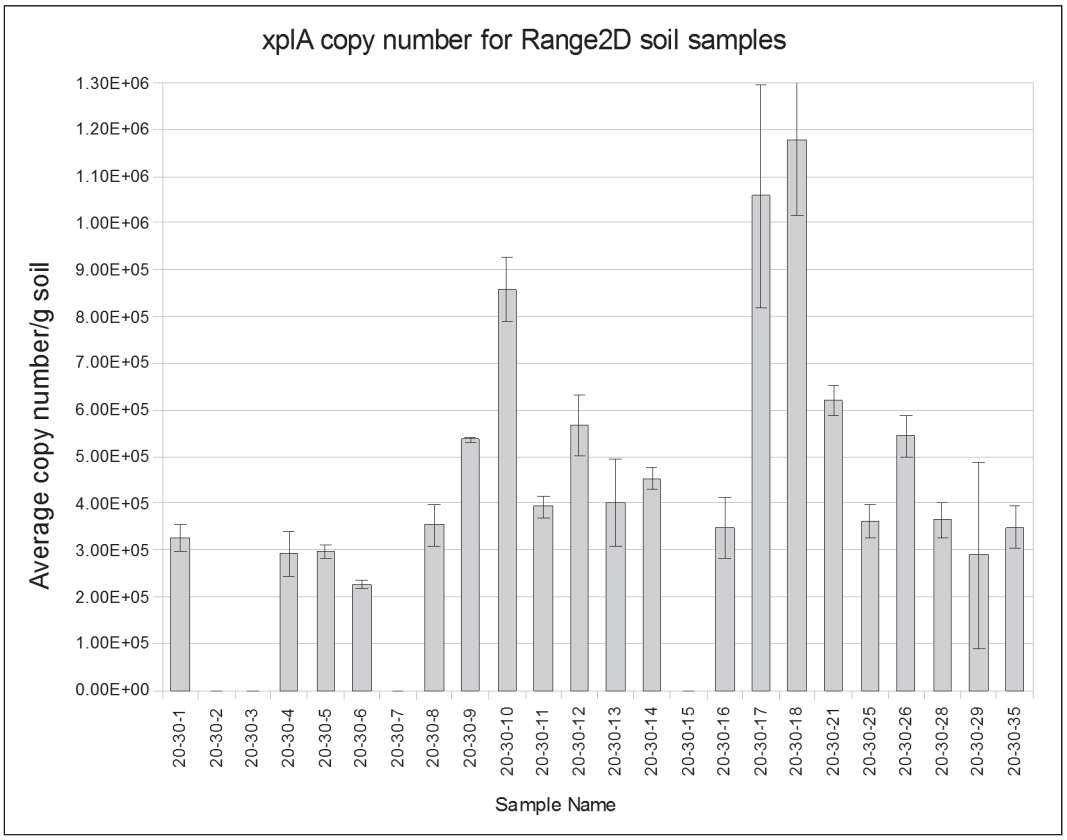

Figure 39. *xplA* gene copy numbers for selected samples from the Grenade Range2D grid. Some quadrants are missing due to insufficient DNA content in soil samples or due to insufficient numbers of completed replicate experiments.

Detection of xplA in IAAAP and UMCD groundwater

In July 2009 the IAAAP groundwater collected from well MW309 had dissolved oxygen levels around 1 mg/L, as well as MNX, DNX, and TNX and reduced levels of RDX at approximately 10 μg/L. In comparison, groundwater collected from well EMW-02 had dissolved oxygen levels that were consistent with aerobic conditions (4 mg/L), a small reduction in RDX levels, and sporadic, low levels of MNX and DNX (< 1 μg/L) present (TetraTech). Groundwater from IAAAP wells MW309 and EMW02 did not contain levels of the *xplA* gene above the detection limit (Table 25). The absence of the *xplA* gene in groundwater at IAAAP probably is a result of the ongoing treatment of the groundwater to stimulate the indigenous anaerobic microbial populations to transform RDX. In contrast, the UMCD treatment influent groundwater had a detectable, but variable number of *xplA* gene copies at 4472 ± 4762 copies/L (Table 25). The aquifer at UMCD is a highly permeable, aerobic aquifer with explosive concentrations in the groundwater influent consistently above 2.1 μg/L for RDX and 2.8 μg/L for TNT (U.S. Army Engineer District, Seattle 2010). The presence and abundance of *xplA* in UMCD groundwater appears to be consistent with favorable conditions in the groundwater for the growth of aerobic RDX degrading bacteria.

Table 25. Quantity of *xplA* gene detected in groundwater and soil.

Source	*xplA* Gene Copies[1]
Groundwater	
IAAAP MW309	9.68 ± 5.56
IAAAP EMW02	18.26 ± 10.04
UMCD, Treatment Influent	4472.00 ± 4762
Soil	
Camp Shelby, MS	139.55 ± 47.82
Ft. Richardson, AK	1618.28 ± 760.68
UMCD, OR	336.84 ± 103.43

[1]*xplA* gene copy values are per liter of filtered groundwater or per gram of soil. Values are averages ± standard deviations of six replicates.

Soil collected from an uncontaminated area near Camp Shelby, Mississippi exhibited *xplA* gene copy numbers that were only slightly above the functional detection limit of 100 gene copies (Table 25). Since the Camp Shelby soil has never been exposed to RDX, this result was not unexpected.

Soil collected from the lagoon washout area at UMCD had a slightly higher abundance of *xplA* gene than observed in the Camp Shelby soil, but the quantity was an order of magnitude lower than determined in the UMCD groundwater (Table 25). Various explosives and transformation products were detected in several batches of homogenized and sieved UMCD soil, including HMX (~ 3900-9600 µg/kg), RDX (ND – 400 µg/kg), TNT (~885 – 1400 µg/kg), 1,3,5-Trinitrobenzene (~120 – 14000 µg/kg), and 4-amino-2,6-dinitrotoluene (ND – 150 µg/kg) (Medina et al. 2012). Finally, soil collected from an impact area at Ft. Richardson, Alaska had a significant quantity of *xplA* gene copies despite the absence of a detectable level of explosives in the homogenized soil (Table 25). The presence of *xplA* in this soil may indicate the historical exposure of the soil microbial community to RDX.

Groundwater was also collected from UMCD during a TNT and RDX push-pull test after amendment with various carbon substrates designed to stimulate TNT and RDX degradation by anaerobic microorganisms. Groundwater (100 to 400 ml) was filtered on-site using (one to three) Sterivex filters from zones treated with lactose, corn syrup, or emulsified oil. Wells from zones treated with corn syrup (WO21-3) and emulsified oil (4-1-3, 4-113, and 4-113-8) had significant *xplA* signals (Figure 40); however, the *xplA* signal decreased with time in well 113 (time point 3 vs. 8) as the RDX migrated away from this well.[1] These results clearly indicate that the type of substrate added to groundwater in the field can significantly affect the biomass and activity of indigenous microorganisms and thus detection and quantification of functional signals. Even though the amendments used at UMCD were designed to stimulate anaerobic degradation, the transient increase in *xplA* gene copy number in some treated areas indicates that groundwater treatment effects are more complicated than expected.

Conclusions

Validation of the *xplA* TaqMan qPCR assay with groundwater and soil collected from military facilities has shown that *xplA* was detected at most locations that have been exposed to long-term explosive contamination. Soil samples from the grenade range at CFB Petawawa were observed to generally have low concentrations of RDX in agreement with observations from other grenade ranges in the United States and Canada (Pennington et al. 2005). The *xplA* gene was detected in most soil samples at CFB

[1] Personal Communication. 2011. M. Michalsen, Environmental Engineer, U.S. Army Engineer District, Seattle.

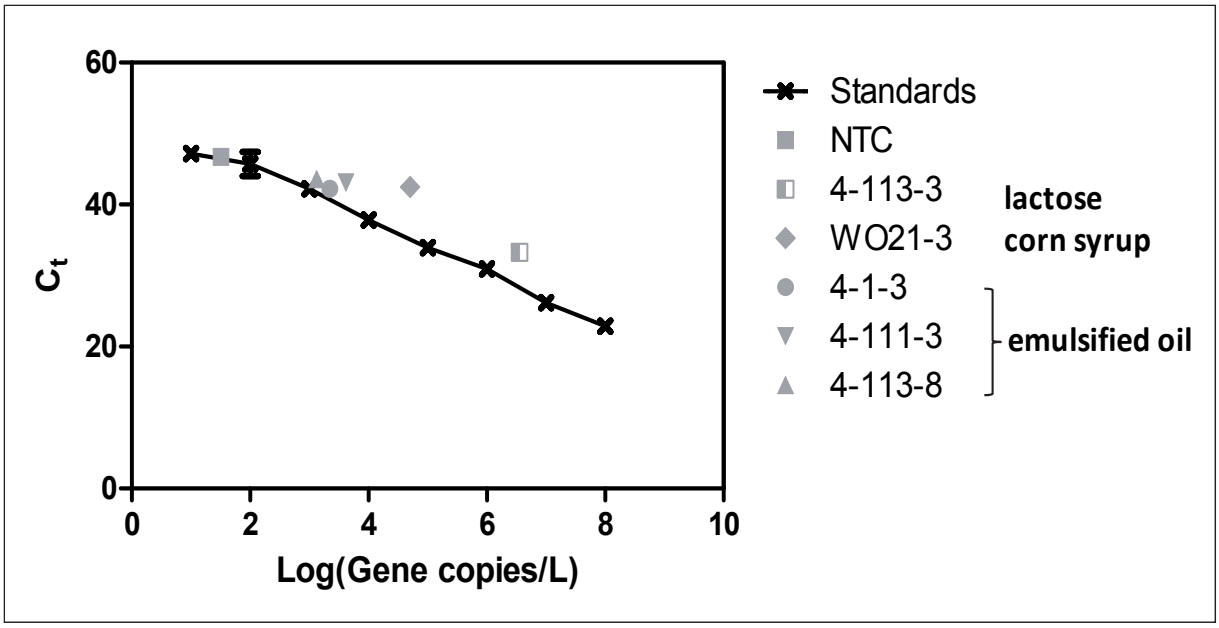

Figure 40. Quantity of *xplA* gene in UMCD groundwater following biostimulation. NTC = no template control.

Petawawa, which implies that the frequent use of this range has selected for RDX-degrading bacteria. Similarly, groundwater from UMCD and soil collected at Ft. Richardson had significant quantities of the *xplA* gene in agreement with historical exposure to explosives. In fact, the highest quantity of *xplA* was detected in the highly aerobic groundwater at UMCD. In comparison, the treatment of the IAAAP groundwater with nutrients designed to stimulate anaerobic microorganisms and the nitrosation of RDX has not selected for bacteria carrying the *xplA* gene. In addition, these data indicated that the *xpl*A qPCR was specific for the aerobic biodegradation pathway of RDX. Interestingly, the *xplA* gene was detected at low levels in soil collected near Camp Shelby despite the fact that this soil has not been exposed to explosives. Thus, these studies implied that the *xplA* biomarker assay has the potential to be used as a qualitative biomarker for detecting the presence of a catabolic potential to degrade RDX under aerobic conditions.

RDX biodegradation in soil and groundwater microcosms

Introduction

The goal of this task was to assess the potential of the *xpl*A TaqMan qPCR assay to detect and quantify *xplA* in soil and groundwater microcosms that had been amended with RDX. A positive correlation between the quantity of *xplA* in the microcosms and the RDX degradation rate would indicate a

potential for the assay to determine the potential for RDX biodegradation in the field.

Methods

CFB Petawawa aerobic and anaerobic soil microcosms

Several Petawawa soil samples (Figure 38) were selected to prepare 1 g scale soil microcosms. The soil was added to glass scintillation vials to which 5 µl of ^{14}C-labelled RDX were added as sole N source. The ^{14}C-RDX stock was diluted in acetone at a concentration of 10000 µg/ml (S. Rocheleau, National Research Council Canada, Montreal, QC). The tubes were left open for 15 min to allow the acetone to evaporate. The final concentration of RDX in the soil was 50 µg/g soil. The soil was mixed to evenly distribute the RDX and then 190 µL of buffer was added to the vial. The buffer was 20 mM KH_2PO_4, pH 6.5 and contained 2.8 mM glucose and 2.8 mM succinate. The buffer for the control vials contained an additional 115 mM sodium azide. Sample vials were sealed with ethanol-rinsed plastic caps lined with Teflon septa. Samples were incubated in the dark for 10 days at 30 ^{o}C. An alkaline trap was used to collect CO_2 in the headspace. Headspace $^{14}CO_2$ was measured using a Beckman scintillation counter on days 0, 1, 2, 3, 4, 7 and 10 of the experiment. Experiments were done in triplicate. All samples used in the mineralization experiment were run with replicate azide killed controls. Statistical analysis was used to determine if a correlation exists between the cumulative yield of $^{14}CO_2$ evolved over the 10-day incubation period and the average number of *xplA* gene copies per gram of soil (Figure 40).

Anaerobic soil microcosms were prepared with soil obtained from the CFB Petawawa collected in 2010. Sterile 60-mL serum bottles contained 7.5 g of soil, 50 ml of anaerobic mineral salts solution, and 10 mg L^{-1} (45 µM) of RDX. Abiotic controls (autoclaved soil) were prepared in parallel. One batch of bottles was supplemented with 1% (v/v) of molasses as the electron donor with either [^{12}C]-RDX or [^{14}C]-RDX. The bottles were sealed, flushed with argon, and incubated statically at 25 ^{o}C. At periodic intervals, replicate microcosms were sacrificed to determine the extent of RDX removal, the production of RDX transformation products, and for DNA extraction. Soil DNA extracts were prepared using the UltraClean Soil DNA Isolation Kit (Mo Bio Laboratories, Inc.). The DNA from triplicate soil samples was pooled and concentrated by filtration through Amicon Ultra 10K centrifugal filter units (Millipore). Soil DNA extracts were stored at -20 ^{o}C prior to PCR

analysis of the *cymA* and 16S rRNA genes in *Shewanella* (Table 26). In addition, aliquots were shipped overnight on dry ice to ERDC for qPCR analysis of the *xplA* gene.

The 50 µL PCR reactions contained ~100 ng of template DNA, 25 pmol of each of the forward and reverse primers, 200 µM of each deoxynucleoside triphosphate (dNTP), 1x PCR buffer, and 2.5 Units of rTaq DNA polymerase (Amersham Biosciences). PCR negative controls were prepared by replacing

Table 26. Primers for *cymA* and 16S rRNA gene of the group *Shewanellaceae.*

Primer	Target gene	Sequence 5'- 3'	Reference
CymA-F	cymA *Shewanellaceae*	TGGCGTGCACTATTYAAACC	(Murphy and Saltikov 2007)
CymA-R	cymA *Shewanellaceae*	TARGGGTGAGCRACRCCTTT	(Murphy and Saltikov 2007)
She211f	16S rRNA gene *Shewanellaceae*	CGCGATTGGATGAACCTAG	(Torodova and Costello 2006)
She1259r	16S rRNA gene *Shewanellaceae*	GGCTTTGCAACCCTCTGTA	(Torodova and Costello 2006)

the template DNA with sterile water. The PCR conditions consisted of an initial denaturation at 95°C for 5 min followed by 35 cycles 94°C for 1 min, 53°C for 1 min, and 72°C for 2 min, and a final extension at 72°C for 10 min. Aliquots of 10 µl of PCR products were loaded on a 1% agarose gel stained with SYBRSafe DNA gel strain (Invitrogen).

Aerobic soil microcosms

Soils collected from Ft. Richardson, Alaska; Camp Shelby, Mississippi; and UMCD, Oregon were used to establish aerobic microcosms. Microcosms consisted of 60- or 125-ml serum bottles containing 5 g of soil with a soil:liquid ratio of 1:4 or 1:10 for soil slurry incubations, or enough liquid to bring the moisture content to between 26.5 and 31.3% (wt/wt) for unsaturated soil incubations. Control microcosms were prepared with autoclaved soil (triplicate 1 h treatments at 121 °C) or $HgCl_2$ at 300 mg/L. The soils were amended with a nitrogen-free mineral salts medium (Crocker et al. 2005) or groundwater, glucose (0.9 g/L) or milk powder (500 mg/L) as carbon sources, and RDX (10 - 40 mg/L or 50 mg/kg). Soil slurries were incubated with shaking at 150 rpm and Ft. Richardson and Camp Shelby microcosms were incubated at 15 °C while UMCD microcosms were incubated at 25-30°C. A parallel set of UMCD microcosms was incubated in

sealed serum bottles amended with a trace amount of [^{14}C]-RDX (2500 dpm/mL) and a final total concentration of 40 mg/L RDX. Mineralization of [^{14}C]-RDX to $^{14}CO_2$ was monitored using a KOH (1N) trap and liquid scintillation counting (Crocker et al. 2005).

At periodic intervals, replicate microcosms were sacrificed to determine the concentration of RDX and to extract DNA. RDX was analyzed from both the aqueous and solid phases. The aqueous phase was mixed with an equal volume of acetonitrile, filtered through 0.45-µm PTFE filters, and analyzed via HPLC. A portion of the soil (1 g) was extracted with 5 ml of acetonitrile for 18 h at 20 °C with sonication. Following centrifugation, the supernatant was filtered and analyzed via HPLC. Soil DNA was extracted using bead beating with the PowerSoil DNA isolation kit (MoBio Laboratories, Inc.) as described above in the section titled "Molecular Detection of xplA in Soil and Groundwater." Quantitative PCR analysis of *xplA* using the TaqMan assay was determined on soil DNA extracts from day 0 and at the end of the incubation period.

Groundwater microcosms

Iowa Army Ammunition Plant groundwater from MW309 and EMW02 (75 ml) was amended with 5 mg/L RDX (added directly from an acetone stock at 8300 mg/L) and 5 mM sodium acetate. A set of sterile control microcosms containing groundwater that had been filtered (0.2 µm polyethersulfone filter) and then autoclaved were similarly amended. All treatments were in triplicate. The aerobic microcosms were incubated at room temperature (22 °C) with shaking at 150 rpm. Anaerobic microcosms were prepared using groundwater that had been purged with a sterile flow of N_2 for 1 h and then immediately placed in an anaerobic chamber (Coy). The sodium acetate stock was similarly purged with N_2 and then autoclaved in a sealed vial. Groundwater for sterile, anaerobic control flasks was filtered, purged with N_2 for 1 h, and then autoclaved in sealed bottles. Anaerobic microcosms were incubated without mixing at 25 °C. Samples (0.6 to 1 ml) were collected periodically and mixed with an equal volume of acetonitrile prior to filtration using a 0.45-µm PTFE filter. The RDX concentration of the samples was determined using HPLC (Crocker et al. 2005). In order to ensure a sufficient DNA quantity for the qPCR assay, the biomass in triplicate vials was pooled by filtration onto 0.45-µM filters. The filters were stored at -80 °C prior to DNA extraction as described in the section titled "Design of the xplA TaqMan Quantitative PCR Assay" for groundwater filtrates.

Results and discussion

CFB Petawawa aerobic and anaerobic microcosms

The total amount of ^{14}C-labeled RDX added to the aerobic microcosms was 15200 dpm. After 10 days, the level of RDX mineralization to CO_2 was comparable in all microcosm communities based on cumulative dpm counts (Table 27). The amount of RDX mineralized to CO_2 did not follow any

Table 27. Cumulative dpm values (after 10 days) in CFB Petawawa aerobic microcosms. The quantity of the *xplA* gene in the original soil samples is shown for comparison.

Sample	Experiment 1	Experiment 2	Experiment 3	Average	Copies *xplA* per gram soil (x 10^5)[1]
20-30-5	2077	4501	8161	4913	2.90
20-30-9	2079	4619	5663	4120.33	5.10
20-30-10	4706	4604	4068	4459.33	9.00
20-30-14	11045	919	4588	5517.33	4.50
20-30-16	4469	511	6692	3890.67	3.50
20-30-17	5634	4187	5350	5057	10.0
20-30-24	5653	3787	5609	5016.33	1.60
20-30-34	6891	5178	8558	6875.67	2.20

[1]qPCR assay used the SybrGreen technique for quantification of PCR product.

trends in relation to the RDX concentration or the *xplA* level of the original soil sample (Figure 41). All the soil communities examined in this experiment definitely possess an RDX degradation phenotype. Cumulative counts for azide-killed controls were in the 40-235 dpm range. No data could be obtained for some samples where insufficient soil quantities were left to perform replicate experiments on a 1-g scale. It is particularly unfortunate in the case of samples 20-30-21 and 20-30-26 (highest RDX levels observed), but these samples were exhausted during optimization of DNA extraction and RDX quantitation attempts.

RDX was transformed in anaerobic CFB Petawawa soil microcosms in the presence or absence of 1% (v/v) of molasses as the electron donor. The microcosms supplemented with 1% molasses degraded 50% of the RDX (~5 mg L^{-1}) in 2 days and the RDX was completely removed after 5 days (Figure 42A). After 12 days, ~10% of the carbon from RDX was recovered as

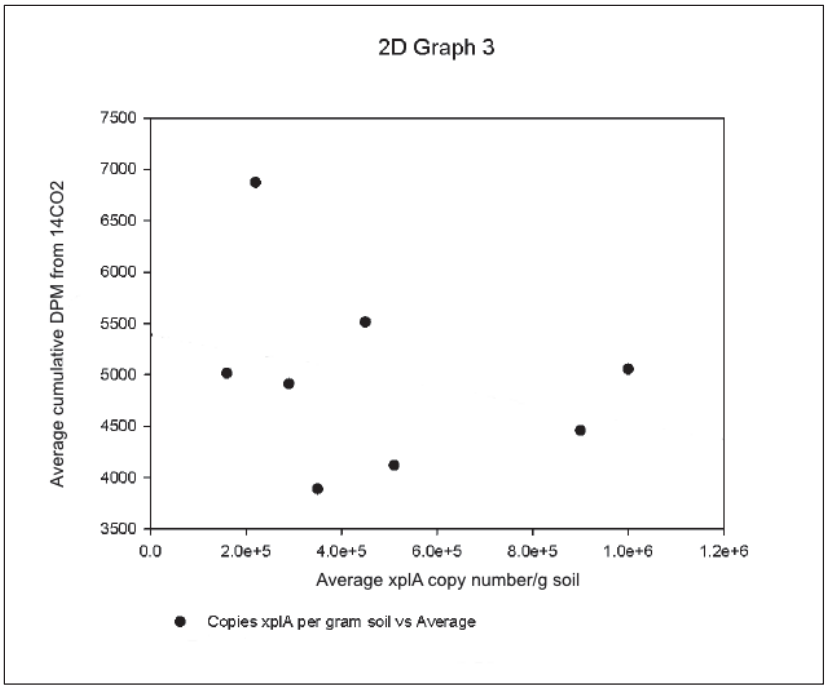

Figure 41. Scatter plot for average cumulative dpm from $^{14}CO_2$ from microcosms versus *xplA* copy number. A regression analysis was performed showing that there is no significant relationship between the two variables ($R^2 = 0.08$, and $p = 0.46$). Samples selected for this analysis were those with three sets of microcosm data that could be averaged for the Day 10 cumulative dpm value.

CO_2. The three nitroso intermediates (MNX, DNX, and TNX) were also detected. Nitrous oxide was observed, indicating that the RDX molecule was also transformed via denitration leading to ring cleavage and decomposition. RDX removal in abiotic control microcosms was negligible. RDX removal in microcosms without molasses was considerably slower; nitroso and denitration products were identified (Figure 42B).

DNA was extracted from the soil microcosms and selected DNA extracts were tested for the presence of the *cymA* gene and *Shewanella* species using PCR. Bacterial 16S rRNA genes were successfully amplified from all DNA samples, indicating that the DNA preparations were adequate for PCR amplification, i.e., that they did not contain impurities that could inhibit PCR amplification (data not shown). The *cymA* gene was successfully amplified from DNA samples extracted from anaerobic RDX-degrading soil slurries RDX (Figure 43). The gene was not detected in soil samples taken at time zero, or in the negative controls. Although the *cymA* was successfully amplified, DNA amplification was not observed for the 16S rRNA gene of *Shewanellaceae*, except for the positive control consisting of *S. oneidensis* MR-1 genomic DNA.

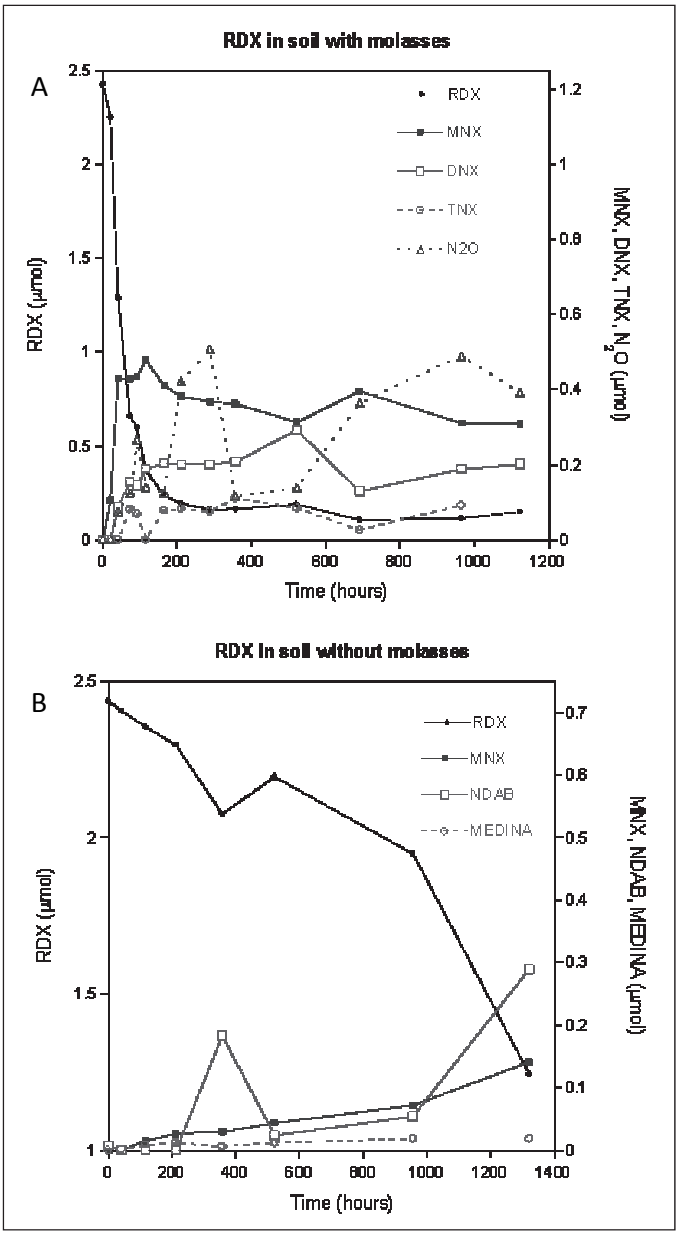

Figure 42. RDX degradation in anaerobic soil microcosms: (A) soil with 1% molasses; (B) soil without molasses.

The DNA extracts were also used to determine the abundance of the *xplA* gene and whether anaerobic conditions affect the presence of bacteria containing this gene. Prior to incubation with RDX, the CFB Petawawa soil had levels of the *xplA* gene above the no template controls (1.5 gene copies), but at a low, insignificant level (~ 55 gene copies). In the microcosms amended with molasses, the levels of *xplA* gene did not change significantly over the incubation period (Figure 44A). The RDX was rapidly degraded (primarily to the nitroso derivatives in these microcosms) indicating that anaerobic conditions were rapidly created. These conditions were therefore

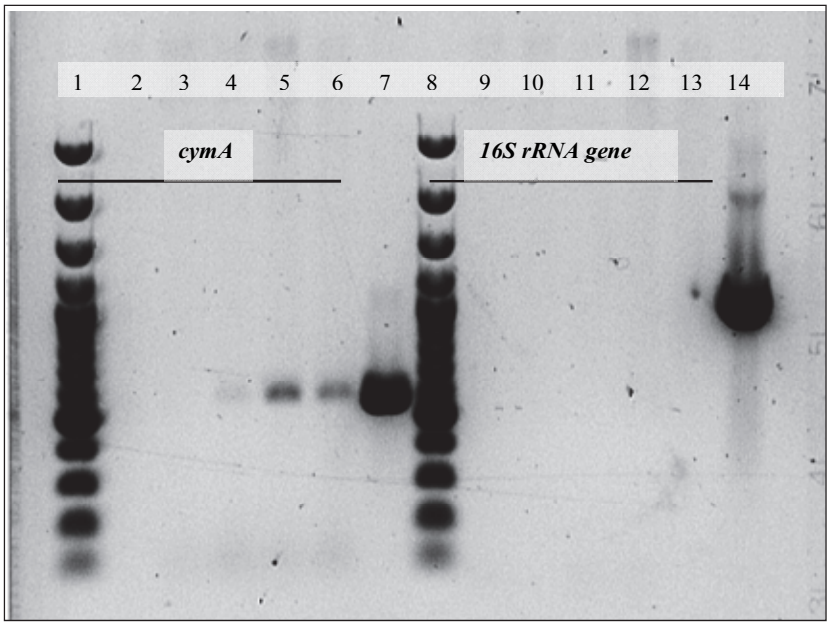

Figure 43. Results of PCR reactions with *cymA* primers and primers for the 16S rRNA gene of *Shewanellaceae* using DNA extracted from anaerobic RDX-degrading slurries as templates. Lanes 1 and 8, 100 bp DNA ladder plus; lanes 2 and 9, amplicons from soil with molasses at 0h; lanes 3 and 10, amplicons from soil with molasses after 41 h; lanes 4 and 11, amplicons from soil with molasses after 212 h; lanes 5 and 12, amplicons from soil with molasses after 1320 h; lanes 6 and 13, amplicons from soil without molasses after 41 h; lanes 7 and 14, amplicons from MR-1 genomic DNA (positive control).

not conducive to the survival of bacteria containing the *xplA* gene. The microcosms that were not amended with molasses degraded RDX slowly with the production of MNX, MEDINA, and NDAB. This indicated that bacteria that degraded RDX via mono-denitration and denitration of MNX were most active in these microcosms. Without the added carbon substrate, bacteria that utilize the nitroso route to transform RDX were not stimulated to the same extent as observed in the molasses-amended microcosms. The difference in the main mechanisms of RDX degradation between the carbon-amended and unamended microcosms was also observed in the analysis of the *xplA* gene copy number. At the earliest time point sampled (212 h), the level of *xplA* was slightly above the detection limit (~ 170 gene copies). The level of *xplA* detected at 1320 h was approximately 80,000 gene copies, but this level had dropped to approximately 500 gene copies by 2136 h (Figure 44B). The reason for the large increase of *xplA* at 1320 h is unknown at this time.

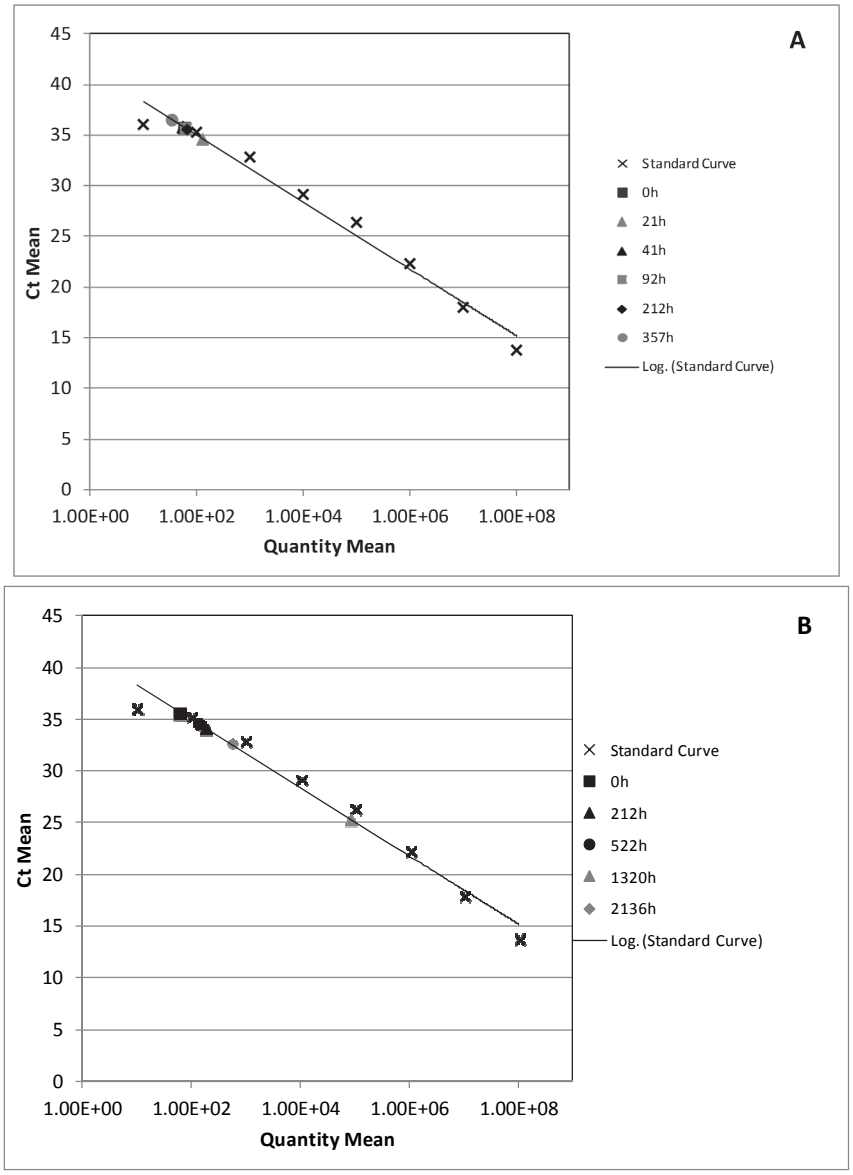

Figure 44. Quantity of *xplA* gene in CFB Petawawa anaerobic microcosms amended with (A) 1% molasses, or (B) unamended.

Ft. Richardson, Camp Shelby, and Umatilla aerobic soil microcosms

Unsaturated soil microcosms containing soil from Camp Shelby degraded approximately 37% of the added RDX in 25 days while the RDX was not degraded in the Ft. Richardson soil microcosms (Table 28). The *xplA* gene was present in the Camp Shelby soil at a low level that did not increase with time despite the degradation of RDX (Table 28). The Ft. Richardson soil contained a moderate level of *xplA* initially; however, the amount of *xplA* decreased during the incubation period (Table 28). Saturated soil microcosms containing UMCD washout lagoon soil degraded RDX slowly at rates

Table 28. RDX degradation and quantity of *xplA* in unsaturated soil microcosms incubated at 15 °C.

Soil	Treatment	RDX concentration (mg/kg)		*xplA* copy number[1]	
		Day 0	Day 25	Day 0	Day 25
Camp Shelby	Live	45 ± 5	28 ± 6	421 ± 205	431 ± 199
	Attenuated	38 ± 4	42 ± 3	185 ± 69	361 ± 321
Ft. Richardson	Live	27 ± 18	30 ± 5	3156 ± 600	797 ± 193
	Attenuated	47 ± 3	54 ± 4	1544 ± 277	4053 ± 3460

[1] Gene copy number has not been corrected for weight of soil extracted.

of 0.001 d^{-1} in the unamended microcosms to 0.009 d^{-1} in the microcosms amended with milk powder, resulting in loss of between 10 and 28% of the RDX in 26 days (Table 29, Figure 45A). The stimulation of RDX degradation by the carbon amendment was also observed by increases in the mineralization rates in the parallel microcosms (Table 29, Figure 45B). Approximately 10% of the [^{14}C]-RDX was mineralized in most of the replicates regardless of nutrient amendment, except in one replicate amended with glucose in which 30% of the [^{14}C]-RDX was mineralized (Figure 45B). Similarly, the stimulation of RDX rates was correlated with an increase in the abundance of the *xpl*A gene. The largest increase in *xplA* abundance was observed in the glucose-amended microcosms, although the degradation rate was not the highest in these microcosms (Table 29). These results indicate that while the *xplA* TaqMan assay may not be suitable as a biomarker to correlate gene abundance with activity, it may have a role as a qualitative tool for detection of a catabolic potential at a field site.

Groundwater microcosms

Aerobic IAAAP groundwater microcosms from wells EMW02 and MW309 amended with RDX at 5 mg/L and acetate at 5 mM did not degrade RDX even though bacterial growth was observed (data not shown). Approximately 10 mg/L of RDX was degraded in anaerobic MW309 groundwater within 14 days. An additional 10 mg/L RDX was added at day 14 to one-half of the microcosms and this was also rapidly degraded within 14 days (Figure 47A). No degradation of RDX was observed in filtered and autoclaved groundwater microcosms (Figure 46B). In contrast, groundwater from well EMW02 did not degrade RDX under anaerobic conditions when amended with acetate (Figures 46C and 46D). This may reflect the low numbers of anaerobic microorganisms in this well or that another carbon source is required to stimulate RDX degradation. With regards to *xplA* gene copy numbers, there was essentially no change in copy number in samples

Table 29. RDX degradation and mineralization rates in UMCD soil slurries compared with the abundance of the *xplA* gene.

Amendment	Degradation rate (d^{-1})[1]	Mineralization rate (d^{-1})[2]	*xplA* (gene copies x 10^3 g^{-1})[1]
Before Incubation	NA[3]	NA	0.34 ± 0.1
Unamended	0.001	0.168	15.00 ± 3.8
Glucose	0.005	0.264 (0.354)[4]	72.00 ± 56
Milk powder	0.009	0.472	8.50 ± 7.7

[1] Determined from microcosms amended with RDX.

[2] Determined from microcosms amended with [^{14}C]RDX.

[3] NA: not applicable.

[4] Value in parantheses is for the one outlying replicate.

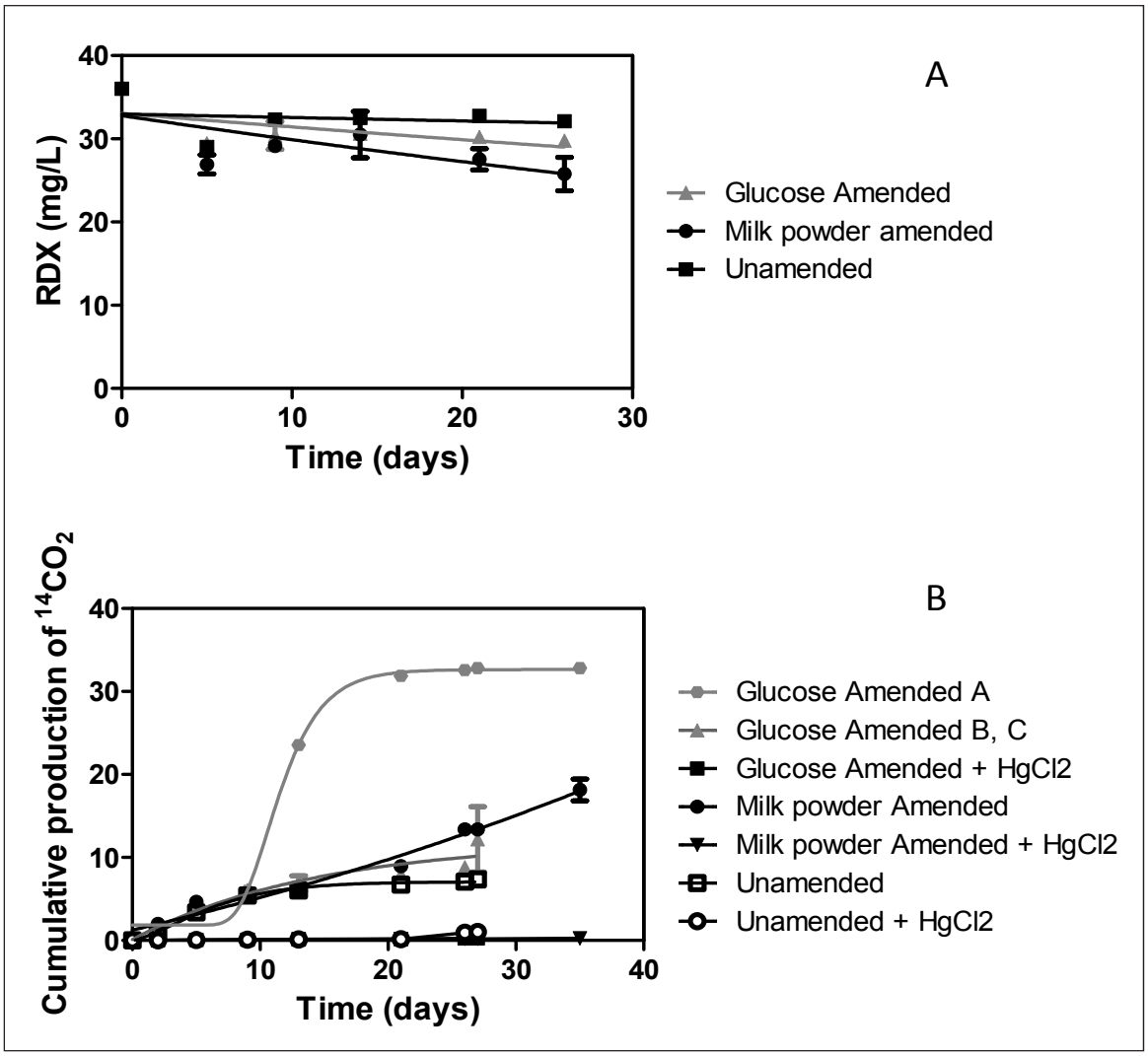

Figure 45. Degradation (A) and mineralization (B) of RDX (40 mg/L) in UMCD soil slurries amended with 5 mM glucose, 500 mg/L milk powder, or no carbon additions (unamended).

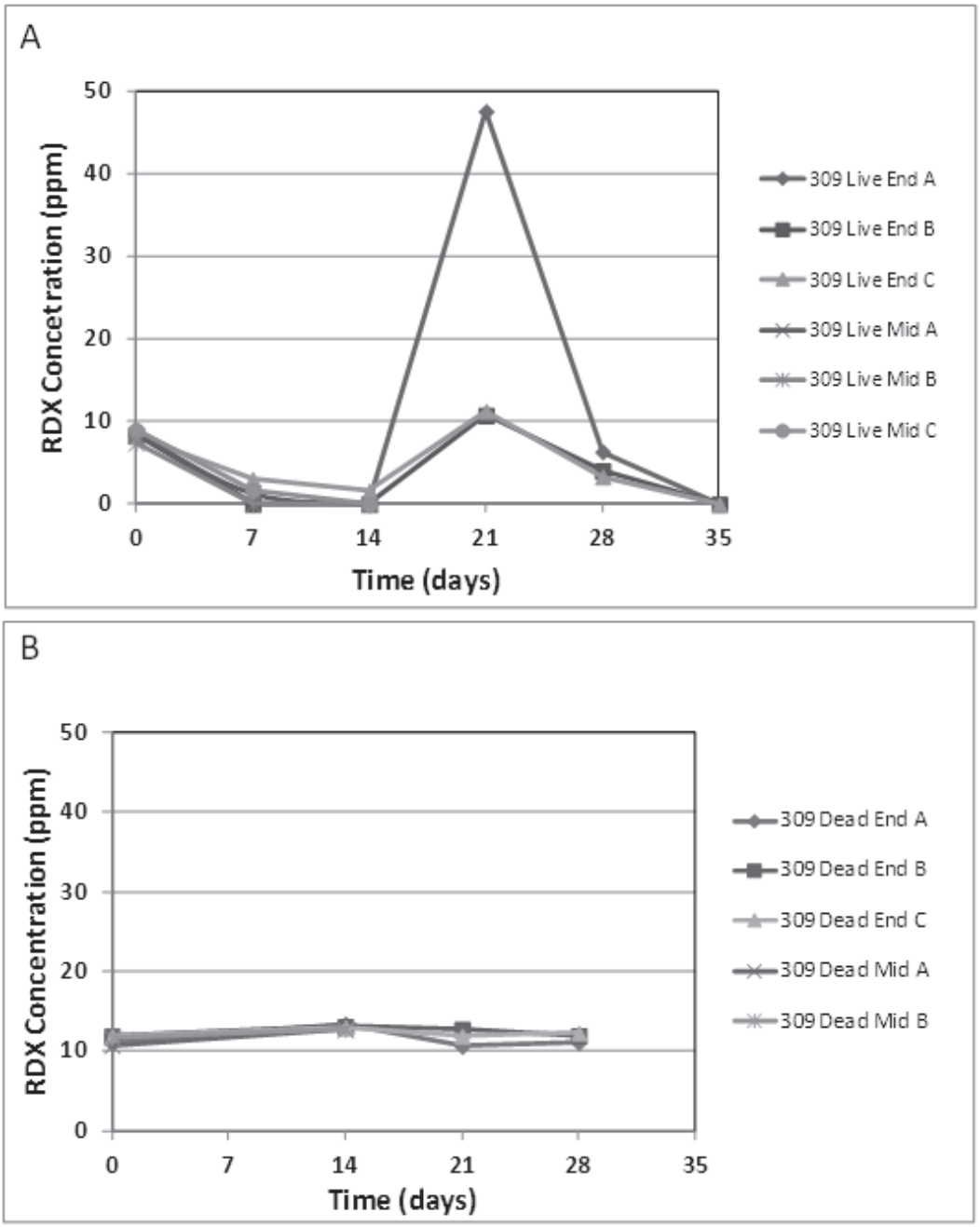

Figure 46. RDX degradation in Iowa Army Ammunition Plant groundwater from monitoring wells (A) MW309; (B) MW309 – 0.2-µm filtered groundwater; (C) MW02; and (D) MW02 - 0.2 µm filtered groundwater. Groundwater was supplemented with 5 mM acetate and 5 mg/L RDX, and incubated under anaerobic conditions for 28 days (Mid) or 35 days (End).

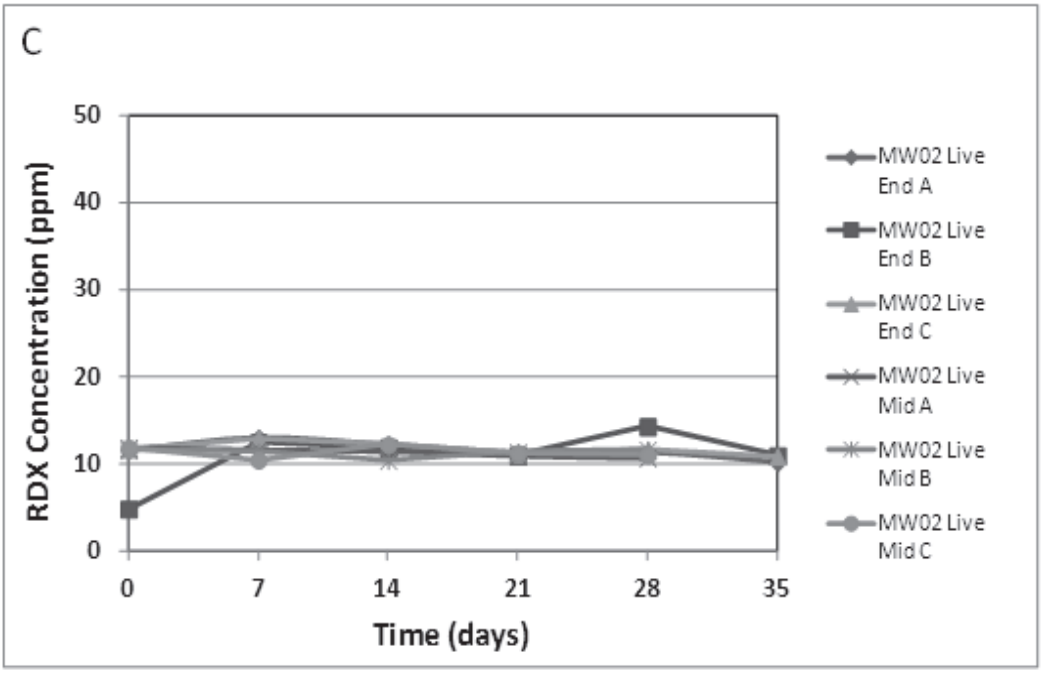

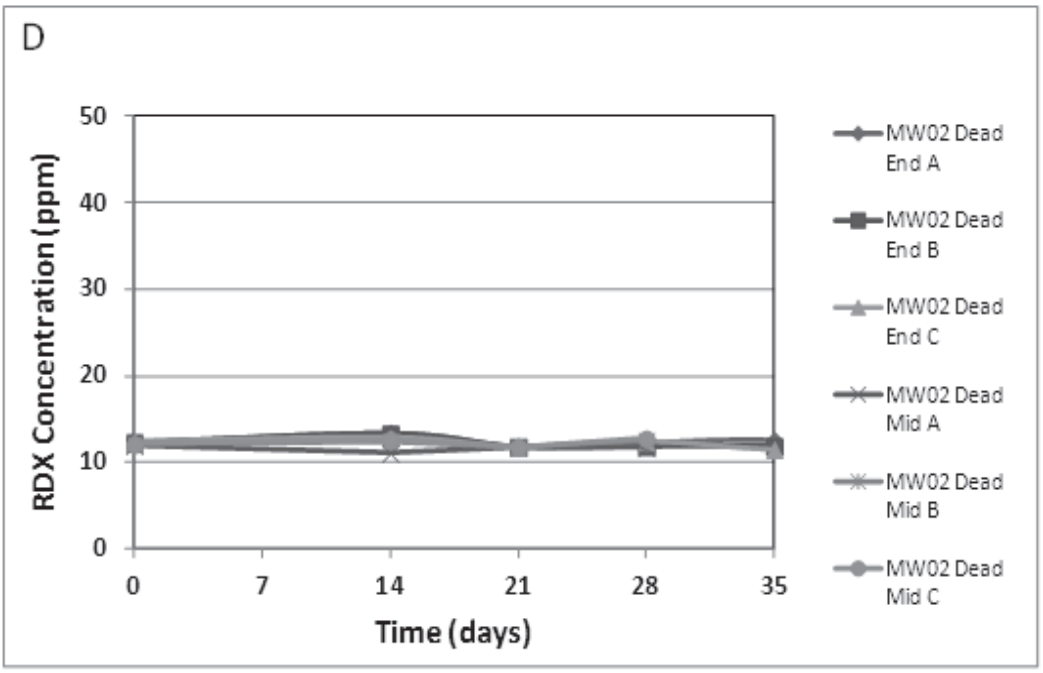

Figure 46. (continued).

from the aerobic and anaerobic EMW02 microcosms (150 – 400 and 65 – 200 *xplA* gene copies, respectively). Similarly, the levels of *xplA* did not change significantly in MW309 microcosms incubated under aerobic conditions (300 – 600 *xplA* gene copies). In comparison, the MW309 anaerobic microcosms exhibited variable levels of *xplA* that were between 400 and 2100 gene copies at day 14 in both live microcosms and sterile microcosms. However, the amount of *xplA* decreased to detection levels (~ 30 gene

copies) by day 35 in live microcosms, while they remained relatively constant in the sterile microcosms.

Conclusions

The qPCR assay used in this study targets the number of DNA copies of a gene in a soil or groundwater sample. Thus, this biomarker assay indirectly assesses bacterial activity by quantifying the potential for the microbial community to degrade RDX. A correlation between the quantity of the *xplA* gene and RDX degradation would help strengthen this line of evidence. In this study, the soils from CFB Petawawa, UMCD, and Camp Shelby degraded RDX under aerobic conditions. These results suggested that the *xplA* TaqMan qPCR assay reliably predicted the catabolic potential at these sites. In addition, the specificity of this qPCR assay for aerobic biotransformation of RDX was observed by the absence of aerobic RDX biodegradation in IAAAP groundwater microcosms. This observation was correlated with an inability to detect the *xplA* gene in this groundwater. However, a correlation between the quantity of *xplA* gene copies and rates of RDX degradation was inconclusive, due to the lack of a significant increasing trend in copy number with the amount of RDX loss. Since only a limited number of samples have been examined, it is possible that this correlation may be supported by additional experiments using different materials and identifying the end-products formed.

6 Conclusions and Implications for Future Research/Implementation

Hexahydro-1,3,5-trinitro-1,3,5-triazine (RDX), is a recalcitrant nitramine explosive with a low sorption capacity that has led to groundwater contamination at some U.S. and Canadian military facilities. The toxicity and persistence of RDX ultimately threatens the long-term sustainability of these facilities, leading to closure of ranges for military training. Training ranges at Camp Edwards, MA were temporarily closed while the extent of explosive soil and groundwater contamination was assessed and restoration plans were implemented. Lower costs of treatment and a minimally invasive approach make *in situ* bioremediation a possible remedial action for contaminated groundwater. However, methods to assess the potential for *in situ* bioremediation of RDX and to monitor treatment are generally lacking. Advances in molecular biology such as high-throughput DNA sequencing and differential gene and protein expression analyses are providing access to biochemical and genetic information on cultivable and uncultivable microorganisms. Gene and protein biomarkers identified by such studies can be used to develop molecular tools that can be applied to detect and monitor metabolic genes and microbial species that are relevant to RDX biodegradation in soil and groundwater.

Project ER-1609 "Identification of Microbial Gene Biomarkers for *in situ* RDX Biodegradation" was conceived to increase the current state of knowledge regarding catabolic pathways, enzymes, and genes associated with RDX biodegradation. *Gordonia* sp. KTR9 and *Shewanella oneidensis* MR-1 were chosen as representative aerobic and anaerobic RDX-degrading bacteria, since they use different mechanisms to transform RDX. Biochemical, physiological, proteomic, and genomic approaches were used to bridge this knowledge gap. Gene targets identified by these methods, as well as existing gene targets (e.g. *xplA*), were examined as potential molecular tools of RDX biodegradation.

This project demonstrated that the genes for aerobic denitration of RDX, *xplAB*, are located on a 182 kb plasmid, pGKT2, in *Gordonia* sp. KTR9. The *xplA* gene encodes a flavodoxin-fused cytochrome P450 enzyme that catalyzes the removal of nitrite (denitration) from RDX. Other genes that cluster with *xplA* were predicted to encode a glutamine synthetase-flavodoxin

reductase fusion protein, GlnAXplB; a second cytochrome P450, Cyp151C; and a GntR-type regulator, XplR. The functions of these novel proteins could not be determined using enzyme assays, expression in *E. coli,* or in deletion mutants of KTR9.

In parallel with KTR9 genome sequencing and annotation efforts, a proteomics approach was initially chosen in order to facilitate the identification of novel proteins in KTR9 associated with RDX degradation. Proteomic analysis of KTR9 grown on RDX as a nitrogen source identified proteins involved in nitrogen assimilation, transcriptional regulation, and the XplA cytochrome P450 that were up-regulated. These same types of genes were up-regulated when KTR9 was grown on RDX as the nitrogen source. In addition, genes involved in transport, nucleic acid/amino acid catabolism/ fatty acid catabolism, and stress/redox imbalance were also up-regulated. These results suggested that the transcriptome response to RDX is likely a reaction to nitrogen limitation rather than a response to RDX. Physiological studies in combination with *xplA* gene expression analyses indicated that inorganic nitrogen sources have significant inhibitory effects on RDX degradation and *xplA* expression. These studies also confirmed that the repression of *xplA* by ammonium and nitrite was not dependent on GlnR, a central regulator of nitrogen uptake and metabolism, but that GlnR may regulate an RDX transport protein. However, this could not be proven for a permease (KTR9-0967), which had been significantly up-regulated in the presence of RDX. Thus, of these five gene targets (*xplA*, *xplR*, *cyp151C*, *glnR*, and KTR9-0967), only *xplA* met criteria as a suitable biomarker.

Shewanella oneidensis MR-1 was shown to efficiently degrade RDX anaerobically (3.5 μmol h^{-1} g^{-1}) via two initial routes: (1) sequential N-NO_2 reductions to the corresponding nitroso (N-NO) derivatives, MNX, DNX, and TNX (94% of initial RDX degradation); (2) denitration followed by ring cleavage to MEDINA, NDAB, HCHO, N_2O, NO_2^-, and NH_4^+. Since little is known about the enzymes that transform RDX by nitrosation or mono-denitration, gene expression and mutagenesis approaches were used to elucidate whether nitroreductase genes, Old Yellow family genes, or other novel genes were associated with RDX transformation in strain MR-1. However, despite the fact that *Shewanella* genomes contain genes for nitroreductases, and Old Yellow family flavoenzymes (Zhao et al. 2010), no evidence was found that these genes were up-regulated by the presence of RDX. In comparison to strain KTR9, the majority of genes up-

regulated in strain MR-1 were involved in nitrogen metabolism, transport, redox balance, and transcriptional regulation.

None of these genes was interrupted by transposon mutagenesis, so that the role of these genes in RDX transformation by MR-1 remains unknown at this time. Interestingly, a gene encoding a tetraheme cytochrome c, *cymA*, was interrupted by transposon mutagenesis. The CymA cytochrome c has a major role as an electron transporter in the reduction of Fe(III)/Mn(IV) oxides, fumarate, nitrate, and dimethylsulfoxide (Myers and Myers 1997; Schwalb et al. 2003). Disruption of this gene in MR-1 led to a significant reduction in the rate of RDX degradation and a shift in the major end products away from the nitroso derivatives towards the ring cleavage products. While a functional gene associated with RDX degradation was not identified in strain MR-1, the data showed that the electron transport system in MR-1 may have a role in RDX transformation.

The multiple approaches used in this study identified only a single gene target that met the criteria as a biomarker of RDX biodegradation. The cytochrome P450 gene, *xplA*, was the only gene that was unique to the RDX biodegradation – namely aerobic denitration, present in a specific group of bacteria, and possessing significant gene homology. The TaqMan qPCR assay that was designed was shown to efficiently and specifically detect the *xplA* gene in only those bacterial strains able to transform RDX by di-denitration to NDAB. Validation of the *xplA* TaqMan qPCR assay with groundwater and soil collected from military facilities showed that *xplA* was detected at most locations that had been exposed to long-term explosive contamination. Most of these soils and groundwater degraded RDX under aerobic conditions, suggesting that the qPCR assay reliably predicted the catabolic potential at these sites. The specificity of the *xplA* assay for aerobic biotransformation of RDX was observed by the absence of the gene in groundwater samples from an aquifer undergoing anaerobic biostimulation, and the absence of aerobic RDX biodegradation in microcosms containing this groundwater. However, a correlation between the quantity of *xplA* gene copies and rates of RDX degradation was inconclusive, due to the lack a significant increasing trend in copy number with the amount of RDX loss. With the limited number of soils and groundwaters examined, this project for now indicates that the *xplA* TaqMan qPCR assay has the potential to be used to detect the presence of a catabolic potential for aerobic RDX degradation.

The fundamental information gained in this study confirmed the role of XplA in aerobic denitration of RDX to ring cleavage products; and confirmed that the fortuitous RDX transformation in *S. oneidensis* MR-1 mainly produces the nitroso derivatives MNX, DNX, and TNX, with minor amounts of ring cleavage products via MEDINA. A functional gene marker was not identified in MR-1, but the transcriptomic and transposon mutagenesis studies indicate that the role of the electron transport system in RDX degradation is important. Future research with targeted gene deletions should be investigated in order to elucidate the various mechanisms and regulations that generate nitroso derivatives versus ring cleavage products. These studies may then identify a suitable biomarker candidate for the detection of *in situ* anaerobic RDX biodegradation.

With regards to XplA, aerobic denitration of RDX will be subjected to regulatory effects in response to nitrogen availability. Excess inorganic nitrogen inhibits RDX degradation in KTR9, with greater inhibition occurring in the presence of ammonium than with nitrite, which suggests that ammonium is preferentially used as the nitrogen source by KTR9. Similarly, concentrations between 100 and 1000 mg/L for ammonium, nitrite, and nitrate have been reported to inhibit RDX degradation rates for other aerobic RDX-degrading *Rhodococcus* species (Bernstein et al. 2011; Coleman et al. 1998; Nejidat et al. 2008). Specifically, it was determined that the expression of *xplA* is repressed under excess nitrogen conditions (greater than 50 mg/L) and up-regulated under nitrogen-limiting conditions (~ <2 mg/L NH_4^+-N or ~ <10 mg/L NO_2^--N). The exact nature of this regulation is unclear at this time and should be further investigated in several of the aerobic RDX-degrading species in order to make inferences regarding RDX biodegradation rates in soils or groundwaters.

Nitrogen inputs into groundwater will most likely come from animal feed lots, fertilizer applications, organic waste disposal, and explosive production facilities. At Camp Edwards, Massachusetts, ammonium levels in groundwater impacted by wastewater were between 0 to 108 μM (Bohlke et al. 2006). Nitrate and nitrite levels in this groundwater were reported to be between 40 and 240 μM and <0.01 μM to around 0.09 μM, respectively. Nitrate levels as high as 30 mg/L in groundwater at Cornhusker Army Ammunition Plant were the result of fertilizer or animal waste applications in the area (Spalding and Fulton 1988). In addition, RDX-contaminated groundwater at UMCD, IAAAP, and in Israel

contained nitrate and nitrite at levels <4 mM[1], nitrate between 0.03 and 0.35 mM, nitrite between 2 and 28 μM,[2] and nitrate up to 3.2 mM (Bernstein et al. 2011), respectively. Generally, these examples indicate that inorganic nitrogen concentrations will be at significant levels to inhibit aerobic RDX biodegradation if the soil or groundwater is near areas that receive external inputs of nitrogen from human activities. Despite the millimolar concentrations of nitrate in UMCD and Israeli groundwater, there is evidence that aerobic RDX degradation is occurring within aerobic portions of the aquifers; as well as the isolation of aerobic RDX-degrading bacteria from the Israeli aquifer (Bernstein et al. 2011), and detection of the *xplA* gene in UMCD groundwater samples.[1]

These data have implications for the role of *xplA* as a biomarker of RDX degradation, as site managers will also be required to measure nitrate and ammonium concentrations in order to determine the impacts of these nitrogen compounds on rates of RDX biodegradation. Since the relationship between RDX degradation rates and inorganic nitrogen concentrations in soils and groundwater was not determined in this project, it can only be suggested that concentrations above 100 to 250 mg/L of ammonium, nitrite, and nitrate will decrease rates of RDX biodegradation, as observed with pure bacterial cultures. Additional research is required to determine reliable guidelines for site managers on the relationship between inorganic nitrogen concentrations and rates of RDX biodegradation, as well as techniques to lower inorganic nitrogen concentrations and enhance aerobic RDX biodegradation rates.

The demonstration that *xplA* can be disseminated to related bacteria by conjugation is significant, as bioaugmentation has not previously been considered or shown to be effective for RDX-contaminated aquifers. Bioaugmentation utilizing *xplA*-containing bacteria may have the beneficial effect of propagating the indigenous microbial population with the ability to degrade RDX, thus reducing treatment times and expenses. The *xplA* qPCR assay would be useful in this scenario, since it could be used to monitor and quantify the increase and spread of this functional gene target. Currently, the *xplA* TaqMan qPCR assay would only be useful for qualitatively evaluating RDX catabolic potential in environmental

[1] Personal Communication. 2011. M. Michalsen, Environmental Engineer, U.S. Army Engineer District, Seattle.

[2] Personal Communication. 2009. R. Arnesth, Senior Project Manager, Geochemist Tetra Tech, Inc., Oak Ridge, TN (provided data files of elemental composition of groundwater).

samples. Since regulators and site managers would be more inclined to adopt molecular tools that can indicate rates of contaminant degradation as proof of active biodegradation, this assay has a limited potential to be used commercially.

Based on a survey of TaqMan qPCR assays that are commercially available, it is predicted that the cost of the *xplA* TaqMan assay will be approximately $250-400 per sample. This cost does not include well installation, as it is expected that existing monitoring wells will be used. The cost does include sample collection, transport, storage, DNA extraction, qPCR analysis, and labor. The assay is expected to minimally add to the cost of site characterization or monitoring with the advantage that data are available within 1 to 2 days compared to 3-4 weeks for microcosm studies or chemical analyses. Unexpectedly, it could not be shown conclusively that the *xplA* TaqMan qPCR assay could be used as a quantitative measure of RDX degradation activity, since only a limited number of soils and groundwaters were examined in this study. Furthermore, a logical analysis of how inorganic nitrogen concentrations in soils and groundwater affect aerobic RDX biodegradation rates has not been conducted to date. Mainly, this is due to the recent discovery of the effects of inorganic nitrogen on RDX degradation in the aerobic RDX-degrading bacteria. Thus, it is recommended that the effectiveness of the *xplA* biomarker assay as a quantitative tool be expanded to include additional field sites; that further optimization of the biomarker assay be considered; and that the regulation of RDX biodegradation by inorganic nitrogen species in the field should be determined.

References

Altschul,S. F., W. Gish, W. Miller, E. W. Myers, and D. J. Lipman. 1990. Basic local alignment search tool. *J Mol Biol* 215: 403-410.

Amon, J., T. Bräu, A. Grimrath, E. Hänssler, K. Hasselt, M. Höller, N. Jessberger, L. Ott, J. Szököl, F. Titgemeyer, and A. Burkovski. 2008. Nitrogen control in Mycobacterium smegmatis: nitrogen-dependent expression of ammonium transport and assimilation proteins depends on the OmpR-type regulator GlnR. *J Bacteriol*. 190:7108-16.

Andeer, P., D. A. Stahl, N. C. Bruce, and S. E. Strand. 2009. Lateral Transfer of Genes for RDX Degradation. *Appl Environ Microbiol* 75: 3258-3262.

Arenskotter, M., D. Broker, and A. Steinbuchel. 2004. Biology of the metabolically diverse genus *Gordonia*. *Appl Environ Microbiol* 70: 3195-3204.

Balakrishnan, V. K., A. Halasz, and J. Hawari. 2003. Alkaline hydrolysis of the cyclic nitramine explosives RDX, HMX, and CL-20: new insights into degradation pathways obtained by the observation of novel intermediates. *Environ Sci Technol* 37: 1838-1843.

Balkwill, D. L., and W. C. Ghiorse. 1985. Characterization of subsurface bacteria associated with two shallow aquifers in Oklahoma. *Appl Environ Microbiol* 50: 580-588.

Beliaev, A. S., D. K. Thompson, T. Khare, H. Lim, C. C. Brandt, G. Li, A. E. Murray, J. F. Heidelberg, C. S. Giometti, J. Yates, III, K. H. Nealson, J. M. Tiedje, and J. Zhoui. 2002. Gene and protein expression profiles of *Shewanella oneidensis* during anaerobic growth with different electron acceptors. *OMICS* 6: 39-60.

Beller, H. R. 2002. Anaerobic biotransformation of RDX (hexahydro-1,3,5-trinitro-1,3,5-triazine) by aquifer bacteria using hydrogen as the sole electron donor. *Water Res*. 36: 2533-2540.

Beller, H. R., S. R. Kane, T. C. Legler, and P. J. J. Alvarez. 2002. A real-time polymerase chain reaction method for monitoring anaerobic, hydrocarbon-degrading bacteria based on a catabolic gene. *Environ Sci Technol* 36: 3977-3984.

Beller, H. R., and K. Tiemeier. 2002. Use of liquid chromatography/tandem mass spectrometry to detect distinctive indicators of *in situ* RDX transformation in contaminated groundwater. *Environ Sci Technol* 36: 2060-2066.

Benndorf, D., and W. Babel. 2002. Assimilatory detoxification of herbicides by *Delftia acidovorans* MC1: induction of two chlorocatechol 1,2-dioxygenases as a response to chemostress. *Microbiology* 148: 2883-2888.

Bernstein, A., E. Adar, A. Nejidat, and Z. Ronen. 2011. Isolation and characterization of RDX-degrading *Rhodococcus* species from a contaminated aquifer. *Biodegradation* 22: 997-1005.

Bhushan, B., A. Halasz, and J. Hawari. 2006. Effect of iron(III), humic acids and anthraquinone-2,6-disulfonate on biodegradation of cyclic nitramines by Clostridium sp. EDB2. *J Appl Microbiol* 100: 555-563.

Bhushan, B., A. Halasz, J. C. Spain, and J. Hawari. 2002a. Diaphorase catalyzed biotransformation of RDX via N-denitration mechanism. *Biochem Biophys Res Comm* 296: 779-784.

Bhushan, B., A. Halasz, J. C. Spain, S. Thiboutot, G. Ampleman, and J. Hawari. 2002b. Biotransformation of hexahydro-1,3,5-trinitro-1,3,5-triazine catalyzed by NAD(P)H: nitrate oxidoreductase from *Aspergillus niger*. *Environ Sci Technol* 36: 3104-3108.

Bhushan, B., A. Halasz, S. Thiboutot, G. Ampleman, and J. Hawari. 2004. Chemotaxis-mediated biodegradation of cyclic nitramine explosives RDX, HMX, and CL-20 by *Clostridium* sp. EDB2. *Biochem Biophys Res Comm* 316: 816-821.

Bhushan,B., S. Trott, J. C. Spain, A. Halasz, L. Paquet, and J. Hawari. 2003. Biotransformation of hexahydro-1,3,5-trinitro-1,3,5-triazine (RDX) by a rabbit liver cytochrome P450: insight into the mechanism of RDX biodegradation by *Rhodococcus* sp. strain DN22. *Appl Environ Microbiol* 69: 1347-1351.

Bohlke, J. K., R. L. Smith, D. N. Miller. 2006. Ammonium transport and reaction in contaminated groundwater: Application of isotope tracers and isotope fractionation studies. *Water Resources Research* 42: W05411.

Bradley, P. M., and R. S. Dinicola. 2005. RDX (hexahydro-1,3,5-trinitro-1,3,5-triazine) biodegradation in aquifer sediments under manganese-reducing conditions. *Bioremed J* 9: 1-8.

Bröker, D., M. Arenskötter, A. Legatzki, D. H. Nies, and A. Steinbüchel. 2004. Characterization of the 101-Kilobase-pair Megaplasmid pKB1, Isolated from the rubber-degrading bacterium *Gordonia westfalica* Kb1. *J Bacteriol* 186: 212-225.

Bryant, C., L. Hubbard, and W. D. McElroy. 1991. Cloning, nucleotide sequence, and expression of the nitroreductase gene from *Enterobacter cloacae*. *J Biol Chem* 266: 4126-4130.

Cabello, P., C. Pino, M. F. Olmo-Mira, F. Castillo, M. D. Roldan, and C. Moreno-Vivian. 2004. Hydroxylamine assimilation by *Rhodobacter capsulatus* E1F1; requirement of the hcp gene (hybrid cluster protein) located in the nitrate assimilation *nas* gene region for hydroxylamine reduction. *J Biol Chem* 279: 45485-45494.

Capyk, J. K., R. Kalscheuer, G. R. Stewart, J. Liu, H. Kwon, R. Zhao, S. Okamoto, W. R. Jacobs, Jr., L. D. Eltis, and W. W. Mohn. 2009. Mycobacterial cytochrome P450 125 (Cyp125) catalyzes the terminal hydroxylation of C27-steroids. *J Biol Chem* 384:35534-35542.

Chang, H.-W., H.-Y. Kahng, S.-I. Kim, J. W. Chun, and K.-H. Oh. 2004. Characterization of *Pseudomonas* sp. HK-6 cells responding to explosive RDX (hexahydro-1,3,5-trinitro-1,3,5-triazine). *Appl Microbiol Biotechnol* 65: 323-329.

Clausen, J., J. Robb, D. Curry, and N. Korte. 2004. A case study of contaminants on military ranges: Camp Edwards, Massachusetts, USA. *Environ Pollut* 129: 13-21.

Coleman, N. V., D. R. Nelson, and T. Duxbury. 1998. Aerobic biodegradation of hexahydro-1,3,5-trinitro-1,3,5-triazine (RDX) as a nitrogen source by a *Rhodococcus* sp. strain DN22. *Soil Biol Biochem* 30: 1159-1167.

Comfort, S. D., P. J. Shea, T. A. Machacek, and T. Satapanajaru. 2003. Pilot-scale treatment of RDX-contaminated soil with zerovalent iron. *J Environ Qual* 32: 1717-1725.

Crocker, F. H., K. J. Indest, and H. L. Fredrickson. 2006. Biodegradation of the cyclic nitramine explosives RDX, HMX, and CL-20. *Appl Microbiol Biotechnol* 73: 274-290.

Crocker, F. H., K. T. Thompson, J. E. Szecsody, and H. L. Fredrickson. 2005. Biotic and abiotic degradation of CL-20 and RDX in soils. *J of Environ Qual* 34: 2208-2216.

Danielsen, S., M. Kilstrup., K. Barilla., B. Jochimsen, and J. Neuhard. 1992. Characterization of the *Escherichia coli* codBA operon encoding cytosine permease and cytosine deaminase. Mol Microbiol 6:1335–1344.

Davis, J. L., A. H. Wani, B. R. O'Neal, and L. D. Hansen. 2004. RDX biodegradation column study: comparison of electron donors for biologically induced reductive transformation in groundwater. *J Hazard Mat* 112: 45-54.

Denef, V. J., M. A. Patrauchan, C. Florizone, J. Park, T. V. Tsoi, W. Verstraete, J. M. Tiedje, and L. D. Eltis. 2005. Growth substrate- and phase-specific expression of biphenyl, benzoate, and C1 metabolic pathways in *Burkholderia xenovorans* LB400. *J Bacteriol* 187: 7996-8005.

Doroghazi, J. R., and D. H. Buckley. 2010. Widespread homologous recombination within and between *Streptomyces* species. *ISME J* 4: 1136-1143.

Faith, J. J., B. Hayete, J. T. Thaden, I. Mogno, J. Wierzbowski, G. Cottarel, S. Kasif, J. J. Collins, and T. S. Gardner. 2007. Large-scale mapping and validation of *Escherichia coli* transcriptional regulation from a compendium of expression profiles. *PLoS Biol* 5: 8e.

Fournier, D., A. Halasz, J. C. Spain, R. J. Spanggord, J. C. Bottaro, and J. Hawari. 2004. Biodegradation of the hexahydro-1,3,5-trinitro-1,3,5-triazine ring cleavage product 4-nitro-2,4-diazabutanal by *Phanerochaete chrysosporium*. *Appl Environ Microbiol* 70: 1123-1128.

Fournier, D., S. Trott, J. Hawari, and J. C. Spain. 2005. Metabolism of the aliphatic nitramine 4-nitro-2,4-diazabutanal by *Methylobacterium* sp. strain JS178. *Appl Environ Microbiol* 71: 4199-4202.

Fournier, D., A. Halasz, J. Spain, P. Fiurasek, and J. Hawari. 2002. Determination of key metabolites during biodegradation of hexahydro-1,3,5-trinitro-1,3,5-triazine with *Rhodococcus* sp. strain DN22. *Appl Environ Microbiol* 68: 166-172.

Fredrickson, J., M. Romine, A. Beliaev, J. M. Auchtung, M. E. Driscoll, T. S. Gardner, K. H. Nealson, A. L. Osterman, G. Pinchuk, J. L. Reed, D. A. Rodionov, J. L. M. Rodrigues, D. A. Saffarini, M. H. Serres, A. M. Spormann, I. B. Zhulin, and J. M. Tiedje. 2008. Towards environmental systems biology of *Shewanella*. *Nat Rev Microbiol* 6: 592-603.

Fuller, M. E., K. McClay, J. Hawari, L. Paquet, T. Malone, B. Fox, and R. J. Steffan. 2009. Transformation of RDX and other energetic compounds by xenobiotic reductases XenA and XenB. *Appl Microbiol Biotechnol* 84: 535-544.

Fuller, M. E., K. McClay, M. Higham, P. B. Hatzinger, and R. J. Steffan. 2010. Hexahydro-1,3,5-trinitro-1,3,5-triazine (RDX) bioremediation in groundwater: are known RDX-degrading bacteria the dominant players? *Bioremed J* 14: 121-134.

Gelfand, J., and D. Yakir. 2008. Influence of nitrite accumulation in association with seasonal patterns and mineralization of soil nitrogen in a semi-arid pine forest. *Soil Biol Biochem* 40: 415-424.

Gregory, K. B., P. Larese-Casanova, G. F. Parkin, and M. M. Scherer. 2004. Abiotic transformation of hexahydro-1,3,5-trinitro-1,3,5-triazine by Fe^{II} bound to magnetite. *Environ Sci Technol* 38: 1414.

Gurtler, V., B. C. Mayall, and R. Seviour. 2004. Can whole genome analysis refine the taxonomy of the genus *Rhodococcus*? *FEMS Microbiol Rev* 28: 377-403.

Halasz, A., and J. Hawari. 2011. Degradation routes of RDX in various redox systems. In *Aquatic Redox Chemistry*, ed. P. G. Tratnyek, T. J. Grundle, and S. B. Haderlein, 441-462. ACS Symposium Series, Vol. 1071. Washington, DC: American Chemical Society.

Halasz, A., J. C. Spain, L. Paquet, C. Beaulieu, and J. Hawari. 2002. Insights into the formation and degradation mechanisms of methylenedinitramine during the incubation of RDX with anaerobic sludge. *Environ Sci Technol* 36: 633-638.

Hawari, J., A. Halasz, C. A. Groom, S. Deschamps, L. Paquet, C. Beaulieu, and A. Corriveau. 2002. Photodegradation of RDX in aqueous solution: a mechanistic probe for biodegradation with *Rhodococcus* sp. *Environ Sci Technol* 36: 5117-5123.

Hawari, J., A. Halasz, T. W. Sheremata, S. Beaudet, C. Groom, L. Paquet, C. Rhofir, G. Ampleman. and S. Thiboutot. 2000. Characterization of metabolites during biodegradation of hexahydro-1,3,5-trinitro-1,3,5-triazine (RDX) with municipal anaerobic sludge. *Appl Environ Microbiol* 66: 2652-2657.

Hewitt, A. D. 2002. *Analysis of nitroglycerine in soils and on mortar fins using GC-TID*. ERDC/CRREL TR-02-3. Hanover, NH: U.S. Army Cold Regions Research and Engineering Laboratory.

Ho, E.-M., H.-W. Chang, S.-I. Kim, H.-Y. Kahng, and K.-H. Oh. 2004. Analysis of TNT (2,4,6-trinitrotoluene)-inducible cellular responses and stress shock proteome in *Stenotrophomonas* sp. OK-5. *Curr Microbiol* 49: 346-352.

Hosada, A., Y. Kasai, N. Hamamura, Y. Takahata, and K. Watanabe. 2005. Development of a PCR method for the detection and quantification of benzoyl-CoA reductase genes and its application to monitored natural attenuation. *Biodegradation* 16: 591-601.

Indest, K. J., F. H. Crocker, and R. Athow. 2007. A TaqMan polymerase chain reaction method for monitoring RDX-degrading bacteria based on the *xplA* functional gene. *J Microbiol Meth* 68: 267-274.

Indest, K. J., C. M. Jung, H.-P. Chen, D. Hancock, C. Florizone, L. D. Eltis, and F. H. Crocker. 2010. Functional characterization of pGKT2, a 182 kb plasmid containing the *xplAB* genes involved in the degradation of RDX by *Gordonia sp.* KTR9. *Appl Environ Microbiol* 76: 6329-6337.

Jackson, R. G., E. L. Rylott, D. Fournier, J. Hawari, and N. C. Bruce. 2007. Exploring the biochemical properties and remediation applications of the unusual explosive-degrading P450 system XplA/B. *Proc Natl Acad Sci* 104: 16822-16827.

Jenkins, T. F., J. C. Pennington, T. A. Ranney, T. E. Berry, Jr., P. H. Miyares, M. E. Walsh, A. D. Hewitt, N. M. Perron, L. V. Parker, C. A. Hayes, and E. G. Wahlgren. 2001. *Characterization of explosives contamination at military firing ranges*. Technical Report ERDC TR-01-5. Vicksburg, MS: U.S. Army Engineer Research and Development Center.

Jenkins, T. F., M. E. Walsh, P. G. Thorne, P. H. Miyares, T. A. Ranney, C. L. Grant, and J. R. Esparza. 1998. *Site characterization for explosives contamination at a military firing range impact area*. Special Report 98-9. Hanover, NH: U.S. Army Cold Regions Research and Engineering Laboratory.

Jung, C. M., F. H. Crocker, J. O. Eberly, and K. J. Indest. 2011. Horizontal gene transfer (HGT) as a mechanism of dissemination of RDX-degrading activity among Actinomycete bacteria. *J Appl Microbiol* 110: 1449-1459.

Karlson, U., D. F. Dwyer, S. H. Hooper, E. R. B. Moore, K. N. Timmis, and L. D. Eltis. 1993. Two independently regulated cytochromes P450 in *Rhodococcus rhodochrous* that degrades 2-ethoxyphenol and 4-ethoxybenzoate. *J Bacteriol* 175: 1467-1474.

Kim, C. C., D. Monack, and S. Falkow. 2003. Modulation of virulence by two acidified nitrite-responsive loci of *Salmonella enterica* serovar Typhimurium. *Infect Immun* 71: 3196-3205.

Kim, S.-I., J. Y. Kim, S. H. Yun, J. H. Kim, S. H. Leem, and C. Lee. 2004. Proteome analysis of *Pseudomonas* sp. K82 biodegradation pathways. *Proteomics* 4: 3610-3621.

Kim, Y. H., I. Kang, H. Bergeron, P. C. Lau, K. H. Engesser, and S. J. Kim. 2006. Physiological, biochemical, and genetic characterization of an alicyclic amine-degrading Mycobacterium sp. strain THO100 isolated from a morpholine-containing culture of activated sewage sludge. *Arch Microbiol* 186: 425-434.

Kitts, C. L., D. P. Cunningham, and P. J. Unkefer. 1994. Isolation of three hexahydro-1,3,5-trinitro-1,3,5-triazine-degrading species of the family Enterobacteriaceae from nitramine explosive-contaminated soil. *Appl Environ Microbiol* 60: 4608-4611.

Kitts, C. L., C. E. Green, R. A. Otley, M. A. Alvarez, and P. J. Unkefer. 2000. Type 1 nitroreductases in soil enterobacteria reduce TNT (2,4,6-trinitrotoluene) and RDX (hexahydro-1,3,5-trinitro-1,3,5-triazine). *Can J Microbiol* 46: 278-282.

Kovach, M. E., P. H. Elzer, D. S. Hill, G. T. Robertson, M. A. Farris, R. M. Roop, and K. M. Peterson. 1995. Four new derivatives of the broad-host-range cloning vector pBBR1MCS, carrying different antibiotic-resistance cassettes. *Gene* 166: 175-176.

Kwon, M. J., and K. T. Finneran. 2006. Microbially mediated biodegradation of hexahydro-1,3,5-trinitro-1,3,5-triazine by extracellular electron shuttling compounds. *Appl Environ Microbiol* 72: 5933-5941.

Kwon, M. J., and K. T. Finneran. 2008a. Biotransformation products and mineralization potential for hexahydro-1,3,5-trinitro-1,3,5-triazine (RDX) in abiotic versus biological degradation pathways with anthraquinone-2,6-disulfonate (AQDS) and *Geobacter metallireducens*. *Biodegradation* 19: 705-715.

Kwon, M. J., and K. T. Finneran. 2008b. Hexahydro-1,3,5-trinitro-1,3,5-triazine (RDX) and octahydro-1,3,5,7- tetranitro-1,3,5,7-tetrazocine (HMX) biodegradation kinetics amongst several Fe(III)-reducing genera. *Soil Sediment Contam* 17: 189-203.

Kwon, M. J., and K. T. Finneran. 2010. Electron shuttle-stimulated RDX mineralization and biological production of 4-nitro-2,4-diazbutanal (NDAB) in RDX-contaminated aquifer material. *Biodegradation* 21: 923-937.

Langille, M. G., and F. S. Brinkman. 2009. IslandViewer: An integrated interface for computational identification and visualization of genomic islands. *Bioinformatics* 25: 664-665.

Larkin, M. J., L. A. Kulakov, and C. C. Allen. 2005. Biodegradation and *Rhodococcus* - masters of catabolic versitility. *Curr Opin Biotechnol* 16: 282-290.

Lee, J. J., S.-K. Rhee, and S.-T. Lee. 2001. Degradation of 3-methylpyridine and 3-ethylpyridine by *Gordonia nitida* LE31. *Appl Environ Microbiol* 67: 4342-4345.

Linos, A., M. M. Berekaa, R. Reichelt, U. Keller, J. Schmitt, H.-C. Flemming, R. M. Kroppenstedt, and A. Steinbüchel. 2000. Biodegradation of cis-1,4-polyisoprene rubbers by distinct actinomycetes: microbial strategies and detailed surface analysis. *Appl Environ Microbiol* 66: 1639-1645.

Lynch, J. C., J. M. Brannon, and J. J. Delfino. 2002. Dissolution rates of three high explosive compounds: TNT, RDX, and HMX. *Chemosphere* 47: 725-734.

Maniatis, T., J. Sambrook, and E. F. Fritsch. 1982. *Molecular cloning: A laboratory manual*. Cold Spring Harbor, NY: Cold Spring Harbor Laboratory Press.

Margolin, A. A., I. Nemenman, K. Basso, C. Wiggins, G. Stolovitzky, R. Dalla Favera, and A. Califano. 2006. ARACNE: an algorithm for the reconstruction of gene regulatory networks in a mammalian cellular context. *BMC Bioinformatics* 7(Suppl 1): S7.

Martel, R., M. Mailloux, U. Gabriel, R. Lefebvre, S. Thiboutot, and G. Ampleman. 2009. Behavior of energetic materials in ground water at an anti-tank range. *J Environ Qual* 38: 72-92.

McLeod, M. P., R. L. Warren, W. W. Hsiao, N. Araki, M. Myhre, C.Fernandes, D. Miyazawa, W. Wong, A. L. Lillquist, D. Wang, M. Dosanjh, H. Hara, A. Petrescu, R. D. Morin, G. Yang, J. M. Stott, J. E. Schein, H. Shin, D. Smailus, A. S. Siddiqui, M. A. Marra, S. J. Jones, R. Holt, F. S. Brinkman, K. Miyauchi, M. Fukuda, J. E. Davies, W. W. Mohn, and L. D. Eltis. 2006. The complete genome of *Rhodococcus* sp. RHA1 provides insights into a catabolic powerhouse. *Proc Natl Acad Sci U. S. A.* 103:15582–15587.

Medina, V. F., H. Knotek-Smith, D. Gent, and A. Morrow. 2012. The results of a laboratory feasibility study for the biological treatment of Umatilla Groundwater. ERDC/EL TR-12-2. Vicksburg, MS: U.S.Army Engineer Research and Development Center.

Moura, I., P. Tavares, J. J. Moura, N. Ravi, B. H. Huynh, M. Y. Liu, and J. LeGall. 1992. Direct spectroscopic evidence for the presence of a 6 Fe cluster in an iron-sulfur protein isolated from *Desulfovibrio desulfuricans* (ATCC 27774). *J Biol Chem* 267: 4489-4496.

Mulbry, W. W. 1994. Purification and characterization of an inducible s-triazine hydrolase from *Rhodococcus corallinus* NRRL B-15444R. *Appl Environ Microbiol* 60: 613-618.

Murphy, J. N., and C. W. Saltikov. 2007. The *cymA* gene, encoding a tetraheme c-type cytochrome, is required for arsenate respiration in *Shewanella* species. *J Bacteriol* 189: 2283-2290.

Muse, W.B., C. J. Rosario, and R. A. Bender. 2003. Nitrogen regulation of the *codBA* (Cytosine Deaminase) Operon from *Escherichia coli* by the nitrogen assimilation control protein, NAC. *J Bacteriol* 185:2920-2926.

Myers, C. R., and J. M. Myers. 1993. Role of menaquinone in the reduction of fumarate, nitrate, iron(III) and manganese (IV) by *Shewanella putrefaciens* MR-1. *FEMS Microbiol Lett* 114: 215-222.

Myers, C. R., and J. M. Myers. 1997. Cloning and sequence of *cymA*, a gene encoding a tetraheme cytochrome c required for reduction of iron(III), fumarate, and nitrate by *Shewanella putrefaciens* MR-1. *J Bacteriol* 179: 1143-1152.

Myers, C. R., and K. H. Nealson. 1988. Bacterial manganese reduction and growth with manganese oxide as the sole electron acceptor. *Science* 240: 1319-1321.

Myers, J. M., W. E. Antholine, and C. R. Myers. 2004. Vanadium(V) reduction by *Shewanella oneidensis* MR-1 requires menaquinone and cytochromes from the cytoplasmic and outer membranes. *Appl Environ Microbiol* 70: 1405-1412.

Nakashima, N., and T. Tamura. 2004. Isolation and characterization of a rolling-circle-type plasmid from *Rhodococcus erythropolis* and application of the plasmid to multiple-recombinant-protein expression. *Appl Environ Microbiol* 70: 5557-5568.

Navarro-Llorens, J. M., M. A. Patrauchan, G. R. Stewart, J. E. Davies, L. D. Eltis, and W. W. Mohn. 2005. Phenylacetate catabolism in *Rhodococcus* sp. strain RHA1: A central pathway for degradation of aromatic compounds. *J Bacteriol* 187: 4497-4505.

Nealson, K. H., and D. A. Saffarini. 1994. Iron and manganese in anaerobic respiration: environmental significance, physiology, and regulation. *Ann Rev Microbiol* 48: 311-343.

Nejidat, A., L. Kafka, Y. Tekoah, and Z. Ronen. 2008. Effect of organic and inorganic nitrogenous compounds on RDX degradation and cytochrome P-450 expression in *Rhodococcus* strain YH1. *Biodegradation* 19: 313-320.

Nyyssonen, M., R. Piskonen, and M. Itavaara. 2006. A targeted real-time PCR for studying naphthalene degradation in the environment. *Microb Ecol* 52: 533-543.

Oh, B.-T., C. L. Just, and P. J. J. Alvarez. 2001. Hexahydro-1,3,5-trinitro-1,3,5-triazine mineralization by zerovalent iron and mixed anaerobic cultures. *Environ Sci Technol* 35: 4341-4346.

Pan, X., M. J. San Francisco, C. Lee, K. M. Ochoa, X. Xu, J. Liu, B. Zhang, S. B. Cox, and G. P. Cobb. 2007. Examination of the mutagenicity of RDX and its N-nitroso metabolites using the *Salmonella* reverse mutation assay. *Mutat Res* 629: 64-69.

Paquet, L., F. Monteil-Rivera, P. Hatzinger, Paul, M. Fuller, and J. Hawari. 2011. Analysis of the key intermediates of RDX (hexahydro-1,3,5-trinitro-1,3,5-triazine) in groundwater: Occurrence, stability and preservation. *J Environ Monitor* 13: 2304-2311

Patrauchan, M. A., M. I. Patrauchan, M. Osanjh, W. W. Ohn, J. Avies, and L. D. Ltis. 2005. Catabolism of benzoate and phthalate in *Rhodococcus* sp. strain RHA1: redundancies and convergence. *J Bacteriol* 187: 4050-4063.

Pennington, J. C., T. F. Jenkins, J. M. Brannon, J. Lynch, T. A. Ranney, T. E. Barry, Jr., C. A. Hayes, P. H. Miyares, M. E. Walsh, A. D. Hewitt, N. M. Perron, and J. J. Delfino. 2001. *Distribution and fate of energetics on DoD test and training ranges: Interim report 1*. Technical Report ERDC TR-01-13. Vicksburg, MS: U.S.Army Engineer Research and Development Center.

Pennington, J. C., T. F. Jenkins, S. Thiboutot, G. Ampleman, A. D. Hewitt, J. Lewis, M. E. Walsh, T. A. Ranney, B. Silverblatt, A. Marois, A. Gagnon, P. Brousseau, J. E. Zufelt, K. Poe, M. Bouchard, R. Martel, D. D. Walker, C. A. Ramsey, C. A. Hayes, S. L. Yost, K. L. Bjella, L. Trepanier, T. E. Berry, Jr., D. J. Lambert, P. Dube, and N. M. Perron. 2005. *Distribution and fate of energetics on DoD test and training ranges: Report 5*. Technical Report ERDC TR-05-2. Vicksburg, MS: U.S.Army Engineer Research and Development Center.

Poupin, P., V. Ducrocq, S. Hallier-Soulier, and N. Truffaut. 1999. Cloning and characterization of the genes encoding a cytochrome P450 (PipA) involved in piperidine and pyrrolidine utilization and its regulatory protein (PipR) in *Mycobacterium smegmatis* mc2155. *J Bacteriol* 181: 3419-3426.

Powell, S. M., S. H. Ferguson, J. P. Bowman, and I. Snape. 2006. Using real-time PCR to assess changes in the hydrocarbon-degrading microbial community in Antarctic soil during bioremediation. *Microb Ecol* 52: 523-532.

Ramakers, C., J. M. Ruijter, R. H. Lekane Deprez, and A. F. M. Moorman. 2003. Assumption-free analysis of quantitative real-time polymerase chain reaction (PCR) data. *Neurosci Letters* 339: 62-66.

Ringelberg, D. B., C. M. Reynolds, M. E. Walsh, and T. F. Jenkins. 2003. RDX loss in a surface soil under saturated and well drained conditions. *J Environ Qual* 32:, 1244-1249.

Ritalahti, K. M., J. K. Hatt, V. Lugmay, K. Henn, E. A. Petrovskis, D. Ogles, G. A. Davis, C. M. Yeager, C. A. Lebron, and F. E. Loffler. 2010. Comparing on-site to off-site biomass collection for *Dehalococcoides* biomarker gene qualification to predict *in situ* chlorinated ethene detoxification potential. *Environ Sci Technol* 44: 5127-5133.

Roh, H., C. P. Yu, M. E. Fuller, and K. H. Chu. 2009. Identification of hexahydro-1,3,5-trinitro-1,3,5-triazine-degrading microorganisms via ^{15}N stable isotope probing. *Environ Sci Technol* 43: 2505-2511.

Ronen, Z., Y. Yanovich, R. Goldin, and E. Adar. 2008. Metabolism of the explosive hexahydro-1,3,5-trinitro-1,3,5-triazine (RDX) in a contaminated vadose zone. *Chemosphere* 73: 1492-1498.

Rylott, E. L., R. G. Jackson, J. Edwards, G. L. Womack, H. M. Seth-Smith, D. A. Rathbone, S. E. Strand, and N. C. Bruce. 2006. An explosive-degrading cytochrome P450 activity and its targeted application for the phytoremediation of RDX. *Nat Biotech* 24: 216-219.

Saffarini, D. A., S. L. Blumerman, and K. J. Mansoorabadi. 2002. Role of menaquinones in Fe(III) reduction by membrane fractions of *Shewanella putrefaciens*. *J Bacteriol* 184: 846-848.

Saito, H., and K. I. Miura. 1963. Preparation of transforming deoxyribonucleic acid by phenol treatment. *Biochim Biophys Acta* 72: 619-629.

Schafer, A., A. Tauch, W. Jager, J. Kalinowski, G. Thierbach, and A. Puhler. 1994. Small mobilizable multi-purpose cloning vectors derived from the *Escherichia coli* plasmids pK18 and pK19: selection of defined deletions in the chromosome of Corynebacterium glutamicum. *Gene* 145: 69-73.

Schwalb, C., S. K. Chapman, and G. A. Reid. 2003. The tetraheme cytochrome CymA is required for anaerobic respiration with dimethyl sulfoxide and nitrite in *Shewanella oneidensis*. *Biochem* 42: 9491-9497.

Segura, A., P. Godoy, P. van Dillewin, A. Hurtado, N. Arroyo, S. Santacruz, and J.-L. Ramos. 2005. Proteomic analysis reveals the participation of energy- and stress-related proteins in the response of *Pseudomonas putida* DOT-T1E to toluene. *J Bacteriol* 187: 5945.

Seth-Smith, H. M. B., J. Edwards, S. J. Rosser, D. A. Rathbone, and N. C. Bruce. 2008. The explosive-degrading cytochrome P450 system is highly conserved among strains of *Rhodococcus* spp. *Appl Environ Microbiol* 74: 4550-4552.

Seth-Smith, H. M. B., S. J. Rosser, A. Basran, E. R. Travis, E. R. Dabbs, S. Nicklin, and N. C. Bruce. 2002. Cloning, sequencing, and characterization of the hexahydro-1,3,5-trinitro-1,3,5-triazine degradation gene cluster from *Rhodococcus rhodochrous*. *Appl Environ Microbiol* 68: 4764-4771.

Sharkey, F. H., S. I. Markos, and R. W. Haylock. 2004. Quantification of toxin-encoding mRNA from *Clostridium botulinum* type E in media containing sorbic acid or sodium nitrite by competitive RT-PCR. *FEMS Microbiol Lett* 232: 139-144.

Sheremata, T. W., A. Halasz, L. Paquet, S. Thiboutot, G. Ampleman, and J. Hawari. 2001. The fate of the cyclic nitramine explosive RDX in natural soil. *Environ Sci Technol* 35: 1037-1040.

Shrout, J. D., P. Larese-Casanova, M. M. Scherer, and P. J. Alvarez. 2005. Sustained and complete hexahydro-1,3,5-trinitro-1,3,5-triazine (RDX) degradation in zero-valent iron simulated barriers under different microbial conditions. *Environ Technol* 26: 1115-1126.

Sielaff, B., and J. R. Andreesen. 2005. Analysis of the nearly identical morpholine monooxygenase-encoding mor genes from different *Mycobacterium* strains and characterization of the specific NADH : ferredoxin oxidoreductase of this cytochrome P450 system. *Microbiology* 151: 2593-2603.

Smith, C. J., and A. M. Osborne. 2009. Advantages and limitations of quantitative PCR (Q-PCR)-based approaches in microbial ecology. *FEMS Microbiol Ecol* 67: 6-20.

Smith, R.V., R. M. Doyle, L. C. Burns, and R. J. Stevens. 1997. A model for nitrite accumulation in soils. *Soil Biol Biochem* 29: 1241-1247.

Spain, J. C. 2000. *Biodegradation of nitroaromatic compounds and explosives*. Boca Raton: Lewis Publishers.

Spalding, R. F., and J. W. Fulton. 1988. Groundwater munition residues and nitrate near Grand Island, Nebraska, U.S.A. *J Contam Hydrol* 2: 139-153.

Strohl, W. R. 1997. *Biotechnology of antibiotics*. New York: Marcel Dekker, Inc., 1-47.

Sunahara, G. I., G. Lotufo, R. G. Kuperman, and J. Hawari. 2009. *Ecotoxicology of explosives*. Boca Raton, FL: CRC Press.

Szecsody, J. E., D. C. Girvin, B. J. Devary, and J. A. Campbell. 2004. Sorption and oxic degradation of the explosive CL-20 during transport in subsurface sediments. *Chemosphere* 56: 593-610.

Taber, H. 1980. Functions of vitamin K2 in microorganisms. In *Proceedings of the 8th Steenbock Symposium held at the University of Wisconsin-Madison,* ed. J. W. Suttie 177-187. Baltimore, MD: University Park Press.

Tang, Y., A. L. Meadows, and J. D. Keasling. 2007. A kinetic model describing *Shewanella oneidensis* MR-1 growth, substrate consumption, and product secretion. *Biotechnol Bioeng* 93: 125-133.

te Poele, E. M., H. Bolhuis, and L. Dijkhuizen. 2008. Actinomycete integrative and conjugative elements. *Antonie van Leeuwenhoek* 94: 127-143.

TetraTech, Inc. 2010. IAAAP off-site background Info.

Thompson, J. D., T. J. Gibson, F. Plewniak, F. Jeanmougin, and D. G. Higgins. 1997. The ClustalX windows interface: flexible strategies for multiple sequence alignment aided by quality analysis tools. *Nucleic Acids Res* 25: 4876-4882.

Thompson, K. T., F. H. Crocker, and H. L. Fredrickson. 2005. Mineralization of the cyclic nitramine explosive hexahydro-1,3,5-trinitro-1,3,5-triazine by *Gordonia* and *Williamsia* spp. *Appl Environ Microbiol* 71: 8265-8272.

Tiffert, Y., P. Supra, R. Wurm, W. Wohlleben, R. Wagner, and J. Reuther. 2008. The *Streptomyces coelicolor* GlnR regulon: Identification of new GlnR targets and evidence for a central role of GlnR in nitrogen metabolism in actinomycetes. *Mol Microbiol* 67:861-80.

Torodova, S. G., and A. M. Costello. 2006. Design of *Shewanella*-specific 16S rRNA primers and application to analysis of *Shewanella* in a minerotrophic wetland. *Environ Microbiol* 8: 426-432.

U.S. Army Engineer District, Seattle. 2010. Final Third Five-Year Review Report for Umatilla Chemical Depot, Hermiston, Umatilla, and Morrow Counties, Oregon.

Van Aken, B., J. M. Yoon, and J. L. Schnoor. 2004. Biodegradation of nitro-substituted explosives 2,4,6-trinitrotoluene, hexahydro-1,3,5-trinitro-1,3,5-triazine, and octahydro-1,3,5,7-tetranitro-1,3,5-tetrazocine by a phytosymbiotic *Methylobacterium* sp. associated with poplar tissues (*Populus deltoides* X *nigra* DN34). *Appl Environ Microbiol* 70: 508-517.

van der Geize, R., and L. Dijhuizen. 2004. Harnessing the catabolic diversity of rhodococci for environmental and biotechnological applications. *Curr Opin Microbiol* 7: 255-261.

van der Geize, R., G. I. Hessels, R. van Gerwen, P. van der Meijden, and L. Dijkhuizen. 2001. Unmarked gene deletion mutagenesis of *kstD*, encoding 3-ketosteroid Δ^1-dehydrogenase, in *Rhodococcus erythropolis* SQ1 using *sacB* as a counter-selectable marker. *FEMS Microbiol Lett* 205: 197-202.

Vindal, V., K. Suma, and A. Ranjan. 2007. GntR family of regulators in Mycobacterium smegmatis: a sequence and structure based characterization. *BMC Genomics* 8: 289.

Waisner, S., L. Hansen, H. Fredrickson, C. Nestler, M. Zappi, S. Banjeri, and R. Bajpai. 2002. Biodegradation of RDX within soil-water slurries using a combination of different redox incubation conditions. *J Hazard Mat* 95: 91-106.

Walsh, M. E., C. M. Collins, C. H. Racine, T. F. Jenkins, A. B. Gelvin, and T. A. Ranney. 2001. *Sampling for explosive residues at Fort Greely, Alaska: Reconnaissance Visit July 2000*. Technical Report ERDC/CRREL TR-01-15. Hanover, NH: U.S.Army Cold Regions Research and Engineering Laboratory.

Wani, A. H, B. R. O.Neal, J. L. Davis, and L. D. Hansen. 2002. Treatability study for biologically active zone enhancement (BAZE) for in situ RDX degradation in groundwater. ERDC/EL TR-02-35. Vicksburg, MS: U.S. Army Engineer Research and Development Center.

Wingfors, H., C. Edlund, L. Hagglund, A. Waleij, J. Sjostrom, R. M. Karlsson, P. Leffler, U. Qvarfort, M. Ahlberg, S. Thiboutot, G. Ampleman, R. Martel, W. Duvalois, A. Creemers, and N. van Ham. 2006. *Evaluation of the contamination by exlosives and metals in soils at the Alvdalen Shooting Range. Part II: Results and discussion*. SE-901 82. Umea: Swedish Defence Research Agency, NBC Defence.

Zhang, B., R. J. Kendall, and T. A. Anderson. 2006. Toxicity of the explosive metabolites hexahydro-1,3,5-trinitroso-1,3,5-triazine (TNX) and hexahydro-1-nitroso-3,5-dinitro-1,3,5-triazine (MNX) to the earthworm *Eisenia fetida*. *Chemosphere* 64: 86-95.

Zhao, J. S., L. Paquet, A. Halasz, and J. Hawari. 2003. Metabolism of hexahydro-1,3,5-trinitro-1,3,5-triazine through initial reduction to hexahydro-1-nitroso-3,5-dinitro-1,3,5-triazine followed by denitration in *Clostridium bifermentans* HAW-1. *Appl Microbiol Biotechnol* 63: 187-193.

Zhao, J.-S., Y. Dent, D. Manno, and J. Hawari. 2010. *Shewanella* spp. genomic evolution for a cold marine lifestyle and *in-situ* explosive biodegradation. *PloS One* 5: e9109.

Zhao, J.-S., A. Halasz, L. Paquet, C. Beaulieu, and J. Hawari. 2002. Biodegradation of hexahydro-1,3,5-trinitro-1,3,5-triazine and its mononitroso derivative hexahydro-1-nitroso-3,5-dinitro-1,3,5-triazine by *Klebsiella pneumoniae* strain SCZ-1 isolated from an anaerobic sludge. *Appl Environ Microbiol* 68: 5336-5341.

Zhao, J.-S., D. Manno, C. Beaulieu, L. Paquet, and J. Hawari. 2005. *Shewanella sediminis* sp. nov., a novel Na^+-requiring and hexahydro-1,3,5-trinitro-1,3,5-triazine-degrading bacterium from marine sediment. *Int J Systematic and Evolutionary Microbiology* 55: 1511-1520.

Zhao, J.-S., D. Manno, and J. Hawari. 2008. Regulation of hexahydro-1,3,5-trinitro-1,3,5-triazine (RDX) metabolism in *Shewanella halifaxensis* HAW-EB4 by terminal electron acceptor and involvement of c-type cytochrome. *Microbiology* 154: 1026-1037.

Zhao,J.-S., D. Manno, C. Leggiadro, D. O'Neil, and J. Hawari. 2006. *Shewanella halifaxensis* sp. nov., a novel obligately respiratory and denitrifying psychrophile. *Inter J Systematic and Evolutionary Microbiology* 56: 205-212.

Zhao, J.-S., J. C. Spain, S. Thiboutot, G. Ampleman, C. Greer, and J. Hawari. 2004. Phylogeny of cyclic nitramine-degrading psychrophilic bacteria in marine sediment and their potential role in the natural attenuation of explosives. *FEMS Microbiol Ecol* 49: 349-357.

Appendix A: Supporting Data

Determination of RDX products/pathways in *Gordonia* sp. KTR9

Strain KTR9 was grown in MSM plus 5 mM succinate and 40 mg L^{-1} RDX. The cell suspensions in each of the three flasks were collected, centrifuged, washed twice with 40 mM phosphate buffer, pH 7.0, and then pooled to provide a cell suspension with an OD_{600} of 3.0. The concentrated KTR9 suspension was used to inoculate four different treatments (210 mL each) of (1) phosphate buffer; (2) phosphate buffer plus 1 mM ammonium sulfate; (3) phosphate buffer plus 90 µM RDX; and (4) phosphate buffer plus 90 µM RDX and 1 mM ammonium sulfate. The initial OD_{600} was between 0.27 and 0.29. The 1 mM ammonium sulfate was added to prevent the use of nitrite by the cells. The RDX was dissolved over 2 to 3 days from crystalline RDX and all treatments were filter-sterilized as above. The cultures were incubated at 30 ^{o}C with shaking (150 rpm). For each time point, 5 mL of culture medium was collected and used to measure the optical density of the culture and RDX concentration. The remaining culture sample was centrifuged at 4000 rpm for 10 min and 3 mL of the supernatant was added to a fresh tube. In addition, 0.5 mL of the supernatant was added to a microcentrifuge tube. Both samples were frozen at -20 ^{o}C prior to shipment to BRI. At BRI, these samples were thawed in cold water for 30 min prior to analysis of RDX, NDAB, MEDINA, formaldehyde, formate, nitrite, and ammonium.

Samples (1 mL) of culture were mixed with 1 mL of acetonitrile and then filtered (0.45-µm Target PTFE syringe filters; National Scientific, Duluth, GA) into autosampler vials. RDX concentrations were determined with an Agilent (Palo Alto, CA) 1100 Series HPLC equipped with a quaternary pump, autosampler, diode array UV absorbance detector (set at 254 nm), and column oven. A Hypersil ODS reverse-phase C-18 HPLC column (100 by 4.6 mm; 5-µm particle size) was used as the primary column, along with a Hypersil ODS C-18 guard column (20 by 4 mm; 5-µm particle size). The system was operated at 39 ^{o}C and at a flow rate of 1.5 mL min^{-1}. The isocratic mobile phase consisted of 68% 20 mM NH_4Cl, 31.4% methanol, and 0.6% butanol. The calibration curve of RDX was linear between 0.1 and 50 mg L^{-1} for 1:1 (v/v) solutions of solvent and water.

Resting cell suspensions of strain KTR9 were monitored for the production of metabolites and end products associated with aerobic biodegradation of RDX (Figure A1). Nitrogen-containing end products such as nitrite, NDAB, and ammonium accumulated in the medium as the RDX was consumed. A transient amount of formaldehyde accumulated and this was subsequently followed by the appearance of formate. Reduced nitroso metabolites, such as MNX, DNX, and TNX, were not produced by metabolism of RDX by KTR9. The presence of MEDINA as an intermediate has not been observed during the biodegradation of RDX by KTR9. For every mole of RDX consumed 1.59 moles of nitrite, 1 mole of NDAB and 1 mole of ammonium was produced. This represented a 92% mass recovery of the nitrogen (Table A1). The carbon recovery was only 78% and was mostly NDAB. The production of carbon dioxide from RDX was not followed in this particular resting cell assay, but approximately 27% of the carbon from RDX has been recovered as carbon dioxide using strain KTR9 (Thompson et al. 2005). The molar ratios and nitrogen and carbon mass balances of the end products from RDX degradation indicate that KTR9 metabolizes RDX by the aerobic denitration pathway.

Optimization of KTR9 growth in different mineral media

Experiments were performed to optimize the concentration of RDX and NH_4Cl that should be used as an N source for gene expression studies. Such conditions were a prerequisite for transcriptomic experiments. KTR9 was grown in a mineral salts medium (MI medium) containing 5 mM glucose, 10 mM glycerol, 5 mM sodium succinate, and 4 mM ammonium sulfate (Thompson et al. 2005). KTR9 was also grown in M9 mineral liquid medium supplemented with Goodies (a mixture of trace elements), 20 mM succinate and 18.7 mM NH_4Cl. Growth was monitored using optical density, protein assay and colony forming units (CFU). KTR9 was also grown on M9 medium with 0.2 and 0.3 mM RDX as the sole N source. Finally, the strain was grown on various concentrations of NH_4Cl to establish which concentration would yield final cell yields similar to those of cultures grown on 0.3 mM RDX.

KTR9 growth on M1 mineral medium was not reproducible (Figures A2 and A3). There were also numerous instances of no growth with this medium. The mineral stock solutions used to prepare this medium were particularly susceptible to precipitation, which may have contributed to the reproducibility issues.

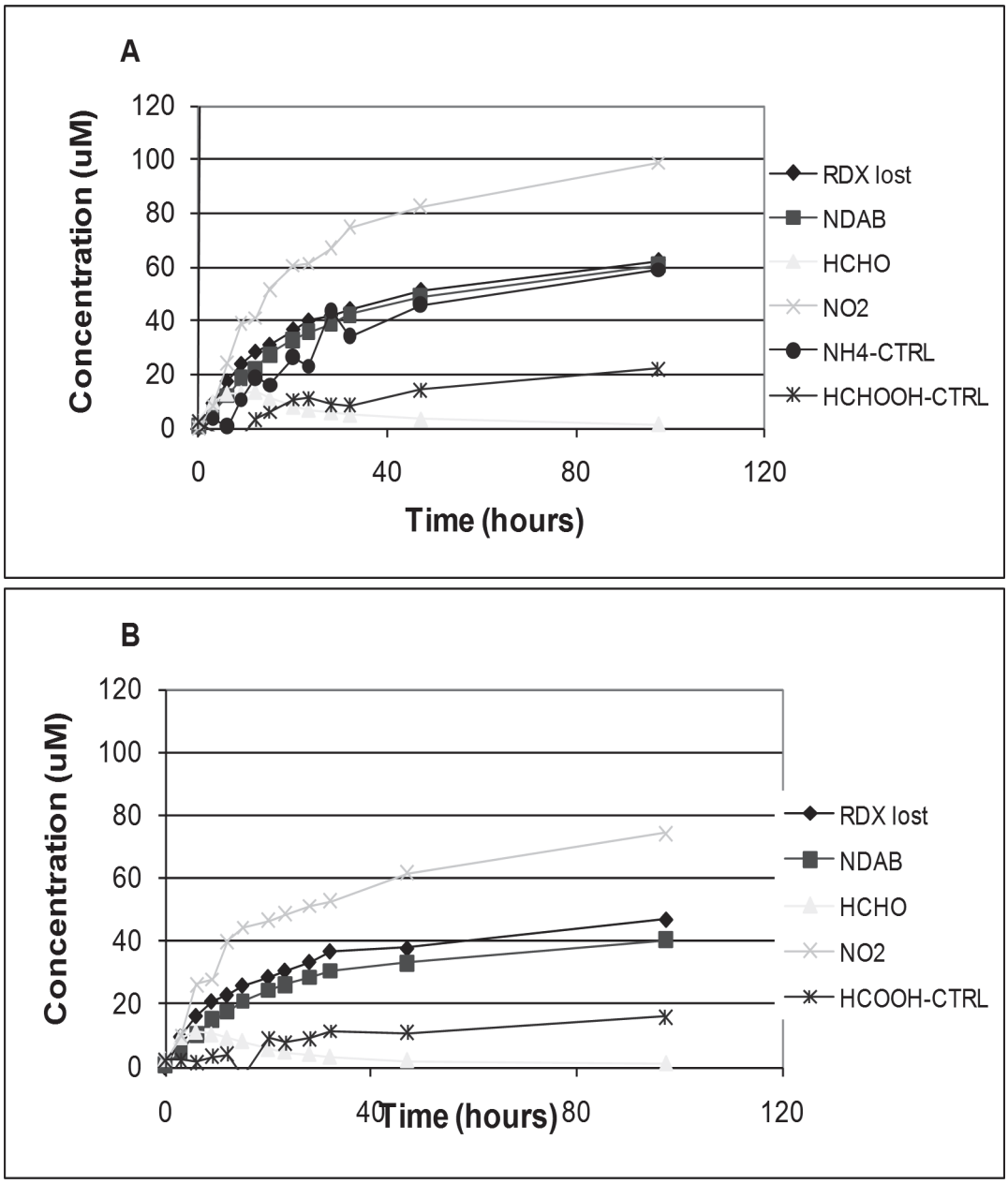

Figure A1. Production of end-products of RDX metabolism by resting cell suspensions of *Gordonia* sp. KTR9. A. RDX B. RDX plus ammonium.

Table A1. Carbon and nitrogen mass balance of RDX and metabolites produced by *Gordonia* sp. KTR9 resting cell suspension in 40 mM phosphate buffer, pH 7.0.

Compound	Amount (uM)	Molar ratio	% Carbon recovery	% Nitrogen recovery
Reactant consumed				
RDX	62.1	1	100	100
Metabolites produced				
Nitrite (NO_2^-)	98.5	1.59	NA	27
Ammonium (NH_4^+)	78.5	0.95	NA	16
4-nitro-2,4-diazabutanal	60.7	0.98	65	49
Formaldehyde	1.4	0.02	1	NA
Formate	35	0.35	12	NA

The initial amount of RDX was 90 uM. The levels of total mass recovery were 78% for carbon and 92% for nitrogen
NA, not applicable

In seeking a better medium, KTR9 was grown in M9 medium supplemented with Goodies. This medium is used to grow other actinomycetes such as *Rhodococcus* (McLeod *et al.* 2006). KTR9 grew robustly and reproducibly in M9 mineral liquid medium supplemented with succinate as sole carbon source and 18.7 mM NH_4Cl as sole N source (Figure A4). KTR9 also grew well in this medium with 0.2 mM to 0.3 mM RDX as N source. The higher RDX concentration was tested to obtain final optical densities which could be useful for RNA harvest (Figure A5). Finally, in order to reach similar final cell yields when using cultures grown on NH_4Cl and on 0.3 mM RDX, the concentration of NH_4Cl was cut to 0.9 mM. This concentration provides an amount of N similar to what the bacterium obtains from 0.3 mM RDX and results in an N-limited culture, rather than a C-limited culture.

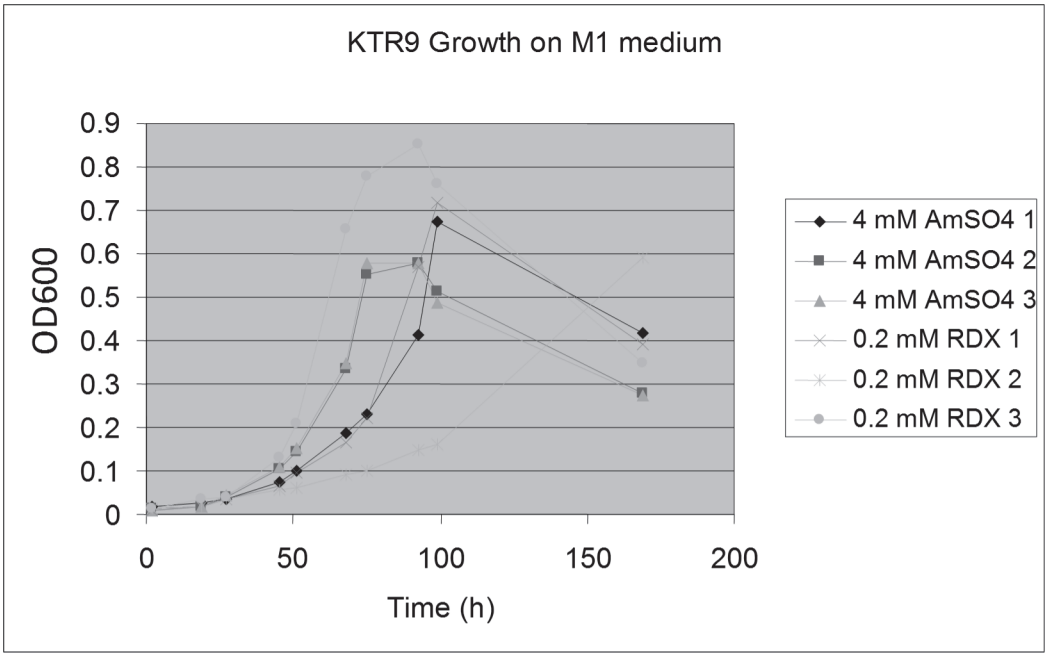

Figure A2. Growth of KTR9 on M1 mineral medium with 20 mM succinate and either 4 mM ammonium sulfate or 0.2 mM RDX as sole nitrogen source (treatments executed in triplicate).

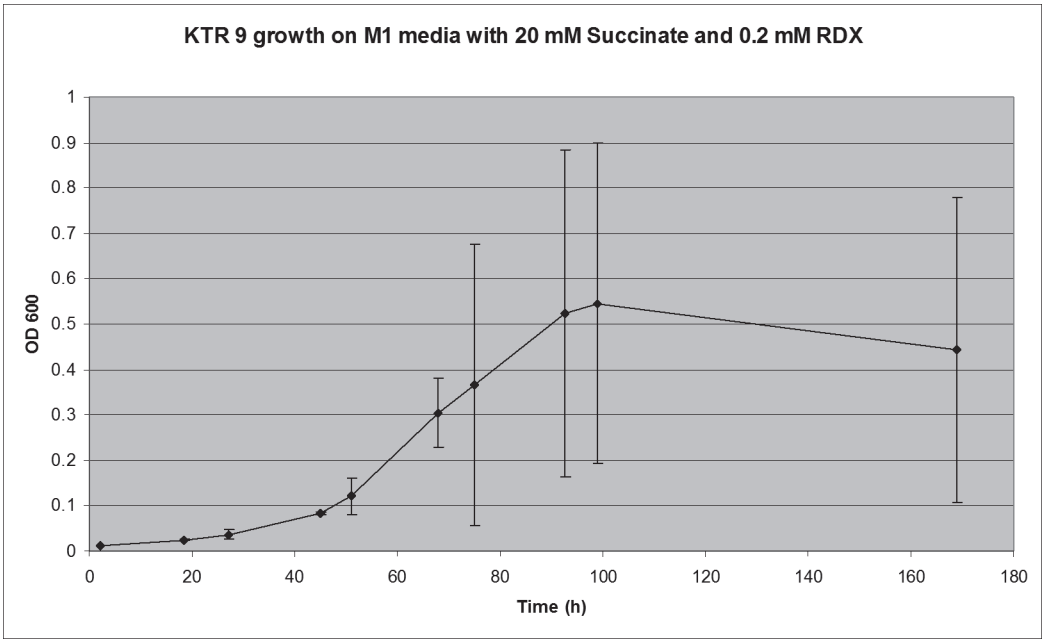

Figure A3. Growth of KTR9 on M1 mineral media with 20 mM succinate and 0.2 mM RDX as sole nitrogen source (n=3).

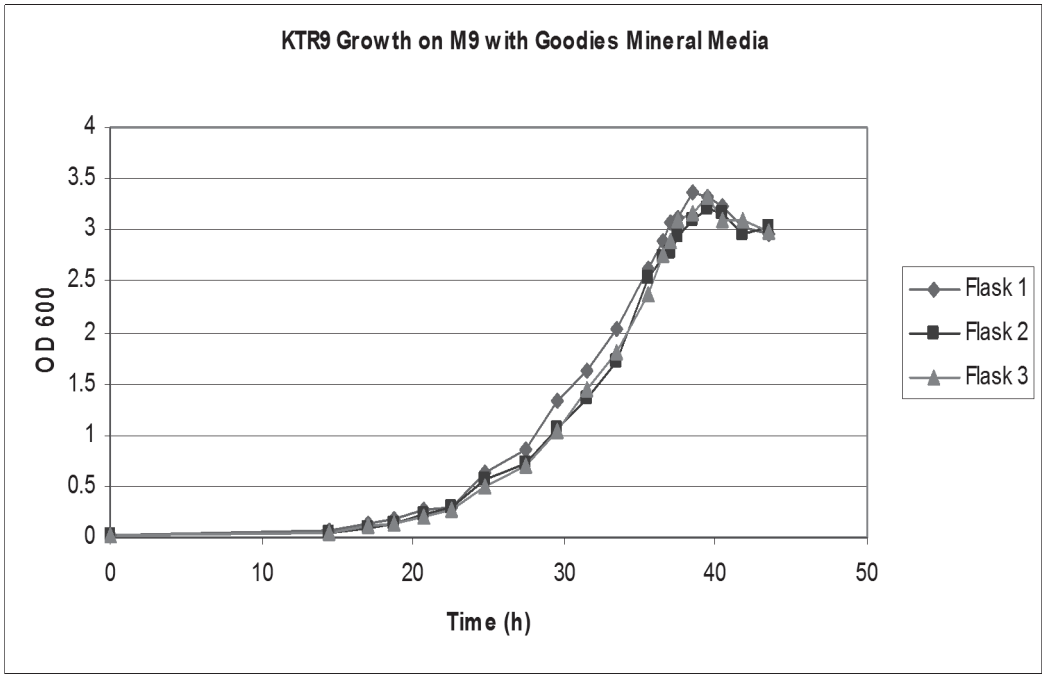

Figure A4. KTR9 growth in liquid culture on M9 mineral medium with Goodies succinate as a growth substrate and 18.7 mM NH_4Cl as sole N source.

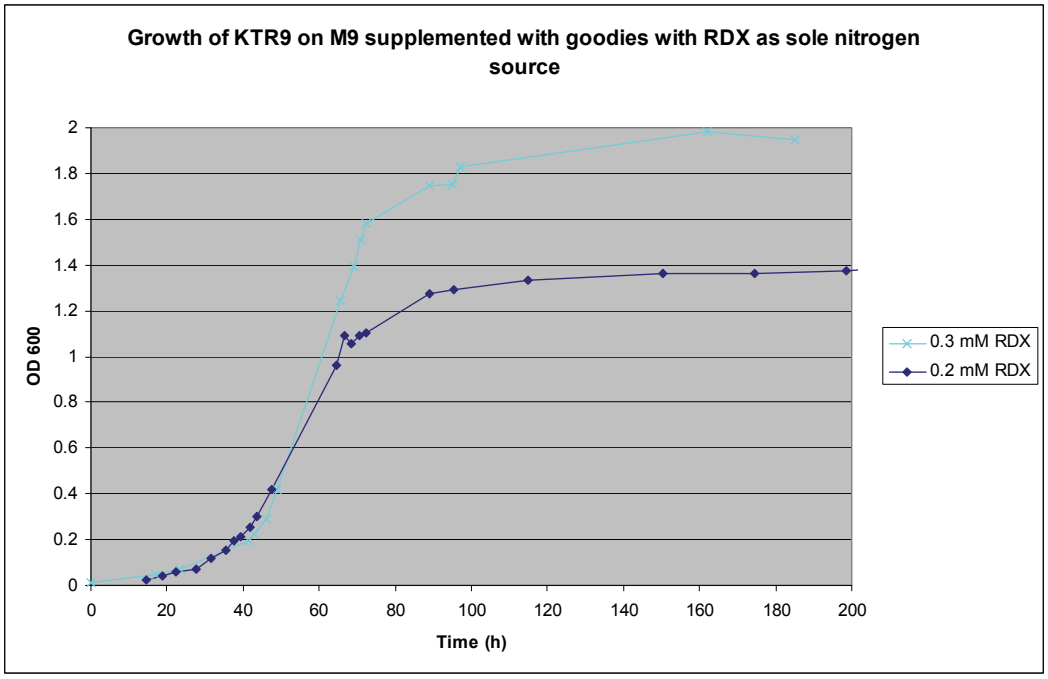

Figure A5. Growth of KTR9 on M9 supplemented with Goodies and RDX as sole N source.

A rapid drop in optical density was consistently observed during the stationary phase of C-limited KTR9 cultures (i.e., with high concentrations of NH_4Cl (Figures A6-A8). Protein and CFU levels remained relatively

stable, although the CFU counts appeared to increase at 62 h, suggesting reductive division. Subsequent experiments have established that this drop in culture OD is associated with C-limited, but not N-limited, cultures. Thus, at a low concentration of NH_4Cl, the spike in OD was not observed.

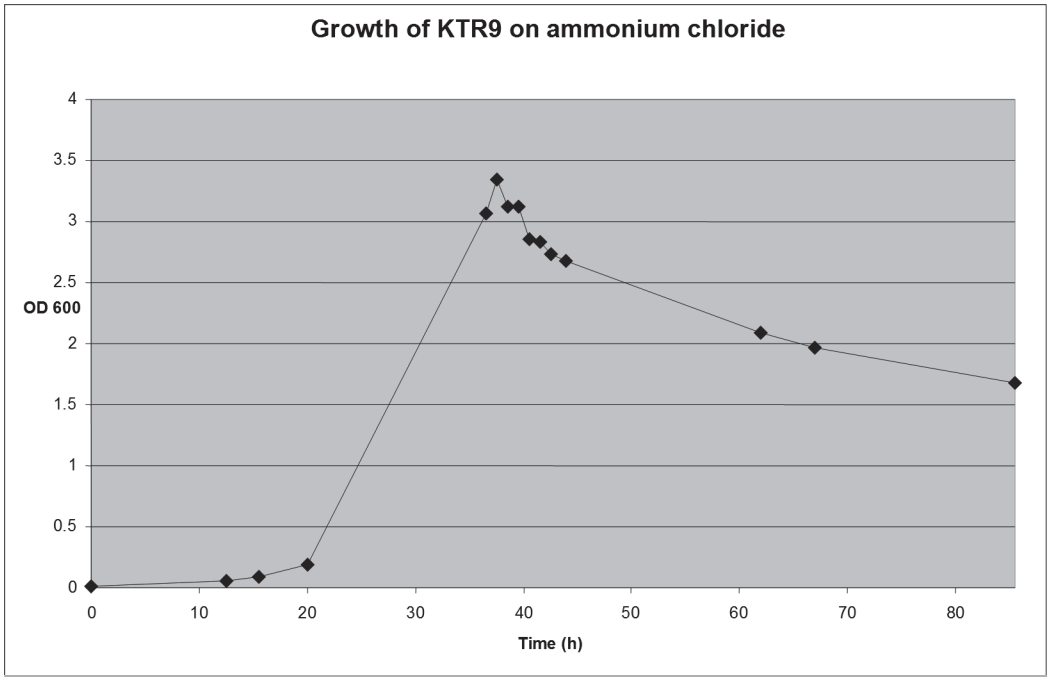

Figure A6. Rapid drop in optical density during the stationary phase when KTR9 growth on M9 medium supplemented with Goodies and 18.7 mM NH_4Cl as the sole N source.

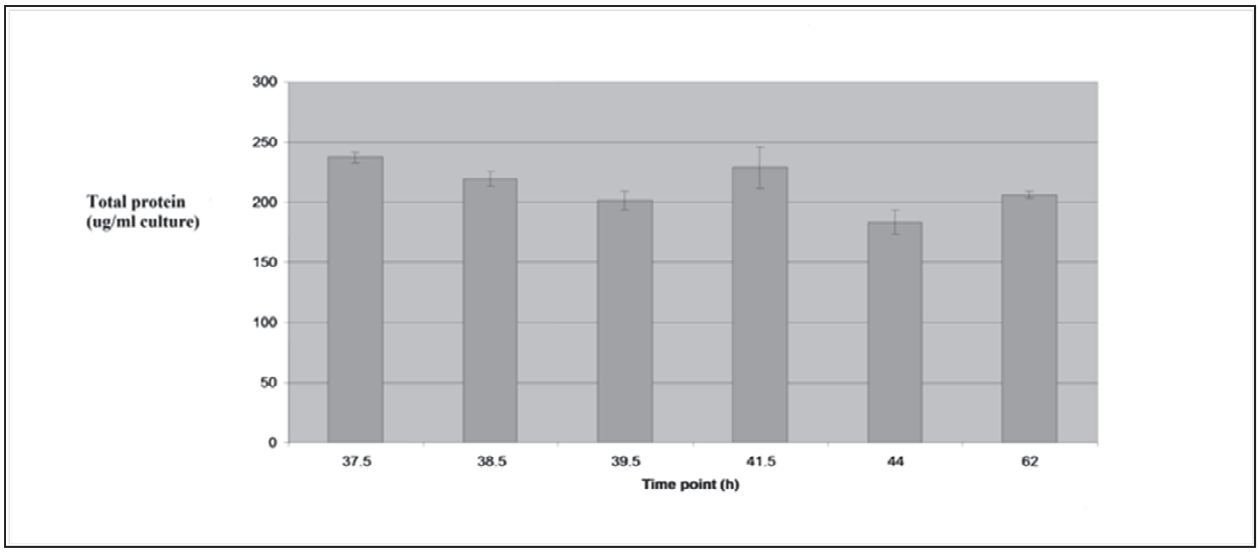

Figure A7. Total protein observed during the stationary phase of KTR9 growth on M9 medium supplemented with Goodies and 18.7 mM NH_4Cl as the sole N source.

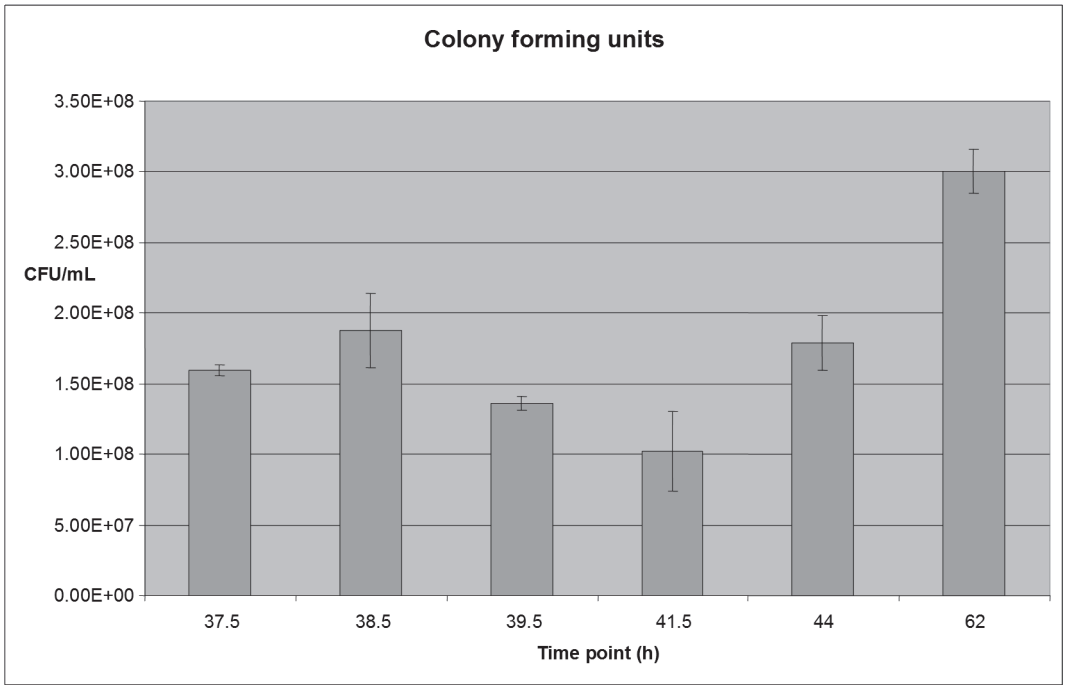

Figure A8. Colony forming units during the stationary phase of growth on M9 medium supplemented with Goodies and 18.7 mM NH_4Cl.

Appendix B: List of Scientific/Technical Publications

A. Articles in peer-reviewed journals:

1. Chen, H.P., Si-H. Zhu, I. CAsabon, S.J. Hallam, F.H. Crocker, W.W. Mohn, K.J. Indest, and L.D. Eltis. 2012. Genomic and transcriptomic studies of an RDX-degrading actinobacterium, Applied Environmental Microbiology doi:10.1128/AEM.02120412
2. Perreault, N.N., F.H. Crocker, K.J. Indest, and J. Hawari. 2012. Involvement of quinone biosynthesis and cytochrome *cymA* genes in the anaerobic metabolism of RDX by *Shewanella oneidensis* MR-1. Canadian Journal of Microbiology 58:124-131.
3. Jung, C. M., Crocker, F. H., Eberly, J. O., and Indest, K. J. 2011 Horizontal gene transfer (HGT) as a mechanism of dissemination of RDX-degrading activity among Actinomycete bacteria. Journal of Applied Microbiology 110: 1449-1459.
4. Indest, K.J., C.M. Jung, H.-P. Chen, D. Hancock, C. Florizone, L.D. Eltis, and F.H. Crocker, 2010, Functional characterization of pGKT2, a 182 kb plasmid containing the *xplAB* genes, involved in the degradation of RDX by *Gordonia* sp. KTR9, Applied Environmental Microbiology 76: 6329-6337.
5. Zhao, J.S., Y. Deng, D. Manno, and J. Hawari, 2010, *Shewanella* spp. genomic evolution for a cold marine lifestyle and *in-situ* explosive biodegradation, PLoS ONE 5(2): e9109. doi:10.1371/journal.pone.0009109.

B. Conference or symposium abstracts:

1. Monteil-Rivera, F. Zorana, R., Perreault, N., Brochu, S., Thiboutot, S., Ampleman, G., and Hawari, J., 2011 Environmental fate of past and future energetic materials (AVT Symposium on Muniton and Propellant Disposal and its Impact on the Environment, Conference Proceedings - North Atlantic Treaty Organisation, Research and Technology Organisation, NATO/PFP unclassified+AUS, AVT-177/RSY-027, Edinburgh, UK, 17-20
2. Crocker, F.H., M. Merritt, W. Mohn, N. Sukdeo, S. Hallam, and K. Indest, 2010, Detection and Quantification of RDX Degradation Activity by qPCR

with the Cytochrome P450 *xplA* gene, 2010 Partners in Environmental Technology Technical Symposium & Workshop. Nov. 30 – Dec. 2, 2010, Washington, DC

3. Kuatsjah, E., N. Sukdeo, A. Page, and S. Hallam, 2010, Optimization of a commercial silica based DNA purification system for recalcitrant soils from a military training range, 2010 Partners in Environmental Technology Technical Symposium & Workshop. Nov. 30 – Dec. 2, 2010, Washington, DC
4. Perreault, N., J. Hawari, K. Indest, and F. Crocker, 2010, Involvement of genes encoding electron carriers in the anaerobic metabolism of RDX by *Shewanella oneidensis* MR-1, 2010 Partners in Environmental Technology Technical Symposium & Workshop. Nov. 30 – Dec. 2, 2010, Washington, DC
5. Sukdeo, N., E. Kuatsjah, A. Page, S. Hallam, S. Zhu, J. Reuther, L.D. Eltis, W.W. Mohn, and F.H. Crocker, 2010, Exploring spatial relationships and the influence of RDX contamination on surface soil microbial populations at Grenade Range 2D, CFB Petawawa, 2010 Partners in Environmental Technology Technical Symposium & Workshop. Nov. 30 – Dec. 2, 2010, Washington, DC
6. Zhu, S., J. Reuther, L.D. Eltis, W.W. Mohn, and F.H. Crocker, 2010, Gene Expression During RDX Degradation by *Gordonia* sp. KTR9, 2010 Partners in Environmental Technology Technical Symposium & Workshop. Nov. 30 – Dec. 2, 2010, Washington, DC
7. Crocker, F.H., K.J. Indest, J. Hawari, and L.D. Eltis, 2009, Development of Genomic and Proteomic Molecular Tools for the Evaluation of *In Situ* RDX Biodegradation, 2009, The Tenth International In Situ and On-Site Bioremediation Symposium May 5-8, 2009, Baltimore, MD
8. Indest, K.J., F.H. Crocker, C.M. Jung, and L.D. Eltis, 2009, Assessing the role of a 182 kb plasmid containing the *xplAB* genes in degradation of RDX by *Gordonia* sp. KTR9, 2009 Partners in Environmental Technology Technical Symposium & Workshop Nov. 30-Dec. 2, 2009, Washington, DC
9. Indest, K.J., F.H. Crocker, and C.M. Jung, 2009, The Molecular Basis of RDX Degradation in *Gordonia* sp. KTR9: The Role of Large Catabolic Plasmids and Horizontal Gene Transfer, 2009 US Army Corps of Engineers Research and Development Conference Nov. 17-19 2009, Memphis, TN

10. Indest, K.J., 2009, The Molecular Basis of RDX Degradation in *Gordonia* sp. KTR9: the Role of Large Catabolic Plasmids and Horizontal Gene Transfer, South Central Branch American Society for Microbiology, Nov. 6-7, 2009, Thibodaux, LA

11. LePuil, M., R. Britto, T. Mattes, J. Livermore, F. Crocker, K. Indest, S. Muffler, B. Caldwell, M. Geraghty, and R. Arnseth, 2009, Comprehensive analysis of RDX biodegradation in off-site groundwater amended with sodium acetate at the Iowa Army Ammunition Plant, 2009 Partners in Environmental Technology Technical Symposium & Workshop Nov. 30-Dec. 2, 2009, Washington, DC

12. Sukdeo, N., A. Page, K.J. Indest, F.H. Crocker, L.D. Eltis, and S. Hallam, 2009, Opening a metagenomic window on microbial community structure and function associated with RDX contamination and degradation in soils, 2009 Partners in Environmental Technology Technical Symposium & Workshop Nov. 30-Dec. 2, 2009, Washington, DC

13. Crocker, F.H,, K.J. Indest, L.D. Eltis, C. Florizone, H-P. Chen, J. Hawari, J-S. Zhao, and N. Perreault, 2008, Identification of Microbial Gene Biomarkers for in situ RDX Biodegradation, 2008 Partners in Environmental Technology Technical Symposium 2-4 Dec. 2008, Washington, DC

14. Crocker, F.H., K. J. Indest, J. Hawari, and L. D. Eltis, 2008, Proteomic and Genomic Approaches to Identify Microbial Biomarkers of *in situ* RDX Biodegradation. Society of Environmental Toxicology and Chemistry North America 29 Annual Meeting 16-20 Nov. 2008, Tampa, FL

C. Textbooks or book chapters:

1. Halasz, A. and J. Hawari, 2011, Degradation routes of RDX in various redox systems. **In** Aquatic Redox Chemistry, American Chemical Society, Washington, D.C. Eds. Paul Tratneyk, Timothy J. Grundl , and Stefan Haderlein. pp 441-462.

D. Awards:

1. Jung, C.M., K.J. Indest, and F.H. Crocker, 2010, Engineer Research and Development Center Research and Development Achievement Award, Horizontal Gene Transfer as a mechanism of dissemination and persistence of RDX-degrading activity at contaminated sites, May 2010.

2. Hawari, Jalal, a co-recipient of The Technical Cooperation Program (TTCP) Achievement Award (October 2011) for significantly advancing the knowledge and understanding of the environmental fate and ecological impact of energetic materials to improve the ecological risk assessment of testing and training ranges at defense installations in TTCP nations
3. Indest, K.J., and F.H. Crocker, 2008, Department of the Army Research and Development Achievement Award, Genome sequencing of *Gordonia* sp. KTR9, October 2008.
4. Indest, K.J., and F.H. Crocker, 2008, Engineer Research and Development Center Research and Development Achievement Award, Genome sequencing of *Gordonia* sp. KTR9, May 2008.

REPORT DOCUMENTATION PAGE

Form Approved
OMB No. 0704-0188

1. REPORT DATE *(DD-MM-YYYY)*	2. REPORT TYPE	3. DATES COVERED *(From - To)*
December 2012	Final	

4. TITLE AND SUBTITLE

Identification of Microbial Gene Biomarkers for *in situ* RDX Biodegradation: ER-1609

5a. CONTRACT NUMBER

5b. GRANT NUMBER

5c. PROGRAM ELEMENT NUMBER

6. AUTHOR(S)

Fiona. H. Crocker, Karl J. Indest, Carina M. Jung, Dawn E. Hancock, Megan E. Merritt, Christine Florizone, Hao-Ping Chen, Gordon R. Stewart, Songhua Zhu, Nicole Sukdeo, Marie-Claude Fortin, Steven J. Hallam, William W. Mohn, Lindsay D. Eltis, Nancy N. Perreault, Jian-Shen Zhao, Louise Paquet, Annamaria Halasz, and Jalal Hawari

5d. PROJECT NUMBER

5e. TASK NUMBER

5f. WORK UNIT NUMBER

7. PERFORMING ORGANIZATION NAME(S) AND ADDRESS(ES)

Environmental Laboratory
U.S. Army Engineer Research and Development Center
3909 Halls Ferry Road, Vicksburg, MS 39180-6199;
Department of Microbiology and Immunology
University of British Columbia, 2350 Health Sciences Mall
Vancouver, British Columbia, Canada V6T 1Z3;
Biotechnology Research Institute, NRC
6100 Royalmount Avenue, Montreal, Quebec, Canada H4P 2R2

8. PERFORMING ORGANIZATION REPORT NUMBER

ERDC/EL TR-12-33

9. SPONSORING / MONITORING AGENCY NAME(S) AND ADDRESS(ES)

U.S. Army Corps of Engineers
Washington, DC 20314-1000

10. SPONSOR/MONITOR'S ACRONYM(S)

11. SPONSOR/MONITOR'S REPORT NUMBER(S)

12. DISTRIBUTION / AVAILABILITY STATEMENT

Approved for public release; distribution is unlimited.

13. SUPPLEMENTARY NOTES

14. ABSTRACT

Objectives of this project were to: (a) elucidate RDX degradation pathways in model RDX-degrading bacteria, (b) design and develop molecular tools to identify genes responsible for RDX biodegradation, and (c) correlate the response of biomarker(s) to concentrations of RDX and/or rates of RDX degradation. *Gordonia* sp. KTR9 and *Shewanella oneidensis* MR-1served as model bacterial systems for the aerobic and anaerobic degradation of RDX, respectively.

Genome annotation and functional characterization of the plasmid pGKT2 in KTR9 revealed that *xplA* gene is both necessary and sufficient for RDX degradation. *Shewanella oneidensis* MR-1 was shown to efficiently degrade RDX anaerobically via two initial routes: (a) sequential N-NO_2 reduction to the corresponding nitroso (N-NO) derivatives; and (b) mono-denitration followed by ring cleavage. The qPCR molecular tools described in this report have the potential to be used by remediation specialists for site characterization, treatment recommendations, and for evaluation and optimization of the treatment process.

The fundamental information gained in this study suggests that XplA-mediated aerobic denitration of RDX may be subjected to inhibitory effects in response to nitrogen availability. Additional research is required to determine reliable guidelines to inform site managers of specific field concentrations of ammonium and nitrate that will increase RDX treatment times. Also, techniques to effectively lower the inorganic nitrogen concentrations to non-inhibitory levels for the aerobic RDX biodegradation pathway will need to be determined.

15. SUBJECT TERMS

Biodegradation
Gordonia
Hexahydro-1,3,5-trinitro-1,3,5-triazine
Proteomics
Quantitative polymerase chain reaction
RDX
Shewanella
Transcriptomics

16. SECURITY CLASSIFICATION OF:			17. LIMITATION OF ABSTRACT	18. NUMBER OF PAGES	19a. NAME OF RESPONSIBLE PERSON
a. REPORT	b. ABSTRACT	c. THIS PAGE			19b. TELEPHONE NUMBER *(include area code)*
UNCLASSIFIED	UNCLASSIFIED	UNCLASSIFIED		174	